Synthesis and Biophysical Studies of Nucleic Acid-Binding Oligomers

By

Riyadh Jaleel Nahi

A Thesis Submitted for the Degree of

Doctor of Philosophy

At

Cardiff School of Chemistry

Cardiff University

United Kingdom

September 2016

DECLARATION

This work has not been submitted in substance for any other degree or award at this or any other university or place of learning, nor is being submitted concurrently in candidature for any degree or another award.

Signed ……(**Riyadh Jaleel Nahi**) Date ……

STATEMENT 1

This thesis is being submitted in partial fulfilment of the requirements for the degree of PhD

Signed …….. (**Riyadh Jaleel Nahi**) Date ……

STATEMENT 2

This thesis is the result of my own independent work/investigation, except where otherwise stated, and the thesis has not been edited by a third party beyond what is permitted by Cardiff University's Policy on the Use of Third Party Editors by Research Degree Students. Other sources are acknowledged by explicit references. The views expressed are my own.

Signed …….. (**Riyadh Jaleel Nahi**) Date ……..

STATEMENT 3

I hereby give consent for my thesis, if accepted, to be available online in the University's Open Access repository and for inter-library loan, and for the title and summary to be made available to outside organisations.

Signed …….. (**Riyadh Jaleel Nahi**) Date ……

Abstract

In general, this thesis describes the design, synthesis, oligomerization and biophysical studies of novel PNA monomers.

Our initial aim was to develop an efficient and inexpensive route for the synthesis of a series of novel alkyne PNA monomers bearing thymine, cytosine, adenine and guanine nucleobases suitable for Fmoc solid phase PNA synthesis strategy. These novel monomers allow functionalising the PNA sequences with alkyne functions at their *N*-terminus during solid phase synthesis. These novel monomers can be exploited in the click reaction applications such as a click ligation of PNA and conjugation of PNA with different substrates such as nucleic acids and proteins. As an application for ligation PNA sequences, the alkyne thymine PNA monomer was incorporated successfully into the target PNA oligomers during oligomerization.

Mimicking the click (CuAAC) reaction linkers of the ligation of PNA oligomers, three novel 1,2,3-triazole functionalised building blocks were designed and prepared suitable for the Fmoc solid phase PNA synthesis strategy. Furthermore, synthesis of these building blocks specifically that is bearing thymine base represents an attempt for modification the original PNA oligomers in order to improve their drawbacks such as poor water solubility and cellular uptake or to enhance their hybridization properties. Our approach to synthesise these monomers is the Click (CuAAC) reaction which is not analogous for the routes that are used for the synthesis of the modified or unmodified PNA monomers. To investigate their effect on the biophysical properties of PNA oligomers, a single monomeric unit of these monomers was incorporated successfully into a series of mixed purine-pyrimidine 8-mer PNA sequences following the standard Fmoc-solid phase PNA synthesis conditions.

In general, The Tm experiments-UV spectroscopy showed that the modified PNA oligomers containing these modified monomers still have a binding affinity with complementary sequences of DNA and RNA. The T_m values indicated that the incorporation of the 1,2,3-triazole functionalised monomers maintained or slightly reduced the thermal stability of the PNA/DNA duplexes, whereas the PNA/RNA duplexes resulted in a significantly reduced thermal stability. All of them are compared to the corresponding unmodified PNA/DNA duplexes.

Acknowledgements

Foremost, I would like to thank my creator (Allah) for giving me a guidance in my life and for seeing me through the completion of this thesis.

I would like to begin by expressing my deepest thank to my supervisor Dr. James Redman for his supervision, advice, guidance and support throughout my PhD. This helped me to improve both my scientific skills and insight into the scientific research.

I would also like to thank the technical and administrative staff at the Cardiff School of Chemistry for their invaluable contribution, in particular, Dr Rob Jenkins, Robin Hicks and Thomas for an efficient NMR and mass spectrometry service.

I would also like to thank Prof. Rudolf Allemann and his group for advices and discussions during group meetings and the use of equipment and facilities.

I am eternally gratefully to my wife, Zeina for her unlimited love, patience and supporting during my PhD and all areas of my life. This PhD is a testament to her faith in me, I hope I have made her proud.

I would also like to say a big thank my family in Iraq, my parents, my parents in law and my brothers and sisters. Thank you for encouraging and praying me during my PhD study.

Finally, I am grateful to Ministry Of Higher Education and Scientific Research (**MOHESR**) of Iraq, for the scholarship and the funding and facilities which allowed me to perform my PhD at Cardiff University in the UK.

Dedicated to

My lovely wife Ziena

&

My beautiful daughters Fatima and Maryam

Abbreviations

A	Adenine
AEG	*N*-(2-aminoethyl) glycine
Bhoc	Benzhydryloxycarbonyl
Boc	*tert*-Butyloxycarbonyl
tBu	*tert*-Butyl
Bn	Benzyl group
BOP	Benzotriazolyl-tris-(dimethylamino) Phosphonium hexafluoro phosphate
Bz	Benzoyl
Cbz	Benzyl carbamate
°C	Degrees Celcius
C	Cytosine
CD	Circular dichroism spectroscopy
cm	Centimetre
d	Doublet
Da	Dalton
DCC	*N,N*'-dicyclohexylcarbodiimide
DCM	Dichloromethane
DHBtOH	3-Hydroxy-1,2,3-benzotriazin-4(3H)-one
DIPCDI	*N,N*'-diisopropylcarbodiimide
DIPEA	Diisopropylethyl amine
DMF	Dimethylformamide
DMSO	Dimethyl sulfoxide
DNA	Deoxyribonucleic acid
ds-DNA	Double-stranded deoxyribonucleic acid
DSC	Differential scanning calorimetry
DVB	Divinyl benzene
EI	Electron impact (in mass spectrometry)
Et	Ethyl

G	Guanine
g	Gram
Fmoc	Fluorenylmethyloxycarbonyl
HA	Hyaluronic acid
HAS2	Hyaluronan synthase 2
HATU	O-(7-Azabenzotriazole-1-yl)-*N*,*N*,*N*′,*N*′-tetramethyluronium hexafluorophosphate
HBTU	O-Benzotriazole-*N*,*N*,*N*′,*N*′-tetramethyl-uronium-hexafluoro-phosphate
HOBt:H_2O	1-Hydroxybenzotriazole monohydrate
HPLC	High-performance liquid chromatography
HRMS	High-resolution mass spectrometry
IR	Infrared
LMRS	Low-resolution mass spectrometry
LNA	Locked nucleic acid
m	Multiplet
Me	Methyl
Mmt	Methoxytrityl [(4-methoxyphenyl)diphenylmethyl]
mp	Melting point
MS	Mass spectrometry
m/z	Mass to charge ratio (in mass spectrometry)
NCL	Native chemical ligation
NMM	*N*-Methylmorpholine
NMP	*N*-Methyl-2-pyrrolidone
NMR	Nuclear magnetic resonance
ODN	Oligodeoxynucleotide
PNA	Peptide nucleic acid
ppm	Parts per million
PyAOP	7-Azabenzotriazol-1-yloxytripyrrolidinophosphonium hexafluorophosphate

PyBOP	Benzotriazol-1-yl-oxytripyrrolidinophosphonium hexafluorophosphate
RNA	Ribonucleic acid
mRNA	Messenger ribonucleic acid
tRNA	Transfer ribonucleic acid
rRNA	Ribosomal ribonucleic acid
RP-HPLC	Reversed-phase high-performance liquid chromatography
s	Singlet
S_N1	Unimolecular nucleophilic substitution
S_N2	Bimolecular nucleophilic substitution
ss-DNA	Single-stranded deoxyribonucleic acid
SPPS	Solid phase peptide synthesis
t	Triplet
T	Thymine
TBTA	Tris-(benzyltriazolylmethyl) amine
TFMSA	Trifluoromethanesulfonic acid
TFA	Trifluoroacetic acid
THF	Tetrahydrofuran
THPTA	Tris-(3-hydroxypropyltriazolylmethyl) amine
TLC	Thin-layer chromatography
T_m	Melting temperature
TMSCl	Trimethylchlorosilane
UV	Ultraviolet

CONTENTS

Chapter Two

Design and Synthesis of Novel PNA monomers:

Results and discussion

Chapter Three

Design and Synthesis of Modified PNA Oligomers:

Results and Discussion

Chapter Six

Experimental

Chapter One

Introduction

1.1 Motivation

The recognition of natural oligonucleotides sequences by a complementary sequence is a fundamental feature in biological systems and is essential for hybridisation-based therapeutic and diagnostic applications.[1,2,3] This principle underpins a possible consideration of antisense or antigene-based inhibition of gene expression, as a practical approach to therapeutics. The mechanism of this recognition depends on Watson-Crick base-pairing between the heterocyclic bases of the antisense oligonucleotide and their complementary nucleobases on the target RNA sequence to form a duplex. Or alternatively, via Hoogsteen base-pairing between an antigene oligonucleotide and its complementary sequence of double-stranded DNA, allowing the third strand antigene to bind around the duplex to form a triplex. These two hybridization mechanisms are only possible through relatively weak hydrogen bond interactions, resulting in highly variable hybridisation efficiencies depending on the number of the nucleotides in each strand sequence.

Currently, DNA and RNA oligonucleotides have found only limited applications in hybridisation based therapeutics owing to their poor permeability and low stability *in vivo*, due predominantly to the susceptibility of their phosphodiester backbone to undergo enzymatic cleavage by the cellular nucleases. Furthermore, they exhibit poor permeability into cells because they are negatively charged compounds. For these reasons, there is a lot of interest in the discovery and development of oligonucleotide analogues that have structural features which lead to improved pharmacological applications. Furthermore, these analogues should also have sufficient chemical and biological stability, and show a significant increase in the binding efficiency with the target oligonucleotide sequence in a high selectivity with lack of sequence restriction.

Peptide nucleic acids (PNA) are one of the most successful examples of the DNA analogues, which have been applied as a biomolecular tool in the recognition of natural oligonucleotides. They, therefore, display promising potential applications such as antisense and antigene based therapeutics, and as such the synthesis and biophysical studies of PNA oligomers, are therefore, described throughout the remainder of this thesis.

However, before describing the experimental work performed it is important to discuss the fundamental oligonucleotides chemistry and how PNA, and other DNA analogues, mimic the structure and function of natural nucleic acids.

1.2 Nucleic Acids: Chemical Structure

Nucleic acids are biological macromolecules that store or transfer the genetic information for all living beings and were first described in 1869 by Friedrich Miescher.[4,5] Subsequent studies have already revealed the fact that there are two nucleic acids differing in their structure and nature of their function, namely DNA (Deoxyribonucleic acid) and RNA (Ribonucleic acid). Structurally, nucleic acids are biopolymers composed of repeating monomeric units called nucleotides (Figure 1.1).

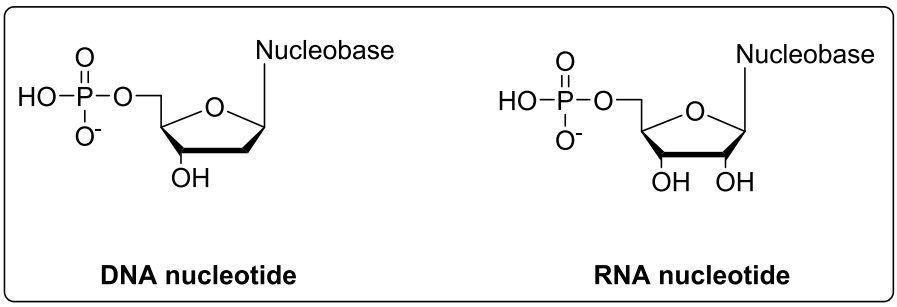

Figure 1.1: Nucleotide structure of DNA and RNA.

Each nucleotide is made up of a pucker-shaped pentose sugar attached at C1 to a nucleobase through a β-glycosidic bond, and at C5 to a phosphate group via a phosphoester linkage. The most substantial difference between DNA and RNA is the nature of the sugar unit. DNA contains a 2-deoxyribose moiety as opposed to the ribose in RNA. Thus, RNA can be distinguished chemically from DNA by its greater instability in alkaline solutions owing to the potential for the additional hydroxyl group on the sugar moiety to be deprotonated then causing hydrolysis of RNA strand.[6] Initial chemical analysis of nucleotides proved that the nucleobases that are attached to the sugar moiety belong either to the pyrimidine or purine families (Figure 1.2). Pyrimidines have a heterocyclic single-ring structure **1** to which they are attached at the N1-position to the sugar unit, whereas the purines are hetero

aromatic bicyclic compounds such as **5** which are connected to the sugar moiety at the N9-position.[7]

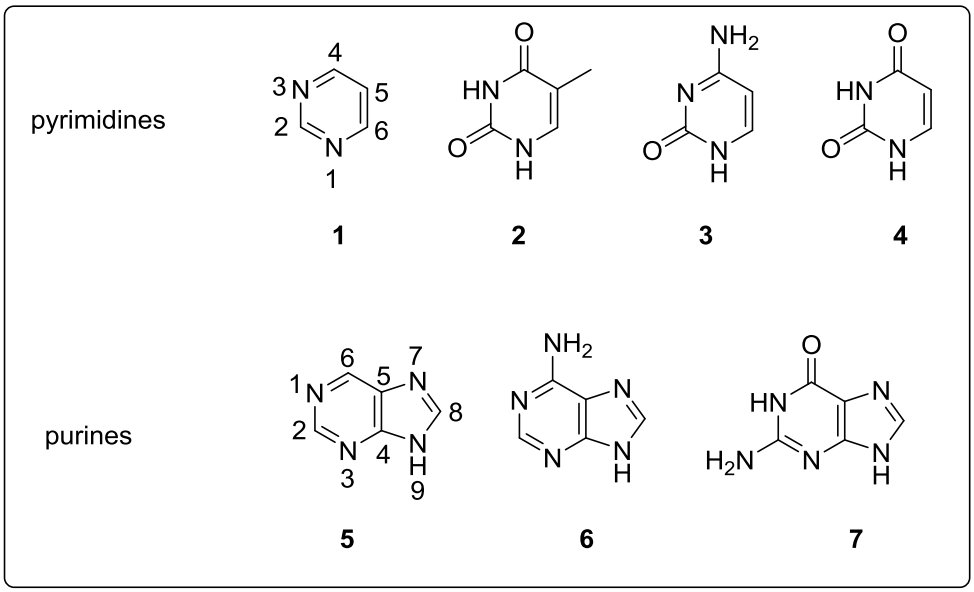

Figure 1.2: Structure of the common pyrimidine and purine nucleobases.

Further, more advanced, chemical investigations have revealed another difference between DNA and RNA which is in the finer structure of the nucleobases. There are four common bases in both DNA and RNA, in DNA these are thymine (T) **2**, cytosine (C) **3**, adenine (A) **6**, and guanine (G) **7**, whereas, in the RNA structure, the thymine base is replaced with uracil base (U) **4**. This difference, although subtle, is highly important in error checking during DNA replication. Cytosine can undergo spontaneous deamination to uracil which could result in an undesired mutation. However, because thymine is expected in DNA, not uracil, the DNA repair enzyme uracil-DNA glycosylase can remove these mutations and repair the sequence.[8]

In both DNA and RNA, the nucleotide monomers are linked by phosphodiester linkages, which are formed between the 5'-phosphate group of one nucleotide and the 3'-hydroxyl of the sugar of the next nucleotide. Consequently, the terminus of the formed oligonucleotide chain is carrying the free 3'-hydroxyl group called the 3'-end while the other terminus is bearing the 5'-phosphate known as the 5'-end. Therefore, their sequences are conventionally depicted from the 5'-end (left hand) to the 3'-end (right hand). Structurally, RNA is a single-stranded polynucleotide folds

upon itself via intramolecular hydrogen bonding into the characteristic secondary and tertiary structures that are essential for the RNA molecule to perform its biological roles.[9,10] In the folded region, most of the nucleobases are complementary and joined together by hydrogen bonds according to Watson-Crick base paring to form a helical structure. This structure helps in the stability of the RNA molecule. Inside living cells, RNA exists in many forms that differ in their size and function. The major classes of RNA in eukaryotic organisms are messenger RNA (mRNA) as a DNA copy, transfer RNA (tRNA) as a coupler between the genetic code and the protein building blocks, and ribosomal RNA (rRNA) as a structural component of ribosomes.

Functionally, RNA plays a key role in the synthesis of protein by transmitting genetic information encoded in DNA and converting it into a variety of different proteins depending on the original DNA sequence. mRNA is transcribed from a DNA source sequence, and in turn transmits this sequence information to the ribosome, where it is 'read' in the blocks of three nucleobases known as codons. Then tRNA carries a specific amino acid, to the site of protein production according to the codon sequence. Moving along the mRNA strand, this combination of functions results in the production of a long chain polypeptides and protein.[9,10]

DNA is the genetic material existing mainly in the nucleus of the cell, but can be found in other cell structures of eukaryotes such as the mitochondria and freely moving around the cytoplasm of prokaryotes. DNA acts as a template and store of the genetic instructions that are used in the development, functioning and replication of all known living organisms (except RNA viruses). Furthermore, DNA controls the synthesis of RNA in the cell.

Inside living cells, DNA almost always consists of two complementary strands of poly nucleotides that are twisted about one another in a spiral (Figure 1.3) to form the famous double-helix structure that was first described in 1953 by Watson and Crick.[11] This helix structure gives the DNA molecule the chemical stability and the ability to copy the information it contains that are necessary to accomplish its functions, by not containing any additional sequence modifying moieties.

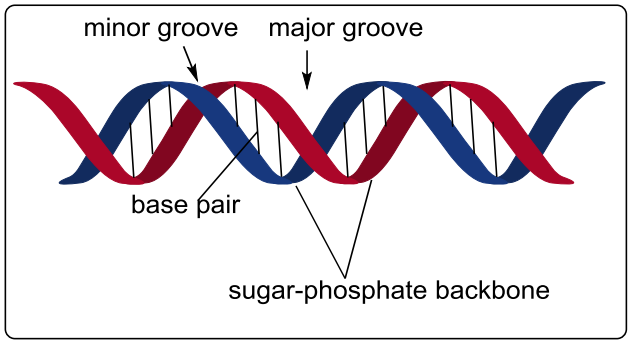

Figure 1.3: An example schematic of the helix of DNA.

Further research into the DNA double helix led to important information about how the strands are held together. The two strands are antiparallel, meaning, from any fixed position; one strand is oriented in the 5' to 3' direction and the other in the 3' to 5' direction. These two strands of DNA are held together by two types of non-covalent binding interactions including the lipophilic interactions between the adjacent bases and the hydrogen bonding between the complementary nucleobases on the opposite strand.

In addition, it has been proven that the thymine base in one strand always pairs only to the adenine base in the other strand via two hydrogen bonds, and similarly, the cytosine base always pairs to the guanine base by three hydrogen bonds. As a consequent, thymine and adenine always have the same concentration, and the amount of cytosine is always equivalent to the amount of guanine.[12] This base pairing is known as Watson-Crick base pairing as shown in Figure 1.4.

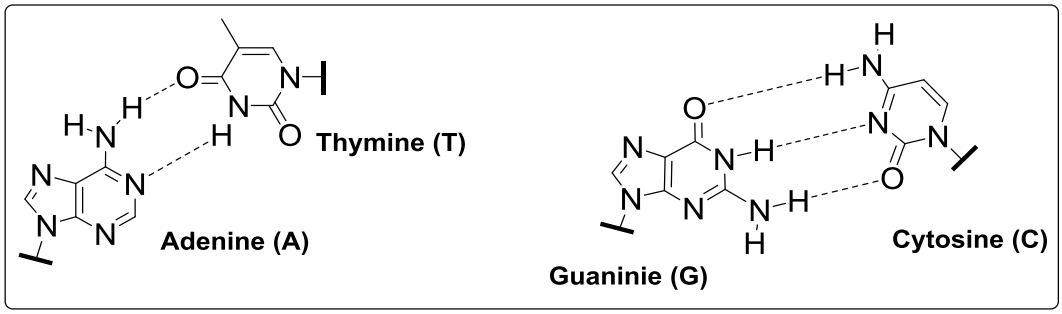

Figure 1.4: Watson-Crick base pairing.

One more feature of the double helix structure is that the two DNA strands are

arranged in such a way to present their sugar-phosphate backbones on the outside of the helix, and their bases are in the centre. This is important as the hydrophobic nature of the nucleobase keeps them on the inside of the double helix of DNA, away from water content in cells. Meanwhile, the phosphate backbone is hydrophilic and retains the backbone on the outside.[11] Consequently, the DNA double helix is stabilised by the fact that the base pairs are stacked one on top of another, which allow for π-π stacking interactions between the heterocyclic rings.

A careful examination of a space-filling model of a double helix of DNA reveals the presence of two types of grooves on its exterior surface between the deoxyribose-phosphate chains. Due to the asymmetry of the sugar moiety and the structurally distinct nature of the upper surface of a base-pair relative from the bottom surface, these grooves are not equal in their size (Figure 1.3). Therefore, they are termed the major groove (ca. 12 Å wide) and the minor groove (ca. 6 Å wide).[13] Practically, DNA-binding proteins use these grooves to interact with a specific DNA sequence without disrupting the base-pairing of the ds-DNA molecule.[14,15] Also, the minor grooves contain water molecules that interact with the keto and amino groups of the nucleobases.[16,17]

Furthermore, the nucleobases have displayed another important alternative base pairing mechanism to Watson-Crick base paring, termed Hoogsteen base pairing which is used to form a triplex.[18,19] In Hoogsteen base pairing, each nucleobase pairs with the complementary nucleobase through two hydrogen bonds. However, acid conditions are required for protonation of the cytosine base, enabling it to form two hydrogen bonds with guanine as shown in Figure 1.5.

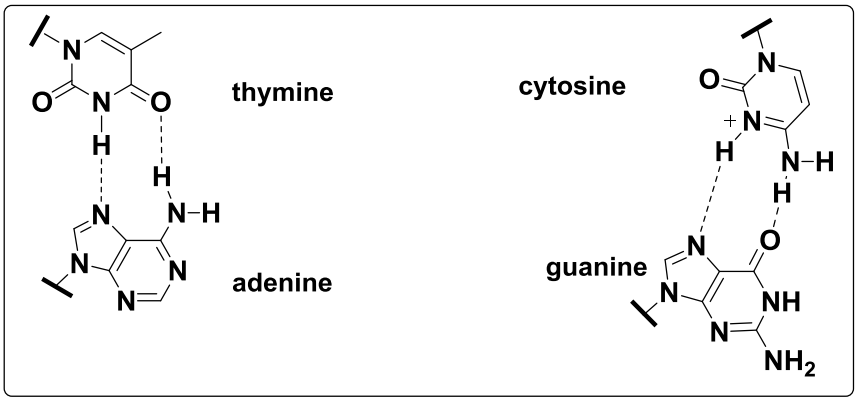

Figure 1.5: Hoogsteen base pairing.

These features of the structure of the double helix are highly important for DNA to achieve its biological activity which allow it to take part in a number of molecular interactions [20] through intercalation, electrostatic, and groove binding mechanisms not only with itself and other nucleic acids but also with other molecules such as proteins,[21,22] drugs,[23] metal ions,[24,25] etc.

1.2.1 Nucleic acids modifications

DNA and RNA oligonucleotides have been used as a tool for antisense and antigene investigations that are helped molecular biologists to discover new gene functions and as a base for future gene therapy applications. However, for *in vivo* applications, there are some problems such as a low biological stability against nucleases, cellular uptake problems and weak DNA binding affinity, which imped their use in certain applications. To overcome these drawbacks, many chemical modifications have been targeted to each of the nucleotide sections, the phosphate backbone, the sugar moiety or the nucleobase.

As the negatively charged phosphodiester linkage of the backbone is readily cleaved by nuclease or protease action,[26] a large number of modifications have been extensively investigated in order to improve its enzymatic stability. These modifications involved altering this linkage partly or wholly to produce neutral, anionic and cationic alternatives. The most common phosphodiester analogues are the phosphorothioate **8**, methyl phosphonates **9**, phosphoramidite **10** and hydroxymethyl phosphonium **11** in which one phosphate oxygen is replaced with a

sulphur atom, methyl, alkyl amine and hydroxymethyl groups, respectively as shown in Figure 1.6.[26-31]

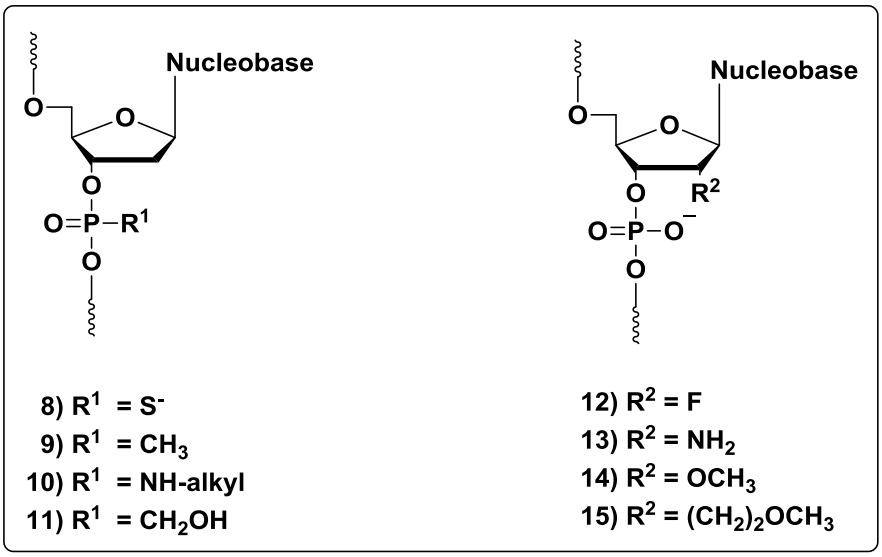

Figure 1.6: Structure of common modifications in antisense oligonucleotides.

In RNA, several interesting modifications have been introduced by replacing the hydroxyl group at the position C2 of the ribose with different groups to enhance its chemical and nuclease stability. The most important analogues at this position are 2'-deoxy-2'-fluorooligoribonucleotide **12**, 2'-deoxy-2'-amine oligoribonucleotide **13**, 2'-O-methyl oligoribonucleotide **14** and 2'-deoxy-2'-C-alkyl oligoribonucleotide **15** as shown in Figure 1.6.[31]

In general, these sugar-phosphate modifications have been examined for antisense applications. Although these modifications displayed an increased resistance to the enzymatic degradation, some associated drawbacks has been resulted such as a lower RNA binding affinity and lower water solubility and lack the binding specifically to proteins than the natural oligonucleotides.[26,30,31] Therefore, further improvements in the design of antisense oligonucleotides need to be made in order to arrive at more ideal therapeutics.

A promising class of nucleic acid modifcations, termed locked nucleic acid (LNA) such as **16** (Figure 1.7), has also been introduced when the ribose sugar of RNA is locked through a bridging methylene group, between the C4 atom and the oxygen

of the hydroxyl group at C2, resulting in a bicyclic RNA analogue.[32,33,34] LNA oligonucleotides have displayed remarkable properties such as resistance to enzymatic degradation, high affinity and excellent specificity toward their complementary DNA or RNA oligonucleotides, with increased thermal stability of their duplexes. These unique properties make this modification to be a promising drug platform for therapeutic applications based upon gene expression.[35,36,37]

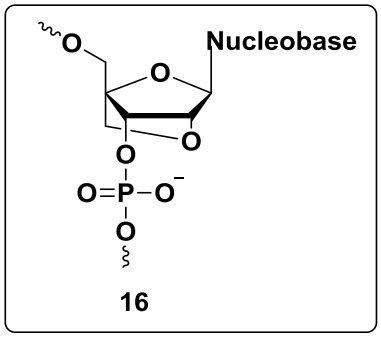

Figure 1.7: Structure of locked nucleic acid LNA **16**.

For more investigations, one more chemically advanced modifications of nucleic acids was reported when the phosphodiester linkage of nucleic acids was replaced with a 1,2,3-triazole ring such as **17** (Figure 1.8).

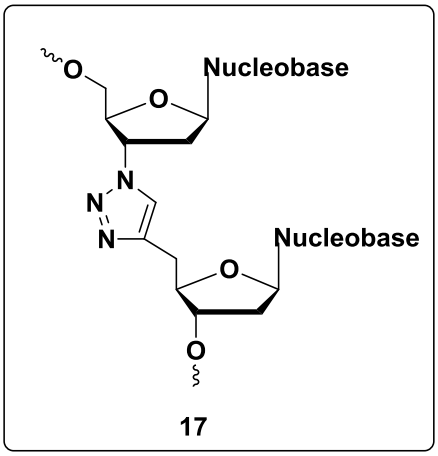

Figure 1.8: Structure of triazole modified DNA oligonucleotide **17**.

Very promising results were reported for the triazole DNA analogues when Isobe *et*

al. in particular found that a polythymidine triazole analogue showed a higher affinity towards polyadenosine oligonucleotides compared to the unmodified DNA.[38]

Currently, one of the most divergent modifications of nucleic acids is one that has wholly replaced the polyanionic sugar-phosphate backbone with a neutral polyamide backbone to make an oligonucleotide analogue called peptide nucleic acid **18** which is abbreviated PNA (Figure 1.9).

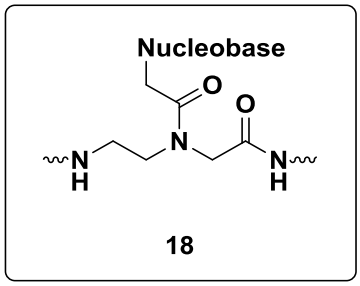

Figure 1.9: Structure of peptide nucleic acid (PNA) **18**.

The astonishing discovery that this polyamide bearing nucleobases can bind with higher affinity and specificity to complementary sequences of nucleic acids obeying Watson-Crick base-pairing rules and has a high resistance to nucleases resulted in the rapid development of a new branch of research focused on diagnostic and therapeutic applications of this highly interesting class of compounds. Thus, the next section is dedicated to peptide nucleic acid (PNA).

1.3 Peptide Nucleic Acid (PNA)

1.3.1 Structure and properties of PNA

Peptide nucleic acid (PNA) is a single strand of nucleobases, was first introduced by Nielsen and his colleagues in 1991[39] as a ligand to bind ds-DNA in the DNA major grooves to form a triplex oligonucleotide. In the PNA sequence, the natural negatively charged sugar-phosphate backbone of nucleic acids was replaced with a neutral achiral polyamide backbone. This new backbone is consisted of repeating units of *N*-(2-aminoethyl) glycine (AEG) linked together by amide bonds in a similar

way to that is used in polypeptides. Therefore, PNAs are also depicted with the *N*-terminus at the left hand and the *C*-terminus at the right hand. Mimicking DNA, the four common nucleobases thymine **2**, cytosine **3**, adenine **6** and guanine **7** (Figure 1.3) are retained and attached to the secondary amine of this backbone via a methylene carbonyl linkage.

Structurally, the original *N*-(2-aminoethyl) glycine PNA monomer backbone was designed to keep the distance between the nucleobases along the PNA oligomer to six bonds (Blue bonds), and three bonds (Red bonds) from the nucleobase to the PNA backbone as shown in Figure 1.10. This maintains the same internuclear distances that are found in the natural oligonucleotides.

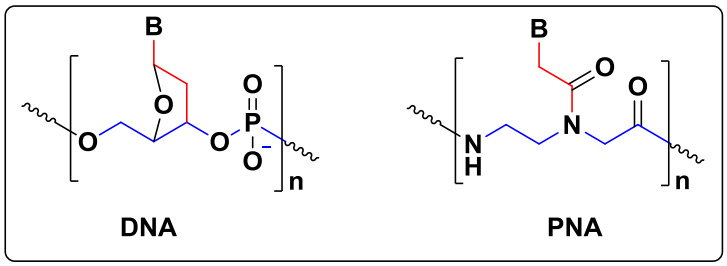

Figure 1.10: Structure of DNA and PNA, B: Nucleobase.

Characteristically, unlike DNA and RNA which are degraded in a depurination reaction, PNAs are fully resistant towards strong acids including HF and even weak bases such as ammonia and piperidine. For this reason, PNA oligomers can be prepared under these conditions.[40] Furthermore, PNAs are also stable in a wide range of temperatures. As PNAs are achiral compounds, they are synthesised without requiring any stereo-selective pathway. In contrast to the nucleic acids, PNAs are particularly more stable in both human serum and cellular extracts as a result of high resistance to biological degradation by nucleases and proteases.[41] Because of PNA's neutral backbone, the electrostatic repulsion between PNA oligomers and the nucleic acids is reduced. Consequently, PNA sequences have a high binding affinity towards complementary sequences of nucleic acids with increased thermal stability of their complexes giving rise to different important applications in molecular biology. An interesting feature, PNA oligomers also display

a greater specificity in binding to complementary DNAs, and also have a high sequence selectivity resulting in the fact that a mismatch in a PNA/DNA and PNA/RNA duplexes is consider more destabilising than a mismatch in a DNA/DNA duplexes.[42]

On the other hand, PNA oligomers are uncharged compounds and hence have some drawbacks such as lower water solubility compared with DNA and RNA with comparable length and purine: pyrimidine ratio and poor cellular uptake. PNA oligomers tend to be aggregated depending on the sequence of the oligomer, G-rich oligomers being the worst.[43,44]

1.3.2 PNA-Nucleic acids hybridizations

1.3.2.1 Duplex formation with complementary ss-DNA and RNA

PNA sequences have a high affinity and sequence selectivity to bind to complementary sequences of single-stranded DNA or RNA obeying Watson-Crick base pairing.[45,46] In contrast to DNA/DNA and DNA/RNA hybridisations that are always antiparallel, the PNA strand can hybridise to the target sequences of ss-DNA or RNA in both parallel and antiparallel orientations to make the corresponding PNA/DNA and PNA/RNA duplexes. In antiparallel hybridisations, the *N*-terminus of the PNA oligomer pairs to the 3' end of DNA or RNA strand, and to the 5' end in the case of the parallel hybridisation (Figure 1.11).

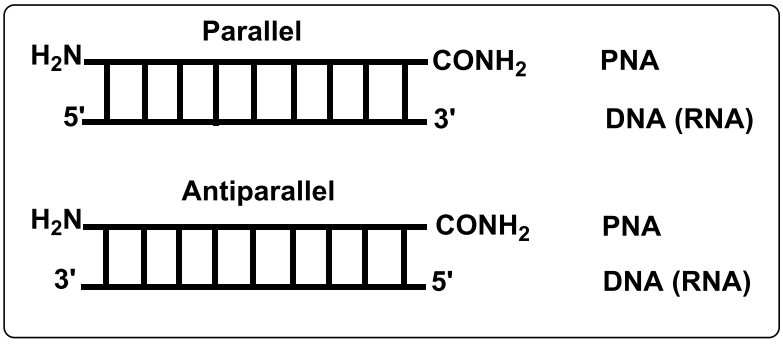

Figure 1.11: PNA/DNA and PNA/RNA duplexes binding orientations.

Similar to DNA/DNA and DNA/RNA duplexes, the hybridization properties of PNA/DNA and PNA/RNA can be assessed with different biophysical techniques such as DSC,[47,48] UV,[49,50] and CD [51,52] through studying the thermal melting temperature (T_m). The T_m is defined as a temperature at which equal amounts of base paired duplex and unpaired single strands are in equilibrium when the free energy change is zero. Interestingly, the thermal studies have demonstrated that the antiparallel hybridisations always show a higher stability than the corresponding parallel hybridisations, and PNA/RNA duplexes are always more stable than PNA/DNA duplexes. More importantly, all these duplexes are much more stable than the corresponding natural oligonucleotide duplexes.[53] The hybridization experiments also have revealed that the T_m values depend on the length of the molecule and the particular nucleotide sequence.[54,45]

Unlike DNA/DNA or DNA/RNA duplexes that are highly dependent on the ionic strength, the thermal stability studies on the effect of NaCl on PNA/DNA and PNA/RNA duplexes practically showed no a significant effect as a result of the uncharged PNA backbone.[55,56] This feature can be exploited when targeting DNA or RNA sequences involved in secondary structures, which are destabilized by low ionic strength.

1.3.2.2 PNA/double-stranded DNA hybridizations

The PNA oligomers were first designed to interact with double-stranded DNA via major groove recognition, through Hoogsteen hydrogen bonding to form a PNA/ds-DNA triplex with strand displacement.[39] However, it has been found that PNA sequence can bind the ds-DNA in a variety of important mechanisms.

Thus, under certain circumstances, a homopyrimidine PNA strand can bind to the complementary strand of double-stranded DNA in the DNA major grooves without displacement of the second strand of DNA to form a conventional triplex formation of PNA/ds-DNA. In this mechanism, the PNA strand is bound to the complementary strand of ds-DNA through Hoogsteen hydrogen bonds, whereas the Watson-Crick hydrogen bonds between two strands of DNA are preserved (Figure 1.12).[30,57]

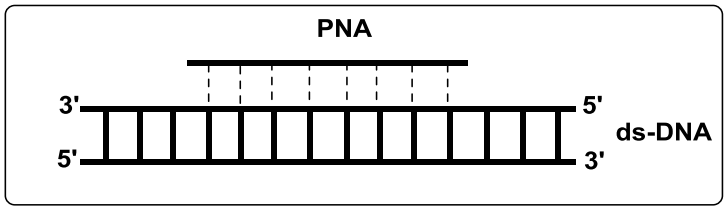

Figure 1.12: PNA/ds-DNA triplex formation, dashed lines are Hoogsteen base pairs.

The stability of the formed triplex PNA/ds-DNA is dependent on the length of PNA oligomers where it has been shown that the melting temperature increases with 1 °C per base. However, this mechanism of hybridization has only been demonstrated in specific cases involving a homo-pyrimidine PNA strand with high cytosine content. Furthermore, triplex formation only happens when the cytosine nucleobase can be protonated at the N3-position under acidic conditions. This protonation makes the cytosine nucleobase able to form a hydrogen bonding that is required for triplex formation, specifically with the N7-position of the guanine nucleobase in the target strand of double-stranded DNA.[57,58]

Since then it has been found that PNA binding to ds-DNA could be accomplished in an alternative mechanism than was described for triplex formation. This alternative is called strand invasion; a mechanism that involves the dissociation of ds-DNA locally into two exposed strands. Then one or both of DNA strands will be targeted by the complementary PNA sequence. This is so called invasion pathway is not limited to one single binding mode, however, as different modes exist such as triplex invasion, duplex invasion and double-duplex invasion.

Due to the increased stability of the resulting hybrid, the triplex invasion mode is the most preferred than the classical PNA/ds-DNA hybridization. Triplex invasion occurs between two homo-pyrimidine PNA strands and ds-DNA in two steps; one PNA strand is hybridised to the complementary DNA strand by Watson-Crick hydrogen bonds, and the other PNA strand by Hoogsteen hydrogen bonds via strand invasion. This forms an internal PNA/DNA:PNA hybrid. The second strand of DNA, which is not complementary to the tow PNA strands, is displaced and left as a single-strand (Figure 1.13).[59-62]

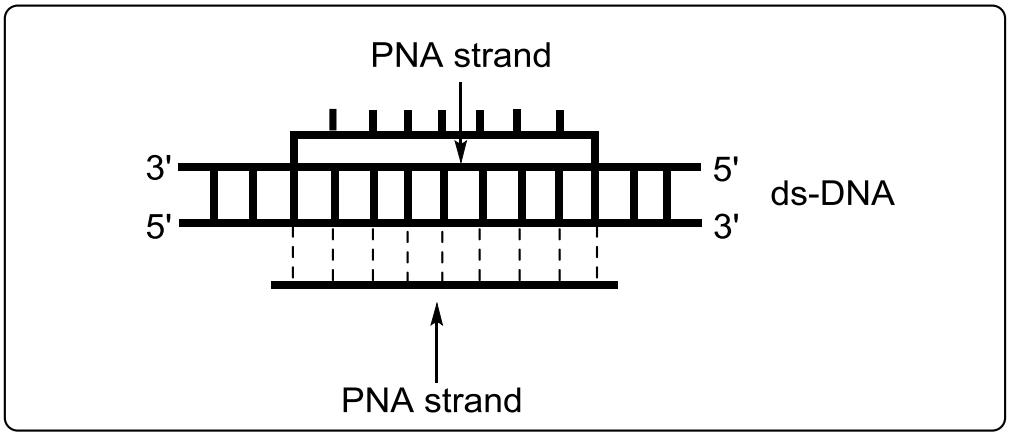

Figure 1.13: PNA/ds-DNA triplex invasion, dashed lines are Hoogsteen base pair.

Since Hoogsteen hydrogen bonds formation requires a protonation of the cytosine nucleobase, a modified base, pseudoisocytosine (J) (Figure 1.14), that carries a permanent proton at the N3-position was used rather than cytosine in the PNA strand aimed for Hoogsteen hydrogen bond.[63] This alternative greatly facilitated the formation of triplex by the invasion mechanism, independently of pH.[62]

Although the stability of the complex that formed via triplex invasion depends on the salt concentration and the length of the PNA oligomers, the complex is extremely stable once triplex invasion is complete. For this reason, binding can be considered irreversible under most experimental conditions.

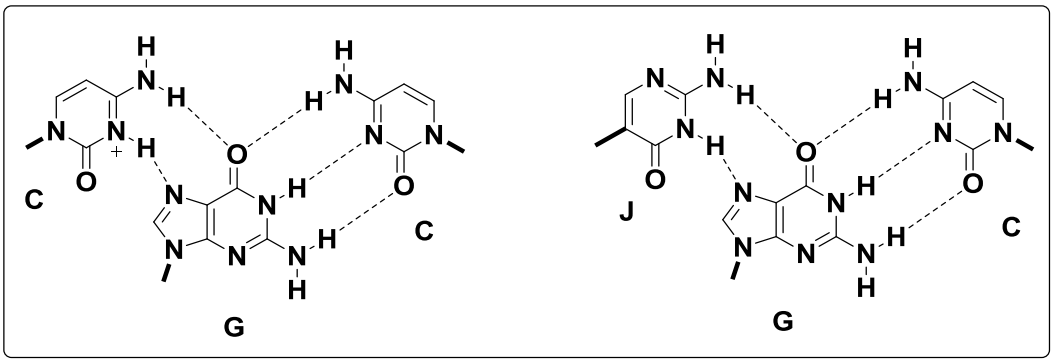

Figure 1.14: Hydrogen bonds in the triplex invasion.

Another binding mode for targeting ds-DNA, is through a duplex invasion mechanism, this time in which only one PNA strand targets the complementary sequence of ds-DNA. In this mode of a strand invasion mechanism, the hybridization

is obeying Watson-Crick base pairing with displacement of the DNA strand non-complementary to PNA (Figure 1.15).

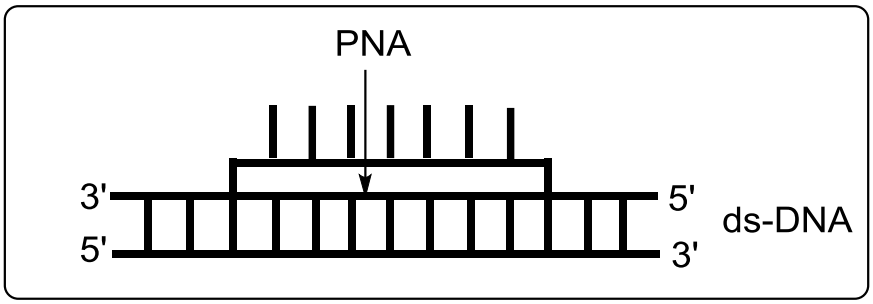

Figure 1.15: Duplex invasion mode of PNA-dsDNA.

In principle, this mechanism of PNA/ds-DNA hybridisation is a very attractive binding mode because it only relies on Watson-Crick base pairing and therefore should not be sequence restricted. The mechanism was first described for a single homopurine PNA targeted to a homopyrimidine ds-DNA sequence.[64] Unfortunately, however this complex is typically much less stable than triplex-invasion complexes although these complexes can exhibit greater stability if the DNA target is negatively supercoiled or if the PNA employed is conjugated to a cationic peptide.

Interestingly, PNA has displayed another binding mode for targeting ds-DNA through double-duplex invasion mechanism. In this hybridization mode, however, a double-stranded DNA can be invaded by two complementary PNA strands through Watson-Crick base pairing, and thus that ds-DNA is locally denatured (Figure 1.16).[65-67] This mechanism of strand invasion is very important because it overcomes the sequence limitations that are associated with triplex and duplex invasion mechanisms. However, there is a drawback with this mechanism in that, due to their neutral backbone, the two complementary PNA strands prefer to hybridise to each other rather than performing strand invasion into the ds-DNA.

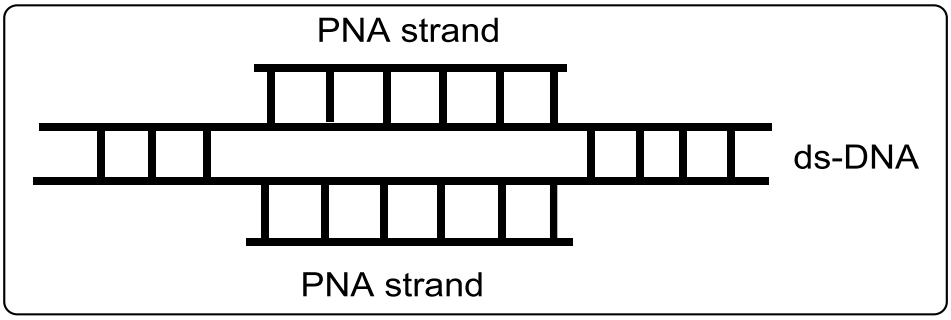

Figure 1.16: Double duplex invasion mode of PNA/ds-DNA hybridisations.

The only way to achieve this mode of hybridisation is by using PNA containing modified nucleobases, such as the 2, 6-diaminopurine (D) and 2-thiouracil (^{S}U) bases in place of adenine and thymine, respectively (Figure 1.17).[68,65] Hybridisation of these bases with each other is restricted by a steric clash between the 2-amino group of the 2,6-diaminopurine and the thio group of 2- thiouracil. Consequently, this modification will prevent or destabilise the interaction between the two PNA strands.

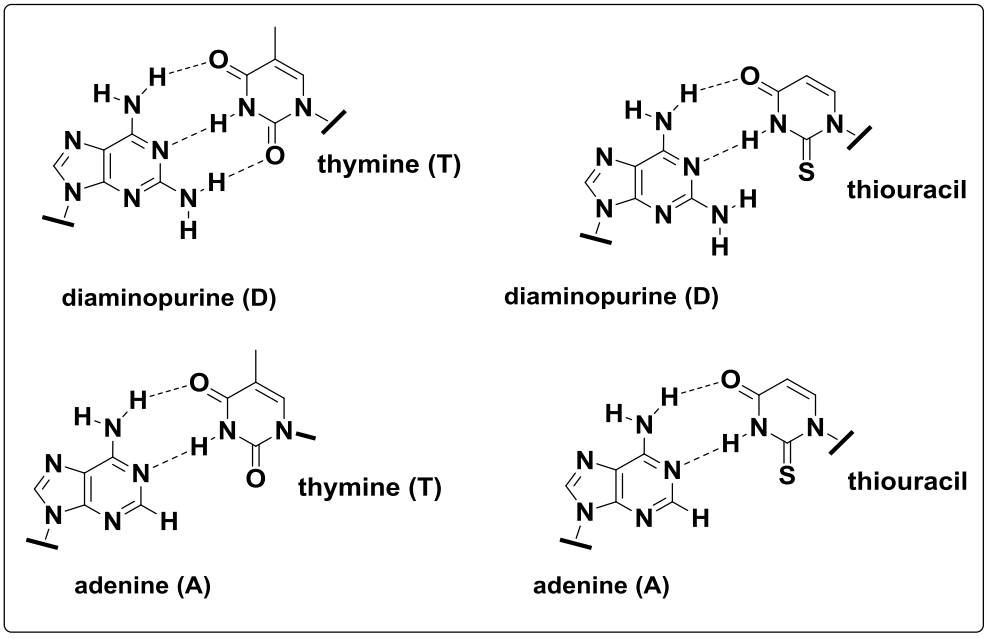

Figure 1.17: Binding of pseudo-complementary bases.

1.3.3 Peptide Nucleic Acids (PNA) as antisense and antigene agents

DNA is the carrier of all the genetic material and directs the protein synthesis through transcription into the messenger RNA (mRNA) which is subsequently translated into proteins. Thus, the gene regulation can occur on an antisense level through blocking the translation process of mRNA into proteins, and on an antigene level through preventing the transcription of DNA into mRNA.

In general, the ability of PNA to bind with high sequence specificity to the complementary DNA or RNA targets has provided a new tool for studying the recognition of nucleic acids and gene regulation. Owing to this ability to interact with the high sequence specificity to a chosen target in gene sequences and their unique physicochemical properties, there has been significant interest in PNA for medicinal and biotechnological applications including therapeutics, diagnostics, and molecular biology. As such PNAs have successfully been used as a tool for antigene or antisense therapeutics strategies, based on strand invasion of double-stranded DNA and duplex formation of single strand RNA, respectively.[69]

One key process in the regulation of gene expression by duplex formation between the PNA antisense, used as an antisense and the complementary mRNA strand via Watson-Crick base pairing is shown in Figure 1.18. Ideally, this mechanism is based on the steric blocking of mRNA sequences thereby inhibiting translation of the target gene.[70,71]

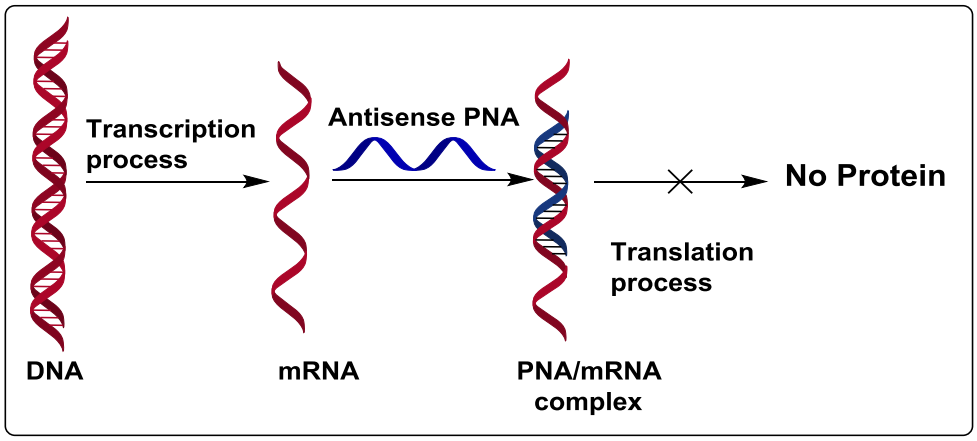

Figure 1.18: General scheme of PNA as antisense agent.

Several examples of PNA-antisense induced downregulation of gene expression have been reported. The mechanism of the antisense effect of conventional oligonucleotides is based on the activation of Ribonuclease H (RNase H) which is essential to cleave the RNA portion of the heteroduplex. Since a PNA/RNA duplex is not a substrate for RNase H, the PNA antisense effect is based on the steric blocking of either mRNA processing, transport into cytoplasm or translation. The efficiency of PNA-based gene silencing, therefore, depends on the stability of the resulting RNA/PNA hybrid.[72,73] In addition, the inhibition of any gene can take place by two different mechanisms. The first mechanism of inhibition involves the mRNA/DNA duplex. Inside the nucleus, mRNA is synthesised according to the initial sequence of DNA from which it is transcribed. Then, the RNaseH enzyme moves in to remove the mRNA strand by degradation, which allows the complementary DNA base pairs to be added to this newly formed strand, thus providing a double-stranded DNA. However, if oligodeoxynucleotides (ODN's) are present in the nucleus, then they will bind to the mRNA and prevent it from forming the new single stranded DNA. This type of mechanism has the advantage that a single ODN can target many mRNA, thus the therapeutic amount of this drug would be very small.

As an antigene agent, PNAs can recognise and hybridise to a complementary sequence of double-stranded DNA in a particular gene as shown in Figure 1.19.

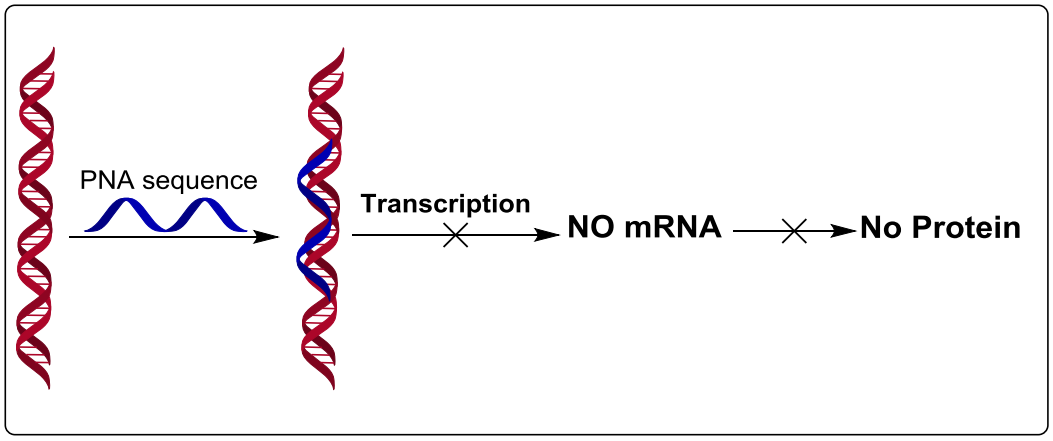

Figure 1.19: General scheme of PNA as antigene agent.

In an antigene application, PNAs are capable of interfering and inhibiting the transcription process of that particular gene through the formation of a stable triplex complex via strand invasion or strand displacement with the double-stranded DNA.[69] Therefore, when PNA binds to DNA to form the triplex complex, the RNA polymerase cannot bind DNA, and so is unable to generate mRNA which in turn prevents the creation of protein.[74] *In vivo*, PNA has also displayed an ability to block plasmid DNA replication,[75] and several studies have confirmed the ability of PNAs to inhibit DNA replication via a triplex structure formation. In short, the PNA2/DNA triplex arrests transcription in vitro and so is, therefore, capable of acting as an antigene-agent.

1.3.4 Solid phase PNA synthesis

The concept of solid phase synthesis (SPS) was developed by Merrifield in 1963 when the first efficient production of a tetrapeptide on a solid support (matrix) was reported.[76] Later, this concept has become a fully established protocol in the chemical synthesis of biologically active oligomers like peptides and nucleic acids. The basic point of the solid phase synthesis methodology is that building blocks having two functional groups are used. One of these functional groups must be temporary protected by a protective group. Therefore, for solid phase peptide synthesis, PNA monomers must have a suitably protected amino group, and their carboxylic functions are free thereby are able to accommodate two amide bonds during oligomerization. A feature that defines the chemistry of the solid phase PNA synthesis is the temporary protecting group of the *N*-terminal amino group of PNA monomers.

Figure 1.20 shows a general scheme of solid phase synthesis cycle of PNA oligomers which involves a repetitive process of temporary deprotection of the primary amino group of growing chains, coupling the activated PNA monomer, and then capping any unreacted amino function via *N*-acylation reaction. Commonly used is acetic anhydride the presence of a base.

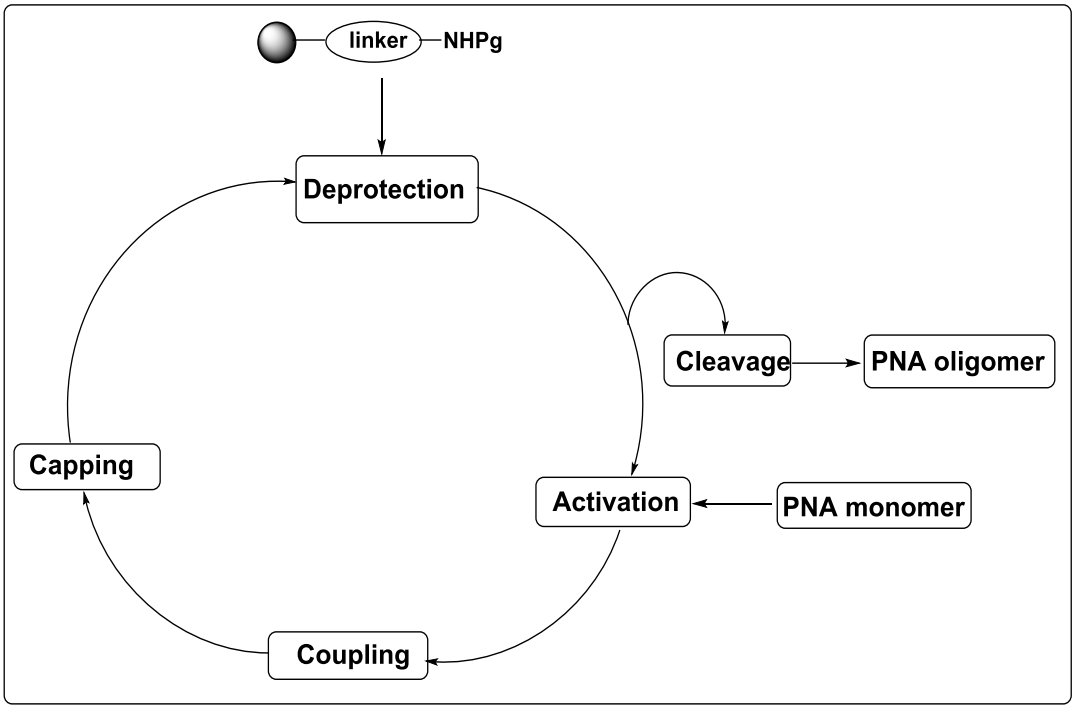

Figure 1.20: General scheme of SPS cycle of PNA oligomers.

Historically, solid phase PNA synthesis was first realised using Boc-protected AEG thymine PNA monomer to give a homothymine sequence.[39] Later, when the acid labile Carboxybenzyl group (Cbz) was employed for protecting the exocyclic amino groups of the bases C, A and G, a new Boc/Cbz strategy was introduced.[77] This strategy quickly became the common protocol for producing mixed purine-pyrimidine PNA oligomers. In this strategy, removal of the *N*-terminal Boc temporary group is carried out by trifluoroacetic acid (TFA), while the orthogonal protecting groups that are used to protect the exocyclic amino function of the nucleobases are removed using trifluoromethanesulfonic acid (TFMSA).

However, the use of TFA in the removal of Boc group can lead to removing the acid labile protecting groups on the exocyclic amino groups on the nucleobase of the growing chains. This deprotection then leads to produce PNA oligomers impurities that are difficult to purify. In the final step, to cleave the PNA oligomer from the solid phase, a strong acid such as hydrogen fluoride (HF) is required. The use of such as strong acids in this process is one of the major drawbacks of this strategy.

To avoid the drawbacks that are associated with the Boc strategy, a milder method was developed and became the most commonly used solid phase PNA synthesis strategy. This approach depends on introducing a base labile fluorenyl methoxycarbonyl group (Fmoc) to protect the primary amino function of PNA monomers. In this strategy, the exocyclic amino function of the nucleobase must be protected with an acid labile protecting group such as Bhoc, Boc and Cbz that are quite stable under Fmoc-deprotection conditions, mostly a solution 20% of piperidine in different solvents such as NMP, DMF, and DCM.

Regardless of the strategy that is used in the solid phase synthesis of PNA oligomers, the carboxyl function of PNA monomers needs an activation. The most commonly used peptide coupling agents for *in situ* PNA monomers' activation are the uronium reagents [78,79] such as HATU **19** and HBTU **20,** and the phosphonium coupling reagents [78,80] such as PyBOP **21** and PyAOP **22** (Figure 1.21). The uronium reagents are less sensitive towards moisture, therefore are more easily handled in solid phase synthesis than the phosphonium reagents. Additionally, The popular carbodiimide condensation reagents such as DCC **23** and DIPCDI **24** (Figure 1.21) also can be used in the solid phase PNA synthesis, mostly in combination with additives such as HOBt and DHBtOH.[80,81]

On the other hand, one major drawback encountered the solid phase PNA synthesis is that the growing PNA oligomers have a tendency for aggregation by folding over upon themselves during the chain elongation. This aggregation can be formed by either intra- or intermolecular interactions thereby leading to a low peptide coupling efficiency. For this reason, PNA oligomers can only be prepared in a limited length of the nucleobases.

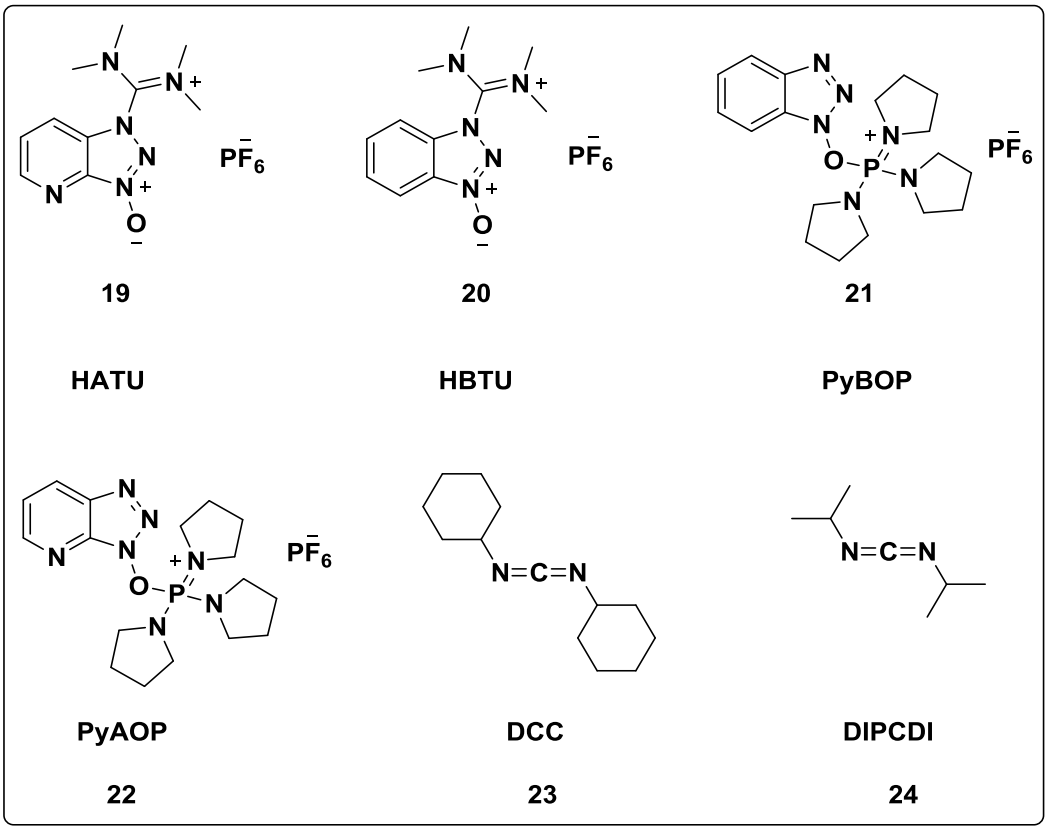

Figure 1.21: The common peptide coupling agents.

1.3.3 Synthesis of PNA monomers

Since PNA's invention, different AEG PNA monomers have been prepared and used in the solid phase PNA synthesis. These monomers differ from each other in the type of orthogonal protecting groups that are used to protect the exocyclic amino function on the nucleobase and the primary amino function of their backbone. Although some PNA monomers are commercially available, they can be synthesised by relatively easy and inexpensive routes.

The key step of the synthesis of PNA monomers such as **27**, involves the coupling of the appropriate nucleobase acetic acid derivative such as **26** to the secondary amine of the protected backbone such as **25**, in the presence of a coupling agent as outlined in Scheme 1.1. The most commonly used coupling agents for synthesis of PNA monomers are the carbodiimides such as DCC **23** and DIPCDI **24** (Figure 1.21), often in the presence of HOBt and DHBtOH.[80]

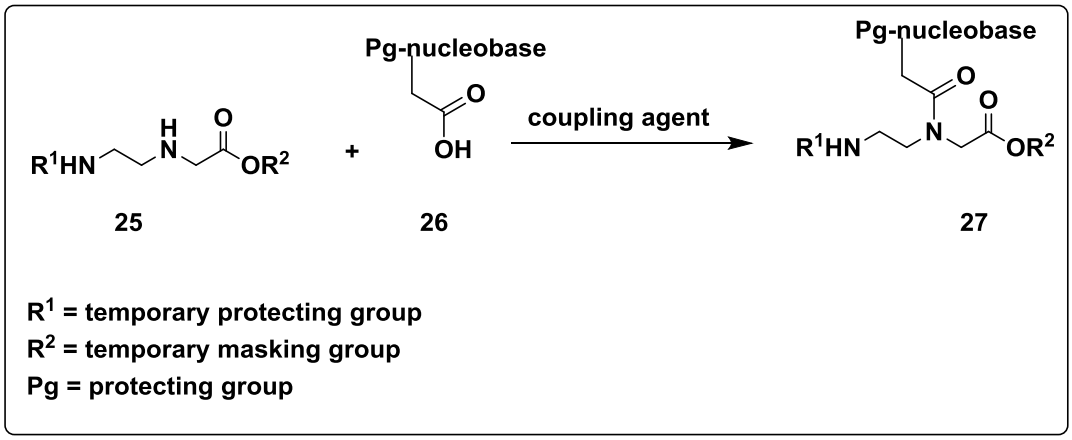

Scheme 1.1: General scheme for the synthesis of AEG PNA monomer.

In some cases, the carboxylic group of the PNA monomer backbone requires a temporary masking group in order to avoid unwanted side reactions such amide bond formation during synthesis of PNA monomers. This masking group will be removed later producing a PNA monomer that is ready for solid phase synthesis procedure.

The AEG PNA monomer backbone is composed of a glycine with a 2-aminoethyl group extension from the amine. There are three efficient retrosynthetic routes have been used routinely for the synthesis of the protected *N*-(2-aminoethyl) glycine PNA monomer backbone, such as **25** as outlined in Scheme 1.2. The most common and inexpensive way is the S_N2 *N*-alkylation of 1,2-diaminoethane (or its mono-protected derivative) **28** with α-haloacetic acid or its esters derivatives **29**. Reductive amination is also a relatively straightforward route for the synthesis of the desired AEG backbone **25**, either using protected amino acetaldehyde **30** with glycine esters **31**[82,83] or compound **28** with glyoxalic acid or its ester derivatives **32**.[84] A few further reaction steps give the desired *N*-protected PNA backbone in a relatively high yield. In order to protect the primary amino function of the AEG PNA monomer backbone, different temporary protecting groups have been used such as Boc,[39,54] Mmt[85] and Fmoc.[86,87] Whereas the secondary amino function of this backbone to which the nucleobase acetic acid derivatives can be coupled, is left free.

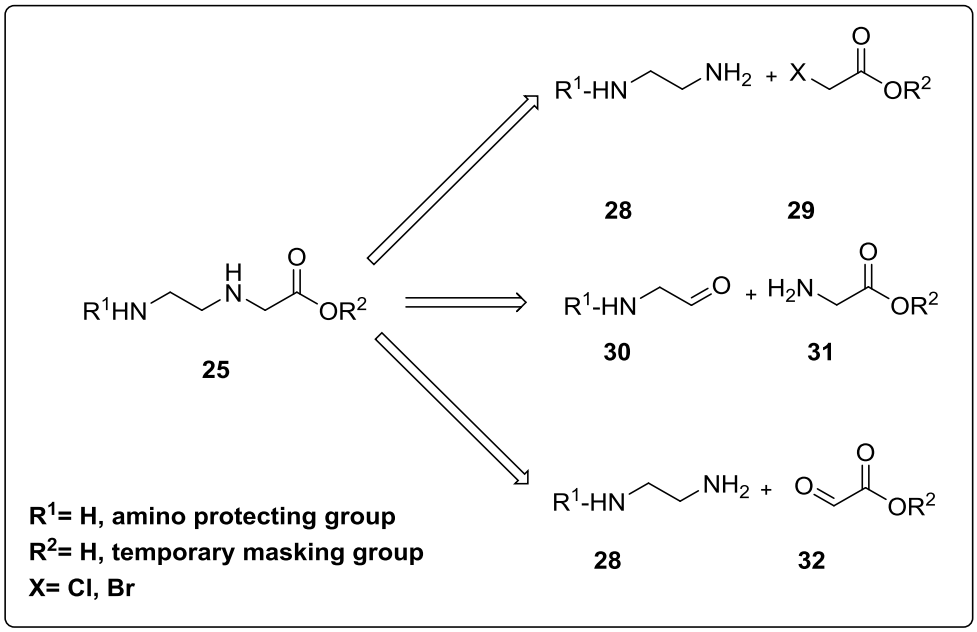

Scheme 1.2: Retrosynthetic analysis of the PNA monomer.

Synthesis of the nucleobase acetic acid derivatives such as **26** involves a selective *N*-alkylation reaction of the pyrimidines or purines bases at N1- and N9-positions, respectively. This is performed using α-haloacetic acid, or its ester derivatives in the presence of different basic reagents such as sodium hydride,[88] and potassium carbonate.[86,89]

In order to avoid undesired reactions such as an amide bond formation during the syntheis of PNA monomers or through the solid phase PNA synthesis, the nucleophilic exocyclic amino functionalities of adenine, cytosine and guanine must be orthogonally protected during the solid phase synthesis. For this purpose, various groups have been reported using a selection of protection groups such as Boc,[90] Bhoc,[91] and Cbz.[86] Futhermore, this protection increases the solubility of PNA monomers in the most common organic solvents.

1.3.5 PNA backbone modifications

Since their invention in 1991,[39] there is an increasing interest in solving the problems that are associated with using the AEG PNA oligomers, such as poor membrane permeability thus limiting its applications for antigene or antisense therapies, low water solubility and self-aggregation. In an attempt to overcome

these drawbacks, many research groups have focused their attention on developing new PNA monomers through backbone and nucleobase modifications.[92] For the work that was performed in this thesis, two series novel PNA monomers consisting of a modified backbone were prepared. We, therefore, present a short overview of PNA monomer backbone modifications in the coming section.

In general, the original *N*-(2-aminoethyl) glycine PNA monomer backbone offers two moieties, namely, 2-aminoethyl and glycine moieties that can be exploited for extension or insertion of a cyclic structure. It also introduces further modification potential at α-, β- and γ-positions that can be used for attachment of a side group (Figure 1.22).

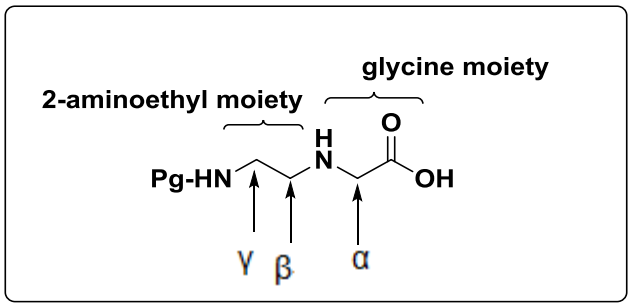

Figure 1.22: The possible sites for modification the PNA monomer backbone.

The earliest attempts to modify the AEG PNA monomers involved extending the original backbone by a methylene group.[93,94] This extra methylene group was introduced into the glycine moiety of AEG PNA monomer backbone by replacing the original *N*-(2-aminoethyl) glycine backbone with *N*-(2-aminoethyl)-β-alanine as outlined in Scheme 1.3. This modification involved hydroamination of methyl acrylate with mono Boc-protected ethylenediamine **33** to produce the extended backbone methyl ester **34** followed by coupling with an acetic acid derivative of thymine. The resultant thymine PNA monomer methyl ester **35** was then hydrolysed to obtain the target thymine PNA monomer **36** (Scheme 1.3).

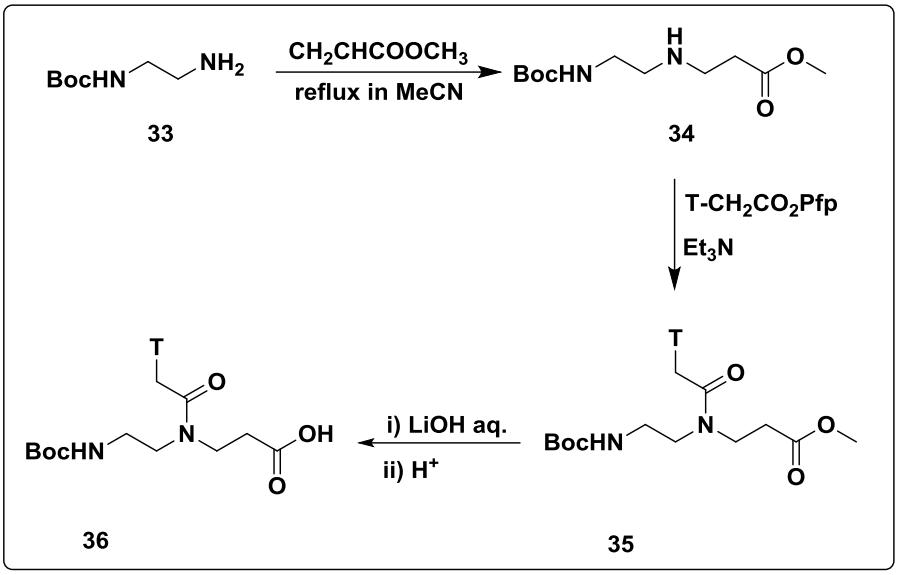

Scheme 1.3: Synthesis of an extended thymine PNA monomer at glycine moiety.

To further investigate the extension effect, the extra methylene group was also introduced into the 2-aminoethyl moiety of the original *N*-(2-aminoethyl) glycine PNA monomer backbone.[93,94] This modifcation was achieved by using 1,3-diaminopropane rather than 1,2-diaminoethane as outlined in Scheme 1.4. Thus, the 1,3-diaminopropane **37** was alkylated with chloroacetic acid, followed by esterification with methanol to give the precursor backbone **38**. The priamry amino group of **38** was then protected with a Boc group by using *tert*-butyl 4-nitrophenyl carbonate. This protected modified backbone **39** was then coupled to thymin-1-yl acetic acid using DCC as a coupling agent in the presence of DHBtOH. A final hydrolysis reaction of the methyl masking group yields the target extended thymine PNA monomer **40** (Scheme 1.4).

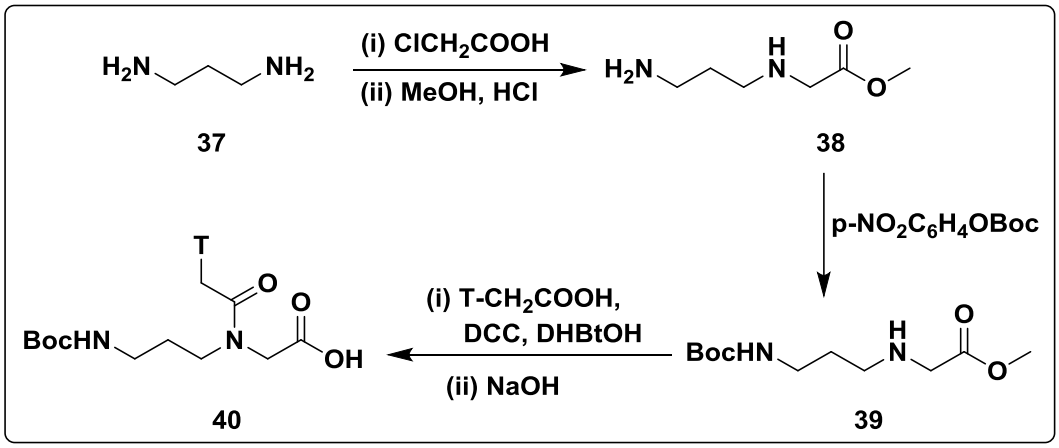

Scheme 1.4: Synthesis of an extended thymine PNA monomer at 2-aminoethyl moiety.

In order to investigate the effect of these extensions on the properties of PNA oligomers, a single monomeric of the extended PNA monomers **36** and **40**, was incorporated into homo-thymine PNA oligomers during oligomerization following the Boc-solid phase synthesis procedure. Biophysical studies showed that the target homopyrimidine PNA oligomers resulted in a lowering of PNA binding affinity towards DNA with significantly reduced melting points (T_m) of PNA/DNA duplexes compare to those derived from unmodified PNA.[94]

In order to enhance the rigidity of the PNA structure, PNA monomers with a modified constrained, chiral, cyclic backbone were synthesised. This modification was done through the incorporation of a cyclic structure such as cyclopentyl [95,96] or cyclohexyl [97,98] into the 2-aminoethyl moiety of the original AEG backbone. Thus, inspired by the general synthetic route that is used in the synthesis of the original AEG PNA monomer backbone, Boc-protected 1,2-diamino cyclopentyl **41** or cyclohexyl **42** was *N*-alkylated with ethyl bromoacetate to produce the modified backbones **43** and **44**, respectively. These modified backbones were then coupled to thymin-1-yl acetic acid, followed by hydrolysis under basic conditions to afford the corresponding thymine PNA monomers **47** and **48** (Scheme 1.5).

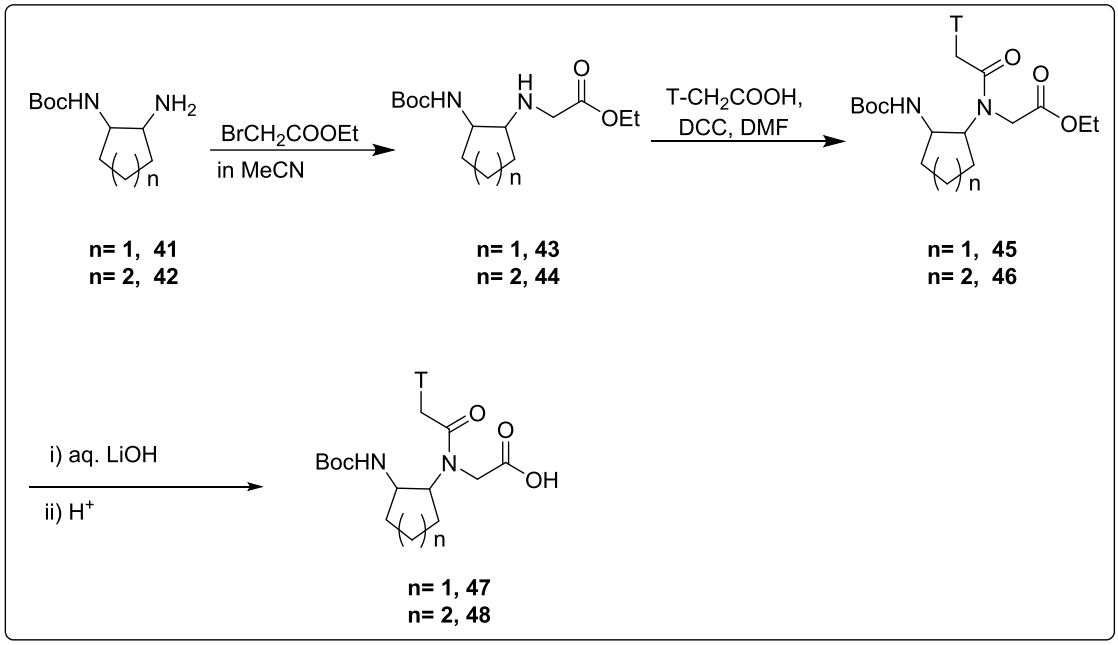

Scheme 1.5: Synthesis of PNA monomers containing a cyclic structure.

To investigate the effect of this type of modification on the PNA properties, a single monomeric unit of **47** and **48** was incorporated into AEG PNA oligomers during Boc-solid phase synthesis strategy. Thermodynamic studies showed that the modified PNA oligomer that is containing of cyclopentyl monomer **47** displayed an improved binding affinity toward DNA with higher thermal stability the corresponding PNA/DNA duplex than the unmodified PNA/DNA duplex. In contrast, the (R, R) isomer of **48** resulted in a drastic decrease in the thermal stability of the corresponding PNA/DNA or PNA/RNA complexes. The PNA oligomers with (S, S) orientated residues, however, were able to bind to complementary sequences of DNA or RNA with a little effect on the thermal stability depending on their number in the PNA sequence.

For more investigations, a fully modified backbone containing a heterocyclic constrained unit was introduced rather than the original AEG PNA monomer backbone as outlined in Scheme 1.6.[99,100] This modified backbone was prepared via condensation of *N*-Boc-glycine aldehyde **49** with L-cysteine methyl ester to give the target backbone in a mixture of *anti* and *syn*-isomer of 2-(Boc-aminomethyl) thiazolidine-4-carboxylic methyl ester **50**. Both isomers were coupled to the

thymine nucleobase via a methylene carbonyl linkage through two steps to produce the intermediates compounds **51** and **52**. Finally, a hydrolysis reaction with an aqueous solution of LiOH afforded the modified thymine PNA monomers *anti* **53** and *syn* **54** (Scheme 1.6).

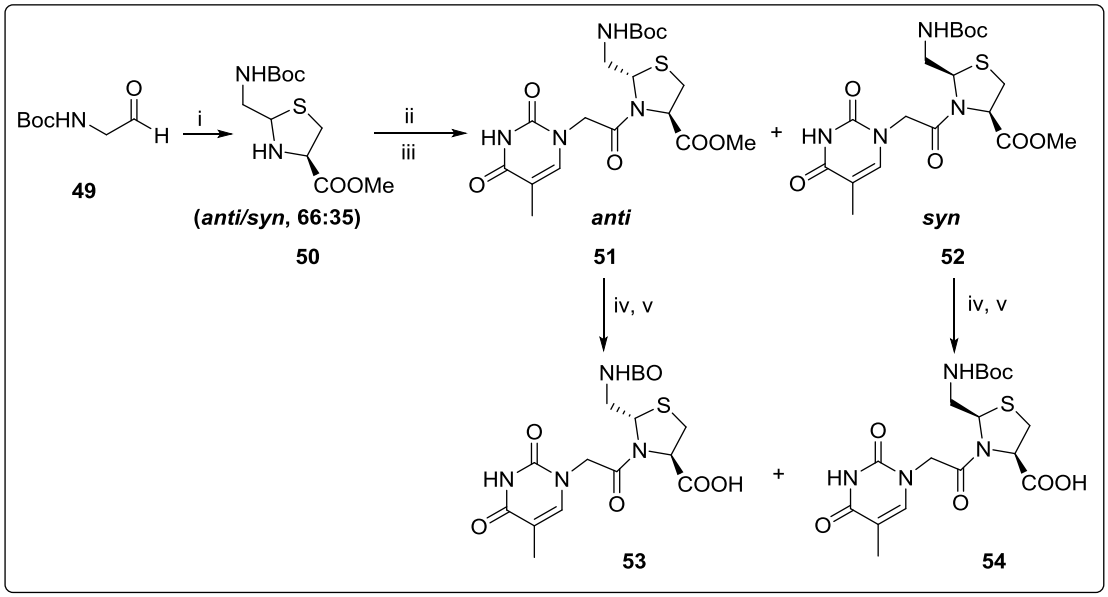

Scheme 1.6: Synthesis of constrained PNA monomer: i) Cys-OMe, pyridine, MeOH; ii) $ClCH_2COCl$, pyridine, CH_2Cl_2, -78 °C; iii) thymine, K_2CO_3, DMF; iv) LiOH, H_2O/dioxane, v) $KHSO_4$.

To investigate the effect of these modifications on the properties of PNA oligomers, a single monomeric unit of heterocyclic constrained thymine PNA monomers **53** and **54**, was inserted into the middle of a 10-mer homothymine AEG PNA oligomer. UV melting experiments showed that the incorporation of these modified PNA monomers does not prevent the binding of the PNA with DNA but does however significantly decrease the stability of PNA/DNA and PNA/RNA triplexes relative to the corresponding unmodified PNA.

A particularly interesting modification to improving the binding affinity, water solubility and cellular uptake of PNA oligomers involves the introduction of a stereogenic centre at the α-, β- and γ-positions of the the AEG PNA monomer backbone (Figure 1.22). Most commonly this is accomplished via the introduction of side chains belonging to proteinogenic amino acids. The most investigated class is

the α-chiral PNA backbone that is prepared by replacing the glycine moiety with an L- or D-chiral amino acid such as alanine, lysine, serine, glutamic acid, aspartic acid, isoleucine and arginine through an analogous synthetic route to that used for the synthesis of AEG PNA monomers.[101,102] The α-chiral thymine PNA monomers such as **58** were the first chiral PNA monomer and were introduced by Nielsen *et al*. in 1994.[101] This modified α-chiral thymine PNA monomer **58** was prepared by saponification reaction of the corresponding ester derivative **57** that was prepared via coupling of thymin-1-yl acetic acid to the precursor for the α-chiral PNA monomer backbone **56**. This precursor backbone **56** was prepared via reductive amination of alanine methyl ester **55** and Boc-amino acetaldehyde **49** as outlined in Scheme 1.7.

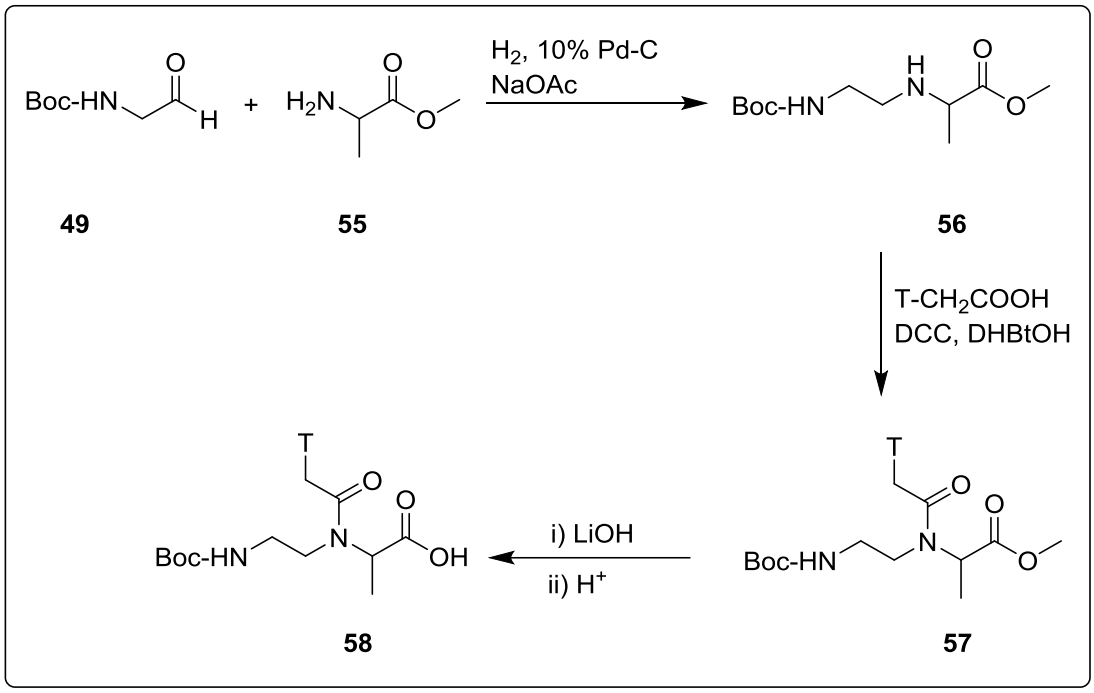

Scheme 1.7: Synthesis of α-chiral PNA monomer.

In general, biophysical studies of PNA/DNA duplexes showed that PNA oligomers carrying the α-chiral PNA monomers, derived from a D-amino acid, have a higher affinity towards complementary DNA than the corresponding L-monomers.[102] Besides that, the PNA/DNA duplexes containing the D-form retained similar thermal stability to the corresponding unmodified duplexes. Whereas the incorporation of L-

form monomers displayed reduced stability. Also, it was found that incorporation of α-chiral thymine monomers that were derived from negatively charged amino acids such as D-glutamic and L-aspartic acids into PNA oligomers such as H-GTxAGATxCACTx-NH_2 reduced the melting temperatures (T_m) of PNA/DNA complexes compared to the unmodified PNA/DNA duplex.[102]

Interestingly, the introduction of a chiral centre at the β-position is expected to influence the conformation and the binding properties of PNA toward DNA because this position corresponds to the C4 of the deoxyribose moiety of the DNA which is a chiral carbon. Although cyclic PNA monomers containing a chiral centre at the β-position of their backbone were reported early, the first modified PNA backbone with a single substituent at the β-position of the original PNA backbone was reported by Sugiyama *et al.* in 2011.[103] This β-modified backbone was prepared by using 1,2-diaminopropane in both S and R forms instead of 1,2-diaminoethane that is commonly used for the synthesis of the original PNA monomer backbone as outlined in Scheme 1.8.

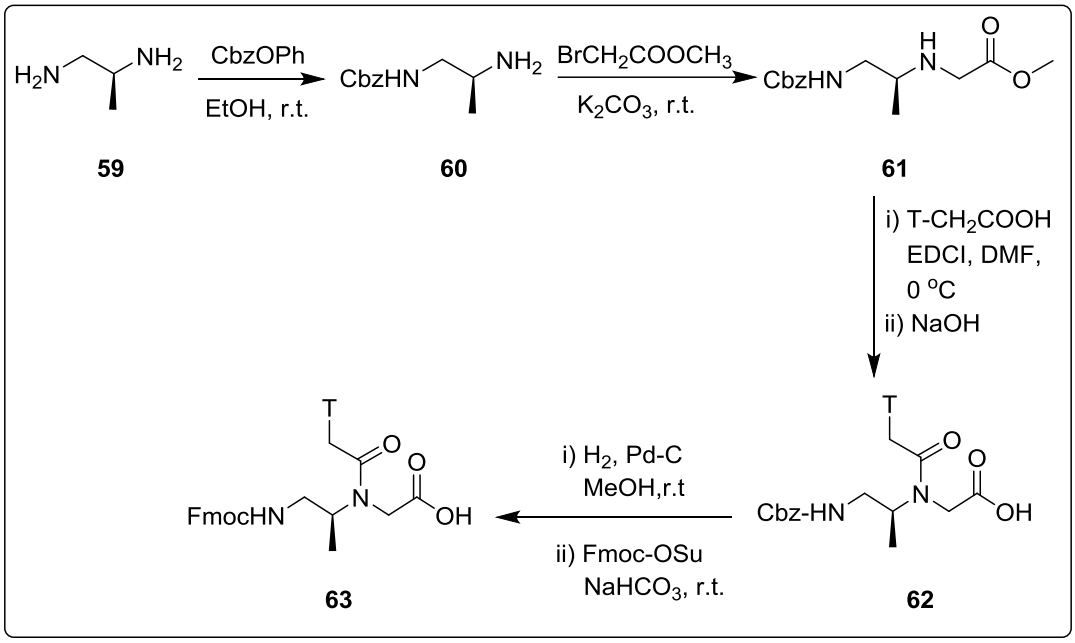

Scheme 1.8: Synthesis of β-chiral thymine PNA monomer.

Thus, 1,2-diaminopropane **59** was selectively mono-protected on the amino group located at C1 with Cbz group using CbzOPh. The resulting intermediate compound

60 was then *N*-alkylated with methyl bromoacetate to produce a β-chiral modified PNA backbone methyl ester **61.** This precursor Cbz-protected PNA monomer backbone methyl ester **61** was then coupled to thymin-1-yl acetic acid followed by hydrolysis reaction under basic conditions to yield a Cbz-protected β-chiral thymine PNA monomer **62**. In the final reaction, the temporary protecting group (Cbz) was replaced with the Fmoc group to obtain Fmoc-protected β-chiral thymine PNA monomer **63** that is ready for solid phase PNA synthesis (Scheme 1.8).

Thermodynamic studies showed that incorporation of the S form of the β-chiral thymine PNA monomer into the PNA oligomers retained the binding affinity and thermal stability of the PNA/DNA duplexes, whereas the incorporation of the R form prevents the formation of PNA/DNA duplex.

Among all the PNA monomer backbone modifications, the introduction of a chiral centre at the γ-position is the most promising one to improve properties of PNA oligomers such as water solubility, binding affinity and thermal stability of PNA/DNA duplexes compared to unmodifed PNA.[104,105] The crystal structure studies of a γ-PNA/DNA duplex illustrates the unique characteristics of this modification, possessing conformational flexibility of PNA oligomers with maintaining sufficient structural integrity of the preferred conformation upon hybridization with single-stranded DNA. Furthermore, the γ-PNA/DNA duplex is induced by the steric clash between and the nitrogen of the tertiary amide of the backbone and its γ-carbon and is stabilized by the sequential base stacking.[106]

Although the γ-modified PNA monomer backbone can be prepared by reductive amination of the Boc-protected amino acetaldehyde with glycine ester derivatives, it can be prepared alterantive way such as Mitsunobu-Fukuyama reaction.[107,92] As an example for the introduction a guanidinium group at γ-position of the original PNA monomer backbone, Boc-protected lysine (guanidine-di-Cbz)-OH acid **49** was first reduced to its alcoholic derivative **65**, followed by coupling with ethyl 2-(2,4-dinitrophenylsulfonamido) acetate to give the intermediated compound **66**. To make the secondary amino function of the target backbone **67** is free, to which the nucleobase acetic acid derivatives can be coupled, the 2,4-dinitrophenylsulfonate protecting group of **66** was removed using a mild base**.** This modified backbone **67**

was then coupled to an appropriate nucleobase acetic acid to give the intermediate a chiral γ-PNA monomer ethyl ester such as **68**. A saponification reaction of **68** yielded the corresponding Boc-protected γ-chiral PNA monomer such as **69** as outlined in Scheme 1.9.

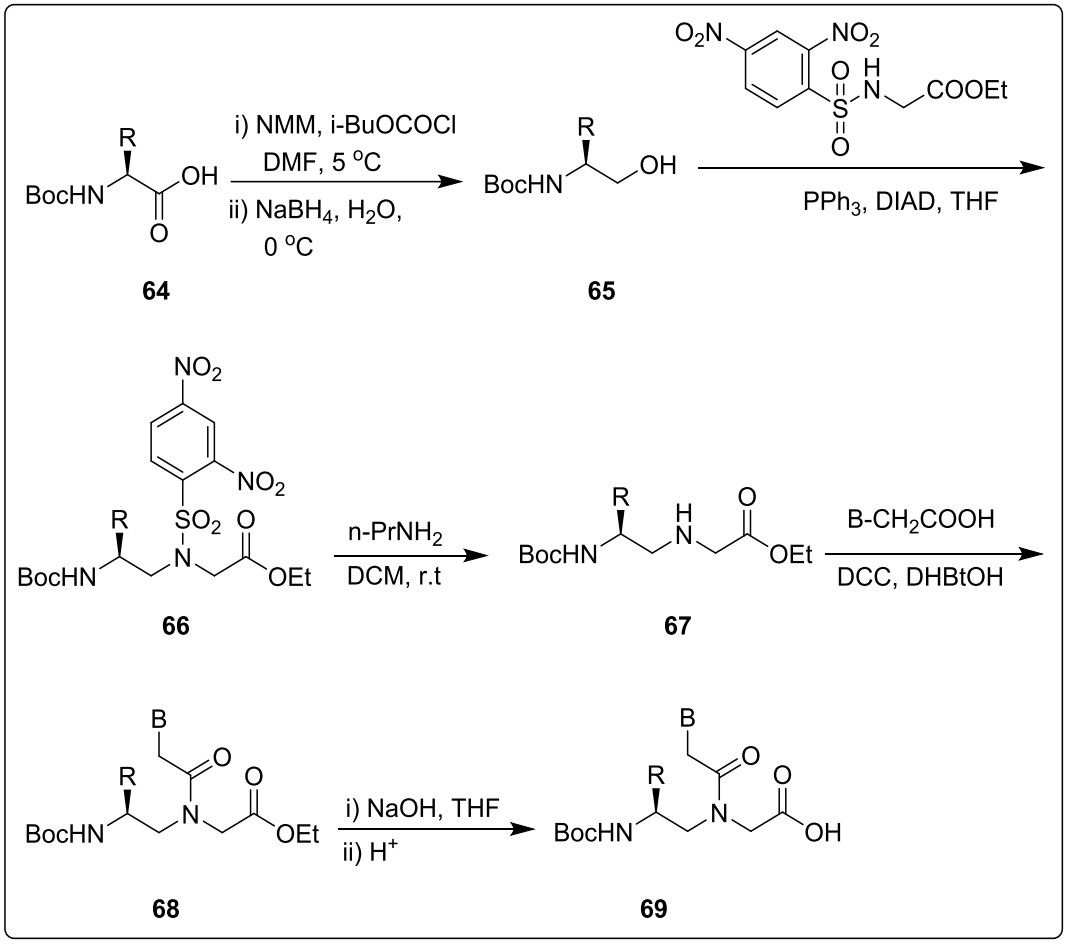

Scheme 1.9: Synthesis of γ-chiral PNA monomers, R: $(CH_2)_4NHC(NHCbz)(NCbz)$, B= nucleobase

Thermodynamic studies showed that the incorporation of a single monomeric unit of γ-guanidine-modified PNA monomer into PNA sequences displayed a higher affinity for complementary DNA and RNA sequences than α-guanidine PNA oligomers.

1.3.7 Ligation of PNA oligomers

Peptide Nucleic Acid (PNA) is mimicking the behaviour of nucleic acids and bind to

complementary sequences of DNA or RNA with much higher affinity and greater recognition specificity. Due to these unique properties, PNA have been exploited to produce an attractive tool for gene targeting applications.[108] In particular, when human natural oligonucleotide segments are targeted, usually oligonucleotides probes forming more than 16 base pairs are required to target a unique sequence.[109] For example, PNA oligomers that are 18-20 nucleobases in length, however, have been used to monitor telomere dynamics,[110] or to inhibit human telomerase.[111] Unfortunately, SPPS has one major disadvantage which is the length limitation. Thus, the synthesis of PNA oligomers longer than 16 nucleobases by SPPS resulted in poor results.[112] This length limitation can be attributed to that the growing PNA oligomers chains can be aggregated by formation of either intra- or intermolecular interactions thereby leading to low coupling efficiencies. Therefore, a different technique using ligation is considered as a promising route for the synthesis of the extended PNA sequences that are difficult to prepare by the standard solid phase methods. Native chemical ligation (NCL) has been developed for ligation of PNA with PNA or conjugation with DNA or peptide. Native chemical ligation allows the combination of two unprotected PNA segments by the reaction between the thiol group of the *N*-terminal cysteine of one PNA oligomers and the *C*-terminal thioester of another PNA oligomer yielding modified PNA sequences.[113-117] However, the efficient synthesis of *C*-terminal thioester PNA oligomers and the ability of a thiol group of cysteine at *N*-terminus to be oxidized to react with another thiol group making a disulfide causing a distorting in the PNA backbone remain limitations to use NCL as a ligation method for PNA sequences.

The advent of the copper (I) catalysed azide-alkyne 1,3-dipolar cycloadditions (CuAAC) known as 'click chemistry' has provided a simple method to link together organic molecules generating 1,2,3-triazole products. This is can be achieved in high yields under mild conditions, and, in the presence of a diverse range of functional groups.[118-120] Furthermore, the azide and alkyne functional groups are mostly inert towards other functional groups i.e. they react only with each other. Moreover, the formed 1,2,3-triazole moiety is of particularly high interest, especially in the area of biological applications, as it has been found to mimic amide bonds and is nearly

impossible to oxidize or reduce and is not toxic.[121] Because of these unique features, it is interesting to consider the use of this click chemistry (CuAAC) in ligation of PNA oligomers via 1,2,3-triazole formation as a linkage.

1.4 CuAAC 'click' reaction: 1,2,3-triazole formation

1.4.1 Historical background

The formation of di-substituted triazole derivatives was first reported in 1893 by Arthur Michael as mentioned in the literature.[122] However, the full synthetic study on the nature of this reaction was reported in 1961 by Rolf Huisgen, and determined to be a 1,3-dipolar cycloaddition reaction between the alkyne and azide functions.[123] This study was revealed that this reaction is relatively slow, but could be achieved at high temperatures to give a reasonable yield, however with lack a regioselectivity and generate a mixture of 1,4- and 1,5-disubstituted triazoles (Scheme 1.10).

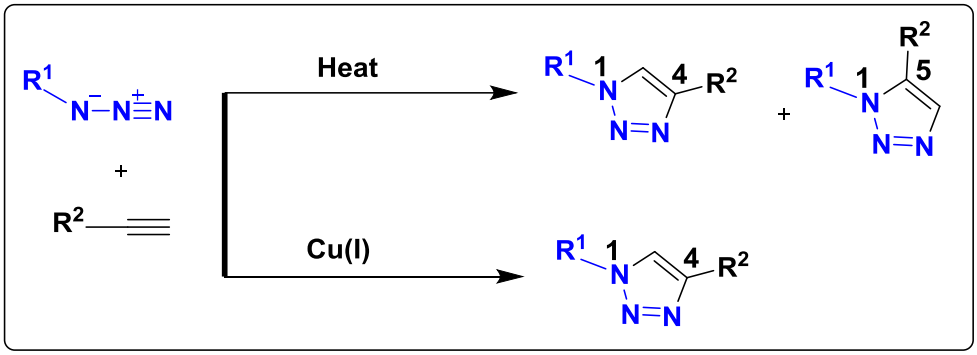

Scheme 1.10: Azide–alkyne 1,3-dipolar cycloaddition reactions.

In 1984, G. Labbe used copper as a catalyst for the synthesis of azidoallene complex and observed a Huisgen azide-alkyne 1,3-dipolar cycloaddition as a side reaction.[124] However, this observation was left without any further investigations until 2001, when a renewed interest in 1,3-dipolar cycloaddition sparked a report by Sharpless and his co-worker when they published a seminal paper to introduce a new strategy for organic synthesis.[118] They defined the term ''click chemistry'' and described the concept as being modular, broad in scope, giving high yields, generating only safe

by-products, stereospecific, and simple to perform. In 2002, the copper (I) species was reported as a catalyst for azide-alkyne cycloaddition independently by two groups: Sharpless in the US [119] and Meldal in Denmark.[120] Both observed that this reaction exclusively gives the 1,4-disubstituted 1,2,3-triazole in high yield. Furthermore, CuAAC copper catalysed reaction can be described as a fast reaction, requiring low temperature, and can be used to covalently attach any fragment containing azide functionality to terminal alkynes, without being affected by the steric or electronics of the substrates.

The generally accepted mechanism of the CuAAC reaction is shown in Figure 1.23. In this mechanism, the copper catalyzed azide-alkyne 1,3-dipolar cycloaddition (CuAAC) proceeds through the coordination between Cu(I) and the terminal alkyne to form an active copper acetylide such as (**A**). This intermediate in turn reacts with the azide component to generate the copper acetylide-azide complex (**B**).

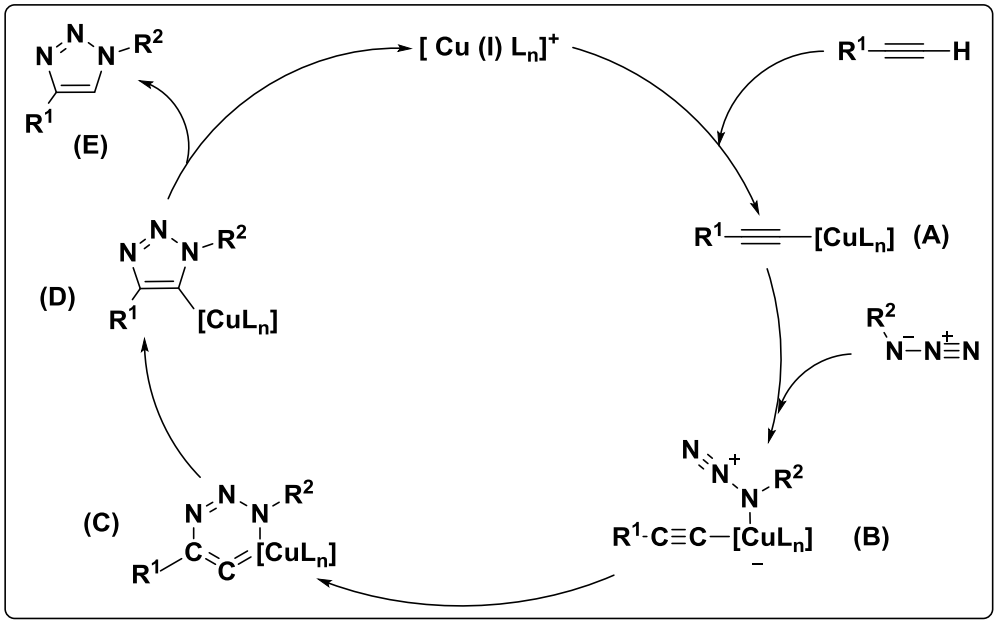

Figure 1.23: A general mechanism of Cu (I) catalysed azide-alkyne reaction.[125] L stands for a ligand or a counter ion. The brackets around ''CuL_n'' symbolize that a bi or polynuclear Cu (I) species is involved in the reaction.

This complex (**B**) then cyclises to form a metallocycle intermediates such as (**C**), following by a rearrangement to form a cyclic compound such as (**D**). Finally, after protonation and dissociation, the reaction ends to produce the final products (**E**) regenerating the Cu (I) catalyst.

The conventional sources of Cu (I) that can be used in this type of Cu (I)-catalyzed reaction are copper (I) iodide and copper (I) acetate. Furthermore, it was found that Cu (I) can be produced *in situ* from a Cu (II) salt, and the most common used is copper sulphate ($CuSO_4$) in the presence of sodium ascorbate as a reducing agent.[126] Although the standard CuAAC reaction solvent is *tert*-BuOH:H_2O (1:1), it can be carried out in other solvents such as DMF, NMP, H_2O, *tert*-BuOH, DMSO, $CHCl_3$, MeOH, and DCM.[126] In a subsequent investigation of the click reaction, it was found that the addition of some heterocyclic chelates could further accelerate CuAAC, and could largely decrease the amount of Cu (I) that is required which is very important in biological systems. For example, the stabilizing ligand tris-(benzyltriazolylmethyl) amine (TBTA) developed in the Sharpless group can protect Cu (I) from oxidation and disproportionation. As a result, the catalytic efficiency was accelerated by 106 fold.[127]

1.4.2 1,2,3-Triazole ring as a bioisostere

Since the copper (I) catalysed azide-alkyne 1,3-dipolar cycloaddition has made the preparation of the 1,2,3-triazole ring relatively easy, it is important to establish the bioisosteric potential of this moiety. The important concept was that the triazole group displays a structural similarity with the amide bond, mimicking a *Z* or an *E*-form depending on its substitution pattern. The 1,4-disubstituted triazole moiety shows similarity with a *Z*-amide bond; where the lone pair of the N3 mimics one of lone pairs of the carbonyl oxygen of the amide bond and the polarized C (5)-H bond can act as a hydrogen bond donor like the amide N–H bond. The electrophilic and polarized C4 is electronically like the amide carbonyl carbon. Since the overall dipole moment of the triazole system is larger than that of the amide bond, its hydrogen bonding donor and acceptor properties are more marked than those of an amide bond, with an enhanced ability to mimic peptide.[128,129]

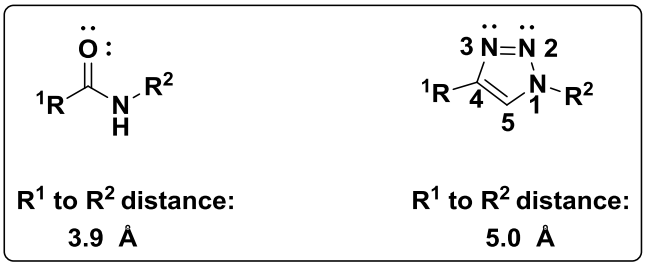

Figure 1.24: Hypothesis of triazoles as a bioisostere of amides bond.

Comparing the structure of a 1,2,3-triazole and an amide bond, some differences are present. For instance, the extra atom C5 in the triazole moiety leads to an increase in the distance between R^1 and R^2 by about 1.1 Å over the typical amide bond. Besides the potential of triazoles in mimicking the amide of the peptide bond, it has also been expected that triazoles might act as bioisosteres of the acyl-phosphate and trans-olefinic moieties.

1.4.3 Applications of 'Click Chemistry' in the field of PNA

The copper (I) catalysed azide-alkyne 1,3-dipolar cycloaddition reaction known as the 'click reaction' has been become an established tool used for synthesis and developed for use with PNA. Thus, it is employed to conjugate PNA with DNA, to label PNA with certain groups such as fluorescent dyes and to ligate fragments of PNA.

As an application of Cu (I) catalysed azide-alkyne cycloaddition reaction in the field of PNA, a DNA-templated, highly efficient and convenient method was developed by Xiaohua Peng *et al.* for the conjugation of PNA-DNA such as **73** via 1,2,3-triazole formation as a linker.[130] The click reaction (CuAAC) was achieved between an alkyne functionalized PNA sequence such as **70** and an azide functionalised DNA sequence such as **71** using a DNA template such as **72**. This reaction was performed in the presence of a water-soluble tris(3-hydroxypropyltriazolylmethyl) amine (THPTA) ligand to prevent DNA template degradation as outlined in Scheme 1.11.

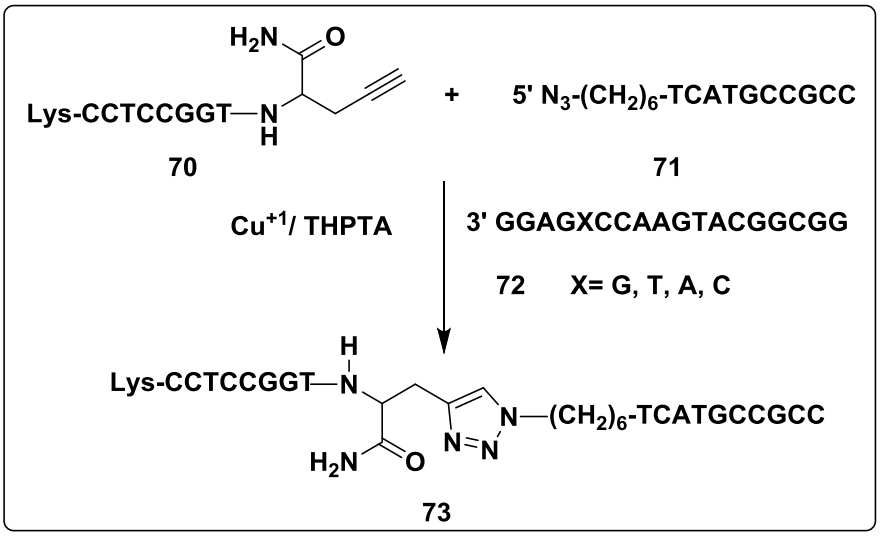

Scheme 1.11: Conjugation of PNA with DNA by click reaction.

Further investigations of this application showed that the efficiency of click conjugation of PNA sequence with DNA sequence depends on the duplex formation between the oligonucleotide starting materials and the DNA template. It was observed that a small yield of the click conjugation product was obtained with mismatched templates.

For click (CuAAC) ligation of PNA-PNA, according to our knowledge, only one study has been reported describing a copper (I) catalysed azide-alkyne cycloaddition so far. As an useful application, Winssinger *et al*. were successful in ligation of two PNA oligomers via 1,2,3-triazole formation as a linkage by click chemistry.[131] This study indicated that an azido functionalised PNA oligomer such as **74** and an alkyne functionalised PNA oligomer such as **75** were ligated together to give the ligation product **77** in an excellent yield using a complementary sequence of DNA as a template **76**. The same conditions that described above for conjugation PNA with DNA were employed for ligation these PNA oligomers as outlined in Scheme 1.12.

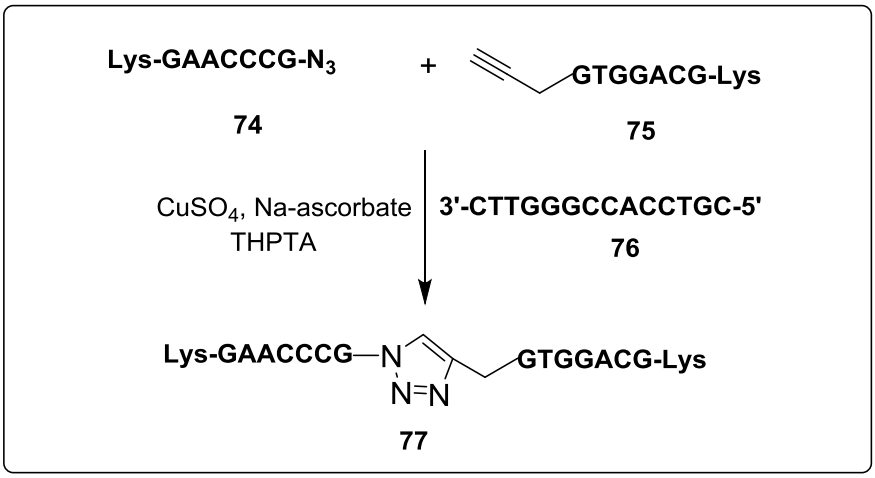

Scheme 1.12: Ligation of PNA-PNA sequence by CuAAC reaction.

Further investigations of this type of application revealed that the click ligation which was performed using an azido component with a single base pair mismatch also afforded the ligation product, however in a lower yield. In addition, no significant reaction yield was observed if the azide component was not complementary to the DNA template. These results are demonstrating the fact that the starting materials alkynoic and azide PNA oligomers must be bound to the DNA template for the click ligation to proceed successfully.

On the other hand, an efficient common strategy to insert the 1,2,3-triazole moiety, into the structure of PNA oligomers, is based on performing the copper (I) catalysed azide-alkyne cycloaddition reaction on the solid support, termed CuAAC-SP.[120,132,133]

As an application for CuAAC-SP in the field of PNA, a new strategy was devised for the synthesis of modified PNA oligomers in which the amide link in their backbone is replaced partially or fully by 1,2,3-triazole ring.[134] This approach involves first synthesising a modified alkyne functionalized PNA monomer, such as **80**, as an alkyne component for the click reaction. Synthesis of this monomer involved S_N2 *N*-alkylation of mono Boc-protected ethylenediamine **33** with propargyl bromide to give a modified PNA monomer backbone **78**. This modified backbone **78** was then reacted with α-chloroacetyl chloride to give the intermediate **79** that was coupled into the thymine nucleobase to afford the target PNA monomer **80** as outlined in Scheme 1.13.

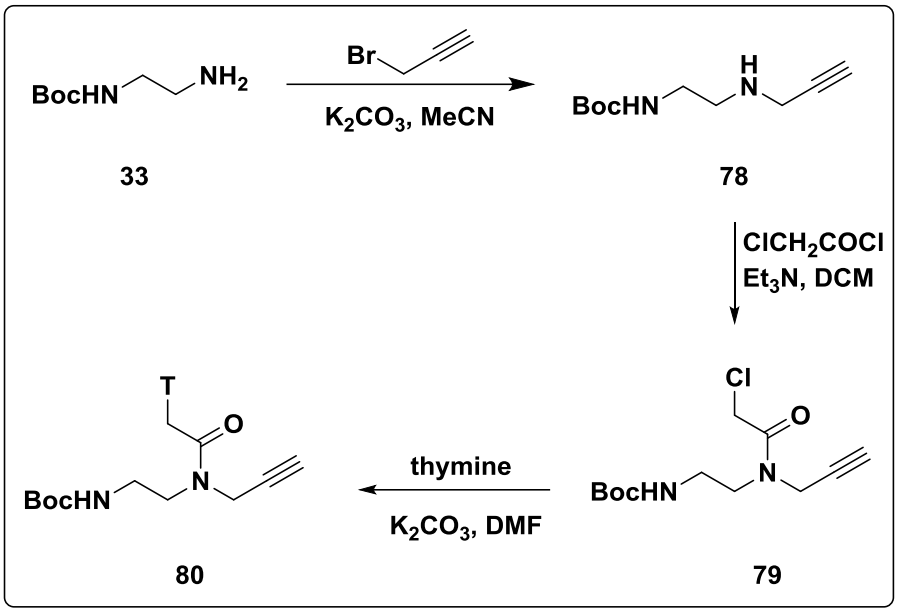

Scheme 1.13: Synthesis of Boc-protected modified thymine PNA monomer.

For performing the click chemistry on the solid support, the commercially available Boc-protected AEG thymine PNA monomer was first coupled into the solid support to give the growing PNA chains such as **81**, followed by Boc-deprotection using TFA. Unlike the solid phase peptide synthesis procedure, the resulted unprotected *N*-terminus was converted *in situ* into an azido group via an azido transfer protocol using triflyl azide (TfN_3) and copper sulfate,[135] generating azido functionalised growing PNA chains such as **82**. The alkynoic thymine PNA monomer **80** was then coupled into these growing PNA chains via a click reaction using copper (I) iodide in the presence of DIPEA introducing the 1,2,3-triazole moiety into the growing PNA chain **83** as a linker instead of the amide bond formation as outlined in Scheme 1.14. This click reaction step can be repeated at the desired position until the required sequence is formed.

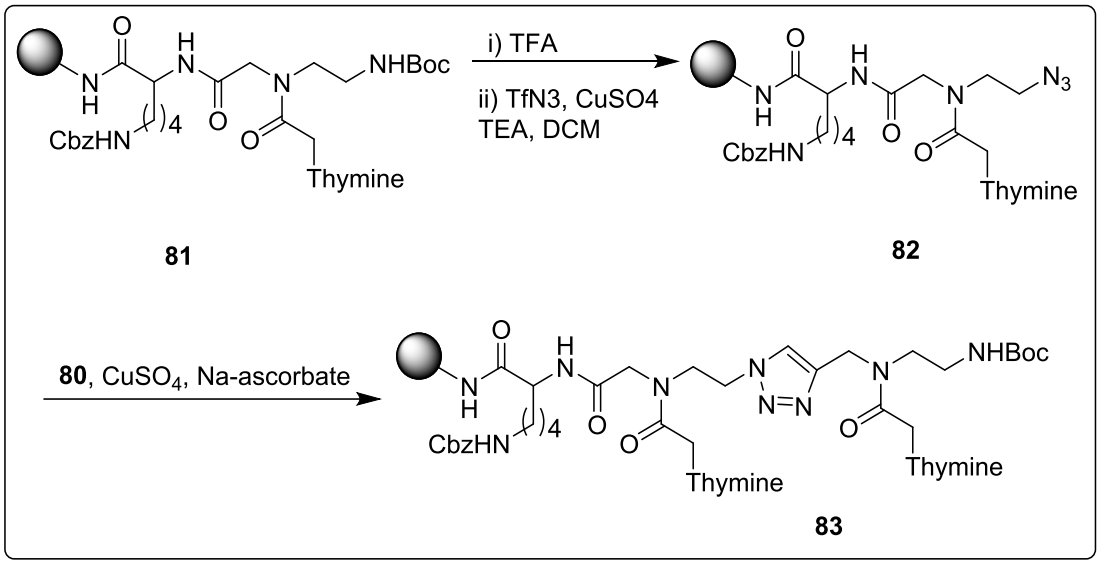

Scheme 1.14: Synthesis of PNA oligomers bearing a 1,2,3-triazole ring.

The hybridization of different triazolyl PNA oligomers with complementary DNA was studied by temperature-dependent UV absorbance measurements. UV-T_m studies showed an improved stability for the PNA2/DNA triplexes that derived from the modified triazole functionalised PNA oligomers than the corresponding unmodified triplexes.

The scope of the CuAAC-SP strategy was explored as a key for the applications of PNA as electrochemical biosensors that are used to discriminate, and therefore detect, single-base mismatches DNA and RNA.[136,137] For example, in order to achieve this goal, a facile method to covalently conjugate a metal complex such as ferrocene to a PNA strand is needed. Thus, for the conjugation of PNA oligomers with ferrocene derivatives via click reaction,[138] the alkyne and azide functions were first introduced at the *N*-terminus of PNA oligomers, such as **85** and **86** respectively. Synthesis of these precursors was achieved by coupling of propynoic acid and azido acetic acid into a growing PNA chain **84** during solid phase PNA synthesis. The click reaction of these precursors **85** and **86** with azido ferrocene and ethynyl ferrocene produced ferrocene labelled PNA oligomers **87** and **88**, respectively as outlined in Scheme 1.15.

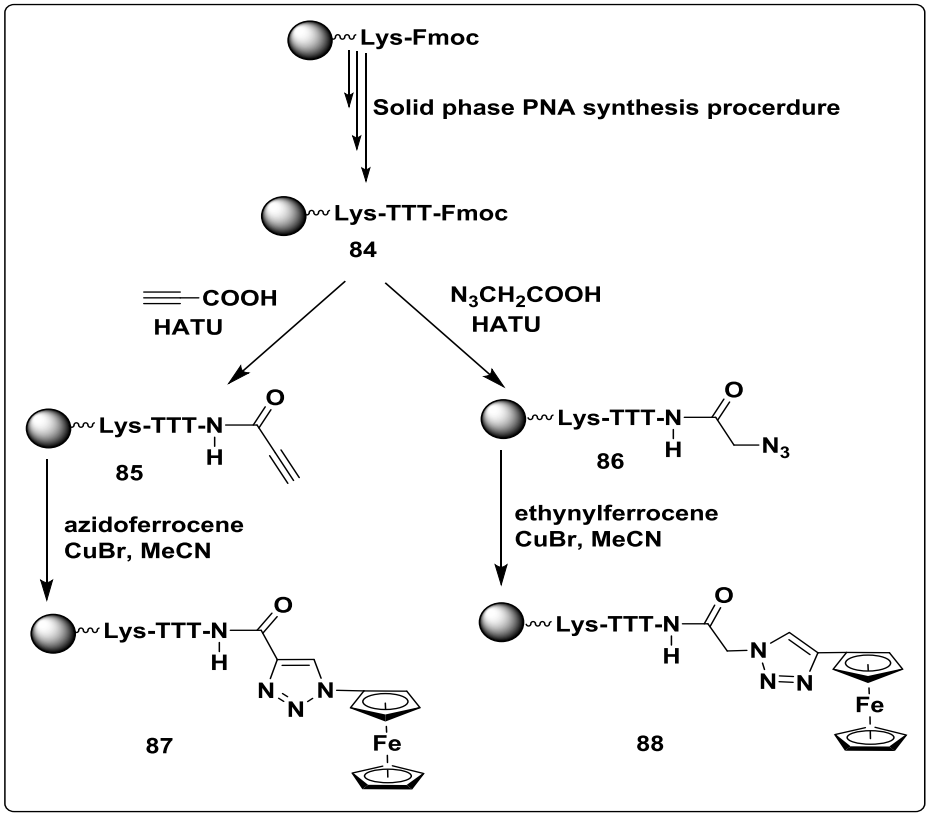

Scheme 1.15: Synthesis of Fc-PNA trimer conjugates.

In another important application of the click (CuAAC) in the PNA field, the CuAAC-SP was used for the synthesis of PNA oligomers containing nucleobase surrogates.[139] In this application, a azide functionalized building block **91** was prepared through coupling of 2-azido acetic acid to the Fmoc protected AEG PNA backbone allyl ester derivative **89** to form the intermediate **90**. The ally temporary masking group of **90** was removed by treatment with $Pd(PPh_3)_4$ in NMM to give the target building block **91** that is ready for solid phase PNA synthesis as outlined in Scheme 1.16.

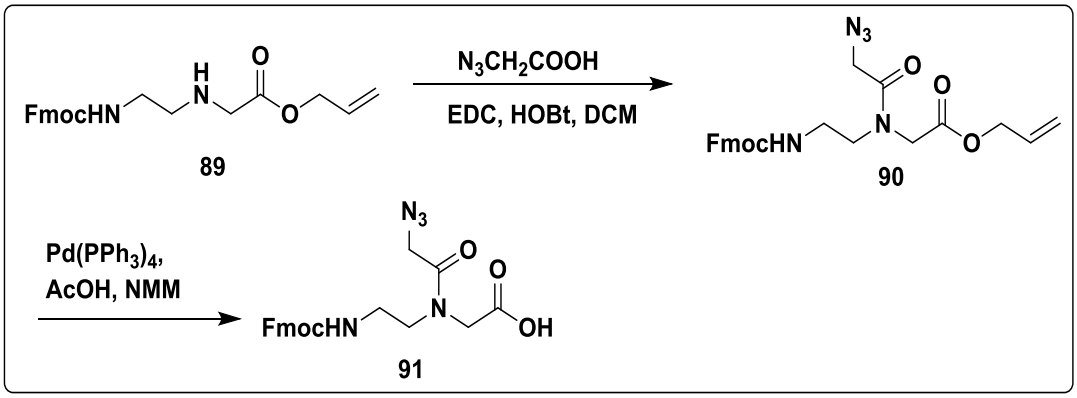

Scheme 1.16: Synthesis of azide-containing PNA monomer **91**.

The modified PNA monomer **91** was incorporated into a 7-mer sequence of PNA during solid phase synthesis. The resin-bound PNA chain with an internal azide residue **92** was then reacted with 2-ethynylfluorene and 1-ethynylpyrene to produce PNA-F **93** and PNA-P **94**, respectively as outlined in Scheme 1.17.

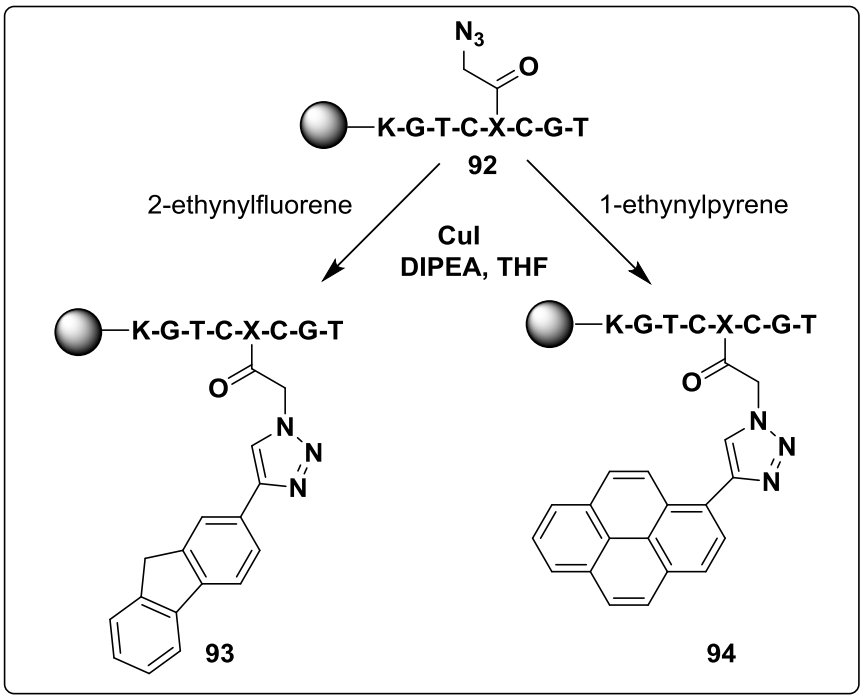

Scheme 1.17: Synthesis of PNA oligomers containing nucleobase surrogates.

For study the effect of this application on the hybridization properties of PNA oligomers, UV-thermal melt analysis of duplexes that were derived from the 7-mers containing PNA-F **93**, PNA-P **94**, and an 11-mer complementary sequence of DNA

with a central abasic site displayed a lower T_m than expected for the corresponding unmodified duplexes.

1.5 Hyaluronic acid

Hyaluronan (HA), **95** (Figure 1.25), also called hyaluronic acid is a member of the glycosaminoglycan family of extracellular matrix component,[140] and can regulate a variety of physiological and pathological functions such as interacting with many receptors and proteins, cell proliferation, cell adhesion, migration and metastatic spread of tumour cells.[141]

HA is a macromolecule, multifunctional and non-sulfated linear glycosaminoglycan (GAG) distributed broadly through vertebrate organs, fluids, connective tissue, epithelial and natural tissue. Its chemical structure was determined in 1954 as a high molecular weight polymer of disaccharide that consists of D-glucuronic acid and *N*-Acetyl-D-glucosamine linked together via alternating β-1,4 and β-1,3 glycosidic bonds [140,141,142] as shown in Figure 1.25. Hyaluronan can be 25,000 disaccharide repeats in length and the average of its molecular weight in the human synovial fluid is about 3×10^6 Da.[143]

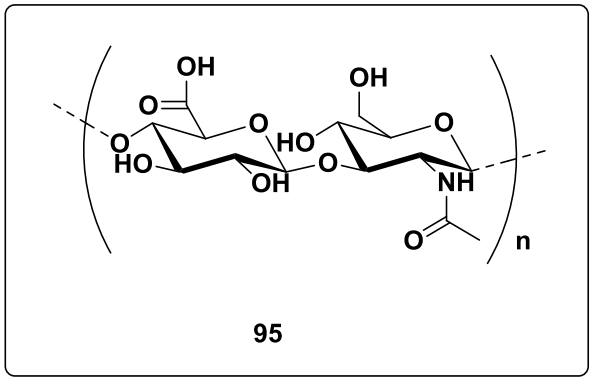

95

Figure 1.25: Structure of Hyaluronan.

Hyaluronan (HA) is synthesised biologically at the inner surface of the plasma membrane of the cell by three isoenzymes of hyaluronan synthase (HAS) in mammals termed as HAS1, HAS2 and HAS3 [140,144,145] which consist of terminal transmembrane or membrane-associated domains flanking a large cytosolic

catalytic domain.[146] In general, increased hyaluronan levels are often associated with elevated activities of growth factors and cytokines that are released in rapidly remodeling tissues as during embryonic development and wound healing or during certain pathological situations, such as inflammation, tumour progression, and vessel thickening.[147] Although all these enzymes are equally capable of synthesising HA, HAS2 is considered the main HA synthase in polymerizing long hyaluronan chain of MW about 2×10^6 Da in adult mammalian tissues.

There are data that suggested that natural antisense mRNA of HAS2 can regulate HAS2 mRNA levels and hyaluronan biosynthesis in a cell culture and may have a regulatory role in the control of the HA biosynthesis.[141] Natural antisense RNA is an endogenous transcript that is complementary an mRNA sequence (sense sequence). Natural antisense RNA (AS) is capable of regulating gene expression in both prokaryotic and eukaryotic organisms. Natural antisense RNAs exert their regulatory effects at multiple levels including transcription, RNA editing, post-transcription, and translation.[148,149] One of our aims in this thesis is looking at gene regulation of HAS2 through preventing the duplex formation inside the living cells between the mRNA of hyaluronic acid synthase (HAS2) and its natural antisense HAS2-AS. This blocking will then help investigating the effect of HAS2-AS on the translation process and protein synthesis, specifically production of HAS2. Our key to achieve this aim is based on using a long complementary sequence of PNA with 30 nucleobases to bind the natural antisense HAS2-AS sequence via a stable duplex formation. HAS2 possesses a natural antisense transcript (NAT) named HAS2-AS1 which is a part of long non-coding mRNA and has a crucial role in the modulation of gene transcription.

HAS2-AS1 is transcribed from the opposite DNA strand of the HAS2 gene localized at 8q24.13 on the minus strand of human chromosome 8 as shown in the literature [150] where the HAS2-AS1 exon 1 sequence lies within intron 1 of the HAS2 gene and the nucleotide sequences of HAS2-AS exons 3 and 4 are located upstream of HAS2. Furthermore, the second HAS2-AS1 exon is complementary to a portion of HAS2 exon 1.

An alternative splicing can generate two HAS2-AS1 NAT isoforms, named long (L) HAS2-AS1 splice-variant, L-HAS2-AS1, which has 257 nucleotide in length and short (S), HAS2-AS1 alternatively-spliced product that has 174 nucleotides. These two isoforms of HAS2-AS1 are complementary sequences to the region starting 70 bp from the presumed transcription start site of human *HAS2*.[151,152] This length variation involves a difference of 83 nucleotides of the HAS2- AS1 exon 2 sequence and thus changes the length of complementary sequence with HAS2. Furthermore, L-HAS2-AS1 shares 257 nucleotides with HAS2 exon 1, while S-HAS2-AS1 has a corresponding 174 nucleotide region of complementarity.[152]

Chapter Two

Design and Synthesis of Novel PNA monomers: Results and discussion

2.1 Introduction

Peptide nucleic acid (PNA) has many advantages over nucleic acids including higher chemical and biological stability, greater mismatch sensitivity, and higher binding efficiency to complementary sequences of nucleic acids associated with higher thermal stability of their complexes. These unique properties make PNA an effective tool in the gene regulation applications. However, these applications are often hampered by inherent drawbacks, such as their limited length that is assembled by solid phase synthesis method, low solubility in water and poor cellular uptake. Therefore, there are considerable ongoing efforts to further improve properties of PNA for both fundamental science and practical applications.

Due to their relatively simple structure, the chemical modifications of AEG PNA monomers have been studied extensively as an approach for improving their oligomers' properties. It is hoped that through these modifications improved probes for nucleic acids recognition, and therapy based on gene regulation can be obtained. Furthermore, more importantly, modification of PNA monomers is necessary not only to overcome the drawbacks that are associated with PNA oligomers toward their DNA or RNA targets. This modification is also to enhance the binding affinity of unmodified PNA oligomers when it is not sufficient for a specific application, or when functionality needs to be used for a specific application.

Several reviews have covered the literature concerning the design and biochemical testing of new chemically modified PNA monomers.[153] As was mentioned in the introduction chapter, modification of PNA monomers can be performed via the *N*-(2-aminoethyl) glycine backbone, the nucleobase and the acetyl linker. Often these changes are not mutually exclusive, and are not regularly used in combination to further tune and enhance the physical and biological properties of the PNA oligomers.

The ease of altering the PNA backbone has encouraged the synthetic organic chemists to develop various PNA monomers as an attempt to improve their oligomers' properties. A large number of chemical modifications of the original AEG PNA monomer backbone have targeted either the glycine unit, or the 2-aminoethyl moiety, or both.[93,94,103] However, only a handful of these modifications appear to

display an advantage in practical biochemical and/or pharmaceutical applications.

The use of Click reaction (CuAAC) within the realm of PNA chemistry has opened various opportunities to expand the applications of PNA in different fields. CuAAC reaction has been used in ligation, conjugation of PNA and insertion of a specific group into PNA sequence leading to the entry of PNA in new therapeutic and biosensor applications. In the current study, we are interested in using a click (CuAAC) reaction to extend PNA sequence as an antisense agent for blocking HAS2-AS sequence that requires a long PNA sequence.

The main results reported in this chapter are concerned with design and synthesis of two classes of novel PNA monomers consisting of modified PNA backbone units, ideally suitable for Fmoc-solid phase synthesis protocol. The first of these classes are alkynoic PNA monomers that allow functionalising the *N*-terminus of PNA sequences with an alkyne function that can be exploited in the click (CuAAC) reaction for ligation of PNA-PNA ligation as described in Chapter 3. Alternatively, synthesis of these modified PNA monomers also makes conjugation PNA with different substrates such as nucleic acid, ferrocene group, protein and sugar possible via click (CuAAC) reaction.

The second class of these novel monomers are the 1,2,3-triazole functionalised building blocks that allow insertion of the 1,2,3-triazole moiety directly into the PNA sequence during oligomerization as an attempt to enhance their hybridization properties with nucleic acids. Furthermore, these modified monomers represent models that can be used to investigate the effect of the click ligation linkers on the PNA properties mimicking the reaction products from ligation of PNA sequences by click reaction (CuAAC) via 1,2,3-triazole formation as click ligation linkages.

2.2 Results and Discussion

2.2.1 Synthesis of novel alkyne functionalised PNA monomers

When we began this project, our attention was turned to develop a new method to extend a specific PNA sequence by ligation of three PNA oligomers via 1,2,3-triazole formation as a biocompatible linker as an antisense agent for blocking HAS2-AS sequence that requires a long PNA sequence. Our approach to achieving this aim is

through a copper (I) catalysed azide-alkyne 1,3-dipolar cycloaddition reaction. Therefore, the correct precursors must be chosen to introduce the alkyne and azide functions at the *N/C*-terminals of PNA oligomers during solid phase synthesis. Thus, our work was first directed towards the synthesis of the azide-alkyne functionalised PNA oligomers. Although there are different commercially available chemicals, such as *N*-Fmoc-propargylglycine and propynoic acid, which can be used to introduce an alkyne function at the *N*-terminus of PNA oligomers during solid phase synthesis, we are particularly interested in the synthesis of a series of novel modified alkyne PNA monomers that allow introducing an alkyne function at the *N*-terminus of PNA sequences.

Synthesis of these novel PNA monomers resulted in an important difference to the commercially available alkyne compounds. Specifically, when these novel monomers are used to introduce the target alkyne function at the *N*-terminus of PNA oligomers for achieving click (CuAAC) applications, it leads to construction of a linker unit bearing a nucleobase. Consequently, this click linker then will be as a modified PNA monomeric unit along the PNA sequence. In contrast, using the commercially available alkyne precursors to introduce an alkyne function at the *N*-terminus of PNA oligomers generates a click reaction linker that is entirely independent of the PNA sequence. This unspecific linker will be as a spacer on the PNA sequence and is thought to negatively affect the PNA properties such as changing the conformation of PNA/DNA duplexes. In other words, the corresponding click ligation linkers of the target alkyne PNA monomers could help to avoid or reduce negative effects on the PNA properties compared to the commercially alkyne precursors.

2.2.1.1 Retrosynthetic analysis of novel alkyne PNA monomer

The synthetic route that has been adopted to synthesise the novel alkyne PNA monomers is inspired by the synthetic route that is commoenly used for the synthesis of standard AEG PNA monomer. Thus, this route is based on the conjugation of the nucleobase acetic acid derivatives to the designed alkyne functionalised PNA monomer backbone by coupling reaction through amide bond

formation. The retrosynthetic analysis suggests a convenient and efficient synthetic route for synthesising the target alkyne functionalised PNA monomers as described in Scheme 2.1.

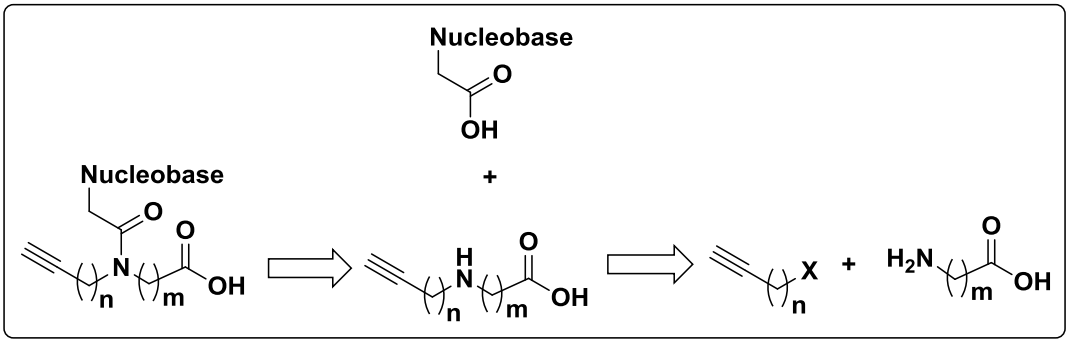

Scheme 2.1: A retrosynthetic route for *N*-alkynoic PNA monomers, n, m= 1, 2, 3.

The first bond to be disconnected is the amide bond between the nucleobase acetic acid and the secondary amino function of the alkyne functionalised backbone. This yields the alkyne functionalised backbone and the nucleobase acetic acid derivative as synthons. The second bond disconnected is that between C1 of an alkynyl group and the amino function of the amino acid compound to give an alkyne group, which could come from an alkynyl halide and an amino compound that can be a proteinogenic amino acid or an alternative amino acid compound.

2.2.1.2 Synthesis of modified alkyne PNA monomer backbone

In the present work, *N*-propargyl glycine ethyl ester was designed and synthesised as the precursor for the alkyne functionalised PNA monomer backbone in our synthetic pathway to synthesise the target PNA monomers. Starting from cheaply available glycine, a new, scalable and cheap route is reported for the synthesis of the target ester backbone as described in Scheme 2.2.

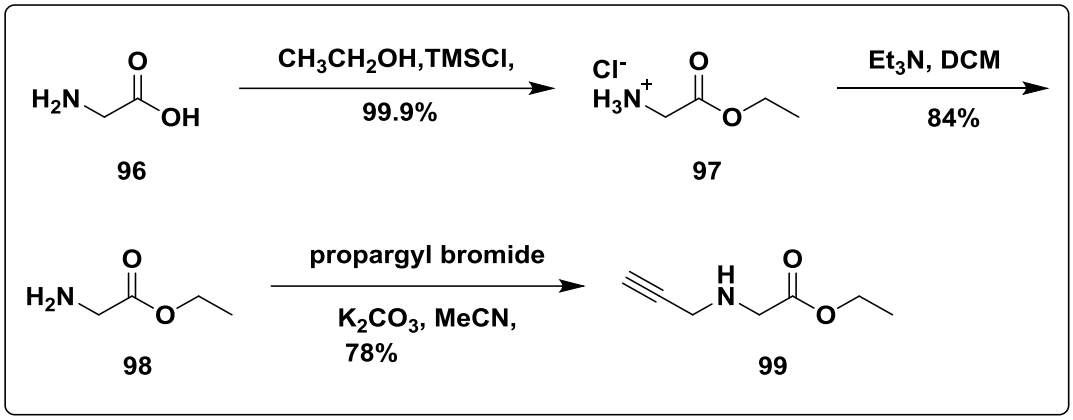

Scheme 2.2: Synthesis of *N*-propargyl glycine ethyl ester **99**.

To allow for two selective *N*-alkylation reactions, the carboxyl function of the glycine **96** was first protected, by esterification with ethanol in the presence of trimethylchlorosilane (TMSCl) to obtain ethyl glycinate hydrochloride **97** in 99.9% yield. This reaction was achieved with relative simplicity through a slightly modified procedure to that was reported in the literature.[154]

The next proposed step of our synthetic route is the *N*-alkylation reaction of **97** with propragyl bromide. In the first attempt, an excess of K_2CO_3 was investigated as a reagent for carrying out this reaction in acetonitrile. However, the protonated primary amine group showed very low activity toward this *N*-alkylation reaction and failed to provide the target compound **99** under these conditions. To avoid this problem, a new step was devised, involving first deprotonating the amino function of compound **97** through treatment of a suspension of compound **97** in dichloromethane with triethylamine and subsequent work up to obtain ethyl glycinate **98** in a yield of 84%. However, as expected, it was noted that compound **98** is particularly prone to undesired side reactions such as formation of 2,5-diketopiperazine,[155] and it cannot be stored for a long time. Consequently, the nitrogen atom of the primary amino group of compound **98** was alkylated immediately using propargyl bromide in the presence of the K_2CO_3 in acetonitrile. After work up and purification by column chromatography, the target alkynoic PNA monomer backbone **99** was obtained in 53% yield. Along with **99**, a significant quantity of *N,N*-di-propargyl glycine ethyl ester side product was also obtained.

In order to synthesise adequate quantities of the four target PNA monomers, we investigated whether the yield of the required product **99** could be improved. Thus, the *N*-alkylation reaction was repeated using an excess of ethyl glycinate **98**. The reaction gave only the desired product **99** in 78% as a yield. The highlightes of our new synthetic route are that it is a simple, high-yielding and gives a product requiring no further purification by column chromatography.

The ^{1}H NMR spectrum recorded for **99** using $CDCl_3$ as a solvent showed the appearance of a narrow triplet peak at 2.20 ppm and a doublet peak at 3.44 that are corresponding to the terminal alkynyl proton coupling to the (CH_2) of alkynyl group ($CH{\equiv}CCH_2$) that is attached to the amino group of ethyl glycinate.

2.2.1.3 Synthesis of nucleobase acetic acid derivatives

Having made the precursor alkyne modified PNA backbone **99**, we turned our attention to synthesise the N1- and N9-nucleobase acetic acid derivatives, particularly the N1-acetic acid derivatives of thymine and cytosine and the N9-acetic acid derivatives of adenine and guanine. A typical selective *N*-alkylation reaction is that of α-haloacetic acid or its ester derivatives, with the free nucleobase which could then be sequentially attached to the appropriate backbone, via amide coupling to construct the target PNA monomers.

More importantly, for the synthesis of cytosine, adenine and guanine PNA monomers, the introduction of an orthogonal protecting group at the reactive exocyclic amino function of each nucleobase is necessary. This prevents an unwanted side reaction from amide bond formation at this position during the synthesis of PNA monomers or through the solid phase synthesis reaction such as coupling and capping reaction, further to improve the solubility of PNA monomers in most organic solvents.

2.2.1.3.1 Synthesis of thymine-1-yl acetic acid

Although the thymin-1-yl acetic acid **100** is commercially available, it can also be prepared by an inexpensive and straightforward method as described in the literature.[156] Thus, the cheap commercially available thymine **2**, was alkylated

selectively at the N1 position with 2-bromo acetic acid in the presence of potassium hydroxide as outlined in Scheme 2.3.

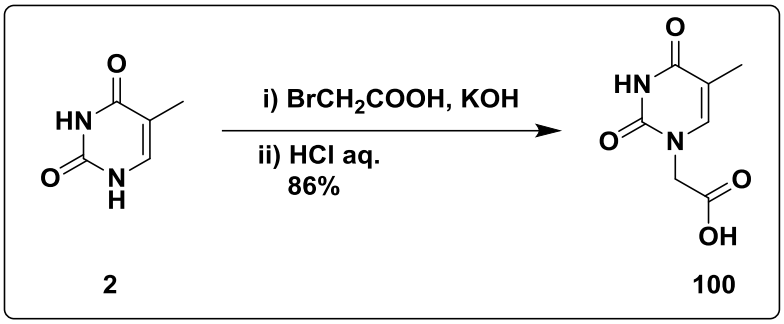

Scheme 2.3: Synthesis of thymine-1-yl acetic acid **100**.

This N1-alkylation reaction takes an advantage of that the amide group at the N1-position, which is susceptible to deprotonation and is consider more nucleophilic than the amide group at the N3-position under these basic conditions. Thus, the controlled addition of chloroacetic acid to the reaction mixture is a key factor to maintain the pH of the reaction suitable for N1-alkylation product. The reaction mixture was worked up to obtain the desired compound **100** in 86% yield as white crystals.

2.2.1.3.2 Synthesis of N^4-benzhydryloxycarbonyl cytosine-1-yl acetic acid

The first step in our synthetic route to synthesis the target compound is N1-alkylation reaction. Many synthetic pathways have been reported in the literature to alkylate cytosine base with α-haloacetic acid ester derivatives.[86,88,157,158] This *N*-alkylation reaction takes advantage of the lower pK_a of the amide group at N1-position, which is more susceptible to deprotonation by a base and thus undergoes alkylation reaction more readily than the primary exocyclic amino group.[159] In the current study, the N1-alkylation of cytosine was carried out using benzyl bromoacetate in the presence of K_2CO_3 in anhydrous DMF to give the desired compound **101** as shown in Scheme 2.4.

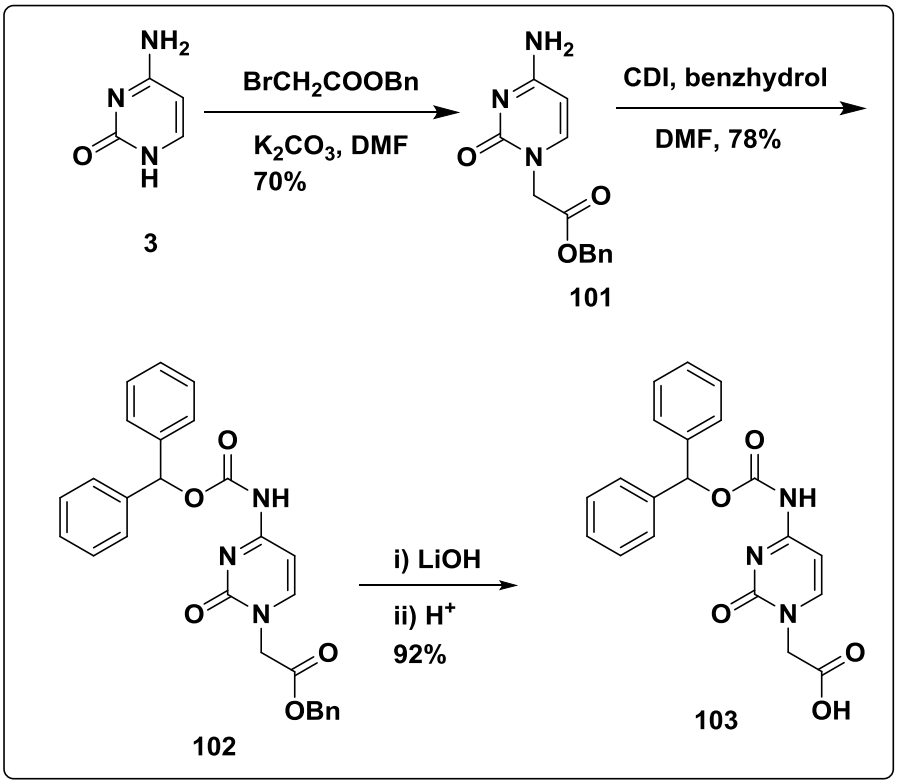

Scheme 2.4: Synthesis of N^4-Bhoc protected- cytosine-1-yl acetic acid **103**.

The acid labile benzhydryloxycarbonyl (Bhoc) group was chosen to protect the exocyclic amino function of **101** according to a simple modification of a procedure that was described in the literature.[91] Thus, the alkylated cytosine **101** was treated with the 1,1-carbonyldiimidazole (CDI) in anhydrous DMF to generate a reactive intermediate isocyanate compound; which subsequently underwent nucleophilic attack with benzhydrol to install the Bhoc group generating the desired compound **102**. Importantly, it was noted that this reaction is very sensitive to moisture because CDI is hydrolysed readily to give imidazole, therefore, all attempts to perform this reaction in non-anhydrous DMF failed to provide the target compound. In the final reaction, the desired Bhoc-protected cytosiny-1-yl acetic acid **103** was obtained in an excellent yield, by hydrolysing compound **102** using an aqueous solution of LiOH.

2.2.1.3.3 Synthesis of N^6-benzhydryloxycarbonyl adenine-9-yl acetic acid

N^6-benzhydryloxycarbonyl-9-adenyl acetic acid **106** was prepared by the same chemistry that was applied for the synthesis of Bhoc-protected cytosiny-1-yl acetic acid **103**, starting from the commercially available adenine **6** as outlined in Scheme 2.5.

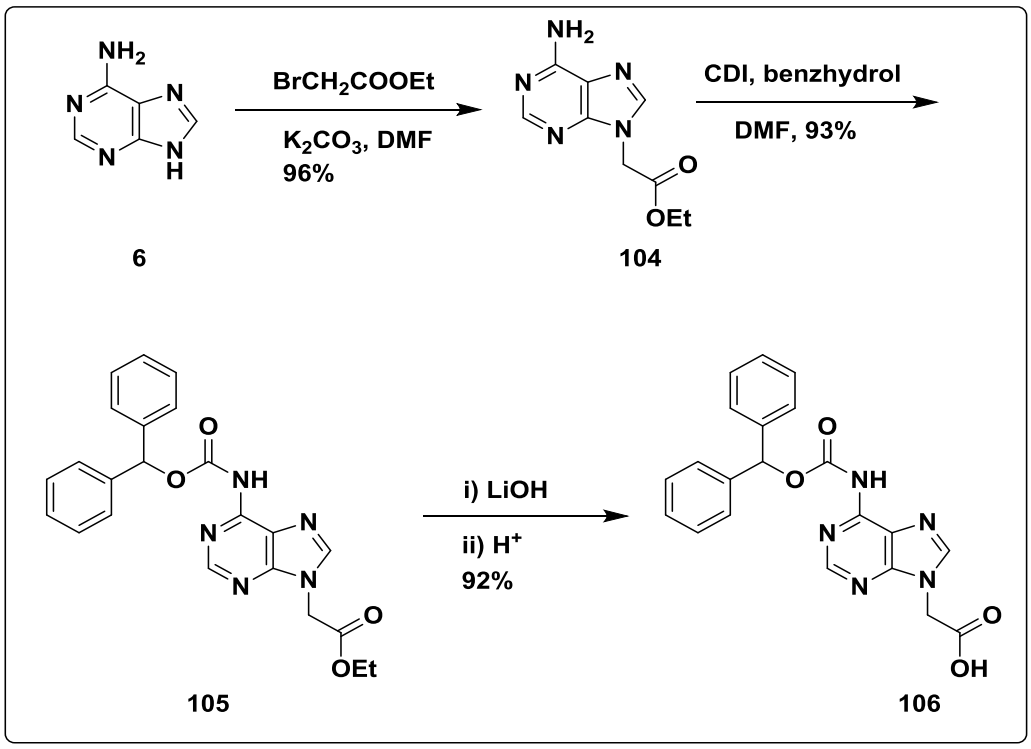

Scheme 2.5: Synthesis of N^6-Bhoc-protected adenine-9-yl acetic acid **106.**

Many methods have also been described in the literature to alkylate adenine selectively at the N9-position with α-haloacetic acid ester derivatives.[86,88,157,158] In the current project, N9-alkylation was carried out with ethyl bromoacetate using K_2CO_3 in anhydrous DMF, following new conditions and work up to obtain the desired compound **104** in an excellent yield. Similar to cytosine, this alkylation reaction also takes advantage of the lower pK_a of the secondary amine at N9-position, which is more susceptible to deprotonation by a base and thus undergoes alkylation more readily than the exocyclic amino function of adenine.[159] As stated for compound **102**, the exocyclic amine of alkylated adenine **104** was protected with

Bhoc group using 1,1-carbonyldiimidazole and benzhydrol in anhydrous DMF, to afford compound **105**. This precursor was followed by hydrolysis with an aqueous solution of LiOH to afford the desired N^6-Bhoc-protected adenine-9-yl acetic acid **106** in an excellent yield (Scheme 2.5).

2.2.1.3.4 Synthesis of N^2-benzhydryloxycarbonyl guanine-9-yl acetic acid

Because guanine has low solubility in most organic solvent and cannot be alkylated selectively at the N9-position,[158,160] the commercially available 2-amino-6-chloropurine **107** has been used as a precursor of the guanine nucleobase as outlined in Scheme 2.6.

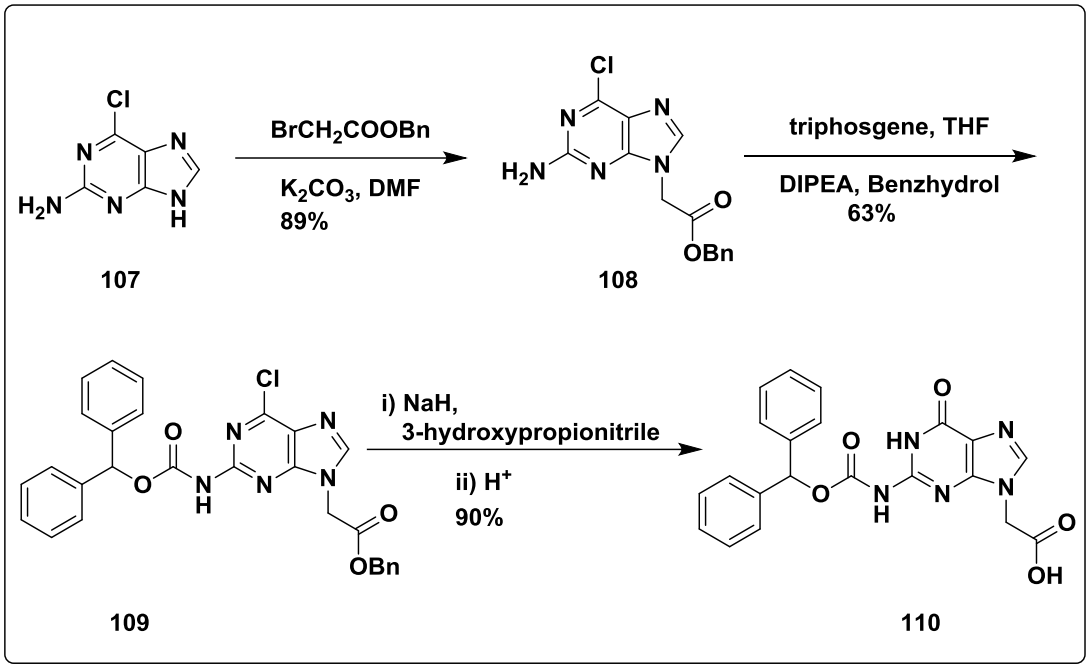

Scheme 2.6: Synthesis of N^2-Bhoc-protected guanine-9-yl acetic acid **110**.

Although numerous methods have been proposed for alkylation of 2-amino-6-chloropurine **107**,[86,88,157] the selective N9-alkylation was achieved with benzyl bromoacetate in the presence of K_2CO_3 in anhydrous DMF according to a modified procedure that was described in the literature [91] to give the desired compound **108** in excellent yield. Due to the exocyclic amino function of the alkylated compound **108** displaying a lack of reactivity with CDI, the Bhoc group was installed at this amino group in a different route than that described for the exocyclic amino group

of compounds **103** and **106.** In this way, triphosgene was used as the precursor to generate a reactive carbonyl intermediate compound, which underwent nucleophilic attack by benzhydrol to afford the desired compound **109**. This reaction was also achieved according to the procedure that was described in the literature.[91] In the final reaction, a nucleophilic displacement of the chlorine atom of **109** was achieved by reaction with 3-hydroxypropionitrile in the presence of sodium hydride. Simultaneous removal of the benzyl ester moiety afforded the desired N^2-Bhoc-protected guanin-9-yl acetic acid **110** in a high yield.

2.2.1.4 Synthesis of ethyl *N*-propargyl-*N*-(nucleobase-yl acetyl) glycinate

Having made the intermediate alkyne-functionalised backbone **99** and nucleobases acetic acid derivatives **100**, **103**, **106** and **110**, we then turned our efforts for combining them in a coupling reaction through amide bond formation. Inspired by the synthetic route that is used for synthesising AEG PNA monomers, we could synthesise the intermediate alkyne functionalised PNA monomers ethyl ester **111**, **112**, **113** and **114** as described in Scheme 2.7.

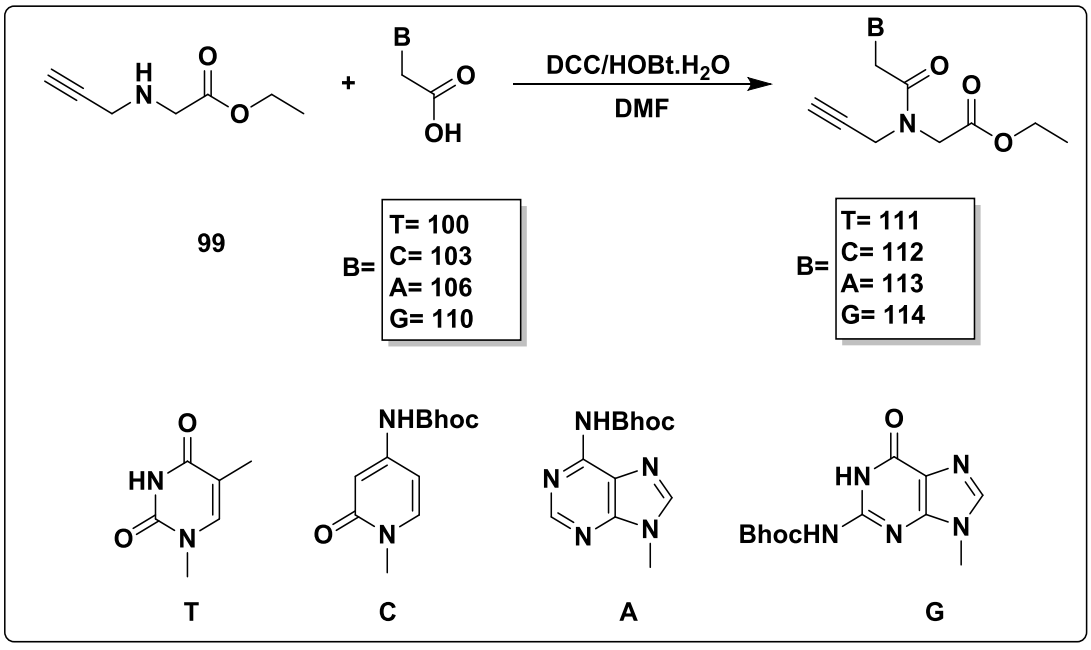

Scheme 2.7: Synthesis of ethyl *N*-propargyl-*N*-(nucleobase-yl acetyl) glycinate.

To carry out this reaction, the carboxyl function of these nucleobase acetic acid

derivatives requires activation. Thus, a solution containing the modified backbone **99** and the appropriate nucleobase acetic acid derivative in anhydrous DMF was treated with DCC in the presence of HOBt·H_2O to give the precursors **111**, **112**, **113** and **114** that were worked up and purified by column chromatography to obtain yields of 74%, 76%, 82%, and 76%, respectively.

The original PNA monomers [161] and *N*-alkyne-*N*-(Cbz-protected nucleobase-yl acetyl) glycine ethyl esters,[162] showed the presence of two rotameric forms in solution. As had been found for these monomers, the ^{1}H NMR and ^{13}C NMR spectra that were recorded for the resultant Bhoc-protected *N*-propargyl PNA ethyl esters **111**, **112**, **113** and **114** also showed splitting of some peaks, which indicates the presence of rotational isomers due to hindered rotation around the tertiary amide bond. This rotational restriction can be ascribed to a pseudo double bond, which means that this kind of monomer exists in two forms visible by the NMR spectroscopy, cis and trans rotamers. By comparing the integrations of the split peaks in the ^{1}H NMR spectra, it was found that the two rotamers were present in a 1:1 ratio.

At this point, the intermediate compounds **111**, **112**, **113** and **114** are not ready to be used in the solid phase synthesis strategies, as their carboxyl functions are still protected with an ethyl masking group. Consequently, they would be unable to form an amide bond during oligomerization.

2.2.1.5 Synthesis of novel *N*-propargyl-*N*-(nucleobase-yl acetyl) glycine PNA monomers

After completing the synthesis of the intermediate PNA monomers ethyl ester **111**, **112**, **113** and **114**, an efficient method was devised to remove the ethyl ester moiety thus, producing the novel alkyne PNA monomers that are ready to be used in the solid phase PNA synthesis. Our first attempt involved a saponification reaction of **111**, **112**, **113** and **114** with an aqueous solution of NaOH (2 M) in THF. Subsequent extraction with ethyl acetate then gave the target alkyne PNA monomers **116**, **117** and **118** in a low yield ranged from 30% to 40%, whereas the thymine monomer **115** was obtained in a slightly improved 60% yield as outlined in Scheme 2.8.

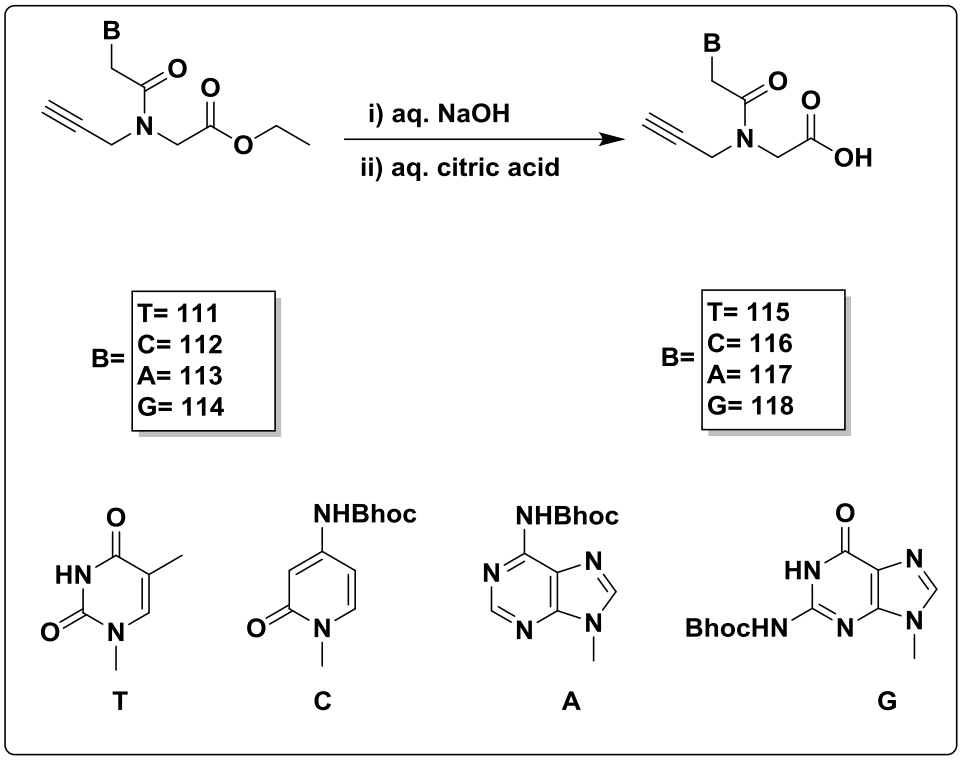

Scheme 2.8: Synthesis of novel alkynoic PNA monomers.

The yields obtained with these conditions were not as high as expected. This is probably due to loss of the products during workup because of their limited solubility in ethyl acetate extraction solvent. The hydrolysis reaction was therefore repeated in 1,4-dioxane using an aqueous solution of NaOH (2 M). Interestingly, an acidification to pH 3 with an aqueous solution of citric acid (20% v/v), led to precipitation of the desired products. These products were then able to be collected directly by vacuum filtration, washed thoroughly with water and dried to afford the novel alkyne PNA monomers. The yields were greatly improved with thymine **115** in 70%, cytosine **116** in 89% yield, adenine **117** in 90% yield and guanine **118** in 84%. All monomers were collected as pale white solids.

As had been seen before, for the precursors **111**, **112**, **113** and **114**, the ^{1}H and ^{13}C NMR spectra recorded for novel alkyne PNA monomers **115**, **116**, **117** and **118** still display splitting of some peaks due to the presence of rotational isomers that are described for their precursors.

As an application to use the novel alkyne PNA monomers in the solid phase PNA synthesis, and according to the PNA sequences that were chosen to be tested in the click chemistry ligation, the alkyne thymine PNA monomer **115** will be used in solid-phase synthesis to introduce the required alkyne moiety at the *N*-terminus of selected PNA sequences as described in Chapter 3. Additionally, one of our aims is also to test the activity of all our novel alkyne PNA **115**, **116**, **117** and **118** monomers toward the click reaction (CuAAC) with a view of synthesising novel PNA monomers containing a 1,2,3-traizole moiety, further explained in the section 2.2.2.

2.2.2 Synthesis of novel PNA monomers containing 1,2,3-triazole ring

Currently, there is a desire to extend PNA sequences through click (CuAAC) reaction via 1,2,3-traizole formation, when the length of PNA that can be prepared by solid phase synthesis is not enough for a specific application. Thus, our motivation to design these novel 1,2,3-triazole functionalised PNA monomers arises from the possibility to obtain new PNA monomers which can be used to demonstrate the effect of 1,2,3-triazole modifications. An entirely different route than that is commonly used for the synthesis of the standard AEG or modified PNA monomers, was designed for the synthesis of these novel PNA monomers. This synthetic route is based on the click (CuAAC) reaction that was developed by Sharpless *et al.*[119] to join an azide function with an alkyne terminus under mild conditions for formation 1,2,3-triazole products.

Herein, to make the target 1,2,3-functionalised building blocks can accommodate two amide bonds during the solid phase PNA synthesis protocols, the alkyne component of the click reaction was designed containing a carboxylic function. Whereas the azide component was designed to introduce an amino group functionality.

2.2.2.1 Synthesis of 2-(Fmoc-amino) ethyl azide

For the present project, the 2-aminoethyl azide was designed as an azide component for the click reaction. Choosing this compound takes advantage of that this precursor can be introduced at the *C*-terminus of a PNA sequence during

oligomerization using Azido Nova-Tag resin. Additionally, in order to avoid the undesired reactions that can occur on the primary amino function of the target monomers during oligomerization, the Fmoc group was chosen to protect the primary amino function of 2-aminoethyl azide. A simple and efficient route was devised for the synthesis of the target 2-(Fmoc-amino) ethyl azide **120**. The key intermediate for the synthesis of the target compound **120** is 2-aminoethyl azide. Several reviews have covered the literature concerning the introduction the azide function to organic compounds.[163] Of these, however, the S_N2 substitution of an alkyl bromide with sodium azide represents a straightforward reaction to introduce an azide function to organic molecules, where the bromide group is a good leaving group, as outlined in Scheme 2.9.

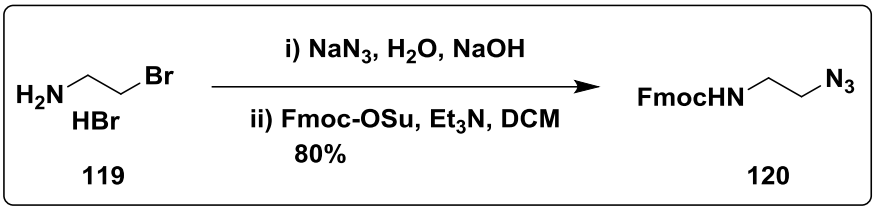

Scheme 2.9: Synthesis of Fmoc-aminoethyl azide **120**.

The commercially available 2-bromoethylamine hydrobromide **119** and sodium azide were stirred in water at 80 °C for 24 hours, according to the procedure that was described in the literature.[164] For the current work, isolation of the intermediate compound 2-aminoethyl azide is undesirable due to its relatively low boiling point and is unnecessary at this stage of this project.

Thus, it was decided to remove this step through extraction of the reaction mixture with dichloromethane. The extraction solution that is containing the expected intermediate compound was then treated with the commercially available Fmoc-succinimide ester in the presence of trimethylamine for two hours. Surprisingly on our first attempt, the primary amine function of the intermediate compound 2-aminoethyl azide was protected successfully by Fmoc group in 80% yield. Consequently, our synthetic route highlighted a simple work up, higher-yielding strategy and required no further purification by column chromatography.

2.2.2.2 Synthesis of novel *N*-[(1-(2-Fmoc-aminoethyl)-1H-1,2,3-triazol-4-yl) methyl]-*N*-(thyminyl-1-yl acetyl) glycine 121

Our first efforts focused on verifying that the click reaction could be applied to our novel alkyne PNA monomers **115**, **116**, **117** and **118**. Each contains an alkyne component in CuAAC reaction for the synthesis of 1,2,3-triazole functionalised PNA monomers. Our efforts focused first on the synthesis of the modified thymine PNA monomer as outlined in Scheme 2.10.

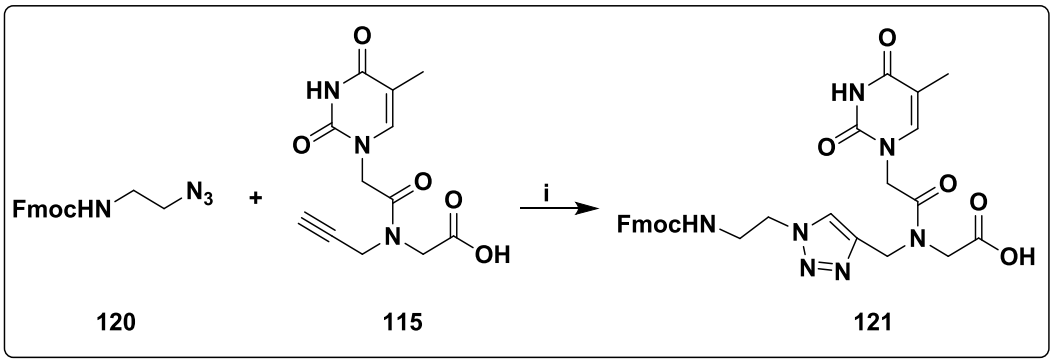

Scheme 2.10: Synthesis of monomer **121**, i) $CuSO_4 \cdot 5H_2O$, Na-ascorbate, *tert*-butanol:H_2O (2:1), 75%

Our initial attempt involved the addition of monomer **115** and 2-(Fmoc-amino) ethyl azide **120** to a solution of (*tert*-butanol: water, 1:1 v/v) containing $CuSO_4 \cdot 5H_2O$ in the presence of sodium ascorbate. The latter of which as reducing agent to produce Cu (I) that is required to achieve CuAAC reaction. However, the starting materials **115** and **120** displayed a limited solubility in the standard click solvent reaction mixture (*tert*-butanol:water, 1:1 v/v) at room temperature. Thus, this attempt proved unsuccessful in generating the desired product. Once the ratio of *tert*-butanol:H_2O was changed to 2:1 v/v, it was enough to dissolve both **115** and **120**. The new solvent system was used with the same reaction constituent as before and left to stir at room temperature. The progress of the reaction was followed by TLC analysis. Although TLC analysis did not show formation a new product, a solid was seen to precipitate from the reaction mixture. Thus, the solid product was collected and characterised by ^{1}H NMR which indicated that this solid is the target compound

121, formed in 20% yield. Since the yield was not optimal, we investigated whether the yield can be improved. Thus, the reaction mixture was heated up to 40 °C and left to stir for overnight, and this was enough to afford the desired product in a 75% yield. Our synthetic pathway highlighted that the product is separated, as a precipitate from the reaction mixture and can be collected by filtration without a further work up and was pure enough to not require column chromatography.

^{1}H NMR spectra recorded for this compound showed that all the signals are previously belonging to the starting materials combined with the correct integration of both starting material and product. However, the disappearance of the signal for the alkynyl proton of **115** at 3.44 and 3.26 ppm along with the appearance of the peaks that are belonging to the thymine moiety and azide component, indicated that 1,2,3-the target compound had been formed. This structure was also verified in the ^{13}C NMR and mass spectra recorded for this compound, in additional to the IR spectrum that showed the disappearance of the peak for the azide group of compound **120**.

Encouraged by the results reported with the novel thymine PNA monomer **121**, and the potential properties of any resulting oligomers, we were motivated to turn our attention to testing the reactivity of the other novel alkyne PNA monomers **116**, **117** and **118** towards the click reaction to obtain their corresponding novel 1,2,3-triazole functionalised PNA monomers. Starting, of course, with their potential in the click reaction, to obtain their corresponding novel 1,2,3-triazole functionalised PNA monomers. All reactions were performed under the same conditions that were used for synthesising monomer **121**.

Unfortunately, these compounds failed to give the desired PNA monomers, owing to the Bhoc protecting group on their exocyclic amino function displaying instability toward the click reaction conditions. The 1H NMR spectra, recorded for the resulting reaction products, confirmed disappearance of the protons belonging to the Bhoc group. In an attempt to overcome this problem modified routes using copper (I) acetate as rather than $CuSO_4 \cdot 5H_2O$, or using DMF instead of *tert*-butanol:H_2O, were attempted but also failed to give the target compounds. Because it was deemed that these monomers were not really required at this stage of the

initial investigations, they were left without further investigations.

2.2.2.3 Synthesis of novel 3-[1-(2-Fmoc-aminoethyl)-1H-1,2,3-triazol-4-yl] propionic acid 123

For further investigation of the potential of the click reaction application in PNA, another novel Fmoc protected monomer **123** was designed and synthesised via a click reaction. This monomer was generated by reacting the synthesised compound **120**, and the commercially available 4-pentynoic acid **122**. Choosing 4-pentynoic acid **122** as an alkyne component of click reaction for synthesis monomer **123**, takes advantage of the fact that this compound **122** can be used to introduce an alkyne function at the *N*-terminus of PNA oligomers during solid phase synthesis for click reaction applications.

Similar to the synthesis of monomer **121**, the synthesised compound **120** was combined with 4-pentynoic acid **122** via the 'click reaction' using $CuSO_4 \cdot 5H_2O$ in the presence of sodium ascorbate as a reducing agent in *tert*-butanol:H_2O (2:1) as outlined in Scheme 2.11.

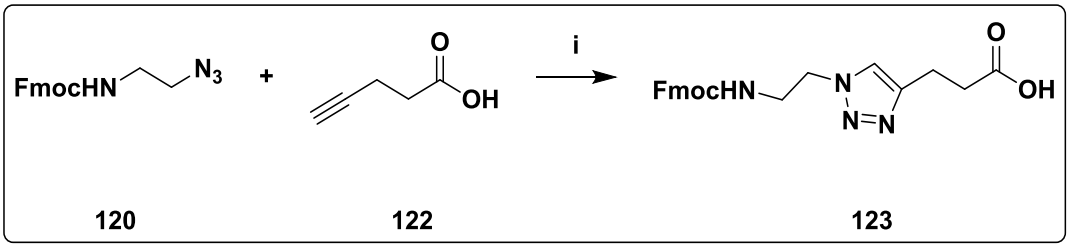

Scheme 2.11: Synthesis of monomer **123**, i) $CuSO_4 \cdot 5H_2O$, Na-ascorbate, *tert*-butanol:H_2O (2:1), 80%.

In the first attempt, the resulting solution obtained was left to stir at room temperature. The progress of the reaction was monitored by TLC analysis. After a few hours, it was seen that a new product was formed beside the starting material. After 24 hours, the reaction was worked up and the crude sample obtained was purified, by column chromatography, to give the titled compound in 50% yield. As an attempt to improve this low yield, the reaction was heated up to 40 °C overnight;

after work up the desired compound **123** was obtained in 80% yield. The ^{1}H NMR spectrum recorded for this compound **123** showed that all the previous signals belonging to the starting materials combined with the correct integration expected for the product and the starting material. However, the appearance of a new singlet at ppm and 7.77 ppm corresponding to the C (5) triazolyl proton, indicated that 1,2,3-triazole ring had been formed. This structure also was verified in the ^{13}C NMR and mass spectra recorded for this compound, and an additional IR spectrum showed the disappearance of the peak for the azide group of the compound.

2.2.2.4 Synthesis of novel *N*-[(1-(2-Fmoc-aminoethyl)-1H-1,2,3-triazol-4-yl) methyl]-*N*-(*tert*-butoxy carbonyl) glycine 126

For further investigations, another novel monomer suitable for Fmoc solid phase peptide synthesis was designed, mimicking the click ligation linker that can be constructed in the PNA sequence when the *N*-propargyl glycine was used to introduce the alkyne function at *N*-terminus of PNA oligomers. Choosing this type of click ligation linkers creates the advantage that this linker will introduce a secondary amino group into the extended PNA sequence. This amino function then will add a positive charge, and therefore will increase water solubility of PNA oligomers and may also increase its attraction to a DNA or RNA target.

For this purpose and to make comparison with monomer **121**, *N*-propargyl glycine was designed as an alkyne component for synthesis of the target novel monomer via click reaction. Again, to avoid undesired reactions during oligomerization, this secondary amino function must be protected orthogonally. Thus, the *N*-Boc-*N*-propargyl glycine **125** that was reported previously by Wakselman *et al.*[165] for a different aim, was chosen to be the precursor for the target *N*-propargyl glycine in our synthetic route. Our synthetic route to the precursor **125** is started from the amino acid glycine **96**. Although the Boc-protected glycine **124** is commercial, it can be prepared in a straightforward and relatively inexpensive method according to the slightly modified procedure that was described in the literature[166] as outlined in Scheme 2.12.

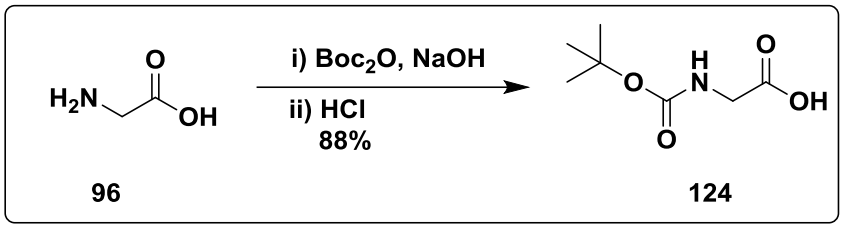

Scheme 2.12: Synthesis of *N*-Boc-protected glycine **124**.

The Boc group was installed on the amino function of glycine by the addition of di-tert-butyl-dicarbonate in isopropanol, to a solution of glycine dissolve in an aqueous solution of NaOH (2 M). The reaction was accomplished under modified conditions and, following workup, the desired compound **124** was isolated in 88% yield and used in the next step without further purification by column chromatography.

The biggest challenge was in *N*-alkylation of the nitrogen atom of the carbamate group with propargyl bromide, as this atom is much less reactive. However, the literature suggested the use of a stronger base i.e. sodium hydride [165] which did indeed lead to a successful reaction as outlined in Scheme 2.13.

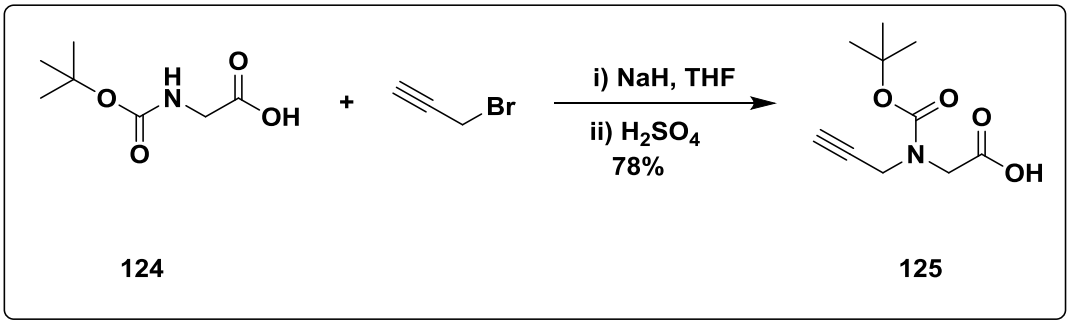

Scheme 2.13: Synthesis of *N*-Boc-*N*-propargyl glycine **125**.

To achieve this reaction successfully, anhydrous conditions are required during the time of reaction. Thus, a solution of **124** in anhydrous THF was cooled to 0 °C under nitrogen gas before being treated with propargyl bromide followed by sodium hydride. Following a simple modified work up, the target compound **125** was obtained in good yield, without requiring further purification by column chromatography.

At this point, compound **125** can be used to introduce the alkyne function at the *N*-

terminus of PNA oligomers during the Fmoc solid phase synthesis strategy. For this reason, we are interested in testing its reactivity toward CuAAC reaction in order to prepare the corresponding monomeric unit. We were then able to study the effect of this novel monomeric unit as seen in a PNA sequence that has been extended by the click reaction.

The click reaction conditions that were investigated for the synthesis of monomers **121** and **123** were used to synthesise the novel monomer **126** as shown in Scheme 2.14.

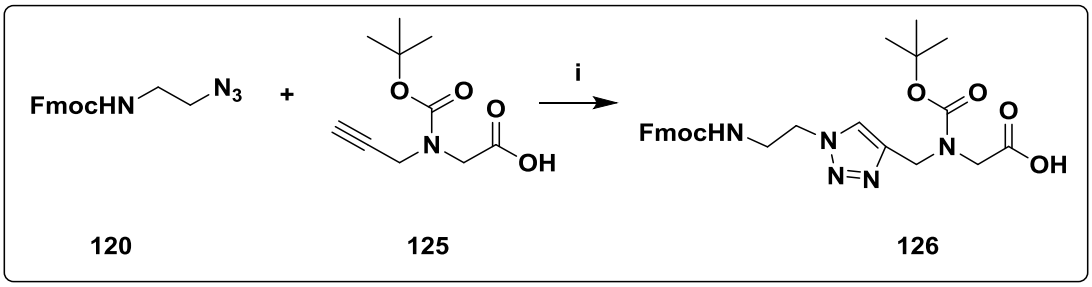

120 **125** **126**

Scheme 2.14: Synthesis of monomer **126**, i) $CuSO_4 \cdot 5H_2O$, Na-ascorbate, *tert*-butanol:H_2O (2:1), 75%.

Thus, compounds **125** and **120** were added sequentially to a solution containing $CuSO_4 \cdot 5H_2O$ and sodium ascorbate in a mixture of *tert*-butanol and water. The resulting reaction mixture was left to stir at 40 °C for overnight. After workup, the crude product was purified by column chromatography to obtain **126** in 75% yield.

The ^{1}H NMR spectra recorded for **126** showed a combination of all the signals from starting materials **120** and **125**, in the correct integration. The disappearance of the signal for the alkynyl proton of **125** at 2.27 ppm along with the appearance of a new singlet 7.75 ppm corresponding to the C (5) triazolyl proton, indicated that 1,2,3-triazole ring had been formed. As it had been seen before, for compound **125**, some of the signals from compound **126** were split in both ^{1}H and ^{13}C NMR spectra. Once again, these implied two rotamers were present.

2.3 Synthesis of Fmoc-protected AEG thymine PNA monomer

Due to the need of obtaining a relatively large number of PNA oligomers during this

study, a large amount of the expensive commercially available Fmoc/Bhoc PNA monomers will be required. As the thymine acetic acid derivative **100** is already prepared for synthesising our novel PNA monomers **115** and **121** in addition to the relative simplicity of the synthesis thymine monomer, therefore, we tried to synthesise it in a relatively low-cost route.

The key intermediate for synthesising Fmoc-protected AEG thymine PNA monomer is the *N*-Fmoc-protected aminoethyl glycine benzyl ester (Fmoc-AEG-OBn). A simple and effective method was adopted to prepare this compound according to the modified procedure that was described in the literature[87] as outlined in Scheme 2.15. Thus, an excess of 1,2-diaminoethane was first mono Boc-protected to **33** using di-*tert* butyl carbonate in acetonitrile. Following removal of excess 1,2-diaminoethane by a simple workup this gave pure compound **33** in a bit higher yield than reported previously. The primary amine function of **33** was alkylated with benzyl bromoacetate in the presence of triethylamine to afford benzyl *N*-(2-Boc-aminoethyl) glycinate backbone **127** in 80% yield.

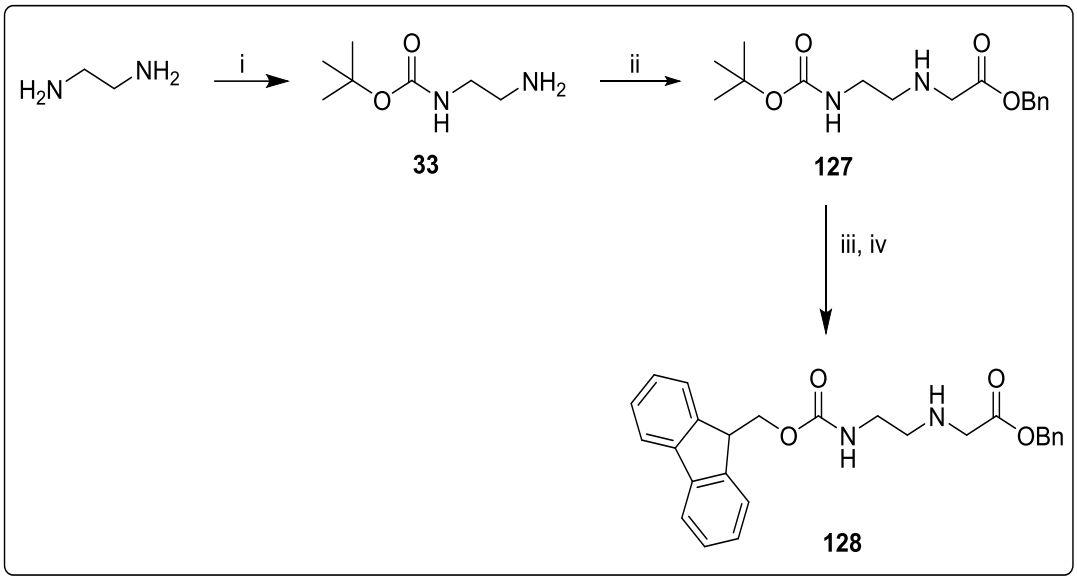

Scheme 2.15: Synthesis of Fmoc protected PNA backbone **128**, i) Boc_2O in THF, 80%, ii) $BrCH_2COOBn$, Et_3N, MeCN, 83%, iii) TFA, DCM, iv) Fmoc-OSu, Et_3N, DCM, 76%.

For the synthesis of Fmoc-protected AEG thymine PNA monomer, the Boc

protecting group was first removed using TFA 95%. The TFA salt intermediate compound was treated with trimethylamine in dichloromethane followed by addition of Fmoc-OSu to produce the Fmoc-protected PNA monomer backbone **128**. After a simple workup, the target backbone was used in the next step without further purification by column chromatography.

As was described for our compounds **111**, **112**, **113** and **114**, the Fmoc protected backbone **128** was coupled to thymin-y-l acetic acid derivative **100** using DCC as a coupling agent in the presence of HOBt·H_2O to give the intermediate Fmoc-protected thymine PNA benzyl ester derivative **129** in a good yield. Removal of the masking benzyl group was achieved by hydrogenation using Pd/C as a catalyst according to the procedure that was described in the literature [167] to afford the target Fmoc-protected AEG thymine PNA monomer **130** as outlined in Scheme 2.16.

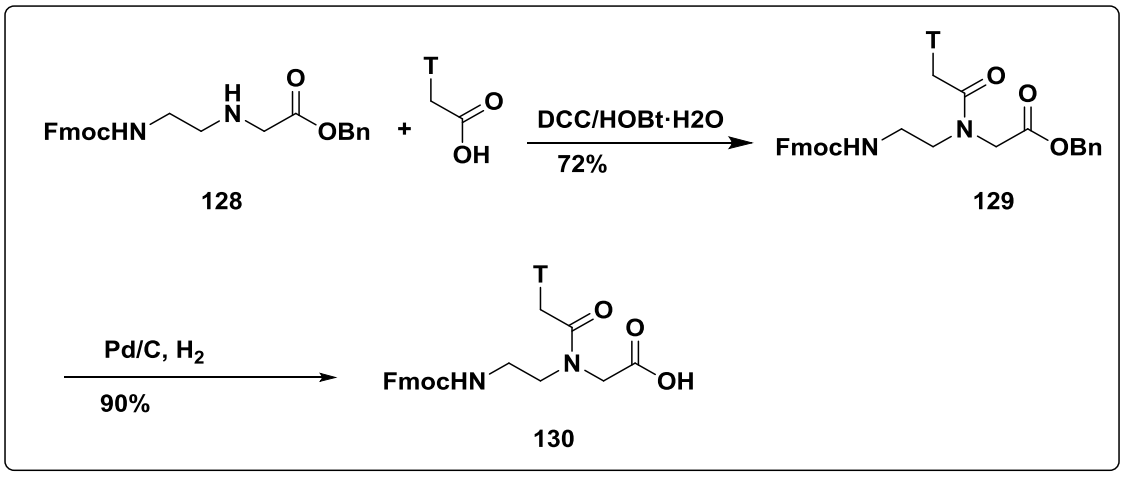

Scheme 2.16: Synthesis of Fmoc-protected AEG thymine PNA monomer **130**.

Chapter Three

Design and Synthesis of Modified PNA Oligomers:

Results and Discussion

3.1 Introduction

Click reaction (CuAAC) is now the method of choice for the conjugation of PNA sequences with nucleic acids and protein and represents a promising way to extend a PNA sequence via ligation through 1,2,3-triazole formation as a linkage. This triazole ring is, in fact, a mimic of the amide bond and a biocompatible group. In principle, it should keep the advantages of standard PNA with stability to degradation and an increased binding affinity toward nucleic acids. However, there are few publications that have demonstrated the effect of the 1,2,3-triazole moiety on the properties of PNA oligomers.

Thus, this chapter will focus on the incorporation of the novel 1,2,3-triazole functionalised PNA monomers **121**, **123** and **126**, that were described in Chapter 2, into AEG PNA oligomers via the Fmoc solid phase peptide synthesis strategy. The resulting PNA oligomers will contain a single unit of these novel monomers. The modified PNA oligomers are then being used in binding studies to investigate the effect of these monomers on the hybridization properties of PNA oligomers. Specifically, their binding affinity and the thermal stability of their complexes with complementary sequences of nucleic acids. Comparisons of the binding properties of these PNA oligomers could then be made against the unmodified PNA oligomer of the same sequence or as an independent monomeric unit as described in Chapter 4. In other words, the modified 1,2,3-triazole functionalised PNA oligomers will be used as models to demonstrate the effect of linkages that can be seen in the PNA sequences that are ligated or conjugated by click reaction.

Further work that is reported in this chapter involves incorporating a novel alkyne functionalized thymine PNA monomer **115** into specific PNA sequences during Fmoc solid phase synthesis strategy in order to introduce an alkyne function at their *N*-terminus. These alkyne functions can then be exploited in the application of the click reaction such as ligation of a PNA sequence. This formed the focus of our preliminary attempt to develop a new method to ligate the alkyne functionalized PNA oligomers with another sequence functionalized with an azide function via CuAAC reaction for a particular goal.

3.2 Solid phase PNA synthesis

Peptide nucleic acid oligomers (PNAs) are polyamide compounds but not peptides because their building blocks are not proteinogenic amino acids. PNAs are synthetic oligonucleotides based upon a pseudo-peptide monomeric unit *N*-(2-aminoethyl) glycine. Therefore, PNA oligomers have been synthesised by the same procedures that are used for the synthesis of polypeptides, i.e. through either solid or solution phase synthesis. Synthesis of PNA is rather similar to that of peptides, in that it can be carried out either from the C or N termini. Most commonly, the synthesis of PNA oligomers is implemented via the automatic or manual solid phase peptide synthesis (SPPS) strategies. Regardless of the strategy chosen, the solid phase synthesis of PNA oligomers proceeds with the following standard synthetic steps: a temporary protecting group removal (deprotection step), a building block coupling (coupling step) and a blocking of the unreacted free amino functions (capping step), as outlined in Scheme 3.1.

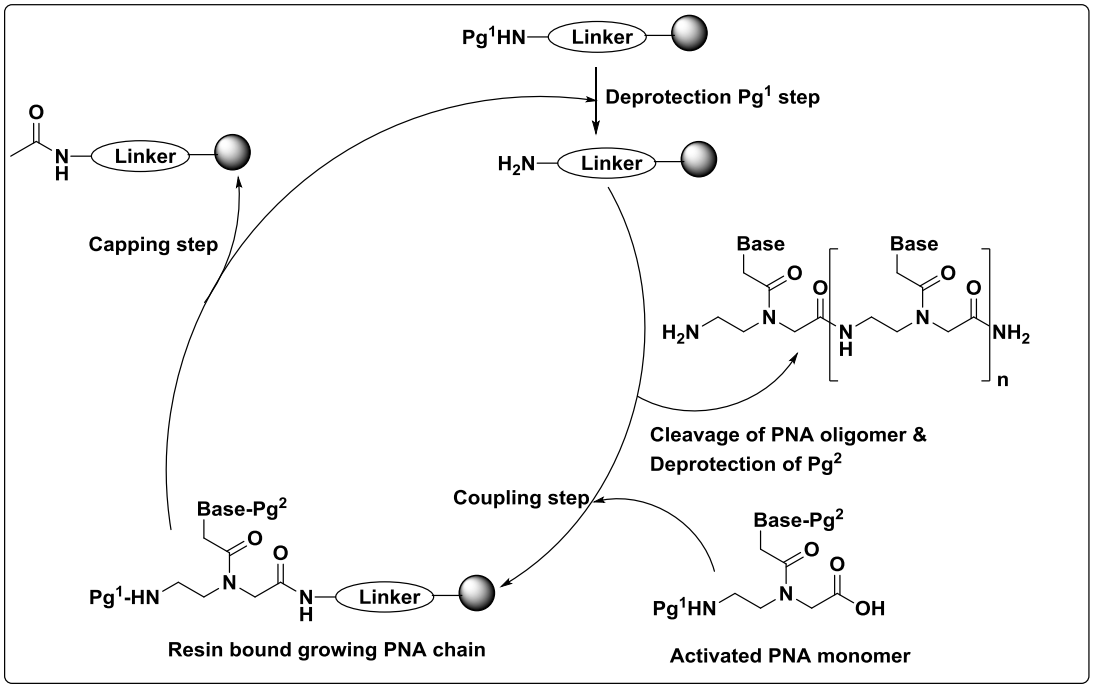

Scheme 3.1: General scheme of solid phase PNA synthesis cycle.

Like polypeptides, the elongation of PNA oligomers takes place by deprotecting the *N*-terminus of the anchored PNA monomer and by coupling to it the activated next

N-protected PNA monomer. In general, solid phase synthesis has many striking advantages over conventional synthesis, including the utility of excess reagents which drives reactions to completion leading to improved yield. Reactions can be worked-up simply by washing the resin and filtering under vacuum, thereby removing the excess of the reagents and any soluble by-products. Practically, the solid phase PNA synthesis conditions are chosen considering the nature of the solid support (resin), and the type of orthogonal protecting groups that are used to protect the exocyclic amine protecting groups on nucleobases and the primary amino function of the PNA monomer backbone.

A typical solid support used in SPPS is made up of an insoluble polymeric material, containing functional sites at which the growing polypeptide chain can be covalently attached. The ideal solid supports are an insoluble resin, with the minimum level of cross-linking to allow it to swell in a solvent while maintaining reasonable physical stability. The swelling opens the resin and thus allows reagents to penetrate its structure, which enables binding of the growing peptide chain at all possible active functional groups within the resin. There are a range of resins that are commercially available, and can be supplied in a functionalized form with a substrate fragment called a linker. The choice of the linker is highly dependent on the temporary protecting group strategy used. Functionalized polystyrene is among the most commonly used solid support.

Although there are many synthetic strategies have been reported for solid phase PNA synthesis, in particular, it is carried out using one of two common standard strategies. The first makes use of Boc-protected PNA monomers and is referred to as the Boc strategy, while the other method involves the use of Fmoc protected PNA monomers, and is thus termed the Fmoc method. Although the basic premise for each method is essentially the same, different conditions are used throughout the two protocols.

3.2.1 Fmoc Methodology

The Fmoc/Bhoc and Fmoc/Boc combinations of protecting groups PNA monomers are the most widely employed in the synthesis of PNA oligomers. This is due to the

mild treatment needed for the cleavage of the oligomer from the resin, and removal of Bhoc and Boc groups simultaneously. Currently, the commercially available Fmoc/Bhoc PNA monomers (Figure 3.1) were used to build all the target novel modified PNA oligomers with incorporation of our novel PNA monomers at the desired positions.

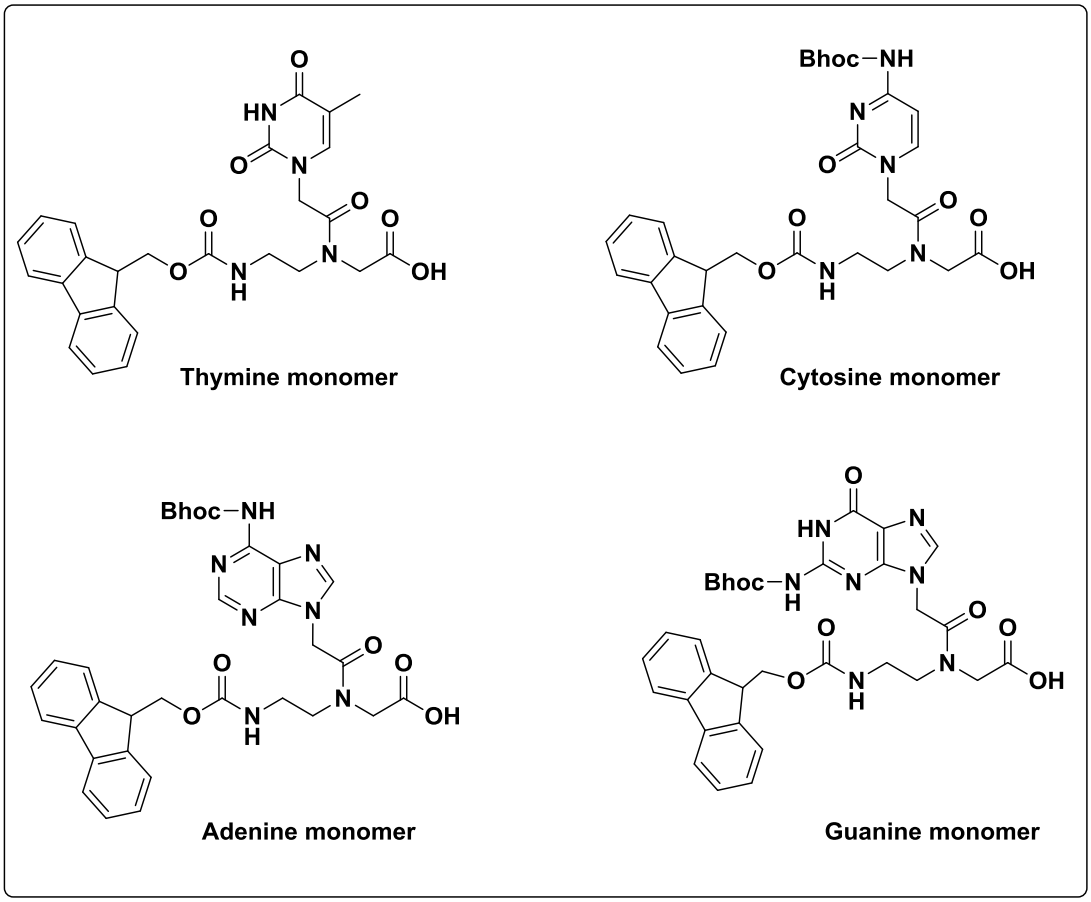

Figure 3.1: Structure of Fmoc/Bhoc protected PNA monomers.

The Fmoc/Boc-protected lysine was incorporated into the target azide and alkyne functionalised PNA oligomers to enhance their water solubility. Furthermore, lysine moiety also was inserted into the synthesised 1,2,3-triazole functionalised PNA oligomers to prepare a model to study its effect on the binding properties of PNA oligomers in the presence of 1,2,3-triazole as click ligation linkage. For the current work, the commercially available Fmoc protected Rink Amide MBHA resin (Figure 3.2) was chosen as a general solid support for synthesising the target PNA oligomers

with the exception of the PNA oligomers that required an azido group. This solid support is a type of Rink amide resins composed of a modified Rink amide linker attached to the (4-methyl benzhydryl amine) (MBHA) resin. This resin yields the PNA oligomers with *C*-terminal amides upon cleavage at the end of the synthesis using TFA. The *C*-terminal azide functionalised PNA oligomers terminus were synthesised on the specific Fmoc protected Azido-Nova Tag resin (*N*-Fmoc-*N*'-azido-PEG-diamine-MPB-AM resin) which is a resin for *C*-terminus labelling of peptide. This solid support is one of the Nova Tag resins that are used for peptide labelling with a group for ligation such as the azido group that is stable under solid phase synthesis conditions such as piperidine and TFA solutions (Figure 3.2). This resin yields the PNA oligomers with *C*-terminal secondary amides substituted with ethyl azide upon cleavage at the end of the synthesis using TFA. For both these two resins, the polymer matrix is a copolymer (styrene + 1% divinyl benzene DVB).

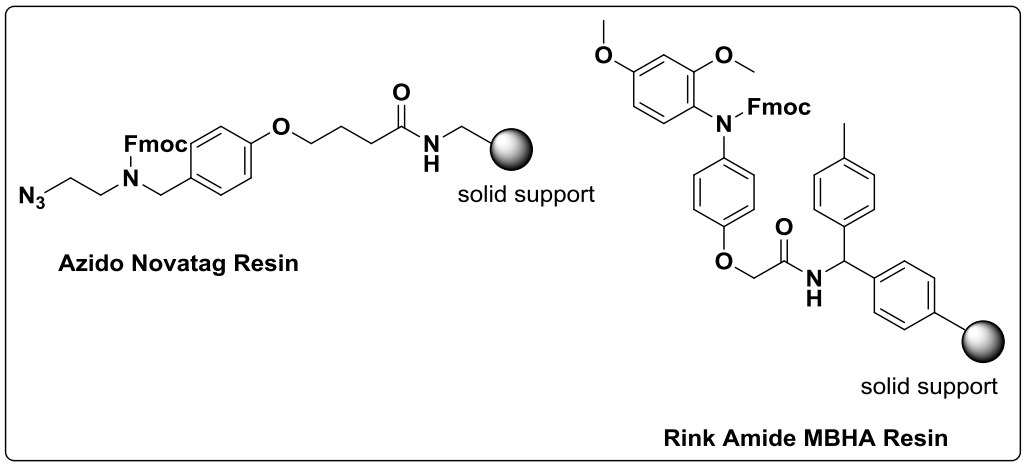

Figure 3.2: Chemical structure of resins that were used in SPS of PNA oligomers.

The synthesis cycle of the target PNA oligomers was achieved manually following standard Fmoc solid phase synthesis strategy. The resins were initially swollen in an appropriate amount of NMP for two hours, then drained by filtration so that all active sites of the solid support were sterically accessible to reagents. In the Fmoc chemistry, the synthesis cycle is started with removal of the Fmoc group from the solid support (resin). For Fmoc removal, numerous procedures in the literature describe a variety of deprotection methods. Most of these pathways are based on

using piperidine and differ primarily in the final concentration of piperidine used which is prepared in different solvents. In the present work, a solution of piperidine (20% v/v) in NMP has proven efficient in removing the Fmoc group. Scheme 3.2 illustrates the mechanism of the deprotection of the Fmoc group using piperidine.

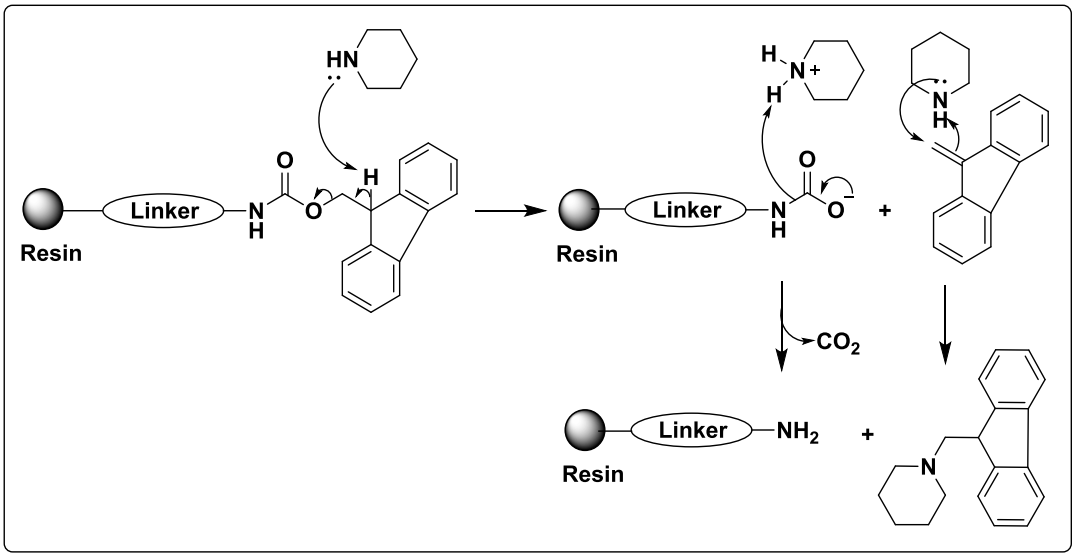

Scheme 3.2: Mechanism of Fmoc deprotection.[168]

When the soluble by-product of the deprotection step was removed by washing and filtration, the free amine group of the resin is ready for the peptide bond formation by a coupling reaction with the carboxyl function of the next monomer. However, prior to this, the carboxyl function of a monomeric unit needs an activation before it is able to couple to the amino function. In this project, the carboxylic acid group of PNA monomers was activated *in situ* by HATU in the presence of DIPEA and 2,6 lutidine in NMP. When mixed, the reaction can be followed by the changing of the colour to a slight yellow. The activated monomer solution was then added to the resin and placed in the shaker for one hour at 25 °C. Scheme 3.3 is outlined the mechanism of activation and coupling of PNA monomers while assembling a PNA oligomer by solid phase synthesis.

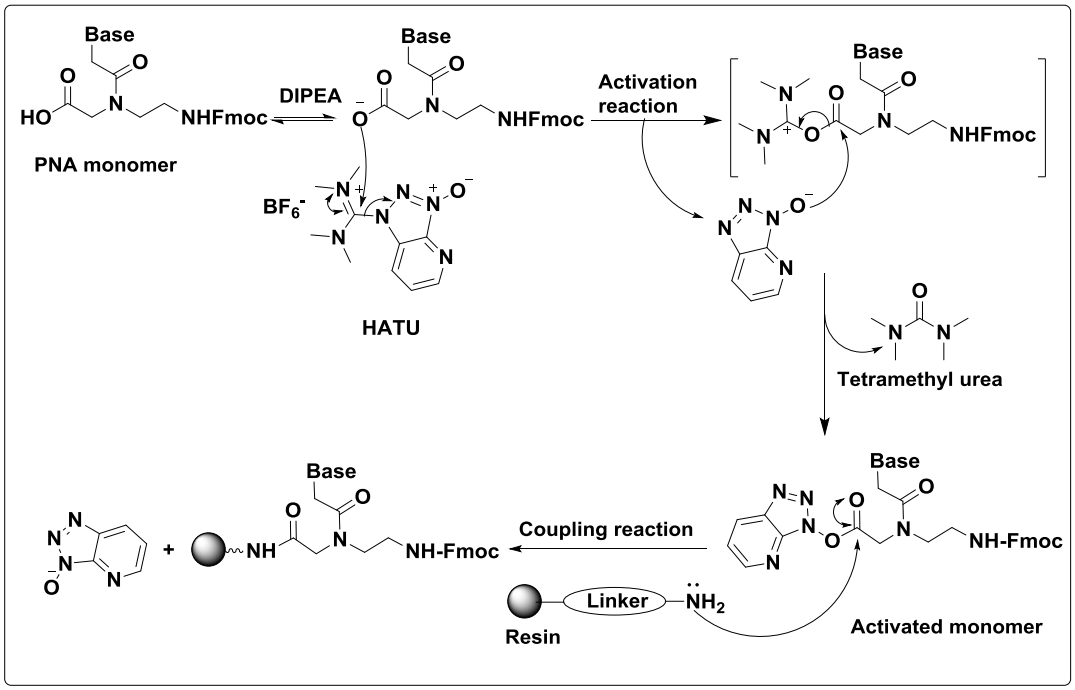

Scheme 3.3: Mechanism of activation, and coupling of a PNA monomer.[78]

However, in the coupling reaction, some of the deprotected amino functions fail to react. These unreacted amino functions should be permanently blocked from further chain elongation, to prevent the formation of PNA oligomers with an internal deletion of monomers. This is important as these oligomeric impurities may be harder to separate from the desired product by HPLC. Thus, the resin-bound growing PNA chain was treated with a solution of acetic anhydride, in the presence of lutidine as a base in NMP for 10 min. This reagent rapidly reacts with the amino group via an acylation reaction. Scheme 3.4 illustrates the mechanism of the capping reaction.

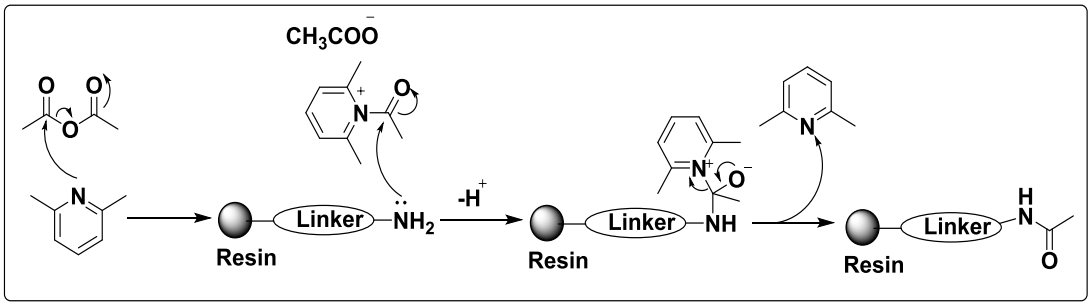

Scheme 3.4: Mechanism of the capping reaction.

These four procedures of Fmoc-deprotection, activation, coupling and capping were repeated until the desired PNA sequences were completed. However, upon completion of the required sequence and after removal of the last *N*-terminal Fmoc group, the support-bound PNA chains remain fully protected. The exocyclic amino groups of the nucleobases remain protected with Bhoc groups, and a Boc group protects the side chain of lysine that had been coupled with the PNA sequences to enhance their water solubility.

Therefore, the final step should involve removal of these protecting groups either before, or during cleavage the PNA sequence from the resin. As the Fmoc/Bhoc chemistry was used to synthesise the target PNA oligomers, the removal of Boc and Bhoc groups can be achieved simultaneously, during the release of the PNA oligomers from the resin, by treatment with TFA. Scheme 3.5 illustrates a proposed mechanism of cleavage PNA oligomer from MBHA Rink amide resin. In order to do this, the resin-bound PNA oligomers were swollen in a cleavage solution consisting of 95% TFA, 2.5% water, and 2.5% *m*-cresol. The latter is a scavenger for the resultant benzhydryl, and *tert*-butyl cations that are generated from the deprotection of Bhoc protected the exocyclic amino group, and Boc-protected lysine side chain, respectively. After two hours, the solution containing the crude product was collected by filtration and concentrated under a flow of nitrogen gas.

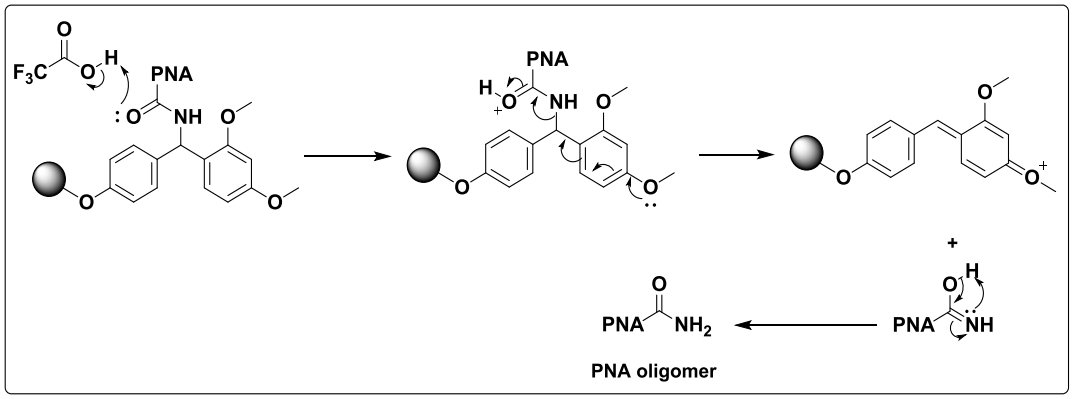

Scheme 3.5: A proposed mechanism of cleavage of PNA oligomers from MBHA Rink amide resin.

The crude mixtures that comprises the desired PNA oligomer, the cleaved protective

groups and the capped PNA sequences were precipitated by addition of diethyl ether and centrifugation. All the target PNA oligomers were purified by reverse phase HPLC and characterised by mass spectrometry.

3.3 Results and Discussion

In this project, a series of new modified PNA oligomers were prepared. Synthesise of these modified PNA was achieved by incorporating versatile novel monomers into a PNA sequence which may display the improved properties over standard PNA oligomers. Furthermore, an alternative application is synthesis of PNA oligomers with sufficient chemical reactivity to allow them to be converted into some desirable products. These protocols have several advantages for instance; synthesis of an oligomer containing a single modified versatile monomer could be used to study the application of click reaction on the PNA oligomers. Or the incorporation of some monomers could offer the possibility of making PNA containing a labile or chemically reactive conjugate.

3.3.1 Rationale for synthesis of functionalised 1,2,3-triazole PNA oligomers

Modification of the PNAs represent a promising way to enhance their properties such as nucleotide recognition, their water solubility, and cellular uptake or to present new functions into their structure for a specific application. In this research, mimicking the linkages that can be seen in extended PNA sequences via click reaction using the corresponding azide and alkyne precursors, three novel compounds **121**, **123** and **126** (Figure 3.3) were designed and prepared suitable for Fmoc solid phase synthesis strategy as described in Chapter two.

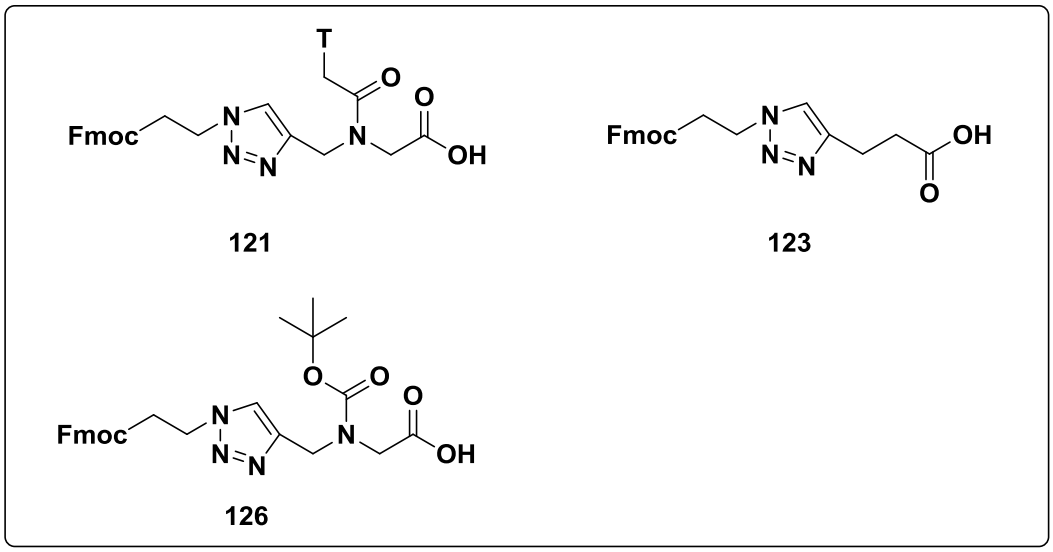

Figure 3.3: Structure of synthesised modified PNA monomers **121**, **123** and **126**.

Thus, once the task of synthesising these monomers was completed, the challenge of incorporating them into PNA sequences using SPS immediately followed. For this purpose, an 8-mer of a mixed pyrimidine-purine, PNA sequence (*N*-terminus **G-A-C-T-T-T-C-T** *C*-terminus) was designed as a model to investigate the effect of these novel PNA monomers on the binding properties of their oligomers. Furthermore, this sequence represents a fragment of PNA sequence that is hoped to be extended by CuAAC reaction to produce a long complementary PNA sequence that is required for blocking the natural antisense sequence (AS) of the mRNA sequence of HAS2.

Thus, based on this sequence, the unmodified 8-mer mixed PNA oligomer **131** (Figure 3.4) was synthesised as a control. Synthesis of this PNA oligomer **131** was carried out using the commercially available Fmoc/Bhoc protected AEG PNA monomers following the standard Fmoc solid phase synthesis strategy that was described in Section 3.2.1.

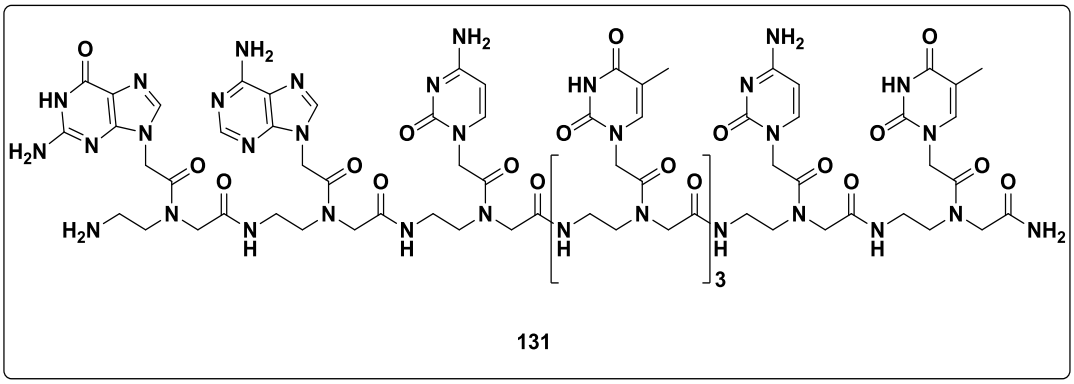

131

Figure 3.4: Chemical structure of the unmodified PNA oligomer **131**.

After cleavage from the resin, the crude PNA oligomer **131** was purified by RP-HPLC and characterised by LC-MS. Mass spectrometric analysis showed that there were peaks for various multiply-charged species of the target sequence **131** (Appendix 1). This PNA oligomer was used as a control sequence for comparing the hybridization properties of the 1,2,3-triazole functionalized PNA oligomers with complementary sequences of DNA and RNA.

3.3.1.1 Solid phase PNA synthesis with incorporation of monomer 121

In order to devise the optimised conditions to incorporate our novel monomers into PNA oligomers, our efforts first focused on the incorporation of the novel Fmoc-protected 1,2,3-triazole functionalised thymine PNA monomer **121** into the unmodified PNA sequence **131** (Figure 3.4).

Thus, this monomer **121** is a key precursor for the synthesis of the internally functionalised 1,2,3-triazole PNA oligomers **132** (Figure 3.5). Synthesis of this modified PNA oligomer **132** was achieved by incorporation of a single monomeric unit of **121** rather than the Fmoc-protected AEG thymine PNA monomer at position 4 of the unmodified PNA oligomer **131** (Figure 3.4)**.** This was done using the standard Fmoc solid phase strategy that was described in Section 3.2.1.

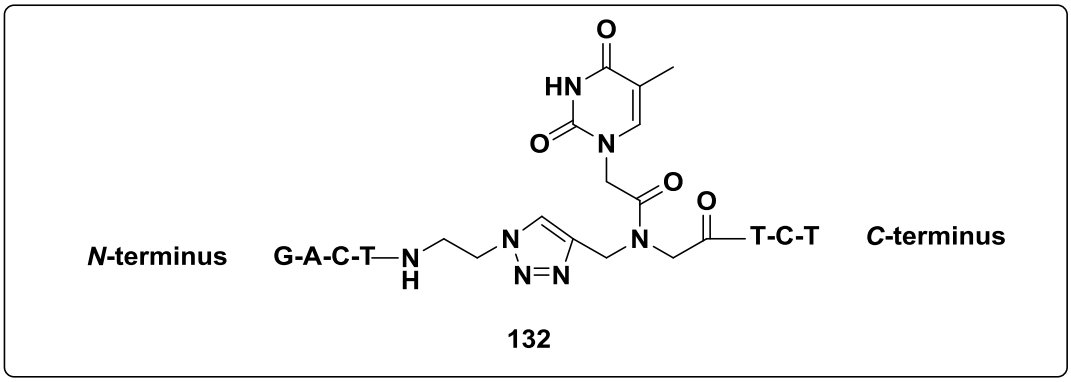

132

Figure 3.5: Structure of modified PNA oligomer **132**.

Incorporation of the triazole functionalised thymine PNA monomer **121** into the PNA sequence **132** (Figure 3.5) has two important benefits. Firstly, it represents an attempt at modifying PNA oligomers in order to improve their properties such as a binding affinity and thermal stability. Therefore, if this novel monomer could support these goals, it would result in a novel method for modification of PNA oligomers with improved properties.

Secondly, incorporation of monomer **121** into the PNA oligomer **132** can simulate the expected triazole monomeric unit that would be seen in the structure of a PNA oligomer that was extended through copper (I) azido-alkyne reaction. This PNA oligomer was produced using a PNA oligomer terminated with an alkyne function by coupling the novel alkyne PNA monomer **115**. Thus, PNA oligomer **132** will be used as a model to investigate the effect of this click ligation linker on the hybridization properties of the extended PNA sequences using click reaction.

Practically, before the incorporation of the novel Fmoc-protected 1,2,3-triazole functionalised thymine PNA monomer **121** into the PNA oligomers, certain characteristics needed investigating. The first potential challenge was determining if this modified monomer will be stable, and whether it can be activated and coupled into PNA oligomers using the conditions used for oligomerisation of the Fmoc/Bhoc protected AEG PNA monomers. In the first attempt for synthesising PNA oligomer **132**, the modified Fmoc protected monomer **121** was coupled to the growing PNA chain by *in situ* activation with HATU in the presence of DIPEA and lutidine in NMP for one hour similar to oligomerisation of AEG Fmoc/Bhoc protected PNA oligomers.

After the cleavage reaction, the crude PNA oligomer was analysed by RP-HPLC and characterised by mass spectrometry. The HPLC analysis showed that the target PNA oligomer **132** was obtained, however in a relatively low yield. Our investigations into why this PNA oligomer resulted in a low yield, it revealed that this monomer has a low solubility in NMP that was used as a solvent for the activation and coupling reactions during the synthesis cycle. Our first attempt to overcome this issue involved replacing the NMP with DMF for dissolving monomer **121**. Conveniently, this led to the target PNA oligomer **132** being obtained in an improved yield.

As mentioned early, PNA oligomers require the attachment of an ionic side chain, preferably at both *N*- and *C*-terminals of their oligomeric chain, to enhance their water solubility and to reduce their self-aggregation. For this purpose, the most commonly used is the commercially available amino acid lysine. In this case, once the PNA sequence is extended via copper (I) catalysed azide-alkyne cycloaddition reaction, the lysine moiety is expected to be neighbouring the ligation linker. To study the effect of this case on the binding properties, such as binding affinity and thermal stability of PNA-nucleic acids complexes, and for comparison with lysine-lacking modified PNA oligomer **132** (Figure 3.5), a new modified PNA oligomer **133** (Figure 3.6) was designed. Synthesis of PNA oligomer **133** was achieved by incorporating a single monomeric unit of Fmoc/Boc-protected lysine amino acid into the structure of the modified PNA oligomer **132** (Figure 3.5) adjacent to the monomeric unit **121**.

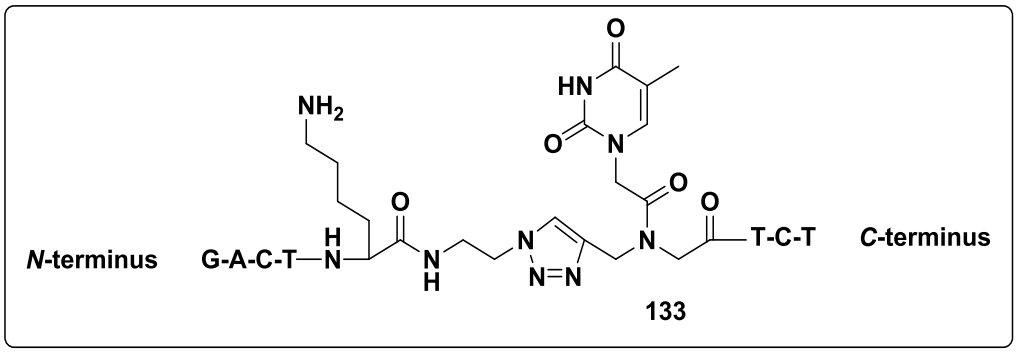

Figure 3.6: Structure of PNA oligomer **133**.

After cleavage reaction, the crude PNA oligomers **132** and **133** were purified by RP-

HPLC and characterized by LC-MS. Mass spectrometric analysis showed that there were peaks for various multiply-charged species of the target PNA oligomers **132** (Appendix 2) and **133** (Appendix 3).

3.3.1.2 Solid phase PNA synthesis with incorporation of monomer 123

An alkyne function can be introduced at the *N*-terminus of PNA oligomers by coupling of the commercially available 4-pentynoic acid during the solid phase peptide synthesis. This opens the possibility to construct a new modified monomeric unit, as a linkage along PNA structure, which can be ligated via the click (CuAAC) reaction. To investigate the effect of this linker on the properties of PNA oligomers, and to make a comparison with novel monomeric unit **121**, a novel monomer **123** was designed. This can be used as a model for general ligation linkages of this type and is synthesised as described in Chapter 2.

In order to investigate the effect of this novel compound **123** on the binding properties of PNA oligomers, a single monomeric unit was incorporated at the central position of the unmodified sequence of PNA oligomer **131** (Figure 3.4). However, incorporation of this independent monomeric unit **123** led to synthesis of a new modified 9-mer PNA oligomer **134** (Figure 3.7) which is longer than the unmodified PNA oligomers **131**, although they have a same number and sequence of the nucleobases.

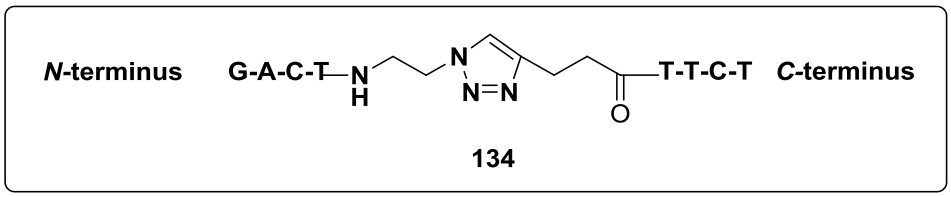

134

Figure 3.7: Structure of PNA oligomer **134**.

Our key for incorporation of novel monomer **123** into the PNA sequence is the manual solid phase PNA synthesis following the standard Fmoc strategy that was described in Section 3.2.1. For the same reasons that were described for the synthesis of the modified PNA oligomer **133** (Figure 3.6), PNA oligomer **135** (Figure 3.8) was designed as a model to investigate the effect of the monomeric unit **123**

adjusting to the lysine moiety.

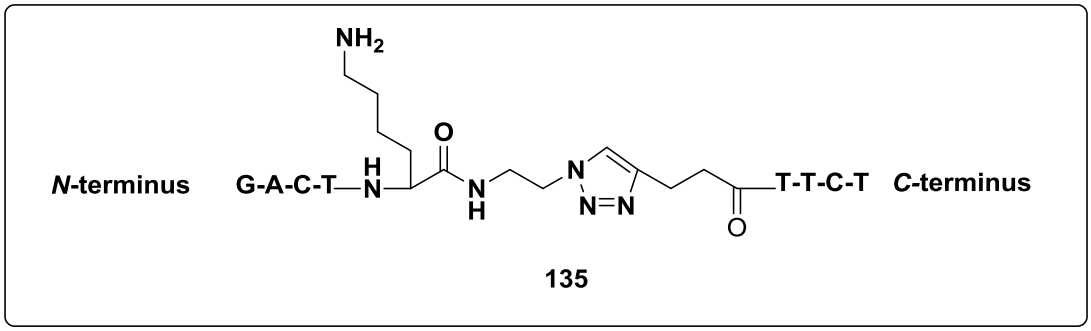

Figure 3.8: Structure of PNA oligomer **135**.

For synthesising the target modified PNA oligomer **135**, a single unit of lysine amino acid was incorporated into the PNA oligomer **134** (Figure 3.7) adjacent to the monomeric unit **123** during Fmoc solid phase synthesis strategy that was described in section 3.2.1. Synthetically, incorporation of the Fmoc-protected monomer **123** and Fmoc/Boc protected lysine amino acid into PNA oligomers **134** and **135** was achieved under the standard conditions that were employed for oligomerization of Fmoc/Bhoc PNA monomers without any problem observed.

HPLC analysis and mass spectra showed that the novel 1,2,3-triazole functionalized monomer **123** was incorporated successfully into the target PNA oligomers **134** and **135**. The crude PNA oligomers **134** and **135** were purified by RP-HPLC and characterized by LC-MS. Mass spectrometric analysis showed that there were peaks for various multiply-charged species of the target PNA oligomers **134** (Appendix 4) and **135** (Appendix 5).

3.3.1.3 Solid phase PNA synthesis with incorporation of monomer 126

Further investigations into the 1,2,3-triazole functionalised PNA oligomers were performed by incorporating the novel Fmoc/Boc-protected triazole functionalised monomer **126** into 8-mer PNA oligomer **131** (Figure 3.4) to generate a new 9-mer modified PNA oligomer **136** as shown in Figure 3.9.

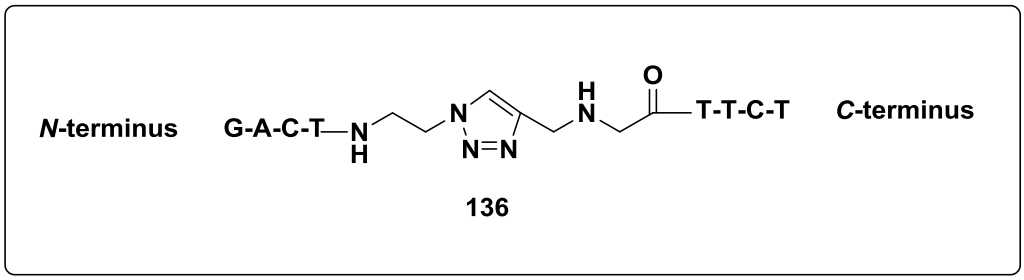

136

Figure 3.9: Structure of PNA oligomer **136**.

As was mentioned in chapter two, our interest in incorporating this monomeric unit is to model the ligation linker that can be seen in the PNA structures that have been ligated via click reaction. This click ligation linker can be formed when the synthesised compound **125** was used introduce an alkyne function to the *N*-terminus of PNA oligomers during oligomerization. Comparing to the novel monomers **121** and **123**, this novel monomeric unit **126** introduces a secondary amino function to the PNA oligomers in addition to the 1,2,3-triazole moiety. Thus, to investigate if this secondary amine enhances their binding affinity and thermal stability of PNA/DNA or PNA/RNA duplexes compared to monomer **123** that does not contain this secondary amino function, the modified PNA oligomer **136** was designed.

Like monomer **123**, a single unit of monomer **126** was incorporated at the central position of the unmodified PNA sequence **131** (Figure 3.4) to produce also a new modified 9-mer PNA oligomer **136** (Figure 3.9). This novel monomeric unit **126** was incorporated successfully into PNA oligomer **136** following the manual Fmoc solid phase peptide synthesis methodology that was described in section 3.2.1. The standard conditions used for oligomerisation the Fmoc/Bhoc protected AEG PNA monomers were used without any problem observed. After cleavage form the resin, the crude PNA oligomer was purified by RP-HPLC and characterised by LC-MS. Mass spectrometric analysis showed that there were peaks for various multiply-charged species of the target PNA sequence **136** (Appendix 6).

3.3.2 Rationale for synthesis of azide-alkyne functionalised PNA oligomers

Peptide nucleic acid oligomers (PNAs) can hybridise to the natural oligonucleotides following Watson-Crick or Hoogsteen base pairing rules, thereby being promising tools for antisense and antigene applications. However, in specific applications, easily synthetically accessible PNA is much shorter in length than the target sequences of nucleic acids. For example, a long sequence of PNA is required for blocking the complementary sequence of HAS2-AS effectively, as in the aim of this study.

Because the solid phase synthesis of PNAs is unable to assemble sequences longer than 20 nucleobases in length,[169] the alternative approach to the chemical synthesis of long PNA oligomers is to join PNA oligomers together by native chemical ligation methods (NCL). Native chemical ligation is an efficient method for the convergent synthesis of proteins and peptides that has been reported to overcome this problem or to conjugate peptide with nucleic acids.[170] NCL allows two peptide fragments to be joined in a covalent peptide bond at the site of ligation and ligation only occurs at the *C*-terminal thiol-ester and *N*-terminal cysteine.

For NCL applications in the PNA field, Mattes *et al*.[115,171] and Ficht *et al*.[172] showed the first applications of a protocol for native chemical ligation (NCL) in templated reactions of PNA oligomers. They designed PNA oligomers, which contained a *C*-terminal glycine thioester, to react with a PNA bearing an *N*-terminal cysteine residue. However, the solid-phase synthesis of PNA-thioesters presents a challenge because *C*-terminus PNA-thioester oligomers cannot be prepared easily by SPPS and they are subject to cyclization reactions which furnish six-membered lactams.[113] Furthermore, as we are interested in ligation of three PNA oligomers, the expected PNA sequence will have two residues of cysteine which is one of the most reactive residues that can possibly influence the proper folding of PNA sequences or can distort and influence the proper folding of PNA by formation of disulfide bonds between each other.

Currently, the copper (I) azide- alkyne cycloaddition reaction (CuAAC) could be represented as a promising method to facilitate ligation of PNA oligomers via formation of triazole ring as a biocompatible chemical linkage, which mimics the

normal amide bond in PNA structure. Herein, we are interested in ligation of three 10-mer mixed purine-pyrimidine PNA oligomers through CuAAC reaction to prepare a long sequence of PNA, specifically for preventing a duplex formation between mRNA of HAS2 and its natural antisense HAS2-AS through blocking HAS2-AS sequences.

This type of approaches for ligation of PNA is required the synthesis of PNA oligomers functionalized with azide and alkyne groups, and then these PNA oligomers can be joined by splint mediated ligation to produce a triazole linkage at the ligation site. To do this, the azide and alkyne functions were chosen to be installed during the solid phase PNA synthesis at the *N*/*C* termini of the target sequences through a linkage that should be stable towards solid phase conditions employed for the deprotection and cleavage of the PNA oligomers from the solid support. Furthermore, all three PNA sequences that were designed to be tested in the click ligation will have a lysine residue at the *C*-terminus in order to enhance their solubility in water.

3.3.2.1 Solid phase synthesis of azide-functionalized PNA oligomer 137

Our first attempt to synthesise the azide/alkyne functionalized PNA oligomers started with synthesis of the designed azide functionalized PNA oligomer **137** (Figure 3.10). Synthesis of the new PNA oligomer **137** was carried out smoothly following the standard procedure of the Fmoc strategy using the commercially available the Fmoc/Bhoc AEG PNA monomers that was described in Section 3.2.1. The particular Fmoc-protected Azido Nova Tag resin was used as a solid support for the synthesis of this PNA oligomer. This resin will introduce the required azido function as a 2-aminoethyl group attached at the *C*-terminus of the target PNA oligomer **137** as shown in Figure 3.10.

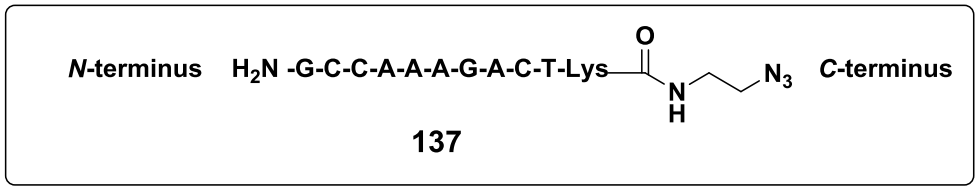

Figure 3.10: Structure of azide-functionalized PNA oligomer **137**.

After cleavage from the resin, the crude PNA oligomer **137** was purified by RP-HPLC and characterized by LC-MS. Mass spectrometric analysis showed that there were peaks for various multiply-charged species of the target sequence **137** (Appendix 7).

3.3.2.2 Solid phase synthesis of azide-alkyne functionalized PNA oligomer 138

As we are interested in ligation of three PNA sequences, one of them should be designed to accommodate two click ligation linkages. For this purpose, the new PNA oligomer **138** was designed to be functionalized with azide function at the *C*-terminus and alkyne function at the *N*-terminus. Similar to the azide functionalized PNA oligomer **137** (Figure 3.10), PNA oligomer **138** was synthesised on the Azido Nova Tag resin following the standard Fmoc solid phase strategy using the Fmoc/Bhoc protected AEG PNA monomers that was described in Section 3.2.1. However, the last coupling of synthesis this PNA oligomer **138** was achieved by using our novel alkyne functionalized PNA monomer **115** rather than the Fmoc-protected AEG thymine PNA monomer. This modified PNA monomer **115** will introduce an alkyne function at the *N*-terminus of the target PNA oligomer **138** as shown in Figure 3.11.

Figure 3.11: Structure of azide-alkyne functionalised PNA oligomer **138**.

Our novel monomer **115** was incorporated successfully at the *N*-terminus of PNA oligomer **138** under the same conditions that were used for oligomerisation of the

Fmoc/Bhoc AEG PNA monomers with no issue observed. After cleavage from the resin, the crude PNA oligomer **138** was purified by reverse phase HPLC and characterized by LC-MS. Mass spectrometric analysis showed that there were peaks for various multiply-charged species of the target sequence **138** (Appendix 8).

3.3.2.3 Solid phase synthesis of alkyne-functionalized PNA oligomer 139

The third target PNA sequence that was chosen to be ligated by the click ''CuAAC'' reaction is the alkyne functionalised PNA oligomer **139** as shown in Figure 3.12.

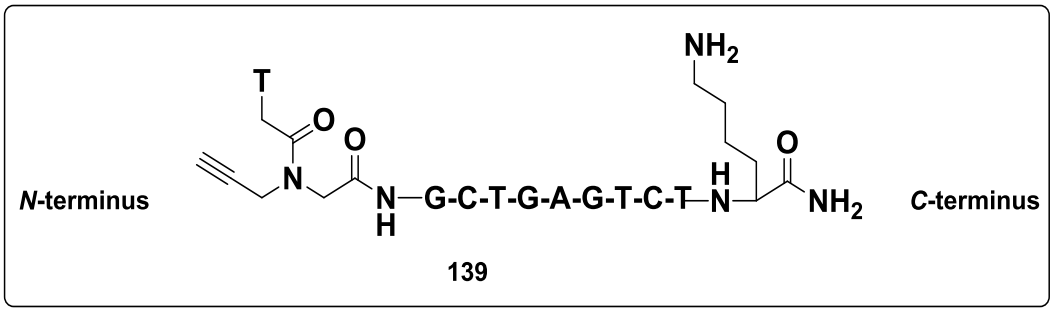

Figure 3.12: Structure of an alkyne functionalized PNA oligomer **139**.

This new PNA oligomer was synthesised on the Rink Amide MBHA resin using the Fmoc/Bhoc AEG protected PNA monomers as described in Section 3.2.1. In order to introduce an alkyne function at the *N*-terminus of the PNA oligomer **139**, the last coupling reaction was achieved smoothly with our novel alkyne functionalised thymine PNA monomer **115**. This modified monomer was also coupled instead of the Fmoc-protected AEG thymine PNA monomer under the same conditions that were used for oligomerization the Fmoc/Bhoc-protected AEG PNA monomers. After cleavage from the resin, the crude PNA oligomer **139** was purified by reverse phase HPLC and characterized by LC-MS. Mass spectrometric analysis showed that there were peaks for various multiply-charged species of the target sequence **139** (Appendix 9).

3.3.3 Preliminary attempt to ligate PNAs via click reaction

Having made the target azide and alkyne functionalized PNA oligomers **137**, **138** and **139**, we turned our attention to trying to ligate them through copper (I)-catalysed

azide-alkyne cycloaddition reaction ''click reaction'' which is a concept that was developed to join an azide and alkyne functionalized organic molecules under mild conditions.

Principally, to enhance the ligation reaction and to ligate the target sequences in the correct order, a templated method is required. In other words, a sequence specific template should bind to the PNA sequences and align the functional groups such that a reaction is facilitated. Furthermore, templates will enhance the proximity of the azide and alkyne functions of the PNA oligomers. Therefore, this preliminary attempt involved a templated two-step methodology for the ligation of the synthesised PNA oligomers **137, 138** and **139** as shown in Scheme 3.6.

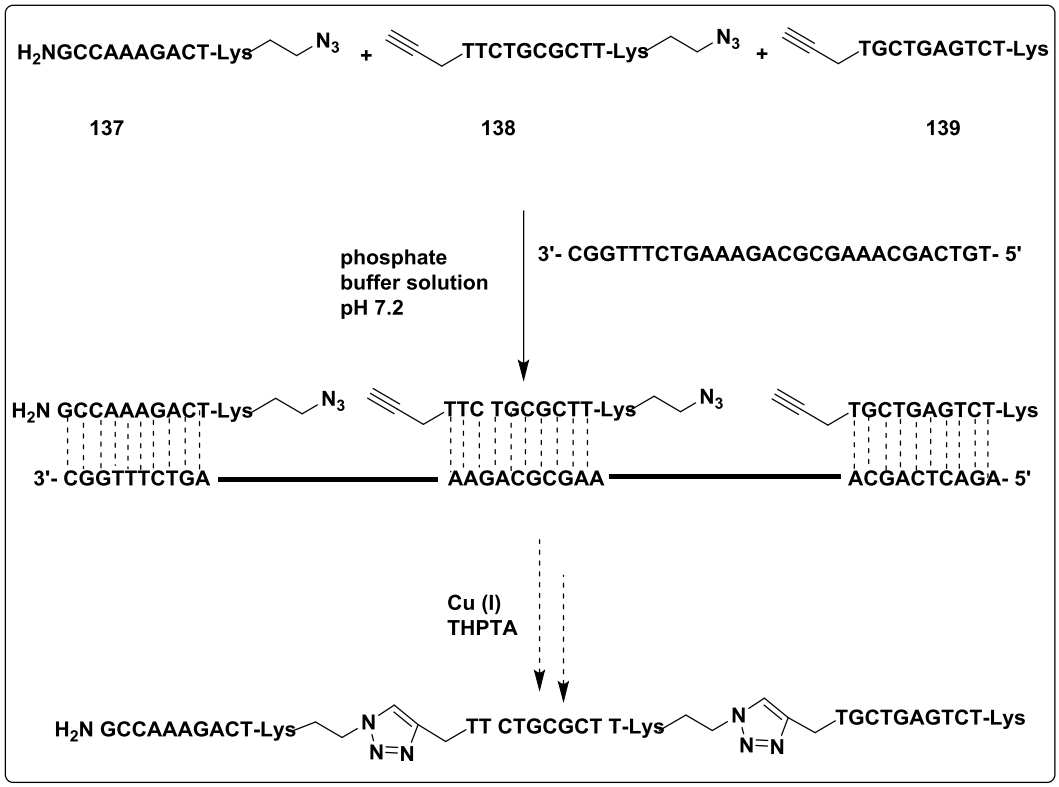

Scheme 3.6: Proposed synthetic route for the ligation of PNA oligomers.

The first step of our method involved hybridising the target PNA oligomers **137**, **138** and **139** with a complementary sequence of DNA as a template. In this study, both antiparallel and parallel complementary sequences were separately used as templates. This hybridization was achieved by mixing the PNA oligomers **137**, **138**

and **139** with a DNA sequence as a template (Table 3.1) in 10 mM phosphate buffer solution containing 10 mM NaCl at pH 7.2. The sample was heated up to 90 °C in a heat block over one hour followed by slow cooling to 4 °C. In the second step, an aqueous solution containing copper (I) in the presence of an excess of sodium ascorbate as reducing agent to keep producing Cu (I) *in situ* during the click ligation reaction. An excess of THPTA was used as a ligand to prevent degradation of the DNA template. Click (CuAAC) ligation was performed using different concentrations of the PNA oligomers, DNA templates, copper source and sodium ascorbate as shown in table 3.1.

Table 3.1: Concentrations used in the copper-catalysed cycloadditions reactions.

No. Exp.	Azido-PNA	Azido-alknyoic PNA	Alkyne-PNA	DNA template	Cu Source	Na-ascorbate	THPTA
1	50.0 nM	50.0 nM	50.0 nM	50.0 nM	$CuSO_4$ 1.0 eq.	5.0 eq.	10.0 eq.
2	50.0 nM	50.0 nM	50.0 nM	60.0 nM	$CuSO_4$ 10.0 eq.	50.0 eq.	25.0 eq.
3	50.0 nM	50.0 nM	50.0 nM	50.0 nM	Cu OAc. 5.0 eq.	0.0 eq.	50.0 eq.
4	50.0 nM	50.0 nM	50.0 nM	60.0 nM	Cu Ac. 20 eq.	100.0 eq.	100.0 eq.

The reactions were kept at room temperature for different times such as 2, 4, 8 and 24 hours before being worked up. The crude reaction mixtures were first analysed RP-HPLC and mass spectrometry. Although the HPLC chromatograms and mass spectrometric analysis showed a disappearance of the peaks belonging to the PNA starting material, they did not show any significant peaks. Therefore, many methods for reverse phase HPLC analysis were set up in an attempt to get the desired product. However, all peaks that were collected by HPLC analysis and checked by mass spectrometry did not show matches with the calculated mass of the expected product or the starting material. Due to the expected product being composed of 30 nucleobases in length, it was believed this long PNA oligomer was still binding to the DNA template tightly by hydrogen bonding and the resultant duplex cannot be denatured under HPLC analysis conditions. An attempt to denature this PNA/DNA

hybridization by addition of TFA was also unsuccessful in making significant changes in HPLC analysis or mass spectra.

A parallel PNA/DNA duplex was considered for further investigation as this is less stable than their corresponding antiparallel duplex and may be denatured easily compared to antiparallel duplex. A parallel complementary DNA sequence was used as a template under the same conditions that were used with antiparallel hybridization for click ligation. However, this attempt also failed to provide the target product.

For further investigations to verify if the target product was still binding to DNA template, two short complementary parallel 8-mer DNA sequences were designed to hybridise with PNA by the ends bearing the azide and alkyne functions. Unfortunately, this attempt was unsuccessful in giving the PNA target sequence. On the other hand, all mass spectra that were run for the crude click ligation reactions did not indicate peaks belonging to the PNA oligomers starting materials and the expected product.

Many efforts and a long time were exerted to optimise this method, as if successful, it would represent a novel and relatively simple method for the ligation of three or more PNA oligonucleotides. Unfortunately, we have been unsuccessful to obtain the target product. However, at this point, we really can not specify if this reaction has failed or not because there is no evidence that confirms which the case is. However, the future work might be led to significant results.

Chapter Four

Biophysical Studies of PNA/DNA and PNA/RNA duplexes

4.1 Introduction

As described previously, peptide nucleic acids (PNAs) are synthetic DNA mimics, in which the negatively charged phosphate-sugar backbone of DNA is replaced by an uncharged achiral poly *N*-(2-aminoethyl) glycine backbone which is connected to a nucleobase via a methylene carbonyl linker. This backbone structure is a key feature of PNAs compared to other DNA analogues. One impressive feature of PNA sequences is their ability to recognize and bind with high affinity and sequence selectivity to complementary sequences of DNA and RNA through Watson-Crick and/or Hoogsteen base pairing. This is predominantly due to the lack of electrostatic repulsion between the neutral PNA strand and the negatively charged nucleic acid strand. Even more interestingly, the formed PNA/DNA and PNA/RNA complexes exhibit a higher thermal stability than their corresponding traditional duplexes and the antiparallel complexes always display much higher thermal stability than parallel hybridization. Moreover, PNA/RNA duplex is more stable than PNA/DNA duplex. An additional consequence of the uncharged nature of polyamide PNA backbone structure is that the thermal stability of PNA/DNA and PNA/RNA complexes are virtually independent of the salt concentration and pH in the hybridization solution. On other words, these thermal stabilities are not significantly affected by changes in the ionic strength.

As a general rule, the melting temperature (T_m) of a PNA/DNA duplex is 1°C on average higher per base pair relative to that of the corresponding DNA/DNA duplex.[173,174] On the other hand, the thermal stability of PNA hybrids is significantly affected by the presence of any mismatching sections.[175,176] Such presence of mismatches in a PNA/DNA duplex is much more destabilising than a mismatch in their corresponding natural nucleic acid complexes. For example, a single base mismatch results in a drop of 15 °C and 11 °C in the T_m of a 15-mer PNA/DNA and DNA/DNA duplex respectively.[136] Specifically, this feature of PNA is responsible for the remarkable discrimination between perfect matches and mismatches offered by PNA probes, and makes PNA sequences so attractive as oligonucleotide recognition tools in biosensor technology. Although, the unique characteristics of PNAs have led to the development of a wide range of important applications, PNAs are not yet a

fully developed tool with some issues still being outstanding. The most problematic of these are their low water solubility, poor cell permeability and a limit to the length of sequences that can be prepared by solid phase peptide synthesis strategies. Thus, in order to overcome these limitation, there is ongoing research on developing and incorporating new monomers into PNA oligomers' structure. In addition to looking for new methods to extend PNA lengths for applications that require long PNA sequences. As the thermal stability of PNA complexes is crucial for their application, it is necessary that all the target modifications improve or maintain the same thermal stability of the modified duplexes, compared to the unmodified duplexes. In general, these complexes mediate the antigene and antisense effects of PNAs via the steric blockade of enzyme complexes responsible for DNA transcription and RNA translation. The binding affinity of PNA oligomers toward nucleic acids and thermal stability of their PNA/DNA and PNA/RNA complexes can be assessed by several different biophysical techniques. The most frequently used of these being temperature dependent UV-spectroscopy (UV-T_m),[50] Circular Dichroism (CD)[50,177] and Differential Scanning Calorimetry (DSC).[178]

4.2 UV-Spectroscopic study of biophysical properties of PNA complexes

The measurement of the UV absorbance as a function of the temperature (UV-Tm) is the standard approach to investigate the hybridization properties of PNA oligomers. In DNA/DNA, RNA/RNA and PNA/DNA complexes, the nucleobases can interact with each other, via their π electron clouds, when the nucleobases in the complex are stacked together when dissolved in water. Because the UV absorbance of the bases is a consequence of π electron transitions, the magnitude of these transitions is highly affected by this base stacking. For this reason, monitoring the UV absorption at 260 nm as a function of temperature has been extensively used to study the thermal stability of PNA/DNA and PNA/RNA duplexes.

Practically, an increase in the temperature induces denaturation of the PNA/DNA or PNA/RNA complexes into their separate individual strands. This occurs because of the diminishing stacking interaction between adjacent bases, and disruption of hydrogen bonds between base pairs, leading to a complete loss of secondary

structure. Consequently, the UV absorbance that is recorded at 260 nm will increase with the temperature, in an effect termed as "hyperchromicity".[179] The process is co-operative, and the plot of the absorbance values at 260 nm vs. temperature is sigmoidal (Figure 4.1). Having the sigmoidal curves indicates the presence of a binding affinity between PNA and nucleic acids, and the midpoint of this sigmoidal transition represents the melting temperature of the formed duplex. This is in turn termed T_m, and is defined as the temperature at which 50% of the complexes have been dissociated.

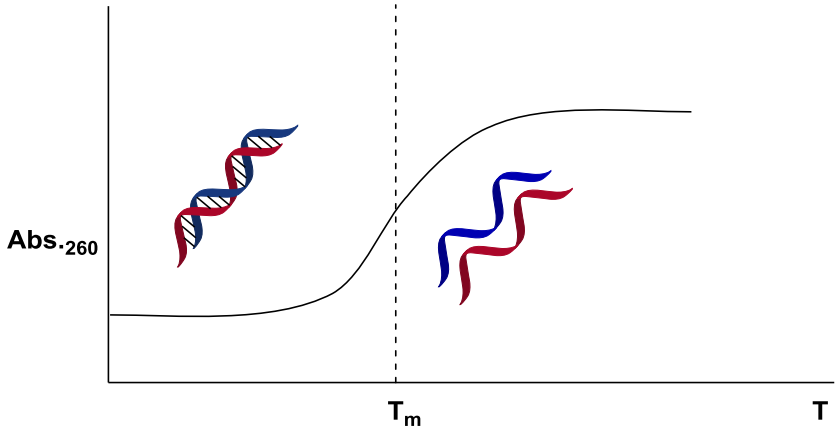

Figure 4.1: The sigmoidal graph of UV-T_m.

The sigmoidal nature of the transition suggests that at any temperature, nucleic acids exist in two states, as duplexes or as single strands, and at varying temperatures the relative proportions of the two states change. A non-sigmoidal (e.g. sloping linear) transition, with low hyperchromicity, is a consequence of non-complementary hybridisation. This chapter addresses the biophysical studies of various modified PNA oligomers, and their hybrids formed with complementary sequences of DNA and RNA, using temperature-dependent UV spectroscopy. The biophysical studies have been carried out on a series of the designed PNA sequences, explored in earlier chapters. The resulting data has allowed us to investigate the effect of the incorporated novel monomeric units on the binding affinity to target nucleic acids, and the resulting duplex stability.

4.3 Results and Discussion

As shown in previous chapters, it is now possible for PNA to be extended by a click (CuAAC) reaction through 1,2,3-triazole formation as the ligation linker. Consequently, based on the structure of the azide and alkyne group precursors, different ligation linkages will be constructed in the structure of the extended PNA sequence. These modified PNA sequence is therefore being longer than the standard AEG PNA sequence and the target nucleic acids sequences despite having the same number of nucleobases. In general, most of the PNA modifications explored resulted in a lower thermal stability compared to their corresponding unmodified complexes.[180] The incorporation of PNA monomers with an extended backbone, into standard PNA oligomers, reduced the thermal stability of the modified PNA/DNA duplexes compared to the corresponding unmodified duplexes.[93] Thus, one challenge to be investigated is that the click reaction will result in an extended monomeric unit in the structure of the extended PNA sequence. For this reason, we are interested in investigating the effect of these click reaction linkages on the binding properties of PNA oligomers. This was achieved by incorporation of a single of monomeric unit of **121**, **123** and **126** (Figure 4.2), at the central position of a specific 8-mer mixed pyrimidine-purine PNA sequence, during the Fmoc solid phase peptide synthesis strategy as described in Chapter three. Thus, a series of modified 1,2,3-tiazole functionalised PNA oligomers were synthesised as models, mimicking the products of the click ligation.

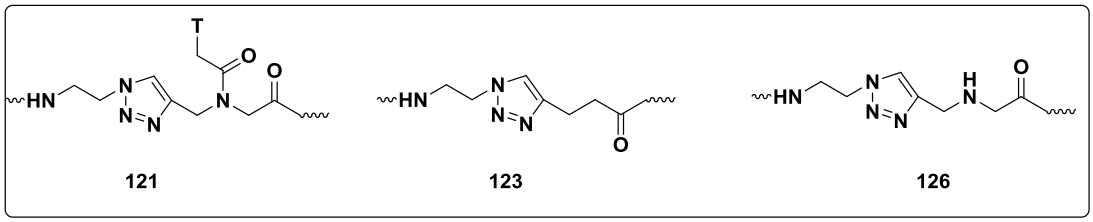

Figure 4.2: Structure of novel monomers **121**, **123** and **126**.

4.3.1 UV-T_m studies of the modified PNA oligomers with DNA

For potential antigene applications, the ability of the target triazole-containing PNA

oligomers to form duplexes was studied with two complementary antiparallel sequences of DNA, an 8-mer (**DNA1**, T_m= 15 °C) and a 9-mer (**DNA2**, T_m=19 °C). As the thermal stability of PNA/DNA duplexes is considerably lowered by the presence of mismatches, the 9-mer sequence was designed with a mismatch nucleobase relative to the target PNA sequences that were prepared as models to investigate the effect of novel monomeric units. This base is located at the centre of **DNA2** sequence to correspond the site of these modified monomeric units in the modified PNA strand during PNA/DNA duplex formation. In the present study, the cytosine deoxynucleotide monomer was chosen for this purpose.

This binding affinity of the modified PNA oligomer and their complexes' stability were evaluated by temperature dependent changes in their UV-absorbance which resulted in distinct melting curves. The absorbance at 260 nm was plotted as a function of the temperature. The T_m values were obtained from an average of the mid-points of the three sigmoidal thermal stability curves for each duplex with the standard deviation for these measurements. The binding properties of all modified PNA/DNA duplexes were analysed compared to their corresponding unmodified **131/DNA1** duplex (T_m= 26.0 ±0.9 °C) and **131/DNA2** (T_m= 28.0 ±0.8 °C)

4.3.1.1 UV-T_m studies of PNA/DNA duplexes modified with monomer 121

In order to investigate the effect of the novel thymine PNA monomer **121** on the binding properties of the corresponding PNA/DNA duplexes, the modified PNA oligomers **132** and **133**, each containing a single monomeric unit of **121**, were first hybridised with an antiparallel complementary 8-mer sequence of DNA (**DNA1**). PNA oligomer **133** containing a single unit of lysine was incorporated adjusting to the monomer **121** as described in Chapter 3**.** The resulting **132/DNA1** and **133/DNA1** duplexes were subsequently studied by T_m-dependent UV-absorbance experiments (Figure 4.3).

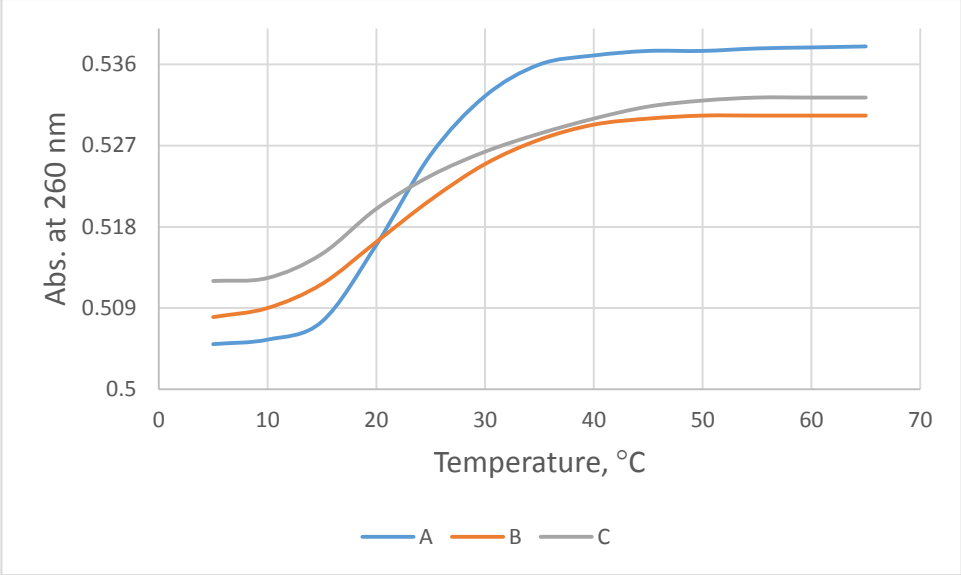

Figure 4.3: Comparison of the UV-melting curves of the duplex formed between **DNA1** and (A) unmodified PNA oligomer (**131**), (B) modified PNA oligomer **132** and (C) modified PNA oligomer **133**. Performed in a buffer of 10 mM potassium phosphate and 10 mM NaCl at pH 7.0.

By the sigmoidal shape of the curves (Figures 4.3) that resulted from UV-melting experiments, it could be concluded that our novel thymine PNA monomer **121** does not prevent the corresponding PNA oligomer **132** from binding to the antiparallel complementary 8-mer sequence of DNA (**DNA1**). Even with the presence of the lysine moiety beside monomer **121**, the corresponding PNA oligomer **133** still displayed an ability to bind to the target DNA sequence. One more item of note can be taken from the shape of the curves belonging to the modified **132**/**DNA1** and **133**/**DNA1** duplexes. These curves are slightly different compared to the unmodified **131**/**DNA1** duplex that resulted in the standard sigmoidal shape. This difference can be attributed to the incorporation of modified PNA monomer **121** which consists of an extended backbone. Consequently, this led to PNA sequences being synthesised that is longer than the unmodified PNA sequence as described in Chapter 3. This, along with the geometry of monomer **121**, results in a strand which may not be as compatible with the duplex formation geometry compared to the AEG PNA monomers.

The T_m values that are given in Table 4.1 indicate that the incorporation of a single

monomeric unit of the novel thymine PNA monomer **121** into PNA oligomer **132** slightly decreased the thermal stability the corresponding modified **132/DNA1** compared to the corresponding unmodified duplex **131/DNA1**. Whereas, incorporation of lysine moiety into the PNA oligomer **133** reduced the thermal stability of the corresponding **133/DNA1** duplex compared to the modified **132/DNA1** and unmodified **131/DNA1** duplexes.

Table 4.1: T_m values of antiparallel PNA/DNA1 duplexes modified with the monomeric PNA unit **121** (**X**). ΔT_m indicates the difference in T_m with the control unmodified **131/DNA1**.

PNA code	**PNA sequence** *N*-terminus *C*-terminus	**DNA1: 3' C-T-G-A-A-A-G-A 5'**	
		UV-T_m °C	**(ΔT_m) °C**
131	**G-A-C-T-T-T-C-T**	**26.0 ± 0.9**	**-**
132	**G-A-C-T-X-T-C-T**	**24.6 ± 0.8**	**-1.4**
133	**G-A-C-T-lys-X-T-C-T**	**23.0 ± 0.8**	**-3.0**

For further investigation, the effect of monomer **121** was also verified in the presence of a mismatch base in the DNA sequence. This was achieved by hybridization of the corresponding PNA oligomers **132** and **133** with antiparallel 9-mer complementary sequence of DNA (**DNA2**). From the shape of the curves (Figure 4.4) that resulted from T_m-dependent UV-absorbance experiments, an important conclusion was reached. The modified **132/DNA2**, **133/DNA2** and even unmodified **131/DNA2** have all given distorted curves, compared to the standard sigmoidal shape. This expected distortion could be attributed to fact that the **DNA2** sequence is longer than the PNA oligomers **131**, **132** and **133**. This difference in the length may be preventing the matching bases from pairing, resulting in slight mismatch character and loss of cooperativity. However, both modified PNA oligomers **132** and **133** also still showed some binding affinity with antiparallel complementary 9-mer DNA sequence (**DNA2**).

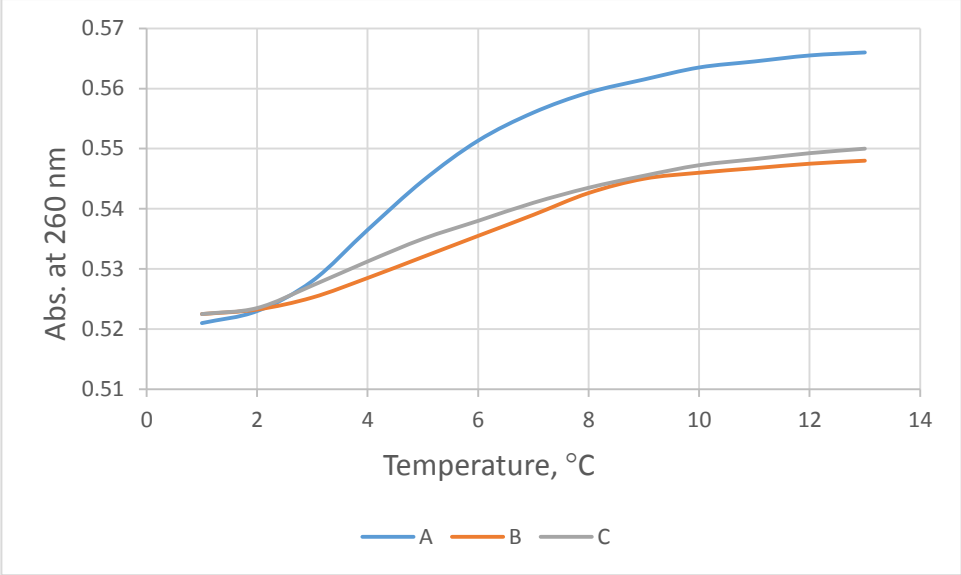

Figure 4.4: Comparison of the UV-melting curves of the duplex formed between **DNA2** and (A) unmodified PNA oligomer **131**, (B) modified PNA oligomer **132** and (C) modified PNA oligomer **133**. Performed in a buffer of 10 mM potassium phosphate and 10 mM NaCl at pH 7.0.

The T_m values (Table 4.2) revealed that the incorporation of a single modified PNA monomer **121** almost kept the same thermal stability of the **132/DNA2** duplex that was resulted for the unmodified **131/DNA2**. However, incorporation of lysine moiety associated with monomer **121** reduced the thermal stability of the corresponding **133/DNA2** duplex compared to both the modified **132/DNA2** and unmodified **131/DNA2** duplexes.

Table 4.2: T_m values of antiparallel PNA/DNA2 duplexes modified with monomeric PNA unit **121 (X)**, ΔT_m indicates the difference in T_m with the control unmodified **131/DNA2** duplex.

PNA code	**PNA sequence** *N*-terminus *C*-terminus	**DNA2: 3' C-T-G-A-C-A-A-G-A 5'**	
		UV-T_m °C	**(ΔT_m) °C**
PNA 131	**G-A-C-T-T-T-C-T**	**28.0 ± 0.9**	**-**
PNA 132	**G-A-C-T-X-T-C-T**	**28.7 ± 0.3**	**+0.7**
PNA 133	**G-A-C-T-lys-X-T-C-T**	**25.0 ± 0.9**	**-3.0**

4.3.1.2 UV-T_m studies of PNA/DNA duplexes modified with monomer 123

As was mentioned in Chapter 3, the novel monomer **123** was incorporated as independent monomer into the model PNA sequence to mimic a new click ligation linker type that can be seen in the structure of the extended PNA sequences. Specifically, 4-pentynoic acid was used to introduce the alkyne function at the *N*-terminus of PNA oligomers. Structurally, unlike monomer **121**, monomeric unit **123** does not contain a nucleobase, thereby this monomeric unit acts as a spacer with no complementarity.

In order to investigate the effect of this type of click ligation, the hybridisation properties of the corresponding modified 9-mer PNA oligomers **134** and **135** were first tested with the antiparallel complementary 8-mer DNA sequence (**DNA1**), and evaluated by temperature dependent UV spectroscopy (Figure 4.5).

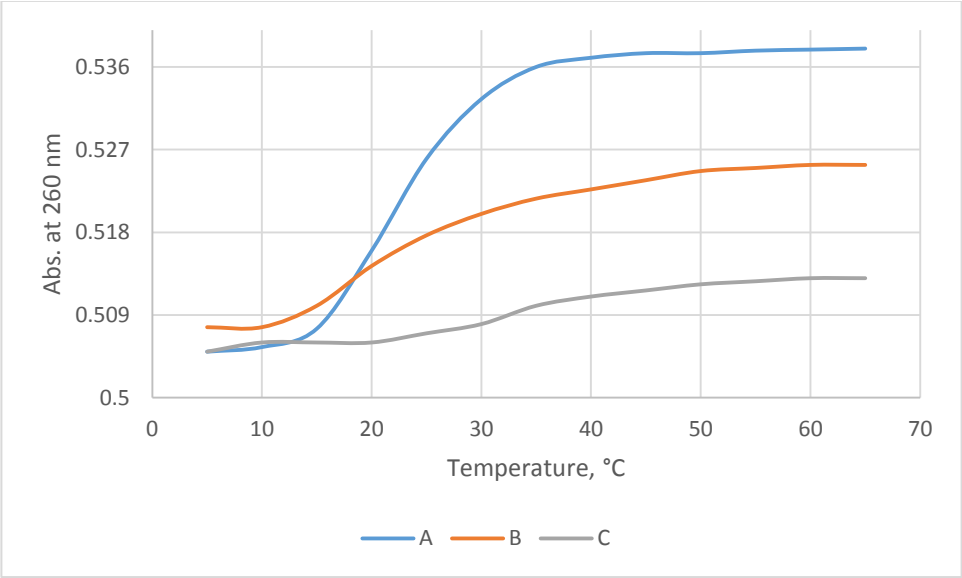

Figure 4.5: Comparison of the UV-melting curves of the duplex formed between **DNA1** and (A) unmodified PNA oligomer **131**, (B) modified PNA oligomer **134** and (C) modified PNA oligomer **135**. Performed in a buffer of 10 mM potassium phosphate and 10 mM NaCl at pH 7.0.

The thermal curves, which are shown in Figure 4.5, demonstrated that although the modified 9-mer PNA oligomer **134** is longer, with one extended monomeric unit **123** than the target 8-mer DNA sequence (**DNA1**), it still has some affinity towards the

duplex formation. However, the incorporation of both the lysine moiety associated with monomer **123** into PNA oligomer **135** reduced the binding affinity towards the DNA target and gave a non-sigmoidal plot. This lack affinity of PNA oligomers **135** can be imputed to that this PNA oligomer is considered the longest of the PNA sequences due to incorporation of both modifications.

Furthermore, the T_m values are listed in Table 4.3 showed that incorporation of a single novel monomeric unit of **123** decreased the thermal stability of the modified **134/DNA1** duplex compared to the unmodified **131/DNA1** duplex

Table 4.3: T_m values of antiparallel PNA/DNA1 duplexes that are modified with monomeric PNA unit **121** (**X**), ΔT_m indicates the difference in T_m with the control unmodified **131/DNA1**.

PNA code	**PNA sequence** *N*-terminus *C*-terminus	**DNA1: 3' C-T-G-A-A-A-G-A 5'**	
		UV-T_m °C	**(ΔT_m) °C**
PNA 131	**G-A-C-T-T-T-C-T**	**26.0 ± 0.9**	**-**
PNA 134	**G-A-C-T-X-T-T-C-T**	**21.7 ± 0.8**	**-4.3**
PNA 135	**G-A-C-T-lys-X-T-T-C-T**	**No duplex**	**-**

Again, to further investigate the effect of this independent monomeric unit **123** on the binding properties of PNA which contain it, the corresponding modified PNA oligomers **134** and **135** were investigated with antiparallel complementary 9-mer **DNA2** sequence. From the general appearance of the shape of the curves (Figure 4.6), it could be concluded that both modified oligomers **134** and **135**, have displayed an improved binding affinity with the **DNA2** sequence compared to their binding affinity with the **DNA1** sequence that was described in Figure 4.5. A reasonable explanation for this is that the difference in the length between these modified PNA oligomers and **DNA2** is less than with **DNA1**.

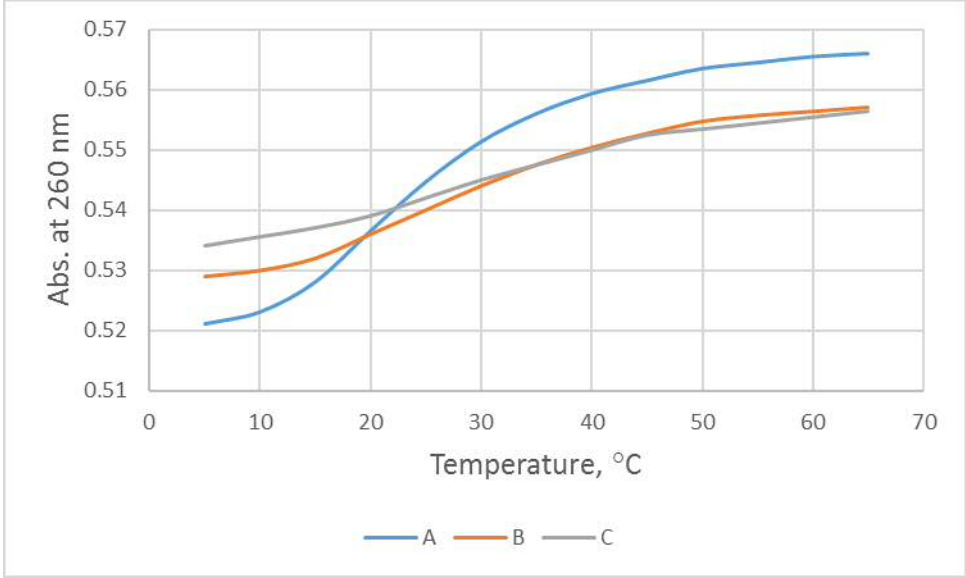

Figure 4.6: Comparison of the UV-melting curves of the duplex formed between **DNA2** and (A) unmodified PNA oligomer **131**, (B) modified PNA oligomer **134** and (C) modified PNA oligomer **135**. Performed in a buffer of 10 mM potassium phosphate and 10m M NaCl at pH 7.0.

The T_m values that are given in Table 4.4 have shown that the incorporation of **123** slightly destabilised the **134/DNA2** and **135/DNA2** duplexes compared to the corresponding unmodified **131/DNA2.** In a general conclusion, incorporation of monomer **123** displayed less thermal stability than monomer **121** for both PNA/**DNA1** and PNA/**DNA2** duplexes.

Table 4.4: T_m values of antiparallel PNA/DNA2 duplexes modified with monomeric unit **123 (X)**, ΔT_m indicates the difference in T_m with control unmodified **131/DNA2**.

PNA code	**PNA sequence** *N*-terminus *C*-terminus	**DNA2: 3' C-T-G-A-C-A-A-G-A 5'**	
		UV-T_m °C	**(ΔT_m) °C**
131	**G-A-C-T-T-T-C-T**	**28.0 ± 0.8**	**-**
134	**G-A-C-T-X-T-T-C-T**	**27.0 ± 0.8**	**-1.0**
135	**G-A-C-T-lys-X-T-T-C-T**	**25.6 ± 0.9**	**-2.4**

4.3.1.3 UV-T_m studies of PNA/DNA duplexes modified with monomer 126

As described for the above monomeric units, **121** and **123**, the novel monomeric unit **126** was studied as a potential click ligation linker of the extended PNA sequence. Specifically, once compound **124** was used to introduce the alkyne function at the *N*-terminus of PNA oligomers. Structurally, like monomer **123**, this monomer does not contain a nucleobase that was attached in monomer **121**, but it contains a secondary amino group that cannot be seen in either **121** or **123**. Thus, to study the effect of including monomeric unit **126** in PNA oligomers on its binding properties, the corresponding PNA oligomer **136** that contains a single monomeric unit of **126** was first hybridised to the complementary antiparallel **DNA1** (Figure 4.7).

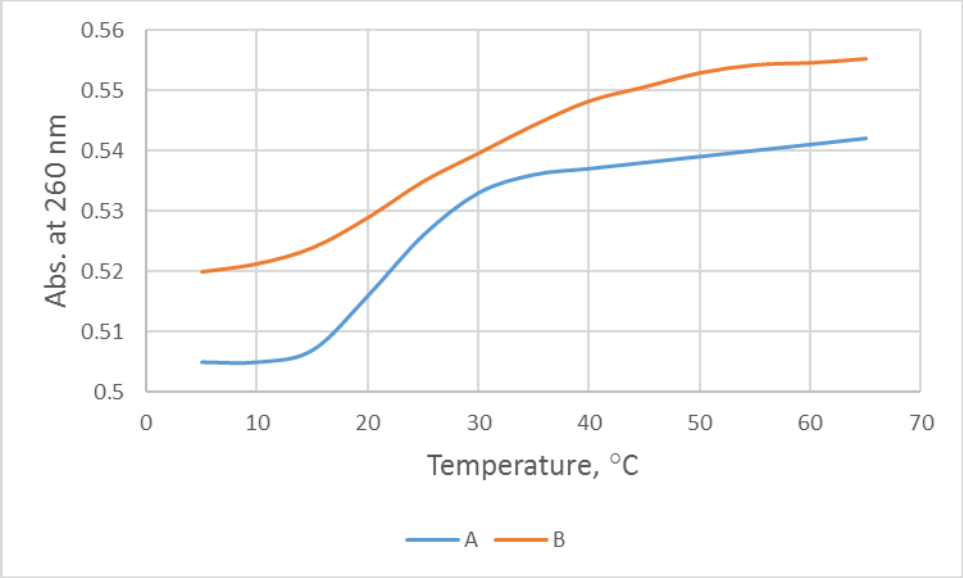

Figure 4.7: Comparison of the UV-melting curves of the duplex formed between **DNA1** and (A) unmodified PNA oligomer **131**, (B) modified PNA oligomer **136**. Performed in a buffer of 10 mM potassium phosphate and 10 mM NaCl 10 at pH 7.0.

From the shape of the curves that are shown in Figure 4.7, it is observed that the incorporation of a single monomeric unit **126** benefitted the binding affinity of the modified PNA oligomers **136**. However, like PNA oligomer **134** the modified PNA

oligomer **136** has an independent extra monomeric unit therefore being longer compared to the **DNA1** sequence. For this reason, the corresponding duplex **136/DNA1** has resulted in a distorted curve which is associated with a slightly decreased thermal stability as given in Table 4.5.

Table 4.5: T_m values of antiparallel PNA/DNA1 duplexes that are modified with monomeric PNA unit **126** (**X**), ΔT_m indicates the difference in T_m with control unmodified **131/DNA1** duplex.

PNA code	**PNA sequence** *N*-terminus *C*-terminus	**DNA1: 3' C-T-G-A-A-A-G-A 5'**	
		UV-T_m °C	**(ΔT_m)**
PNA 131	**G-A-C-T-T-T-C-T**	**26.0 ± 0.9**	**-**
PNA 136	**G-A-C-T-X-T-T-C-T**	**24.0 ± 0.9**	**-2.0**

As described for others PNA oligomers, the biophysical properties of the PNA oligomer **136** was also studied by hybridising with the 9-mer DNA sequence **DNA2**, to investigate whether this secondary amine group of this monomeric unit **126** can support this monomer to make a hydrogen bond with the spacer cytosine base on the DNA2 sequence. This was also performed using T_m-dependent UV absorbance experiments. The shape of the curve, belonging to the **136/DNA2** hybrid (Figure 4.8), allows us to conclude that the modified oligomer **136** has displayed an improved sigmoidal shape over the previous corresponding **136/DNA1**. This result also can once again be ascribed to the reduction in the difference in a length between the **136** and **DNA2** sequence, compared to **136** and **DNA1**.

The T_m values that are given in Table 4.6 have shown that incorporation of a single monomeric unit of compound **126** almost maintained the thermal stability of the modified **136/DNA** compared to the corresponding unmodified **131/DNA2**.

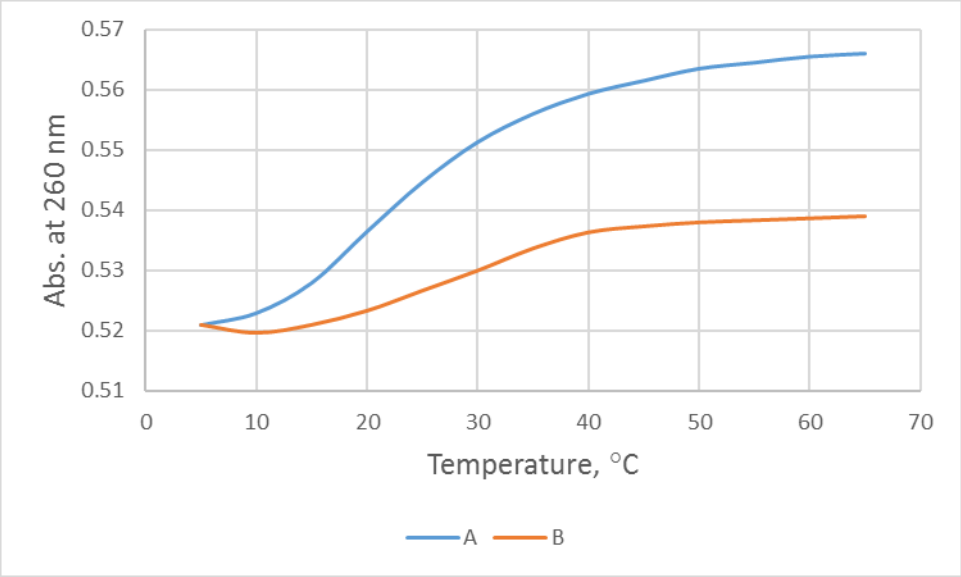

Figure 4.8: Comparison of the UV-melting curves of the duplex formed between **DNA2** and (A) unmodified PNA oligomer **131**, (B) modified PNA oligomer **136**. Performed in a buffer of 10 mM potassium phosphate and 10 mM NaCl at pH 7.0.

Table 4.6: T_m values of antiparallel PNA: DNA2 duplexes modified with monomeric PNA unit **126 (X)**, ΔT_m indicates the difference in T_m with control unmodified **131/DNA2** duplex.

PNA code	**PNA sequence** *N*-terminus *C*-terminus	**DNA2: 3' C-T-G-A-C-A-A-G-A 5'**	
		UV-T_m °C	**(ΔT_m) °C**
131	**G-A-C-T-T-T-C-T**	**28.0 ±0.9**	**-**
136	**G-A-C-T-X-T-T-C-T**	**28.6 ±0.9**	**+0.6**

4.3.2 UV- T_m studies of modified PNA oligomers with RNA

This section describes the hybridisation properties of the modified PNA oligomers with a complementary antiparallel RNA sequence (5' **AGAAAGUC** 3'), therefore displaying any differences in property enhancement between the DNA/PNA hybrids and the RNA/PNA hybrids.

As mentioned previously RNA/PNA hybrids tend to show more affinity towards each other and increased stability over their DNA counterparts, however it is important

to see how modifying the PNA monomers affects this observation. The binding properties of all modified PNA/RNA duplexes were analysed to their corresponding unmodified **131/RNA** duplex (T_m= 37 ±0.8 °C). As described for modified PNA/DNA1 duplexes, the modified PNA/RNA duplexes displayed distorted curves compared to the standard sigmoidal shape. Again, this distortion could be attributed to fact that the modified PNA sequences are longer than RNA sequences. This difference in the length may be preventing the matching bases from pairing, resulting in slight mismatch character and loss of cooperativity. Consequently, this may be leading to a change in the conformation of PNA/RNA duplexes thereby resulting in a decreased thermal stability.

4.3.2.1 UV- T_m studies of PNA/RNA duplexes modified with monomer 121

The modified PNA oligomers **132** and **133** that are containing a single unit of monomer **121** were hybridized to a complementary antiparallel RNA sequence to form PNA/RNA duplexes. Thus, this will use as a model to investigate the effect of the novel thymine PNA monomer **121** on the binding properties of potential RNA antisense PNA oligomers. The hybridisation properties were studied by T_m-dependent UV absorbance experiments. From the sigmoidal shape of the curves shown in Figure 4.9, it can be concluded that both modified PNA oligomers **132** and **133** still displayed the ability to bind with the antiparallel RNA sequence.

The melting profiles of PNA/RNA duplexes that have been derived from PNA oligomers **132** and **133** are listed in Table 4.7. However, these results showed that incorporating the monomeric unit **121** significantly destabilised the **132/RNA** duplex by (-13.8 °C) and **133/RNA** duplex by (-11.1 °C) compared to the unmodified **131/RNA** duplex.

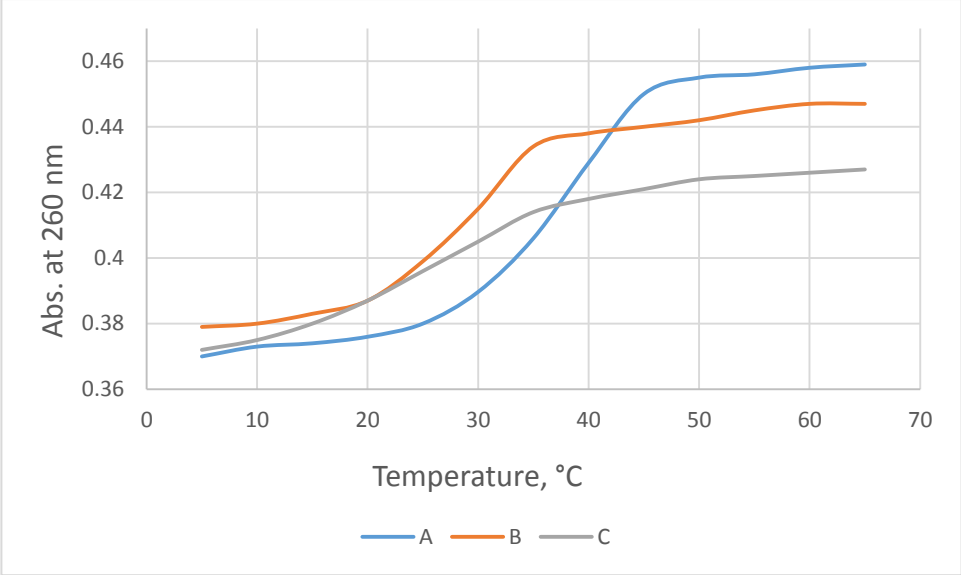

Figure 4.9: Comparison of the UV-melting curves of the duplex formed between RNA and (A) unmodified PNA oligomer **131**, (B) modified PNA oligomer **132** and (C) modified PNA oligomer **133** in a buffer of 10 mM potassium phosphate and 10 mM NaCl at pH 7.0.

Table 4.7: T_m values of antiparallel PNA/RNA duplexes modified with monomeric unit **121 (X)**, ΔT_m indicates the difference in T_m compared with control unmodified **131/RNA**.

PNA code	**PNA sequence** *N*-terminus *C*-terminus	**RNA: 3' C-U-G-A-A-A-G-A 5'**	
		UV-T_m °C	**(ΔT_m)**
131	**G-A-C-T-T-T-C-T**	**37.0 ± 0.8**	**-**
132	**G-A-C-T-X-T-C-T**	**23.2 ± 0.9**	**-13.8**
133	**G-A-C-T-lys-X-T-C-T**	**25.9 ± 0.9**	**-11.1**

4.4.2.2 UV- T_m studies of PNA/RNA duplexes modified with monomer 123

To investigate the effect of novel monomeric **123** on the potential RNA antisense PNA, the corresponding modified PNA oligomers **134** and **135** were hybridised as well with an antiparallel complementary RNA sequence. The hybridisation properties were also studied by T_m-dependent UV absorbance (Figure 4.10). To a

certain extent, the shape of thermal curves indicates that the modified PNA oligomers **134** and **135** still have an affinity towards binding the antiparallel complementary RNA sequence.

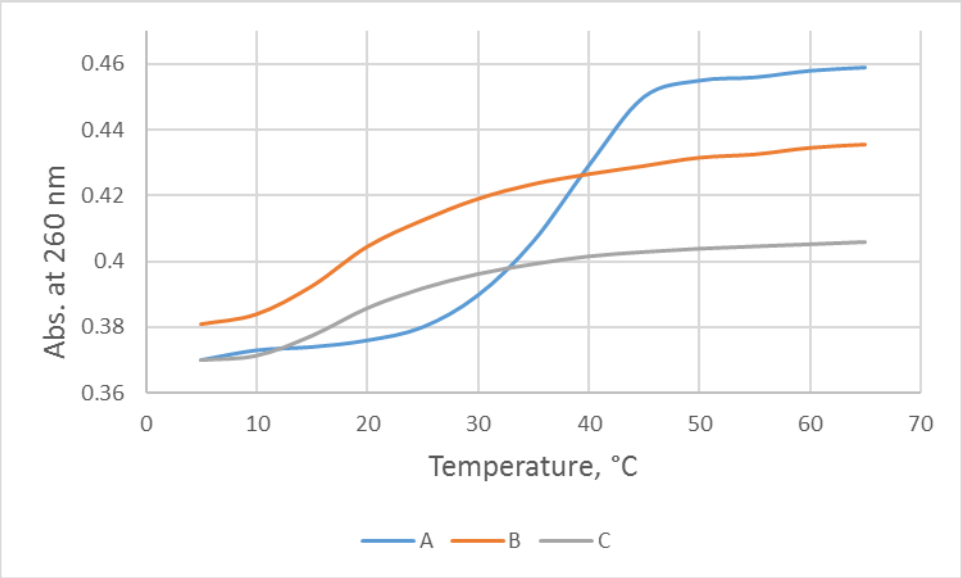

Figure 4.10: Comparison of the UV-melting curves of the duplex formed between RNA and (A) unmodified PNA oligomer **131**, (B) modified PNA oligomer **134** and (C) modified PNA oligomer **135**. Performed in a buffer of 10 mM potassium phosphate and 10 mM NaCl at pH 7.0.

However, the T_m values (Table 4.8) showed that the inclusion of novel monomeric **123** extremely reduced the thermal stability of the PNA/RNA duplexes, which resulted from the use of PNA oligomers **134** and **135**, by -15.7 °C and -16.0 °C respectively. These are significant reductions compared to the use of the unmodified **131/RNA** duplex.

Table 4.8: T_m values of antiparallel PNA/RNA duplexes modified with monomeric PNA unit **123** (**X**), ΔT_m indicates the difference in T_m compared with the control unmodified **131/RNA** hybrid.

PNA code	PNA sequence	RNA: 3' C-U-G-A-A-A-G-A 5'	
	N-terminus *C*-terminus	UV-T_m °C	(ΔT_m) °C
131	**G-A-C-T-T-T-C-T**	**37.0 ± 0.8**	**-**
134	**G-A-C-T-X-T-T-C-T**	**21.3 ± 0.9**	**-15.7**
135	**G-A-C-T-lys- X-T-T-C-T**	**21.0 ± 0.8**	**-16.0**

4.4.2.3 UV -T_m studies of PNA/RNA duplexes modified with monomer 126

The modified PNA oligomer **136** was used as a model to investigate the effect of another expected click ligation linker, which can also be seen in the structure of an extended PNA sequence for potential antisense application. This linkage was modelled by incorporation of a single monomeric unit of monomer **126** at a specific position. The hybridisation properties of the modified PNA oligomer **136** were investigated by testing its ability to hybridise with a complementary antiparallel RNA sequence. The hybridisation properties were studied by T_m-dependent UV absorbance (Figure 4.11). Judging by the shape of the curves shown in Figure 4.11, the modified oligomer **136** still has an affinity towards binding the antiparallel complementary RNA sequence.

The T_m values that are given in Table 4.9 have shown that introduction of this independent monomeric unit **126** into PNA oligomer **136** reduced the thermal stability of the corresponding **136/RNA** duplex by -11.5 °C compared to the corresponding unmodified **131/RNA** duplex.

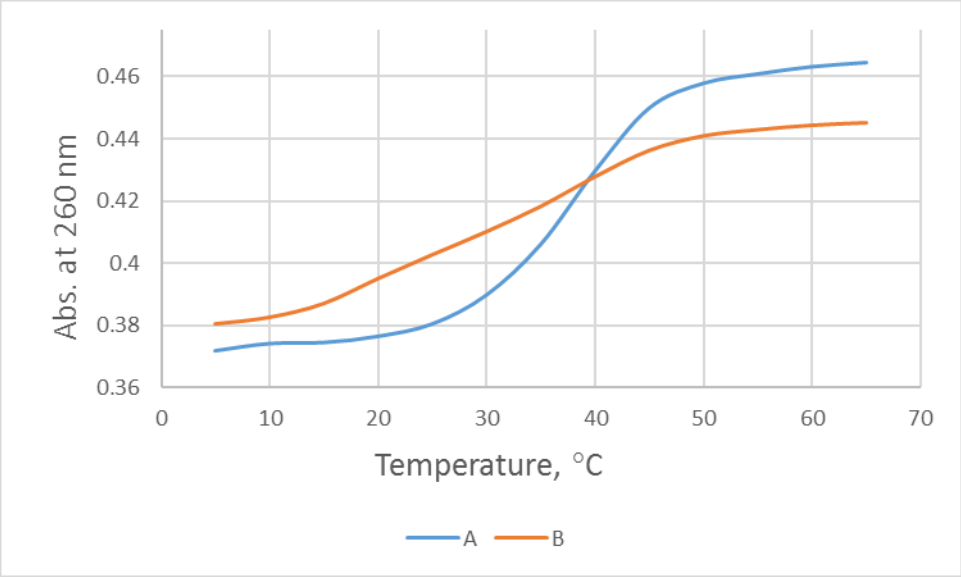

Figure 4.11: Comparison of the UV-melting curves of the duplex formed between RNA with (A) unmodified PNA oligomer **131**, (B) modified PNA oligomer **136**. Performed in a buffer of 10 mM potassium phosphate and 10 mM NaCl at pH 7.0.

Table 4.9: T_m values of antiparallel PNA/RNA duplexes modified with monomeric PNA unit **126** (**X**), ΔT_m indicates the difference in T_m compared with the control unmodified **131/RNA** hybrid.

PNA code	**PNA sequence** *N*-terminus *C*-terminus	**RNA: 3'C-U-G-A-A-A-G-A 5'**	
		UV-T_m °C	**(ΔT_m)**
131	**G-A-C-T-T-T-C-T**	**37.0 ± 0.8**	-
136	**G-A-C-T-X- T-T-C-T**	**25.5 ± 0.9**	**- 11.5 °C**

Chapter Five

Conclusions and Future Work

5.1 Conclusions

The work that is described in this thesis mainly deals with the synthesis of two classes of novel PNA monomers as well as their application as building blocks in the Fmoc solid phase PNA synthesis strategy for modified PNA oligomers that will be used in specific applications.

Since PNA is being considered as a substrate for the copper (I) catalysed azide-alkyne cycloaddition for different applications, the alkyne group required for the reaction would be at the *N*/*C*-terminus of the PNA oligomers. A new and efficient synthetic route was consequently developed to synthesise novel *N*-alkyne functionalized PNA monomers bearing thymine, Bhoc-protected cytosine, Bhoc-protected adenine, and Bhoc-protected guanine. These monomers are used to introduce an alkyne group at the *N*-terminus of PNA oligomers.

An *N*-propargyl PNA monomer bearing thymine base **115** was incorporated successfully into PNA oligomers **138** and **139** under the same conditions that were used for oligomerisation of the AEG PNA monomers following the Fmoc solid phase synthesis strategy. Whereas the incorporation of *N*-alkyne PNA monomers of cytosine, adenine and guanine was not attempted because it was deemed that these monomers were not required at this stage of our initial investigations.

As an application for ligation PNA by click reaction, we tried to use the CuAAC reaction to implement a novel DNA-templated method to ligate three azide and alkyne functionalized mixed pyrimidine-purine PNA oligomers. Antiparallel and parallel complementary DNA sequences were used as templates.

Many attempts at click ligation were made involving the use of Cu (II) or Cu (I) salts in the presence of an excess of Na-ascorbate to keep producing Cu (I) by reducing Cu (II) that was used as a starting material or produced *in situ* from oxidation of Cu (I). Furthermore, an excess of THPTA was used to avoid the DNA template degrading. All attempts were unsuccessful in achieving this aim. Although HPLC chromatograms and mass spectra that were run for click reaction mixture did not show the peaks that are belonging to the desired product or PNA oligomers starting materials, we really can not specify if this reaction failed or not.

We have successfully used Cu (I) catalysed azide-alkyne cycloaddition to synthesise three novel 1,2,3-triazole functionalized monomeric suitable for Fmoc solid phase peptide synthesis. Our strategy involved investigating new conditions to connect the *N*-alkyne PNA monomer bearing thymine base **115** PNA monomer to the synthesised Fmoc-protected 2-aminoethyl azide **120** to afford novel 1,2,3-triazole functionalised thymine PNA monomer **121**. Compound **120** was then clicked with the commercially available 4-pentynoic **122** and the synthesised *N*-propargyl-*N*-Boc glycine acid **125** to give the novel monomeric units **123** and **126** respectively.

These modified 1,2,3-triazole functionalised monomers have shown an ability to be incorporated into PNA sequences that were used as models in the evaluation of their effect on the binding properties of the potential antisense and antigene PNA agents. The incorporation of these monomers into PNA oligomers was done easily under the same conditions that are used for oligomerization of the Fmoc/Bhoc PNA monomers without any significant issue observed.

The thermodynamic profiles of hybridization studies that was studied by T_m-dependent UV spectroscopy indicate that all the novel 1,2,3-tiazole functionalised **121**, **123** and **126** monomers have unevenly maintained the binding affinity and slightly reduced thermal stability of their oligomers towards both antiparallel complementary DNA sequences 8-mer (DNA1) and 9-mer (DNA2). Also, it was demonstrated that the incorporation of a lysine moiety beside monomer **121** reduced the thermal stability of the corresponding **133/DNA1** and **133/DNA2** duplexes. Whereas, the introduction of a lysine moiety beside monomer **123** prevents the corresponding PNA oligomer from binding the 8-mer DNA sequence (**DNA1**) and reduced the thermal stability of the corresponding **135/DNA2** duplex.

For antisense investigations, all the modified 1,2,3-triazole functionalised PNA oligomers have displayed an ability to bind an antiparallel complementary 8-mer RNA sequence. However, their duplexes resulted in a reduced thermal stability compared to the corresponding unmodified PNA/RNA duplex.

However, we think these changes in the binding affinity and thermal stability maybe are not going to be a problematic issue for click ligation because if the click ligation was successful, then it would have a longer PNA sequence. So, any detrimental

effect resulting from a click linker would be more than compensated by the increases in the number of nucleobases.

The encouraging results of novel Fmoc-protected 1,2,3-triazole functionalised thymine PNA monomer **121** lead us to believe that our novel alkyne monomers **115**, **116**, **117** and **118** will be suitable to introduce an alkyne function at the *N*-terminus for ligation of PNA by click reaction. This will lead to construction of ligation linkages that are maybe are capable of maintaining the binding affinity and thermal stability of extended PNA sequences compared to the other linkages that do not contain nucleobase.

5.2 Future work

As PNA/DNA duplexes have resulted in encouraging binding properties, future investigation for biological applications can be achieved for the novel 1,2,3-triazole functionalised thymine PNA monomer **121**, for instance, by studying its effect on the cellular uptake of the corresponding PNA oligomers further to investigate if this modified monomer has a metabolic stability.

Future work could be utilising the *tert*-butyloxycarbonyl group (Boc) that has proven a stability toward click reaction conditions to protect the exocyclic amino function of cytosine, adenine and guanine bases of the *N*-alkyne PNA monomers. This protection will help to overcome the deprotection issue of Bhoc group to yield novel 1,2,3-triazole functionalised PNA monomers suitable for Fmoc solid phase PNA synthesis strategy and could be used to develop a new analogue of PNA.

For the future, the effect of the 1,2,3-triazole functionalised monomeric units **121**, **121** and **126** on the on the conformation of PNA/DNA and PNA/RNA duplexes can be studied by CD spectroscopy. In addition, this technique can be used as a complementary tool to T_m-dependent UV spectroscopy to evaluate the effect of these monomeric units on thermal stability of their corresponding PNA/DNA and PNA/RNA duplexes.

For ligation of PNAs by click reaction, continued research could involve more studies to understand what happened with this reaction. Firstly, what happened to the PNA oligomers starting material if the click ligation of PNA oligomers is not going toward

the desired product. If it is believed that there is a product still binding to the DNA template, then an efficient method should be devised to denature PNA/DNA-template hybrid and remove the DNA template.

Further investigations could include the effect of proximity of the azide and alkyne terminus of PNA oligomers that are hybridising with a DNA template. That can be achieved by introducing a long chain containing an azide or alkyne group into PNA sequences.

Furthermore, a new strategy such as performing the ligation of PNA sequences on the solid support may be led to better results.

Finally, an alternative approach based on the bio-orthogonal chemistry can be useful for ligation of PNA oligomer in cells in a copper-free reaction where a cyclooctyne is used as an alkyne terminus. That would avoid any toxicity problems with the copper salt.

Chapter Six
Experimental

6.0 Experimental

6.1 Synthesis of PNA monomers

Chemicals and solvents

All solvents including anhydrous DMF were purchased from commercial suppliers and used without further purification. Anhydrous THF and MeCN were collected from a solvent purification system. Chemicals were purchased from Acros, Aldrich, Fluka, Molekula, Alfa Aesar and Novabiochem and were used without further purification.

Melting Points

Melting points were determined on a Gallenkamp melting point apparatus fitted with a mercury thermometer and are uncorrected.

NMR Spectroscopy

All ^{1}H NMR and ^{13}C NMR spectra were recorded on a Bruker DPX 400 (400 MHz for ^{1}H NMR and 100 MHz for ^{13}C NMR) or a Bruker 500 (500 MHz, for ^{1}H NMR and 125 MHz for ^{13}C NMR). Chemical shifts are given in parts per million, where all spectra were calibrated using chemical shifts reported relative to the residual deuterated solvent signals in $CDCl_3$ [7.26 ppm for ^{1}H (singlet) and 77.0 for ^{13}C (central line of triplet)], DMSO-d6 [2.50 ppm for ^{1}H (central signal of quintuplet) and 39.7 ppm for ^{13}C (central line of septuplet)]. Coupling constants (*J*) values are quoted in Hertz (Hz).

Mass Spectrometry

Mass spectrometry was performed at the Cardiff University, UK, by the analytical services team.

IR Spectroscopy

Infrared spectra were recorded at Cardiff University, UK, on an FT/IR–660 plus spectrometer operating from 4000 – 500 cm^{-1} as a thin film or as KBr disc.

Procedures

Synthesis of ethyl glycinate 98

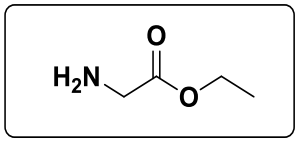

To a stirred suspension of glycine **96** (7.5 g, 100 mmol) in ethanol (100 ml) at room temperature, TMSCl (25 ml, 200 mmol) was slowly added. The resulting mixture reaction was then stirred for 24 h at room temperature. The reaction mixture was then concentrated on a rotary evaporator to dryness. The solid product was dried under high vacuum for 2 hours to yield the desired compound ethyl glycinate hydrochloride **97** (14.9 g, 99.9 %) as white crystals.

Triethylamine (7.5 ml, 71.7 mmol) was slowly added to a stirred suspension of ethyl glycinate hydrochloride **97** (10.0 g, 71.6 mmol) in dichloromethane (100 ml) at 25 °C. The resulting solution was then stirred for 20 min at the same temperature. The solvent was evaporated on a rotary evaporator, and the residue was dissolved in ethyl acetate (25 ml). The resulting solution was filtered to remove triethylammonium chloride, washed with brine (2 × 25 ml). The organic phase was dried over Na_2SO_4 and concentrated to obtain the target product **98** (6.2 g, 84%) as pale green oil.

^{1}H NMR (400 MHz, $CDCl_3$); δ= 4.15 (q, *J*= 8.0 Hz, 2H, OCH_2CH_3), 3.38 (s, 2H, NCH_2CO), 1.45 (s, 2H, NH_2), 1.23 (t, *J*= 8.0 Hz, 3H, CH_2CH_3).

^{13}C NMR (100 MHz, $CDCl_3$); δ= 174.11, 60.55, 43.62, 13.99.

LRMS-ES$^+$ (*m/z*): Calc. for $C_4H_{10}NO_2$ $[M+H]^+$= 104.1, found 104.01.

Synthesis of ethyl *N*-propargyl glycinate 99 [183]

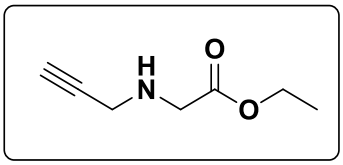

To a stirred solution of ethyl glycinate **98** (5.0 g, 48.5 mmol) dissolved in dry CH_3CN containing K_2CO_3 (9.0 g, 65.2 mmol), a solution of 3-bromopropyne (80% w/v in toluene), (3.0 ml, 33.6 mmol) was added in one portion. The reaction mixture was then stirred for 8 hours at room temperature. The solvent was evaporated on a rotary evaporator. The paste residue was dissolved in ethyl acetate (50 ml), filtered, washed with water (2 × 25 ml) and brine (2 × 25 ml). The organic phase was dried over anhydrous Na_2SO_4 and concentrated to give the desired product **99** (5.4 g, 78%) as pale yellow oil.

^{1}H NMR (400 MHz, $CDCl_3$): δ = 4.17 (q, *J*= 7.01 Hz, 2H, OCH_2CH_3), 3.47 (s, 2H, NCH_2COO), 3.44 (d, *J*= 2.30 Hz, 2H, $CH_2C{\equiv}CH$), 2.20 (t, *J*= 2.30 Hz, 1H C≡CH), 1.84 (s, br, 1H, NH), 1.25 (t, *J*= 7.01 Hz, 3H, CH_2CH_3).

^{13}C NMR (100 MHz, $CDCl_3$): δ= 171.72, 81.11, 71.94, 60.63, 48.99, 37.4, 14.04.

HRMS-APCl$^+$ (*m/z*): calc. for $C_7H_{12}NO_2$ $[M+H]^+$ =142.0868, found= 142.0863.

Synthesis of thymin-1-yl acetic acid 100 [156]

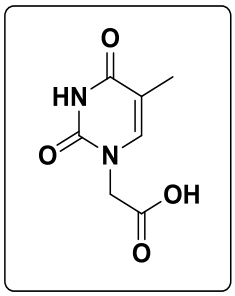

To a stirred aqueous solution of KOH (7.0 g, 124.8 mmol) dissolved in water (30 ml) was added thymine **2** (5.0 g, 39.6 mmol). The resulting solution was then heated to 40 °C before addition a solution of bromoacetic acid (8.3 g, 59.7 mmol) dissolved in water (15 ml) dropwise over 20 min. The reaction mixture was stirred for a further 30 minutes at this temperature. The reaction mixture was cooled to room temperature and acidified with a concentrated solution of hydrochloric acid until pH 5.5. The resulting solution was then kept in a fridge for two hours. The precipitate formed (unreacted thymine) was removed by filtration. The filtrate was then acidified with a concentrated solution of hydrochloric acid until pH 2.0 and placed in a freezer for 2 hours. The resultant white precipitate was collected by filtration and dried under high vacuum to give the titled compound **100** (6.3 g, 86%) as white crystals; melting point (mp): 252-254 °C [lit.[181] mp: 252-253 °C].

^{1}H NMR (400 MHz, DMSO-d6): δ = 11. 35 (s, 1H, NH), 7.51 (s, 1H, CH=C), 4.37 (s, 2H, NCH_2COOH), 1.75 (s, 3H, CH_3).

^{13}C NMR (100 MHz, DMSO-d6): δ = 170.15, 164.84, 151.45, 142.22, 108.87, 48.89, 12.31.

LRMS-ES^{+} (*m/z*): calc. for $C_7H_9N_2O_2$ $[M+H]^+$ =185.10, found= 185.07.

Synthesis of benzyl cytosin-1-yl acetate 101[91]

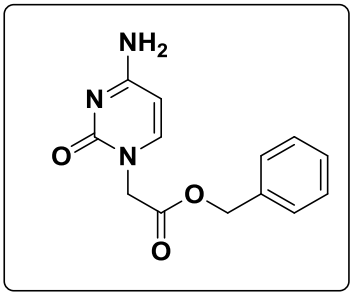

A suspended solution of cytosine **3** (5.0 g, 45.0 mmol) and potassium carbonate (12.0 g, 86.8 mmol) in anhydrous DMF (40 ml) was stirred at 100 °C for two hours. The reaction mixture was then cooled in an ice-water bath and benzyl bromoacetate (7.5 ml, 47.3 mmol) was added in one portion. The reaction mixture was then stirred for a further one hour before being removed from the ice-water bath. The reaction mixture was stirred at room temperature for 12 hours. The solvent was evaporated by a rotary evaporator. The paste residue was triturated with water (50 ml) and stirred for 10 minutes. The precipitate was collected by filtration and dried under high vacuum to give the titled compound **101** (8.2 g, 70%) as a pale white solid, melting point (mp): 242-245 °C.

^{1}H NMR (400 MHz, DMSO-d6); δ= 7.58 (d, *J* = 7.5 Hz, 1H, Cyt-C6), 7.35-7.39 (m, 5H, Ar-H), 7.16 (br, 1H, NH), 5.69 (d, *J*= 7.5 Hz, 1H, Cyt-C5), 5.16 (s, 2H, OCH_2Ph), 4.51 (s, 2H, NCH_2COO).

^{13}C NMR (100 MHz, DMSO-d6); δ= 168.9, 166.6, 156.03, 146.51, 135.96, 128.66, 128.33, 128.1, 93.82, 566.30, 50.24.

HRMS-EI^{+} (*m/z*): calc. for $C_{13}H_{14}N_3O_3$ $[M+H]^+$ = 260.0957, found= 260.0959.

The spectroscopic data are in agreement with the literature.[182]

Synthesis of benzyl (N^4-(benzhydryloxycarbonyl) cytosine-1-yl acetate 102 [91]

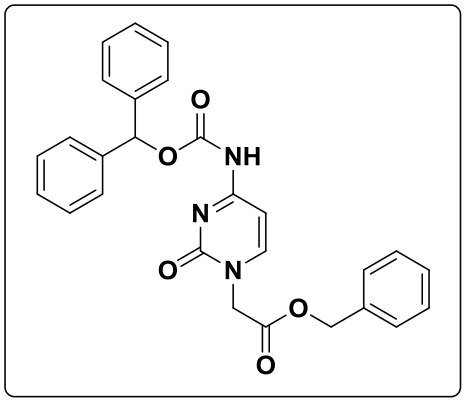

To a stirred solution of compound **101** (5.0 g, 19.3 mmol) dissolved in anhydrous DMF (30 ml) was added 1,1-carbonyldiimidazole (6.0 g, 37.0 mmol) in one portion. The reaction mixture was stirred at 60 °C for two hours before addition of benzhydrol (5.0 g, 27.1 mmol). The reaction mixture was then stirred for 12 hours at the same temperature. The solvent was evaporated on a rotary evaporator. To the residue was added water (100 ml) and the resulting solution was stirred for 30 minutes. The white precipitate that formed was collected by filtration, washed with diethyl ether (2 × 50) and dried under high vacuum to give the desired compound **102** (7.0 g, 78%) as a white solid, melting point (mp): 182-185 °C.

^{1}H NMR (400 MHz, DMSO-d6); δ= 11.07 (br., 1H, NH), 8.65 (d, *J*= 8.0 Hz, 1H, Cytosinyl C(6)-H), 7.48-7.27 (m, 15H, Ar-H), 6.98 (d, *J*=8.0 Hz, 1H, CH, Cytosinyl C(5)-H), 6.80 (s, 1H, Ph_2CHOCO), 5.18 (s, 2H, $COOCH_2Ph$), 4.69 (s, 2H, NCH_2COO).

^{13}C NMR (100 MHz, DMSO-d6); δ= 168.14, 163.68, 155.24, 152.57, 150.63, 140.56, 135.76, 128.78, 128.67, 128.40, 128.15, 128.10, 126.70, 94.25, 77.57, 66.44, 50.71.

HRMS-ES$^+$ (*m/z*): Calc. for $C_{27}H_{23}N_3O_5Na$ $[M+Na]^+$ = 492.1535, found= 492.1551.

Synthesis of N^4-(benzhydryloxycarbonyl) cytosin-1-yl acetic acid 103 [91]

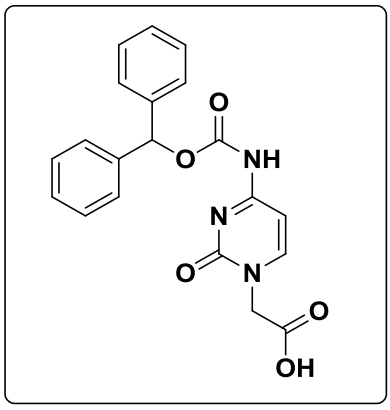

Benzyl (N^4-(benzhydryloxycarbonyl) cytosin-1-yl acetate **102** (6.0 g, 12.8 mmol) was dissolved in a mixture of acetonitrile, methanol, ethanol and water (78 ml, 2:2:1:1). To the resulting solution was added a solution of anhydrous lithium hydroxide (5.2 g, 217.0 mmol) dissolved in water (40 ml). The resulting reaction mixture was stirred at room temperature for 15 minutes. The reaction mixture was cooled in an ice bath before being treated with a solution of citric acid (15.0 g, 78.1 mmol) dissolved in water (65 ml). The resulting solution was stirred for further 10 minutes before collecting the precipitate by vacuum filtration. The precipitate was washed several times with water and dried under high vacuum to afford the titled product **103** (4.4 g, 92%) as a white powder, melting point (mp): 320-323 °C.

^{1}H NMR (400 MHz, DMSO-d6); δ= 11.03 (s (br), 1H, NH), 8.01 (d, *J*= 7.2 Hz, 1H, CH, Cytosinyl C(6)-H), 7.47-7.27 (m, 10H, Ar-H), 6.945 (d, *J*= 7.20 Hz, 1H, CH, Cytosinyl C(5)-H), 6.79 (s, 1H, CHOCO), 4.51 (s, 2H, NCH_2COOH).

^{13}C NMR (100 MHz, DMSO-d6); δ= 170.06, 163.86, 155.79, 153.00, 151.21, 140.94, 128.80, 128.12, 126.43, 94.26, 77.80, 59.97.

HRMS-ES-ve (*m/z*): calc. for $C_{20}H_{16}N_3O_5$ $[M-H]^-$ = 378.109, found= 378.109.

Synthesis of ethyl adenin-9-yl acetate 104 [91]

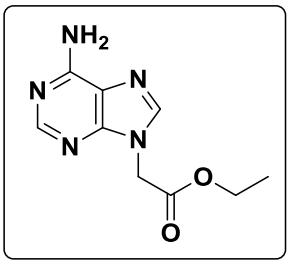

Potassium carbonate (10.0 g, 72.4 mmol) and adenine **6** (5.0 g, 37.0 mmol) were suspended in anhydrous DMF (50 ml). The resulting suspension was stirred at 100 °C for 30 minutes. The reaction mixture was then cooled in an ice bath and ethyl bromoacetate (4.1 ml, 37.0 mmol) was added via syringe over 5 minutes. The stirred reaction mixture was maintained for a further one hour at the same temperature. The reaction mixture was then allowed to stir at the ambient temperature for four hours. The solvent was evaporated by a rotary evaporator to dryness. The solid residue was triturated with water (50 ml) and stirred for 15 minutes. The precipitate was collected by filtration under vacuum and dried under high vacuum to obtain the desired compound **104** (7.8 g, 96%) as a pale white solid, melting point (mp): 217-220 °C.

^{1}H NMR (400 MHz, DMSO-d6); δ= 8.2 (s, 1H, adeninyl-C(2)-H), 8.1 (s, 1H, adeninyl-C(8)-H), 7.27 (s, 2H, NH_2), 5.06 (s, 2H, NCH_2COO), 4.14 (q, *J*= 7.2 Hz, 2H, OCH_2CH_3), 1.18 (t, *J*= 7.2 Hz, 3H, CH_2CH_3).

^{13}C NMR (100 MHz, DMSO-d6); δ= 168.12, 156.02, 152.89, 149.73, 141.32, 118.46 61.39, 43.96, 14.02.

HRMS-EI^{+} (*m/z*): calc. for $C_9H_{11}N_5O_2$ = 221.0913, found= 221.0135.

Ethyl (N^6-benzhydryloxycarbonyl) adenin-9-yl acetate 105 [91]

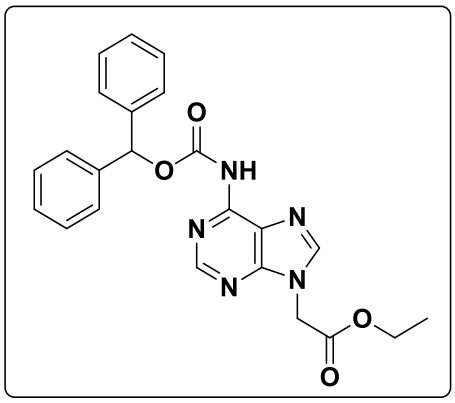

To a stirred solution of ethyl adenin-9-yl acetate **104** (5.0 g, 22.6 mmol) dissolved in anhydrous DMF (30 ml) was added 1,1-carbonyldiimidazole (5.9 g, 36.2 mmol) in one portion. The reaction mixture was heated to 100 °C and then maintained at this temperature for two hours. The temperature was reduced to 60 °C, and benzhydrol (6.2 g, 33.9 mmol) was added in one portion. The resulting reaction mixture was then stirred at 60 °C overnight. The reaction mixture was cooled to the ambient temperature and water (200 ml) was added. The resulting reaction mixture was then stirred for 30 minutes, and the precipitate was collected by filtration under vacuum, washed with cold diethyl ether and dried under high vacuum to give the desired compound **105** (9.1 g, 93%) as a white solid, melting point (mp): 109-112 °C.

^{1}H NMR (400 MHz, DMSO-d6); δ=10.98 (s, 1H, NH), 8.6 (s, 1H, adeninyl-C(2)-H), 8.45 (s, 1H, adeninyl-C(8)-H), 7.52-7.27 (m, 10H, Ar-H), 6.83 (s, 1H, Ph_2CHOCO), 5.20 (s, 2H, NCH_2COO) 4.175 (q, *J*= 7.1 Hz, 2H, OCH_2CH_3), 1.21 (t, *J*= 7.1 Hz, 3H, OCH_2CH_3).

^{13}C NMR (100 MHz, DMSO-d6); δ=167.77, 152.14, 151.87, 151.22, 149.96, 144.8, 141.32, 128.54, 127.77, 126.57, 122.66, 77.41, 61.60, 44.29, 14.00.

HRMS ES$^+$ (*m/z*): calc. for $C_{23}H_{22}N_5O_4$ $[M+H]^+$ = 432.1672, found= 432.1689.

Synthesis of (N^6-benzhydryloxycarbonyl) adenin-9-yl acetic acid 106 [91]

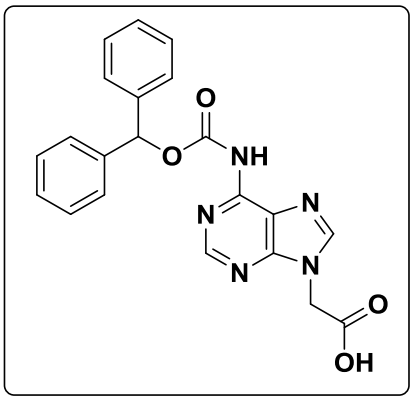

To a stirred solution of ethyl (N^6-benzhydryloxycarbonyl) adenine-9-yl acetate **105** (5.0 g, 11.6 mmol) dissolved in a mixture of ethanol and acetonitrile (30 ml, 1:1) was added a solution of anhydrous lithium hydroxide (4.8 g, 200.0 mmol) dissolved in water (50 ml). The reaction mixture was then stirred for exactly 10 minutes at room temperature, followed by addition of water (10 ml). The stirred reaction mixture was then cooled in an ice-water bath before being treated with a solution of citric acid (30 g, 183 mmol) dissolved in water (80 ml). The precipitate was collected by filtration under vacuum, washed with water several times and dried under high vacuum to give the desired compound **106** (6.0 g, 92%) as a white solid, melting point (mp): 282-285 °C.

^{1}H NMR (400 MHz, DMSO-d6); δ= 10.95 (s, 1H, NH), 8.61 (s, 1H, adeninyl-C(2)-H), 8.44 (s, 1H, adeninyl-C(8)-H), 7.53-7.25 (m, 10H, Ar-H), 6.82 (s, 1H, Ph_2CHOCO), 5.06 (s, 2H, $NHCH_2COO$).

^{13}C NMR (100 MHz, DMSO-d6); δ= 169.63, 152.52, 152.11, 151.61, 149.73, 146.07, 141.24, 128.96, 128.19, 126.91, 122.96, 77.82, 45.0.

HRMS ES$^+$ (*m/z*): calc. for $C_{21}H_{18}N_5O_4$ $[M+H]^+$ = 404.1359, found= 404.1349.

Synthesis of benzyl 2-amino-6-chloropurin-9-yl acetate 108 [91]

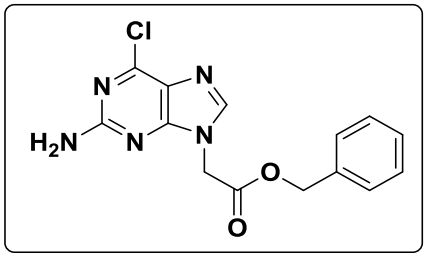

2-Amino-6-chloro purine **107** (4.5 g, 26.54 mmol) and potassium carbonate (5.5 g, 37.8 mmol) were suspended in an anhydrous DMF (50 ml). The stirred suspension solution was heated to 100 °C for 30 minutes. The mixture reaction was then cooled in an ice bath to less than 10 °C, followed by addition of benzyl bromoacetate (4.2 ml, 26.6 mmol) in one portion. The reaction mixture was then stirred for further four hours at room temperature. Water (200 ml) was then added. The resulting solution was cooled in an ice bath and stirred for further one hour. The precipitate was collected by vacuum filtration and dried under high vacuum to give the desired compound **108** (7.8 g, 89%) as a white solid, melting point (mp): 169-172 °C.

^{1}H NMR (400 MHz, DMSO-d6); δ= 8.12 (s, 1H, guaninyl-C(8)-H), 7.42-7.43 (m, 5H, Ar-H), 7.01 (s, 2H, NH_2), 5.20 (s, 2H, $COOCH_2Ph$), 5.07 (s, 2H, NCH_2COO).

^{13}C NMR (100 MHz, DMSO-d6); δ= 167.62, 159.99, 154.28, 149.58, 143.44, 135.47, 128.47, 128.37, 128.06, 123.01, 66.81, 44.23.

HRMS-ES+ (*m/z*): calc. for $C_{14}H_{12}N_5O_2$ NaCl $[M+Na]^+$ = 340.0577, found= 340.0590.

Synthesis of benzyl N^2-(benzhydryloxycarbonyl)-6-chloropurin-9-yl acetate 109 [91]

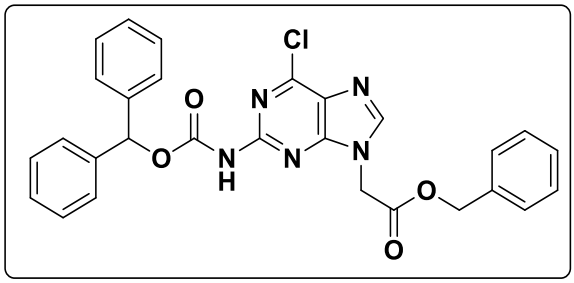

To a stirred solution of benzyl 2-amino-6-chloropurine-9-yl acetate, **108** (5.0 g, 15.7 mmol) dissolved in dry tetrahydrofuran (50 ml) at 0 °C was added triphosgene (1.8 g, 6.0 mmol) in one portion. The reaction mixture was maintained at the same temperature for one hour before addition of DIPEA (7.0 ml, 40.2 mmol) over 30 minutes. The temperature of the reaction was then allowed to rise to the room temperature, followed by addition of benzhydrol (3.5 g, 19.0 mmol). The resulting reaction mixture was stirred for 8 hours. The solvent was evaporated by a rotary evaporator. The residue was dissolved in CH_2Cl_2 (50 ml), washed with water (3 × 50 ml), dried over Na_2SO_4 and concentrated to dryness. The paste residue was triturated with diethyl ether and stirred for one hour. The formed precipitate was collected by filtration and dried under high vacuum to yield the desired compound **109** (5.2 g, 63%) as a pale yellow solid, melting point (mp): 70-75 °C.

^{1}H NMR (400 MHz, DMSO-d6); δ= 11.02 (s, 1H, NH), 8.51 (s, 1H, guaninyl-C(8)-H), 7.36-719 (m, 15H, Ar-H), 6.81 (s, 1H, Ph_2CHOCO), 5.21(s, 2H, $COOCH_2Ph$), 5.18 (s, 2H, NCH_2COO).

^{13}C NMR (100 MHz, DMSO-d6); δ= 168.43, 153.61, 152.80, 151.42, 149.72, 147.21, 141.32, 135.77, 128.97, 128.76, 128.50, 128.46, 127.27, 127.16, 126.94, 126.70, 77.56, 67.39, 44.96.

HRMS-ES+ (*m/z*): calc. for $C_{28}H_{23}N_5O_4Cl$ $[M+H]^+$ = 528.1439, found= 528.1443.

Synthesis of N^2-(benzhydryloxycarbonyl) guanin-9-yl acetic acid 110 [91]

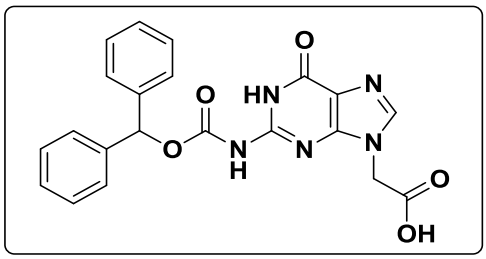

A stirred suspension of sodium hydride (60% in oil, 1.84 g, 46.0 mmol) in dry THF (50 ml) was cooled in a dry ice/acetone bath for 20 minutes, followed by addition of 3-hydroxypropionitrile (3.1 ml, 46.0 mmol) in one portion. The resulting solution was then stirred at 0 °C for two hours before addition of compound **109** (5.0 g, 9.5 mmol). The resulting reaction mixture was stirred for 12 hours at room temperature. The solvent was removed under vacuum, and the residue was dissolved in water (50 ml). The resulting solution was acidified with an aqueous solution of citric acid (20% w/v) until pH 3. The formed precipitate was collected by filtration, washed with diethyl ether and dried under high vacuum to give the titled compound **110** (3.5 g, 90%) as a pale white solid melting point (mp): 220-224 °C.

^{1}H NMR (400 MHz DMSO-d6); δ = 11.71 (s, 1H, COOH), 11.24 (s, 1H, NH), 7.94 (s, 1H, guaninyl-C(8)-H), 7.47-7.30 (m, 10H, Ar-H), 6.86 (s, 1H, Ph_2CHOCO), 4.88 (s, 2H, $NHCH_2COOH$).

^{13}C NMR (100 MHz, DMSO-d6); δ = 169.35, 155.38, 153.93, 149.49, 147.41, 140.55, 140.17, 128.82, 128.22, 126.63, 119.79, 78.38, 44.80.

HRMS-ES$^+$ (*m/z*): Calc. for $C_{21}H_{23}N_5O_5$ $[M+H]^+$ = 420.1308, Found= 420.1304.

Synthesis of ethyl *N*-propargyl-*N*-(thymin-1-yl acetyl) glycinate 111 [162]

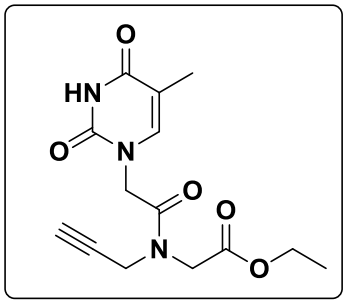

Ethyl *N*-propargyl glycinate **99** (2.0 g, 14.2 mmol), thymin-1-yl acetic acid **100** (2.6 g, 14.0 mmol), DCC (3.0 g, 14.5 mmol) and HOBt·H_2O (2.2 g, 14.4 mmol) were dissolved in anhydrous DMF (25 ml). The resulting mixture was then stirred for 12 hours at room temperature. The reaction mixture was filtered to remove the formed DCU, and DMF was removed by a rotary evaporator. The residue was dissolved in dichloromethane (50 mL), washed with aqueous solutions of Na_2HCO_3 (1 M, 25 ml), $KHSO_4$ (1 M, 25 ml), and brine (2 × 25 ml). The organic phase was dried over anhydrous ($MgSO_4$) and the solvent was removed under reduced pressure to yield a pale orange foam which was purified by column chromatography (EtOAc/MeOH, 10:1) to give the title compound **111** (3.2 g, 74%) as pale yellow foam.

^{1}H NMR (400 MHz; $CDCl_3$) (two rotational isomers observed); δ= 8.70 (s, 1H, thyminyl N(3)-H) 7.00 and 6.96 (s, 1H, thyminyl (C6)-H), 4.67 and 4.45 (s, 2H, NCH_2CON), 4.30-4.17 (m, 6H, $C{\equiv}CCH_2NCH_2COOCH_2$), 2.30 and 2.48 (t, 1H, *J*= 2.4 Hz, C≡CH), 1.7 (s, 3H, thyminyl C(5)-CH3), 1.30 and 1.25 (3H, *J*= 6.8 Hz, OCH_2CH_3).

^{13}C NMR (100 MHz; $CDCl_3$) (two rotational isomers observed); δ= 168.9 and 168.5, 167.1 and 166.5, 151.3, 141.1, 110.3, 77.1 and 76.6, 74.6 and 73.8, 62.3 and 61.7, 48.1 and 48.0, 47.7, 38.0 and 36.3, 14.0 and 14.1, 12.2.

HRMS-ES$^+$ (*m/z*): calc. for $C_{14}H_{18}N_3O_5$ $[M+H]^+$ = 308.1246, found = 308.1256.

FT-IR ($CDCl_3$ film, cm^{-1}): 3242 (str. C-H, C≡CH), 2920 and 2832 (str. aliphatic CH), 2100 (str. C≡C), 1712 (str. C=O amide, 1678 (str. C=C), 1653 (str. C=O).

Synthesis of ethyl *N*-propargyl-*N*-[(*N*^{4}-benzhydryloxycarbonyl) cytosin-1-yl acetyl] glycinate 112

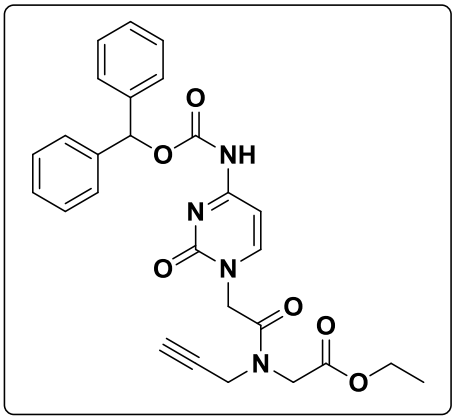

Ethyl *N*-propargyl glycinate (2.8 g, 19.8 mmol) **99**, *N*^{4}-(benzhydryloxycarbonyl) cytosin-1-yl acetic acid **103** (5.0 g, 13.2 mmol), DCC (2.78 g, 13.5 mmol) and HOBt·H_2O (2.0 g, 13.2 mmol) were sequentially were added in DMF (50 ml). The reaction mixture was stirred at 25 °C for overnight. The reaction mixture was filtered to remove the formed DCU, and the solvent was removed under vacuum. The residue was dissolved in DCM (50 ml), filtered and washed with water (2 × 25 ml), brine (2 × 25 ml), dried over Na_2SO_4. The solvent was removed on a rotary evaporator. The formed foam was purified by column chromatography (EtOAc/MeOH, 9:1) to yield target compound **112** (5.0 g, 76%) a pale white foam.

^{1}H NMR (400 MHz, $CDCl_3$) (two rotational isomers observed); δ= 7.80 (b, 1H, NH), 7.62 and 7.56 (d, *J* = 7.74, 1H, Cytosinyl-C(6)-H), 7.26-7.37 (m, 10H, Ph_2CHO), 7.19 and 7.20 (d, *J* = 7.74, 1H, Cytosinyl-C(5)-H), 6.82 (s, 1H Ph_2CHO), 4.84 and 4.60 (s, 2H $NCOCH_2N$), 4.38 and 4.28 (d, *J*= 2.44 Hz, 2H, $NCH_2C{\equiv}C$), 4.34 and 4.16 (s, 2H, NCH_2CO), 4.24 and 4.5 (q, *J*= 7.1 Hz, 2H, OCH_2CH_3), 2.34 and 2.20 (t, *J*= 2.44 Hz, 1H, C≡CH), 1.16 and 1.22 (t, *J*= 7.1 Hz, 3H, OCH_2CH_3).

^{13}C NMR (100 MHz, $CDCl_3$) (two rotational isomers were observed); δ= 168.99 and 168.56, 167.02 and 166.87, 162.87, 155.74, 151.66, 149.73 and 149.56, 139.29, 128.68, 128.29, 127.02, 95.25, 79.12, 77.3 and 77.2, 74.48 and 73.76, 62.16 and 61.59, 49.41 and 49.16, 48.12 and 47.61, 36.39 and 33.96, 14.14 and 14.12.

HRMS-ES$^+$ (*m/z*): calc. for = $C_{27}H_{26}N_4O_6Na$ $[M+Na]^+$: 525.1750, found= 525.1730.

FT-IR max ($CHCl_3$ film, cm^{-1}); 3270 (str. C≡C-H), 2980 and 2880 (str. CH, aliphatic), 2130 (str. C≡C), 1744 (str. CO ester), 1678 (str. C=C aromatic), 1629 (str. C=O).

Synthesis of ethyl *N*-(propargyl)-*N*-[N^6-(benzhydryloxycarbonyl) adenine-9-acetyl] glycinate 113

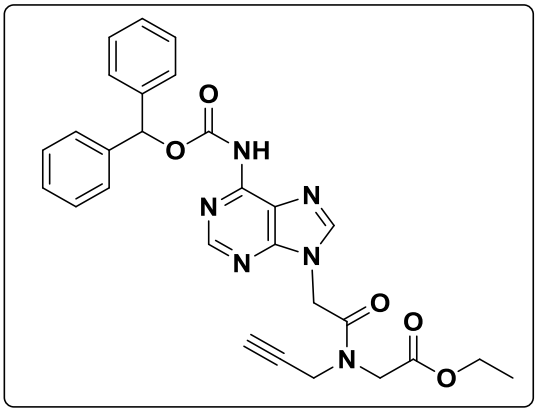

To a stirred solution of N^6-(benzhydryloxycarbonyl) adeninyl-9-yl acetic acid **106** (3.0 g, 7.4 mmol) in DMF (50 ml), DCC (1.6 g, 7.8 mmol), HOBt·H_2O (1.2 g, 7.5 mmol) and ethyl *N*-propargyl glycinate (1.2 g, 8.5 mmol) were added sequentially. The resulting reaction mixture was stirred at 25 °C for overnight. The reaction mixture was filtered to remove the formed DCU after which the solvent was removed under vacuum. The crude residue was dissolved in acetonitrile and filtered. The solvent evaporated on rotary evaporator to dryness. The formed foam was purified by column chromatography (EtOAc/MeOH, 9:1) to yield target compound **113** (3.2 g, 82%) as a pale white solid, melting point (mp): 125-128 °C

^{1}H NMR (400 MHz; $CDCl_3$) (two rotational isomers were observed); δ= 8.72 and 8.70 (s, 1H, adeninyl (C2)-H), 8.45 (br s, 1H, NH), 8.07 and 8.06 (s, 1H, adeninyl C(8)-H), 7.42-7.24 (5H, m, Ph), 6.98 (s, 1H, Ph_2CHO), 5.20 and 5.00 (s, 2H, $NCOCH_2N$), 4.32 and 4.31 (d, *J*= 2.4 Hz, 2H, $NCH_2C{\equiv}$), 4.38 and 4.45 (s, 2H, NCH_2CO), 4.15 and 4.10 (q, *J*= 7.1 Hz, 2H, OCH_2CH_3), 2.29 and 2.44 (t, 1H, *J*= 2.4 Hz, CH≡C), 1.24 and 1.31 (t, 3H, *J*= 7.1 Hz, OCH_2CH_3).

^{13}C NMR (100 MHz; $CDCl_3$) (two rotational isomers were observed); δ= 169.7 and 168.5, 166.3 and 166.0, 152.78, 151.7 and 151.6, 150.7 and 150.6, 149.4 and 149.29, 144.3 and 143.9, 139.7, 128.61, 128.17, 128.14, 127.34, 78.7, 74.9 and 74,06, 61.7 and 61.6, 47.8 and 47.5, 40.06 and 43.39, 37.99 and 36.37, 14.14 and 14.10.

HRMS-ESI$^+$ (*m/z*): calc. for $C_{28}H_{27}N_6O_5$ $[M+H]^+$ = 527.2043, found = 527.2035.

FT-IR max (film $CHCl_3$, cm^{-1}): 3190 (str. C-H of aromatic ring), 2957 (str. C-H of aliphatic), 1763 (str. C=O), 1749 (str. C=O), 1680 (str., C=C, Aromatic).

Synthesis of ethyl *N*-(propargyl)-*N*-[N^2-(benzhydryloxycarbonyl) guanine-9-acetyl] glycinate 114

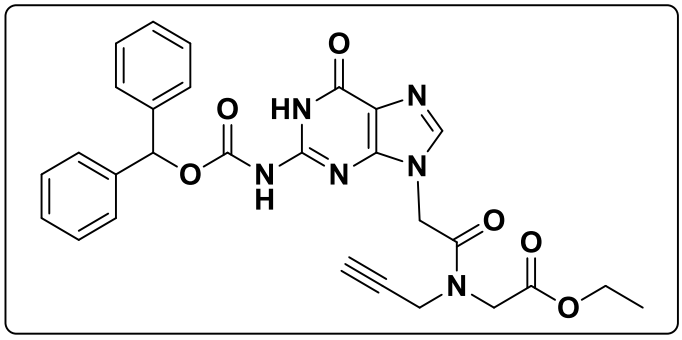

Ethyl *N*-propargyl glycinate **99** (1.2 g, 8.5 mmol), N^2-(benzhydroloxycarbonyl) guanin-9-yl acetic acid **110** (3.0 g, 7.153 mmol), DCC (1.6 g, 7.8 mmol) and HOBt·H_2O (1.2 g, 7.8 mmol) were dissolved in DMF (50 m). The reaction mixture was stirred for overnight at 25 °C then filtered to remove DCU after which the solvent was removed under vacuum. The residue was dissolved in dichloromethane (50 ml), filtered and concentrated. The residue was re-dissolved in acetonitrile (50 ml) to remove remaining DCC after which the solvent was evaporated until dryness. The formed foam was purified by column chromatography (EtOAc/MeOH, 9:1) to yield target compound **114** (3.5 g, 76%) a pale-yellow powder, melting point (mp): 145-148 °C.

^{1}H NMR (400 MHz, $CDCl_3$) (two rotational isomers observed); δ= 11.28 (br. 1H, NH),

7.53 (m, 1H, guaniniyl C(9)-H), 7.35-7.27 (m, 10H, Ar), 6.80 (s, 1H, Ph_2CHOCO), 4.94 and 4.47 (s, 2H, NCH_2COO), 4.34-3.8 (m, 6H, OCH_2, $CH_2C{\equiv}C$, NCH_2CON), 2.44 and 2.34 (t, *J*= 2.5 Hz, 1H, C≡CH), 1.21 and 1.17 and (t, *J*= 7.1 Hz, 3H, CH_3).

^{13}C NMR (100 MHz, $CDCl_3$) (two rotational isomers observed); δ= 168.87 and 168.75, 166.47 and 166.40, 156.0, 153.22, 149.19, 147.06, 140.19, 139.06 and 138.89, 128.17, 128.42, 127.09, 79.69, 77.2, 74.65 and 73.81, 61.66 and 61.42, 47.70 and 47.36, 44.20 and 41.52, 37.99 and 36.23, 14.14 and 14.09.

HRMS-ES$^+$ (*m/z*): calc. for $C_{28}H_{27}N_6O_6$ $[M+H]^+$= 543.1992, found= 543.1993.

FT-IR (film CHCl3, cm^{-1}); 2984 (str. CH, aliphatic), 1744 (str. C=O ester), 1678 (str. C=C aromatic), 1629 (str. C=O).

Synthesis of *N*-propargyl-*N*-(thymin-1-yl acetyl) glycine 115

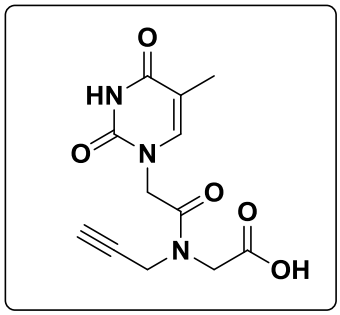

To a stirred solution of ethyl *N*-propargyl *N*-(thymin-1-yl acetyl) glycinate **111** (2.0 g, 6.5 mmol) dissolved in 1,2-dioxane (10 ml) at room temperature was added an aqueous solution of NaOH (10 ml, 24.9 mmol). The mixture reaction was stirred at room temperature for 15 minutes. The reaction mixture was acidified with 20% aqueous solution of $KHSO_4$ until pH 3. The resulting precipitate was collected and dried in high vacuum for 3 hours to give the desired compound **115** (1.3 g, 70%) as a pale white solid, melting point (m.p.): 138-140 °C.

^{1}H NMR (400 MHz, DMSO-d6) (two rotational isomers observed); δ= 12.91 (br, 1H, COOH), 11.31 (s, 1H, thyminyl N(3)-H), 7.34 and 7.34 (s, 1H, thyminyl C(6)-H), 4.71 and 4.53 (s, 2H, $NCOCH_2N$), 4.33 and 4.26 (s, 2H, $\equiv CCH_2N$), 4.17 and 4.04 (s, 2H, NCH_2CO), 3.44 and 3.26 (s, 1H, C≡CH), 1.7 (s, 3H, CH_3).

^{13}C NMR (100 MHz, DMSO-d6) (two rotational isomers observed); δ= 170.51 and 170.2, 167.76 and 167.29, 164.84, 151.40, 142.61, 108.82, 79.39 and 78.59, 76.26 and 75.49, 48.05, 46.96 and 47.59, 12.41.

HRMS-ES$^-$ (*m/z*): calc. for $C_{12}H_{12}N_3O_5$ $[M-H]^-$ = 278.0777, found= 278.0781.

FT-IR (cm^{-1}): 3277 (str. C-H, C≡CH), 2990 and 2832 (str. aliphatic CH), 2200 (str. C≡C), 1737 (str. C=O amide, 1678 (str. C=O), 1653 (str. C=O).

Synthesis of *N*-propargyl-*N*-[*N*^{4}-(benzhydryloxycarbonyl) cytosin-1-acetyl] glycine 116

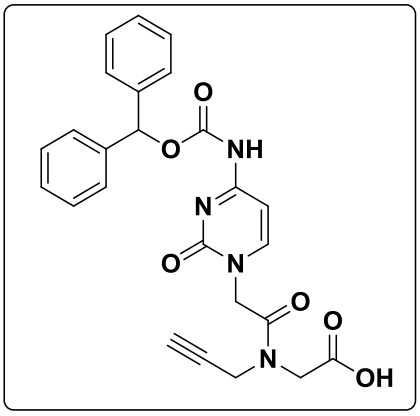

To a stirred solution of ethyl *N*-propargyl-*N*-[*N*^{4}-(benzhydryloxycarbonyl) cytosin-1-acetyl] glycinate **112** (4.0 g, 8.0 mmol) in 1,4-dioxane (8 ml) at room temperature was added an aqueous solution of NaOH (15 ml, 30.0 mmol). The resulting reaction mixture was stirred for exactly 10 minutes then the reaction was quenched by addition a solution of citric acid (20% w/v) until pH 3. The precipitate formed was stirred for further 5 minutes before collecting by filtration under vacuum. The precipitate was dried under high vacuum for three hours to afford the novel PNA monomer **116** (3.3 g, 89%) as a white solid, melting point (mp): 125-127 °C.

^{1}H NMR (400 MHz, DMSO-d6) (two rotational isomers observed); δ= 8.56 (br., 1H, NH), 7.96 (m, 1H, Cytosinyl-C(6)-H), 7.48- 7.25 (m, 10H, Ar), 6.94 (m, 1H, Cytosinyl-C(5)-H, 6.79 (s, 1H, Ph_2CHO), 4.88 and 4.68 (s, 2H, NCH_2COO), 3.5-4.5 (m, 4H, $C{\equiv}CCH_2N$, NCH_2CO), 2.45 and 2.26 (t, *J*= 2.62 Hz, 1H, C≡CH).

^{13}C NMR (100 MHz, DMSO-d6) (two rotational isomers observed); δ= 170.83 and 171.42, 170.43 and 169.61, 169.61, 155.74, 151.66, 149.73 and 149.56, 139.29, 128.68, 128.29, 127.02, 95.25, 79.12, 77.3 and 77.2, 74.48 and 73.76, 49.41 and 49.16, 48.12 and 47.61, 36.39 and 33.96.

HRMS-ES$^+$ (*m/z*): calc. for $C_{25}H_{24}N_4O_6Na$ $[M+Na]^+$ = 497.1437, found= 497.1441.

FT-IR max (cm^{-1}); 3270 (str. CH, C≡C-H), 2980 and 2880 (str. CH, aliphatic), 2230 (str. C≡C), 1744 (str. C=O), 1678 (str. C=C aromatic), 1629 (str. C=O), 1558.

Synthesis of *N*-propargyl-*N*-[*N*^{6}-(benzhydryloxycarbonyl) adenin-9-acetyl] glycine 117

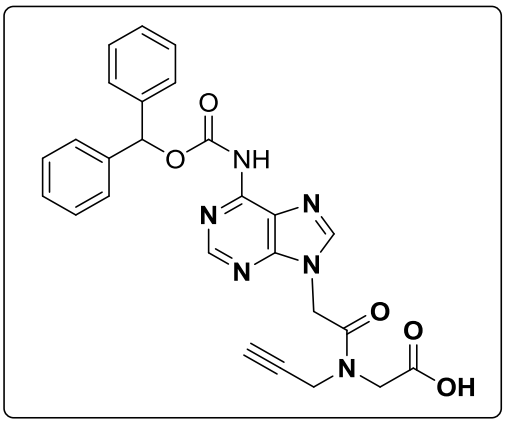

To a stirred solution of ethyl *N*-propargyl-*N*-[*N*^{6}-(benzhydryloxycarbonyl) adenin-9-acetyl] glycinate **113** (2.0 g, 3.8 mmol) in 1,4-dioxane (10 ml) at room temperature, an aqueous solution of NaOH (10 ml, 20mmol) was added. The reaction mixture was stirred at room temperature for 20 minutes. After this time, the reaction was acidified with an aqueous solution of citric acid (20% w/v) until pH 3. The formed precipitate was collected by filtration under vacuum. The wet precipitate was dried in high vacuum for 3 hours to give the novel PNA monomer **117** (1.7 g, 90%) as a pale white powder, melting point (mp)**:** 155-158 ˚C.

^{1}H NMR (400 MHz, DMSO-d6) (two rotational isomers observed); δ= 10.96 (br, 1H, NH), 8.62 and 8.61 (s, 1H, adeninyl-C(2)-H), 8.40 and 8.39 (s, 1H, adeninyl-C(8)-H), 7.55-7.25 (m, 10H, Ar), 6.86 (s, 1H, Ph_2CHO), 5.43 and 5.25 (s, 2H, NCH_2CON), 4.49

and 4.20 (d, *J*= 2.45 Hz, 2H, $CH_2C{\equiv}CH$), 4.42 and 4.07 (s, 2H, NCH_2COO), 3.35 and 3.30 (t, *J*= 2.45 Hz, 1H, C≡CH).

^{13}C NMR (100 MHz, DMSO-d6) (two rotational isomers observed); δ= 171.8 and 171.4, 170.7 and 170.4, 169.61, 151.7 and 151.6, 150.7 and 150.6, 149.7 and 149.29, 144.3 and 143.9, 139.7, 128.61, 128.17, 128.14, 127.34, 78.7, 74.9 and 74.06, 47.8 and 47.5, 40.06 and 43.39, 37.99 and 36.37.

HRMS-ESI$^+$ (*m/z*): calc. for $C_{26}H_{23}N_6O_5$ $[M+H]^+$ = 499.1730, found= 499.1729.

FT-IR max (cm^{-1}): 3190 (str. C-H of aromatic ring), 2957 (str. C-H of aliphatic), 2270 (str. C≡C), 1724 (str. C=O), 1670 (str.C=C), 1616 (str., C=C, Aromatic).

Synthesis of *N*-propargyl-*N*-[*N*^{2}-(benzhydryloxycarbonyl) gunain-9-acetyl] glycine 118

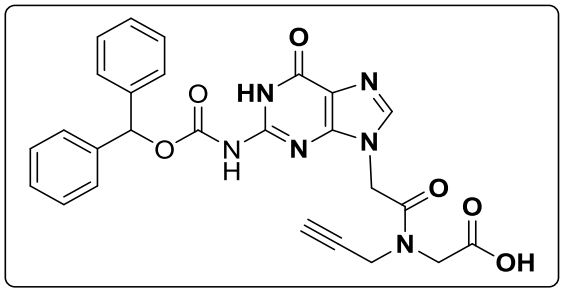

To a stirred solution of ethyl *N*-propargyl-*N*-[4-N-(benzhydryloxycarbonyl) guanine-9-acetyl] glycinate **114** (1.0 g, 1.8 mmol) dissolved in 1,4-dioxane (10 ml), was added in one portion an aqueous solution of NaOH (10 ml, 20.0 mmol). The reaction mixture was stirred at room temperature for 20 minutes. After this time, the reaction mixture was cooled with an ice-water bath and stirred for further five minutes and then was acidified with an aqueous solution of citric acid (20% w/v) until pH=3. The resulting precipitate was stirred for a further five minutes and collected by filtration under vacuum and dried under high vacuum for 3 hours to give the desired novel PNA monomer **118** (0.81, 84%) as a pure white powder, melting point (mp): 195-198 ˚C.

^{1}H NMR (400 MHz, DMSO-d6) (two rotational isomers observed); δ= 11.78 (br. 1H,

OH), 11.26 (br., 1H, NH), 7.91 (m, 1H, gauninyl-C(8)-H), 7.50-7.28 (m, 10, Ar), 6.87 (s, 1H, Ph_2CHO), 5.21 and 5.64 (s, 2H, NCH_2CON), 4.45 and 4.38 (s, 2H, NCH_2COOH), 4.20 and 407 (s, 2H, $CH_2C{\equiv}CH$), 3.53 and 3.30 (s, 1H, $CH{\equiv}C$).

^{13}C NMR (100 MHz, DMSO-d6) (two rotational isomers observed); δ = 170.84 and 170.6, 167.47 and 166.9, 156.0, 153.22, 149.19, 147.5, 141.1, 139.06 and 138.89, 129.05, 128.9, 128.4, 126.88, 79.05, 78.4, 74.65 and 73.81, 61.66 and 61.42, 47.70 and 47.36, 44.20 and 43.52, 36.0 and 33.8.

HRMS-ES$^+$ (*m/z*): calc. for $C_{26}H_{23}N_6O_6$ $[M+H]^+$= 515.1679, found= 515.1680.

FT-IR ($CHCl_3$ film, cm^{-1}): 3251 (str. C≡C-H), 2983 (str. aliphatic CH), 1681 (str. C=O), 1612 (str. C=O), 1571 (str. C=C).

Synthesis of 2-(*N*-Fmoc amino) ethyl azide 120

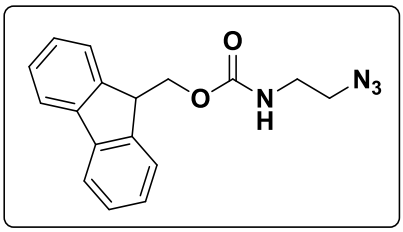

2-Bromoethylamine hydrobromide **119** (5.0 g, 24.4 mmol) and sodium azide (4.0 g, 61.5 mmol) were dissolved in water (100 ml). The resulting solution was stirred and heated up 80 °C for 20 hours. The reaction mixture was cooled to room temperature followed by addition NaOH (2.0 g, 50.0 mmol). The resulting solution was stirred for further 15 minutes before being extracted with DCM (4 × 50 ml). The combined organic layer was dried over $MgSO_4$ and concentrated to about 60 ml. To this solution, Fmoc succinimide ester (3 g, 8.9 mmol) and triethylamine (2.5 ml, 17.8 mmol) were added. The reaction mixture was stirred for two hours at room temperature. The reaction mixture was then washed with water (5 × 50 ml), brine (3 × 50 ml). The organic phase was dried over $MgSO_4$ and concentrated under vacuum. The residue was cooled in an ice bath to give the target compound **120** (2.2 g, 80%) a white solid product, melting point (mp): 85-88 ˚C.

^{1}H NMR (400 MHz, $CDCl_3$); δ= 7.75 (d, *J*= 8.93 Hz, 2H, Ar-CH), 7.57 (d, *J*= 8.93 Hz, 2H, Ar-CH), 7.39 7.30 (m, 4H, Ar-CH), 5.03 (bs, 1H, NH), 4.41(d, *J*= 6.29 Hz, 2H, $CHCH_2O$), 4.21 (t, *J*= 6.29 Hz, 1H, $CHCH_2O$), 3.43 (t, *J*= 3.5 Hz, 2H, $NHCH_2$), 3.5 (t, *J*= 3.55 Hz, 2H, CH_2N_3).

^{13}C NMR (100 MHz, $CDCl_3$); δ= 156.44, 143.9, 141.39, 127.83, 127.16, 125.11, 120.11, 69.89, 51.14, 47.26, 40.54.

HRMS-ESI$^+$ (*m/z*): Calc. for $C_{17}H_{16}N_4O_2$ $[M+H]^+$ = 309.1352, found= 309.1347.

FT-IR ($CHCl_3$ film, cm^{-1}): 2988 and 2875 (str. aliphatic CH), 2100 (str. azide group), 1681 (str. C=O), 1543 (str. C=C).

Synthesis of *N*-[(1-(2-Fmoc-aminoethyl)-1H-1,2,3-triazol-4-yl) methyl]-*N*-(thyminyl-1-yl acetyl) glycine 121

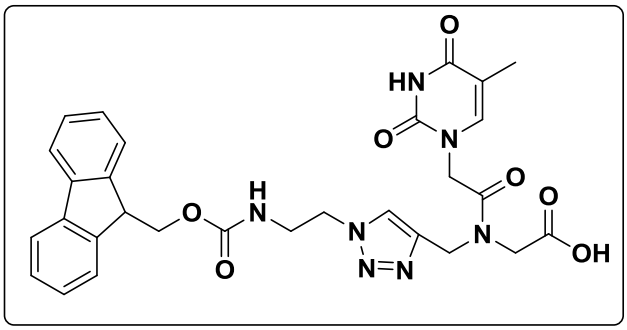

To a stirred solution of $CuSO_4{\cdot}5H_2O$ (40 mg, 0.16 mmol) in water (0.5 ml) was added a solution of sodium ascorbate (60 mg, 0.3 mmol) dissolved in water (0.5 ml), followed by addition of *tert*-butanol:water (20 ml 2:1). *N*-propargyl *N*-(thymin-1-yl acetyl) glycine **115** (0.3 g, 3.1 mmol) and compound **120** (0.95 g, 3.1 mml) were sequentially added. The reaction mixture was heated to 40 °C and stirred for 22 hours. The precipitate formed was collected by filtration, washed with ethyl acetate and dried under high vacuum to obtain the target compound **121** (1.5 g, 75%) as a pale white powder, melting point (mp): 197-200 °C.

^{1}H NMR (500 MHz, DMSO-d6); δ= 11.30 (br. 1H, NH-thyminyl), 7.96 (s, 1H, C=CH-triazolyl), 7.88 (d, *J*= 5.0 Hz, 2H, Ar-CH), 7.65 (d, *J*= 5.0 Hz, 2H, Ar-CH), 7.55 (br, 1H, CONH), 7.5-7.25 (m, 5H, C=CH-thyminyl, Ar-H), 4.80 and 4.66 (s, 2H, NCH_2CON), 4.5-

3.25 (m, 9H, $CHCH_2O$, $NCH_2CH_2NCH_2$), 1.71 (s, 3H, CH_3).

^{13}C NMR (125 MHz, DMSO-d6); δ= 167.84, 164.61, 156.61, 151.0, 144.26, 142.0, 140.50, 135.83, 128.24, 124.4, 125.0, 120.5, 108.0, 66.56, 49.66, 48.7, 48.02, 46.2, 42.0, 12.25.

HRMS-ESI$^+$ (*m/z*): calc. for $C_{29}H_{30}N_7O_7$ $[M+H]^+$ = 588.2207, found = 588.2197

FT-IR (Disc KBr, cm^{-1}): 3311 (s, amide NH), 2962 and 2885 (str., CH, aliphatic), 1690 (str. C=O), 1664 (str. C=O), 1544 (str. C=C aromatic).

Synthesis of 3-[1-(2-Fmoc-aminoethyl)-1H-1,2,3-triazol-4-yl] propionic acid 123

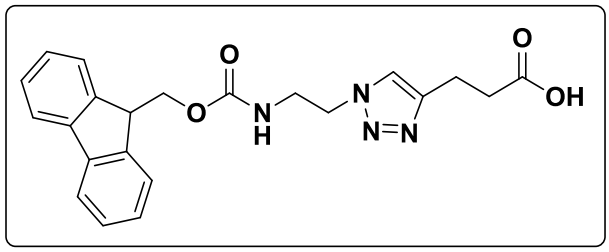

A solution of sodium ascorbate (100 mg, 0.50 mmol) dissolved in water (0.5 ml) was added to a stirred solution of $CuSO_4 \cdot 5H_2O$ (65.0 mg, 0.30 mmol) dissolved in water (0.5 mL), followed by addition a mixture of *ter*t-butanol:water (10 ml, 2:1). To the resulting solution were sequentially added compound **120** (1.5 g, 4.9 mml) and 4-pentynoic acid **122** (0.5 g, 5.1 mmol). The reaction mixture was stirred at room temperature for overnight. The residue was dissolved in ethyl acetate (25 ml), and washed with water (2 × 25 ml) and brine (2 × 25 ml). The organic phase was dried over Na_2SO_4, filtered and concentrated. The crude product was purified by column chromatography to give the titled compound **126** (1.2 g, 80%) as pale yellow solid, melting point (mp):164-166 °C.

^{1}H NMR (400 MHz, DMSO-d6); δ= 12.14 (s, 1H, COOH), 7.9 (d, *J*= 7.02 Hz, 2H, Ar-CH), 7.77 (s, 1H, CH=C) 7.66 (d, *J*= 7.02 Hz, 2H, Ar-CH), 7.50 (br, 1H, NH), 7.4 (t, *J*= 7.9 Hz, 2H, Ar-CH), 7.34 (t, *J*= 7.9 Hz, 2H, Ar-CH), 4.36 (t, *J*= 5.94 Hz, 2H, CH_2-N-triazole), 4.31 (d, *J*= 6.3 Hz, 2H, $CHCH_2O$), 4.21 (t, *J*= 6.3 Hz, 1H, $CHCH_2O$), 3.40 (q, *J*= 5.3 Hz, 2H, $CONHCH_2$), 2.82 (t, *J*= 7.2 Hz, 2H, CH_2CH_2COOH), 2.56 (t, *J*= 7.2 Hz, 2H,

CH_2COOH).

^{13}C NMR (100 MHz, DMSO-d6); δ= 173.77, 156.63, 146.11, 144.33, 141.24, 128.10, 127.55, 125.63, 122.76, 120.58, 66.89, 49.19, 47.18, 41.06, 39.0, 21.27.

HRMS-ESI$^+$ (*m/z*): calc. for $C_{22}H_{22}N_4O_4$ $[M+H]^+$ = 407.1719, found = 407.1722.

FT-IR (Disc KBr, cm^{-1}): 3311 (s, amide NH), 3100 (str. C-H, Aromatic) 2962 and 2885 (str., CH, aliphatic), 1734 (str. C=O, COOH), 1695 (str. C=O, OCON), 1544 (str. C=C aromatic).

Synthesis of *N-tert*-butoxycarbonyl-glycine 124 [166]

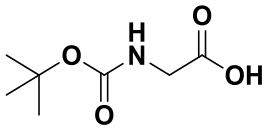

To a stirred solution of glycine **96** (1.5 g, 20.0 mmol) in an aqueous solution of NaOH (40 ml, 1N) was added in portions a solution of di-*tert*-butyl carbonate (5.5 g, 25.2 mmol) dissolved in isopropanol (30 ml). The resulting solution was stirred at room temperature for two hrs and then washed with light petroleum ether (b.p 40-60 °C) (2 × 50 ml). The aqueous phase was acidified to pH 3 with a solution of H_2SO_4 (2 N) and was then extracted with chloroform (3 × 50 ml). The combined organic layer was dried over anhydrous Na_2SO_4 and evaporated on the rotary evaporator to give the desired compound **124** (3.1 g, 88%) as white crystals, melting point (mp): 89-92 °C, [lit.[166] mp: 93 °C].

^{1}H NMR (400 MHz, $CDCl_3$); δ= 12.46 (br, 1H, OH), 7.10 (br, 1H, NH), 3.56 (d, *J*= 8.0 Hz, 2H, NCH_2CO), 1.37 (s, 9H, $(CH_3)_3$).

^{13}C NMR (100 MHz, $CDCl_3$); δ= 173.56, 156.14, 80.09, 41.7, 28.27.

HRMS-ESI$^-$ (*m/z*): calc. for $C_7H_{12}NO_4$ $[M-H]^-$ = 174.076, found = 174.0760.

FT-IR (Disc KBr cm^{-1}): 3292-3488 (br, OH), 3133 (NH str, amide), 2927 and 2850 (str. aliphatic C-H), 1737 (str. C=O of COOH), 1635 (str. C=O of amide).

Synthesise of *N*-(*tert*-butoxycarbonyl)-*N*-(prop-2-yn-1-yl) glycine 125 [165]

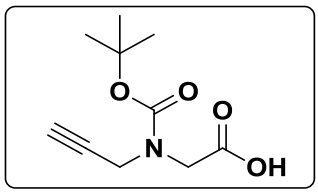

To a stirred solution of *N*-Boc-protected glycine, **124** (1.5 g, 8.6 mmole) dissolved in dry THF (100 ml) was added a solution of propargyl bromide 80% w/v in toluene (6.0 ml, 66.0 mmol). The resulting reaction mixture was cooled in an ice-water bath and kept under nitrogen atmosphere, and sodium hydride (60% in mineral oil, 0.175 g, 24.0 mmol) was added in portions. The resulting mixture reaction was stirred for a further two hours at 0 °C, and then the ice-water bath was removed. The reaction mixture was stirred at room temperature for overnight. The solvent was evaporated on a rotary evaporator and the residue was dissolved in water (50 ml) and washed with diethyl ether (20 ml). The aqueous phase was acidified to pH 2 with a solution of hydrochloric acid (1.0 N). The resulting solution was extracted with ethyl acetate (3 × 50 ml). The combined organic layer was dried over anhydrous $MgSO_4$, filtered and evaporated to give the desired product **125** (1.42 g, 78%), melting point (mp): 98-100 °C.

^{1}H NMR (400 MHz, $CDCl_3$) (two rotational isomers observed); δ= 10.37 (br, 1H, COOH), 4.22 and 4.18 (s, 2H, NCH_2COO), 4.15 and 4.11 (s, 2H, $NCH_2C{\equiv}$), 2.27 (s, 1H, C≡CH), 1.48 and 1.44 (s, 9H, C $(CH_3)_3$).

^{13}C NMR (100 MHz, $CDCl_3$) (two rotational isomers observed); δ= 175.2 and 174.01, 155.3 and 154.7, 82.1 and 81.9, 79.0 and 78.75, 73.44 and 72.18, 47.4 and 47.0, 37.6 and 37.0, 28.56 and 28.5.

HRMS-ESI$^-$ (*m/z*): calc. for $C_{10}H_{15}NO_4$ $[M-H]^-$ = 212.0923, found = 212.0916.

FT-IR ($CDCl_3$ film, cm^{-1}): 3311 (s, C≡H), 2981 and 2927 (str., aliphatic CH), 2300 (str. C≡C) 1740 (str. C=O, COOH), 1650 (str. C=O, OCON).

Synthesis of *N*-[(1-(2-Fmoc-aminoethyl)-1H-1,2,3-triazol-4-yl) methyl]-*N*-(*tert*-butoxycarbonyl) glycine 126

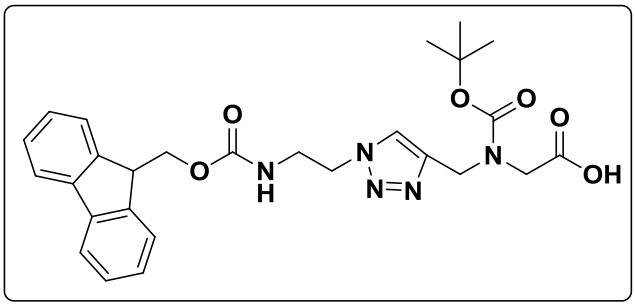

To a stirred solution of $CuSO_4 \cdot 5H_2O$ (50 mg, 0.20 mmol) dissolved in water (0.5 ml) was added a solution of sodium ascorbate (90 mg, 0.45 mmol) dissolved in water (0.5 mL). To the resulting solution, a mixture of *tert*-butanol:water (9 ml, 6:3) was added, followed by addition of *N*-propargyl-*N*-*tert*-butyloxycarbonyl glycine **125** (0.5 g, 2.3 mmol) and the azide component **120** (0.95 g, 3.1 mmol) sequentially. The mixture was then stirred at 40 °C overnight. The solvents were removed under vacuum. The residue was dissolved in ethyl acetate (25 ml), and washed with water (2 × 25 ml) and brine (2 × 25 ml). The organic phase was dried over Na_2SO_4, filtered and concentrated to give a yellow foam which was purified by column chromatography to give the titled compound **126** (1.2 g, 75%) as pale yellow solid, melting point (mp): 78-80 °C.

^{1}H NMR (400 MHz, Acetone-d6); δ 7.74 (s, 1H, C=CH, triazolyl), 7.88 (d, *J*= 8.0 Hz, 2H, Ar-CH), 7.65 (d, *J*= 8.0 Hz, 2H, Ar-CH), 7.39-7.31 (m, 4H, Ar-CH), 4.46-4.36 (m, 4H, CH_2CH_2-triazole, CH_2OCON), 4.28 (t, *J*= 8.2 Hz, 1H $CHCH_2OCON$), *4*.21 (t, *J*= 7.5 Hz, 2H, $CONHCH_2$), 4.1 and 3.95 (s, 2H, NCH_2COO), 3.64 (s, 2H, CH_2NCO), 1.30 and 1.28 (s, 9H, $(CH_3)_3$).

^{13}C NMR (100 MHz, $CDCl_3$); δ = 173.12, 157.03, 155.76, 144.12, 141.63, 128.13, 127.47, 125.49, 125.05, 124.26, 120.38, 81.46, 67.22, 50.45, 47.49, 43.22, 41.30, 28.76 and 28.58.

HRMS-ESI$^+$ (*m/z*): calc. for $C_{27}H_{31}N_5O_6$ $[M+H]^+$ = 522.2353, found= 522.2352.

FT-IR ($CDCl_3$ film, cm^{-1}): 2962 and 2885 (str., aliphatic C-H), 1734 (str. C=O, COOH), 1695 (str. C=O, OCON), 1525 (str. C=C aromatic).

Synthesis of *tert*-Butyl (2-aminoethyl) carbamate 33 [87]

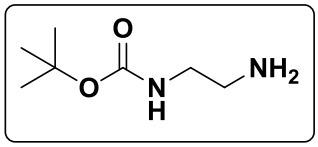

To a stirred solution of 1,2-diaminoethane (20 ml, 299 mmol) dissolved in THF (40 ml) at room temperature, a solution of Boc-anhydride (3.3 g, 15.114 mmol) dissolved in tetrahydrofuran (50 ml) was slowly added. The reaction mixture was stirred at room temperature for 12 hours. After this time, the solvent was evaporated on a rotary evaporator and the residue was dissolved in ethyl acetate (50 ml) and washed with brine (2 × 25 ml), and water (2 × 25 ml). The organic phase was dried over Na_2SO_4 and concentrated to give the desired product (2.0 g, 80%) as a pale-yellow oil.

^{1}H NMR (400 MHz, $CDCl_3$); δ = 5.05 (br, 1H, NH), 3.10 (q, *J*= 8.0 Hz, 2H, $NHCH_2CH_2$), 2.27 (t, *J*= 8.0 Hz, 2H, CH_2NH_2), 1.41 (s, 9H, $(CH_3)_3$).

^{13}C NMR (100 MHz, $CDCl_3$); δ = 156.13, 78.26, 43.12, 41.53, 28.07.

LRMS-ES$^+$ (*m/z*): calc. for $C_7H_{16}N_2O_2$= 160.1, found = 160.104.

Synthesis of benzyl (2-((*tert*-butoxycarbonyl) amino) ethyl) glycinate 127 [87]

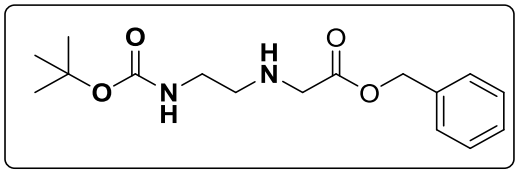

To a stirred solution of *tert*-butyl (2-aminoethyl) carbamate **33** (2.0 g, 12.517 mmol), triethylamine (1.8 ml, 12.917 mmol) and benzyl bromoacetate (1.4 ml, 12.658 mmol) were dissolved in acetonitrile. The reaction mixture was stirred at room temperature for 2 hours and then filtered. The solvent was removed under vacuum, and the residue was dissolved in ethyl acetate (50 ml), washed with brine (2 × 25 ml), water (2 × 25 ml). The organic phase was dried over Na_2SO_4, filtered, and concentrated to give the titled compound **127** (2.5 g, 83%) as a pale red oil.

^{1}H NMR (400 MHz, $CDCl_3$); δ = 7.2-7.35 (m, 5H, Ar), 5.1 (s, 2H, OCH_2Ar), 5.05 (br, 1H, NH), 3.39 (s, 2H, NCH_2COO), 3.15(q, *J*= 5.7 Hz, 2H, $NHCH_2$), 2.79 (t, *J*= 5.7 Hz, 2H, CH_2NH), 1.78 (br, 1H, NH), (s, 9H, $(CH_3)_3$).

^{13}C NMR (100 MHz, $CDCl_3$); δ= 172.62, 156.26, 135.6, 128.7, 128.58, 128.50, 77.69, 50.56, 48.89, 40.26, 28.53.

LRMS-ES$^+$ (*m/z*): calc. for $C_{16}H_{25}N_2O_4$ $[M+H]^+$ = 309.2, found= 309.204.

Synthesis of benzyl *N*-(2-Fmoc-aminoethyl) glycinate 128 [87]

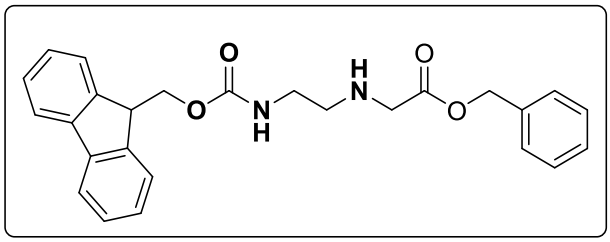

To a stirred solution of benzyl 2-((2-((*tert*-butoxycarbonyl) amino) ethyl) amino) acetate **127** (2.0 g, 8.120 mmol) dissolved in DCM (20 ml) in an ice-water bath was added TFA (15 ml) in one portion. The resulting reaction mixture was stirred for 15 min at room temperature. The solvent was removed under vacuum and the residue was washed with chloroform (25 ml) and then decanted. DCM (25 ml), triethylamine (2.5 ml, 17.924 mmole), Fmoc-OSu (2.7 g, 8.120 mmol) were added and the reaction mixture was stirred for further two hours at room temperature. The reaction mixture was washed with water (3 × 50 mL), brine (3 × 25 ml) dried over Na_2SO_4, filtered, and concentrated to give the target compound **128** (2.1 g, 76%) a red oil.

^{1}H NMR (400 MHz, $CDCl_3$); δ 7.61 (d, *J*= 7.4 Hz, 2H, Ar-CH), 7.49 (d, *J*= 7.4 Hz, 2H, Ar-CH), 7.42–7.28 (m, 9H, Ar-CH), 5.68 (br, 1H, NH), 5.1 (s, 2H, $COOCH_2Ph$), 4.3 (d, *J*= 7.0 Hz, 2H, $CHCH_2O$), 4.22 (t, *J*= 7.0 Hz, 1H, $CHCH_2O$), 3.25 (s, 2H, $NHCH_2COO$), 3.19 (q, *J*= 5.4 Hz, 2H, $NHCH_2$), 2.58 (t, *J*= 5.4 Hz, 2H, CH_2NH), 1.76 (br, 1H).

^{13}C NMR (100 MHz, $CDCl_3$); δ= 172.52, 156.66, 144.18, 141.3, 135.6, 127.28, 125.0, 120.0, 66.5, 50.44, 48.67, 48.2, 40.0.

LRMS-ES$^+$ (*m/z*): calc. for $C_{26}H_{26}N_2O_4$ $[M+H]^+$ = 430.5 found = 430.52.

Synthesis of benzyl *N*-(2-Fmoc-aminoethyl)-*N*-(thymin-1-yl acetyl) glycinate 129 [86]

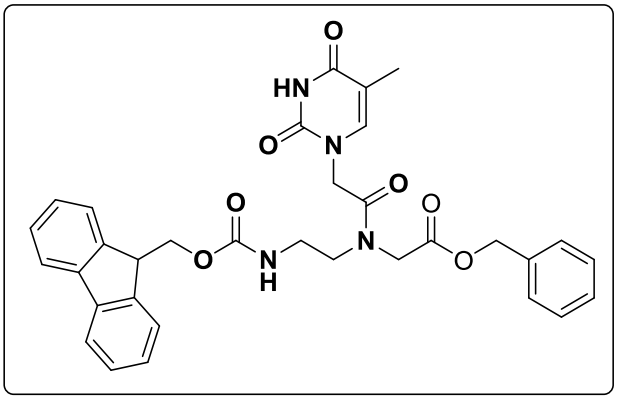

To a stirred solution of compound **128** (1.99 g, 5.428 mmol) dissolved in DMF (25 ml), DCC (1.1 g, 5.428 mmol), and HOBt.H_2O (0.765 g, 5.0 mmol) and thymine acetic acid derivative **100** (1.0 g, 5.428 mmol) were sequentially added. The reaction mixture was stirred at room temperature overnight. The formed DCU was removed by filtration, and the solvent was then evaporated under vacuum to dryness. The residue was dissolved in DCM (50 ml), filtered and washed sequentially with $NaHCO_3$ 5% w/v (2 × 50 ml), $KHSO_4$ 1 M aqueous (2 × 50 ml) and brine (2 × 50 ml). The organic phase was dried over Na_2SO_4 and concentrated. The resulting foam was triturated with a mixture of THF/ hexane (25 ml, 5:20). The precipitate that formed was collected by filtration and dried under high vacuum to give the titled compound **129 (**2.1 g, 72%) as a foam.

^{1}H NMR (400 MHz, $CDCl_3$) (two rotational isomers); δ= 7.88 (d, *J*=7.3 Hz, 2H, Ar-CH), 7.68 (d, *J*=7.3 Hz, 2H, Ar-CH), 7.48-7.25 (m, 11H, Ar-H, thymin-C(6)-H), [5.22 (s, min) and 5.13 (s, maj) 2H, OCH_2Ph], [4.69 (s, maj) and 4.51 (s, min), 2H, $NHCH_2CO$], 4.10-4.40 (m, 5H, $CHCH_2OCO$, NCH_2COO), 3.0-3.50 (m, 5H, $NHCH_2CH_2$)), 1.76 (s, 3H, CH_3)

^{13}C NMR (100 MHz, $CDCl_3$); δ= 169.6, 167.8, 164.8, 156.7, 151.3, 144.2, 141.1, 136.1, 128.8, 128.6, 1285, 128, 4, 128.2, 127.9, 127.4, 125.4, 120.4, 67.0, 66.3, 48.3, 12.3.

LRMS-ES$^+$ (*m/z*): calc. for $C_{33}H_{33}N_4O_7$ $[M+H]^+$ = 597.2, found 597.21.

Synthesis of *N*-(2-Fmoc-aminoethyl)-*N*-(thymin-1-yl acetyl) glycine 130 [86]

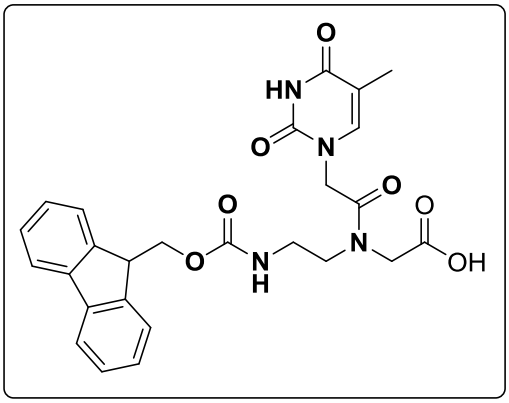

Compound **129** (0.5 g, 1.0 mmol) was dissolved in the minimal amount of an acetone:MeOH solution (1:1, v/v). To the resulting solution was added Pd/C (100 mg) and the reaction flask was placed under an atmosphere of H_2 at 0 °C for 1 hour. The suspension was stirred at room temperature for a further 2 h. The solvent was removed and the residue suspended in MeOH (100 ml). The suspension was filtered through celite, and the solvent removed by rotary evaporator to yield the tilted compound **130** (0.22, 90%) as white solid, melting point (mp)= 215-218 °C [lit.[86] mp: 216-219 °C].

^{1}H NMR (400 MHz, $CDCl_3$) (two rotational isomers observed); δ= 11.2 (s, 1 H), 7.9 (d, *J*=7.3 Hz, 2H Ar-H), 7.68 (d, *J*=7.3 Hz, 2H, Ar-H), 7.20-7.48 (m, 5H, Ar-H and thyminy-C(6)-H), [4.69 (s, maj.) and 4.51(s, min), 2H, NCH_2COO] 4.4-4.10 (m, 5H, $CHCH_2OCO$, NCH_2CON), 3.5-3.1(m, 5H, $NHCH_2CH_2$), 1.76 and 174 (s, 3H, CH_3).

^{13}C NMR (100 MHz, DMSO-d_6) (two rotational isomers observed); δ= 168.1 and 167.7, 164.9, 156.8 and 156.5, 151.5, 144.3, 142.6, 141.15, 128.1, 127.5, 125.7, 120.5, 108.58, 65.98, 48.2 and 47.1, 12.38 and 12.33.

LRMS-ES$^+$ (*m/z*): calc. for $C_{26}H_{26}N_4O_7$ $[M+H]^+$ = 506.2, found 506.205.

6.2 Solid phase PNA synthesis

Monomers and reagents for solid phase PNA synthesis

Standard Fmoc/Bhoc protected PNA monomers were purchased from Link Technologies. Fmoc-Lys (Boc)-OH**,** HATU and NMP reagent were purchased from Novabiochem. 2,6-Lutidine, DIPEA (*N*,*N*-diisopropylethylamine), acetic anhydride were obtained from Sigma-Aldrich. Piperidine, m-cresol and TFA were purchased from Fisher scientific.

Reversed-phase high-performance liquid chromatography (RP-HPLC)

RP-HPLC chromatograms was recorded on a Merck-Hitachi La Chrom D-7000 series instrument with a Merck reverse phase C18 E column (4.6 × 100 mm) and a UV diode array detector which was set at 260 nm. The column was set at 30 °C with flow rate 0.5 ml/min. The analysis was performed on the mobile phase consisting of H_2O (A) and MeCN (B) acidified with 0.1 % TFA. Gradient elution from 95% to 5% water in 30 minutes.

Ultra-high performance liquid chromatography-mass spectrometry (UPLC-MS)

Mass spectra of the synthesised PNA oligomers were recorded at the Cardiff University, UK using positive ESI mode on a Waters Synapt G2-Si spectrometer with Acquity UPLC and an Acquity UPLC BEH C18 column (50 × 2.1 mm; 1.7 µm).

General Procedure for Synthesis of PNA oligomers

Resins preparation

In the current study, two different Fmoc-protected resins Rink Amide MBHA resin (Substitution 0.34 mmole/g) and Azido-Nova Tag (Substitution 0.35 mmole/g) were used in the synthesis of the target modified PNA oligomers. The appropriate resin was added to a fritted plastic vessel. The outlet of the syringe was connected to a membrane pump via a collecting tank. NMP was added for resin swelling and left at least two hours before the solvent was removed by vacuum filtration.

Fmoc-deprotection/Coupling-activation/Capping cycle

For Fmoc removal, a solution of piperidine in NMP (20% v/v) was added and shaken for 10 min at room temperature. The solvent was removed by vacuum filtration, and this step was repeated. The resin was then washed with NMP (3 × 2 min). To a solution containing the required monomer (4 eq.) and HATU (4.5 eq.) in NMP was added a solution of DIPEA (10 eq.) and 2,6-lutidine (10 eq.). The resulting solution was mixed for five min. before being added to the reaction vessel containing the resin bound free amino function. The resulting solution was shaken for 60 min at 25 °C. The solvent was removed by vacuum filtration, and the resin beads were washed with NMP. Followed by addition of a solution of a mixture of acetic anhydride (5 µL), lutidine (6 µL) and NMP (85 µl). The resulting solution was shaken for 10 min. at room temperature, filtered and washed efficiently with NMP. This deprotection/coupling/capping cycle was repeated for all building blocks until the required PNA sequence was synthesised.

Finally, for removal of the *N*-terminal Fmoc group and drying the resin-bound PNA oligomers, a solution of piperidine in NMP (20% v/v) was added and shaken for 10 min. at room temperature. The solvent was removed by vacuum filtration, and this step was repeated. The resin was the washed three times with each of NMP, chloroform methanol and diethyl ether and finally dried *in vacuo*.

Cleavage of the PNA oligomer from resin and deprotection of side chains

To the resin-bound PNA oligomer was added a solution (1 ml) of a mixture of TFA (95%), water (2.5%) and *m*-cresol (2.5%). The resulting mixture reaction was shaken for two hours at room temperature. The filtrate was then collected, and the resin was washed with TFA (200 µl). All cleavage solutions were combined and concentrated to about the 0.5 ml under a stream of nitrogen gas. Diethyl ether (1.5 ml) was added to induce the precipitation of the PNA oligomers. The sample was centrifuged at 4 °C for 10 minutes at 11000 rcf. The ether was carefully decanted without removing any precipitated PNA. The precipitate was re-suspended in diethyl ether and centrifuged three more times. The PNA oligomers were dried under vacuum and then dissolved in 1 ml of a mixture of H_2O/ACN (1:1). All the

crude samples were purified by HPLC and characterised by mass spectrometry.

Purifications of the synthesised PNA oligomers

The crude PNA oligomers were purified by RP- HPLC with UV detection at 260 nm. Semi-prep column C18 (5 µm, 250 × 10 mm, Jupiter Phenomenex, 300 Å) was utilized, eluting with water + 0.01% TFA (eluent A) and acetonitrile + 0.01% TFA (eluent B); elution gradient: from 95% A to 95% B in 25, flow: 1 ml/min. The resulting pure PNA oligomers were characterized by LCMS-ESI with gave positive ions consistent with the final products.

PNA oligomer 131

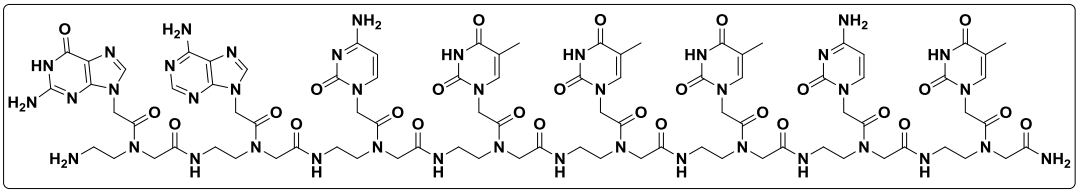

Chemical Formula: $C_{86}H_{111}N_{41}O_{27}$, Exact Mass: 2149.9, Molecular Weight: 2151.1

RP-HPLC, retention time: 8.71 min

ESI-MS: *m/z* = found 1076.0 (calc. 1075.95; $[M+2H]^{2+}$), found 717.9 (calc. 717.6; $[M+3H]^{3+}$), found 538.7 (calc. 538.475; $[M+4H]^{4+}$), found 431.1 (calc. 430.98; $[M+5H]^{5+}$).

PNA oligomer 132

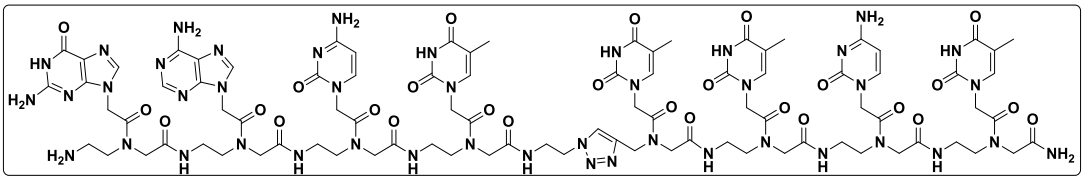

Chemical Formula: $C_{89}H_{114}N_{44}O_{27}$, Exact Mass: 2230.9, Molecular Weight: 2232.2

RPHPLC retention time: 9.33

ESI-MS: *m/z* = found 1116.9 (calc. 1116.45; $[M+2H]^{2+}$), found 744.8 (calc. 744.6; $[M+3H]^{3+}$), found 559.0 (calc. 558.7; $[M+4H]^{4+}$).

PNA oligomer 133

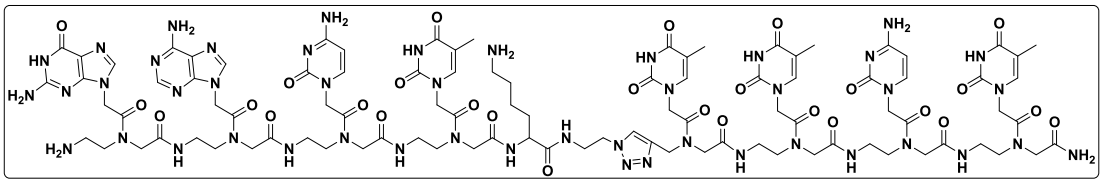

Chemical Formula: $C_{95}H_{126}N_{46}O_{28}$, Exact Mass: 2359.0, Molecular Weight: 2360.3

RPHPLC retention time: 8.63

ESI-MS: ***m/z*** = found 1180.5 (calc. 1180.5; $[M+2H]^{2+}$), found 787.6 (calc. 786.3; $[M+3H]^{3+}$), found 591.0 (calc. 590.75; $[M+4H]^{4+}$), found 473.0 (calc. 472.8; $[M+5H]^{5+}$).

PNA oligomer 134

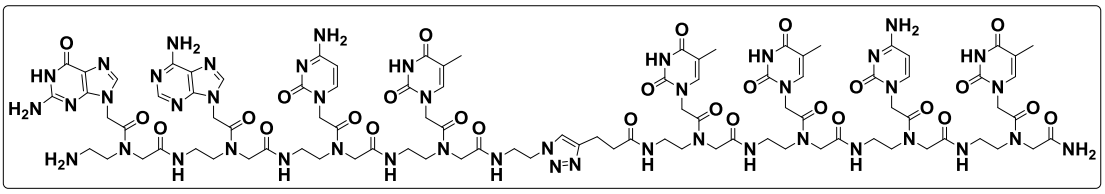

Chemical Formula: $C_{93}H_{121}N_{45}O_{28}$, Exact Mass: 2315.9, Molecular Weight: 2317.3

RPHPLC retention time= 13.12

ESI-MS: ***m/z*** = found 1159.8 (calc. 1158.95; $[M+2H]^{2+}$), found 773.4 (calc. 772.96; $[M+3H]^{3+}$), found 580.3 (calc. 579.97; $[M+4H]^{4+}$), found 462.8 (calc. 464.1; $[M+5H]^{5+}$).

PNA oligomer 135

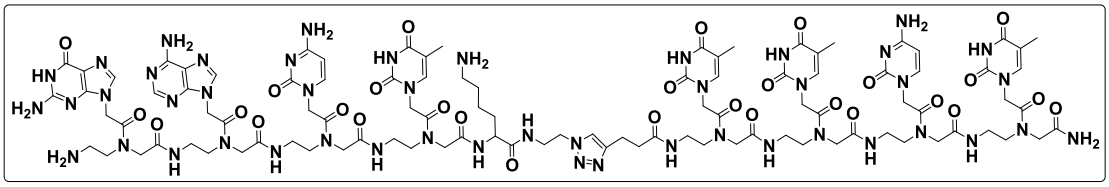

Chemical Formula: $C_{99}H_{133}N_{47}O_{29}$, Exact Mass: 2444.0, Molecular Weight: 2445.5

RPHPLC retention time: 12.61

ESI-MS: ***m/z*** = found 1223.5 (calc. 1223.0; $[M+2H]^{2+}$), found 816.3 (calc. 815.6; $[M+3H]^{3+}$), found 612.2 (calc. 612.0; $[M+4H]^{4+}$).

PNA oligomer 136

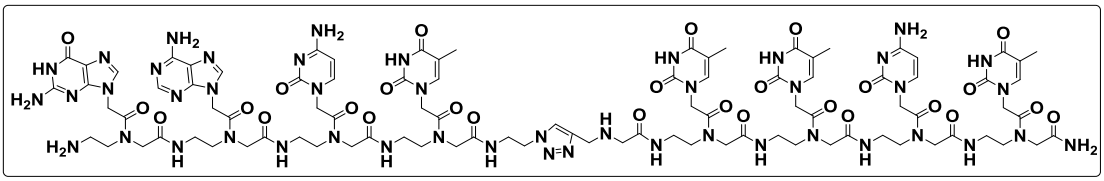

Chemical Formula: $C_{93}H_{122}N_{46}O_{28}$, Exact Mass: 2331.0, Molecular Weight: 2332.3

RPHPLC: Retention time = 9.09

ESI-MS: *m/z* = found 1167.0 (calc. 1166.5; $[M+2H]^{2+}$), found 778.4 (calc. 778.0; $[M+3H]^{3+}$), found 584.1 (calc. 583.75; $[M+4H]^{4+}$).

Azide functionalised PNA oligomer 137

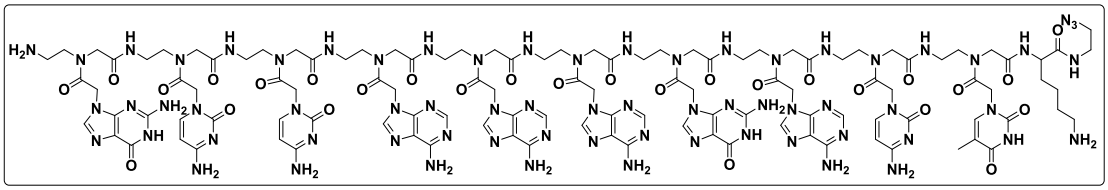

Chemical Formula: $C_{115}H_{149}N_{67}O_{28}$; Exact Mass: 2916.2; Molecular Weight: 2917.9

RPHPLC: Retention time = 9.28

ESI-MS: *m/z* = found 1459.3 (calc. 1459.1; $[M+2H]^{2+}$), found 973.4 (calc. 973.06; $[M+3H]^{3+}$), found 730.3 (calc. 730.1; $[M+4H]^{4+}$), found 584.5 (calc. 584.24; $[M+5H]^{5+}$), found 487.2 (calc. 487.03; $[M+6H]^{6+}$), found 417.8 (calc. 417.6; $[M+7H]^{7+}$).

Azide-alkyne functionalised PNA oligomer 138

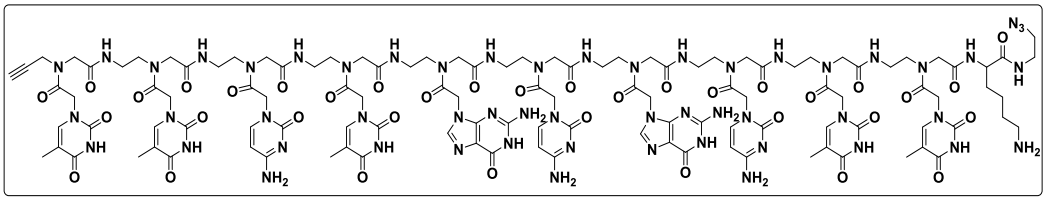

Chemical Formula: $C_{116}H_{150}N_{54}O_{36}$, Exact Mass: 2875.2, Molecular Weight: 2876.8

RPHPLC: Retention time = 9.9

ESI-MS: *m/z* = found 1438.8.0 (calc. 1438.6; $[M+2H]^{2+}$), found 959.8 (calc. 959.4; $[M+3H]^{3+}$), found 720.0 (calc. 719.8; $[M+4H]^{4+}$), found 576.3 (calc. 576.04; $[M+5H]^{5+}$), found 480.1 (calc. 480.2; $[M+6H]^{6+}$).

Alkyne functionalized PNA oligomer 139

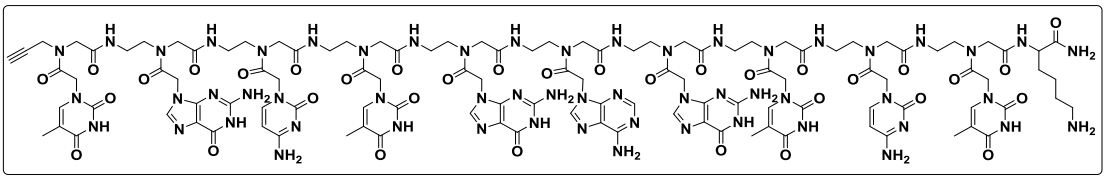

Chemical Formula: $C_{115}H_{146}N_{56}O_{34}$, Exact Mass: 2855.1, Molecular Weight: 2856.8

RPHPLC: Retention time = 10.51

ESI-MS: ***m/z*** = found 1429.0 (calc. 1428.55; $[M+2H]^{2+}$), found 953.1 (calc. 952.7; $[M+3H]^{3+}$), found 715.1 (calc. 715.77; $[M+4H]^{4+}$), found 572.4 (calc. 572.02; $[M+5H]^{5+}$), found 477.2 (calc. 476.85; $[M+6H]^{6+}$).

6.3 UV-T_m measurements

Samples preparation

DNA and RNA sequences were purchased from Sigma-Aldrich Company (Table 6.1).

Table 6.1: Physical data of nucleic acids that were used in the T_m -UV spectroscopy experiments.

Oligo name	Sequences (5'-3')	Pur	Mw	T_m	µg	nmol	µl for 100 µM
DNA1	AGAAAGTC	HPLC	2443	15.0	87.5	35.8	358
DNA2	AGAACAGTC	HPLC	2732	19.0	34.1	12.7	125
RNA	AGAAAGUC	HPLC	2557	8.9	255.1	99.7	997

PNA oligomers were prepared in our lab. Stock solutions of PNA oligomers, DNA and RNA, were prepared in distilled water, and their concentrations were determined on the basis of absorbance from the molar extinction coefficient of corresponding nucleobases i.e. C = 6.6, T = 8.6, A = 13.7 and G = 11.7 [$(mmol)^{-1}$ cm^{-1}] following Beer Lambert's Law (A = εcl). Phosphate buffer was prepared by mixing both potassium

phosphate monobasic (KH_2PO_4), sodium phosphate dibasic (K_2HPO_4) buffers and 0.1 mM NaCl in amounts appropriate for the desired pH= 7.0. PNA complexes with the antiparallel complementary nucleic acid oligomers were prepared by mixing stoichiometric quantities (1:1) of the involved oligomers with the DNA or RNA sample in 1 ml buffer of 10 mM sodium phosphate and 10 mM NaCl, at pH 7.0. The samples were annealed at 90 °C in a heat block for 5 min followed by slow cooling to 4 °C slowly over one hour and then were transferred to quartz cuvette, sealed with a Teflon stopper.

All UV melting experiments were performed on Shimadzu UV-2600 UV-Visible Spectrophotometer equipped with a heat controller. The absorbance at 260 nm was recorded in steps from 5-65 °C. Nitrogen gas was purged through the cuvette chamber below 20 °C to prevent the condensation of moisture on the cuvette walls. All measurements were recorded three times. Cuvette of 1.0 cm path length and 1.0 ml volume was used for all experiments.

The absorbance at 260 nm was plotted as a function of the temperature. The T_m values were obtained from average of the mid-points of the three sigmoidal thermal stability curves for each duplex with calculated the standard deviation for these measurements.

References

(1) Germer, K.; Leonard, M.; Zhang, X. *Int. J. Biochem Mol. Biol.* **2013**, *4*, 27–40.

(2) Niemietz, C.; Chandhok, G.; Schmidt, H. *Molecules* **2015**, *20*, 17944–17975.

(3) Khodakov, D.; Wang, C.; Yu, D. *Adv. Drug Deliv. Rev.* **2016**, *105*, 3–19.

(4) Dahm, R. *Dev. Biol.* **2005**, *278*, 274–288.

(5) Cobb, M. *Curr. Biol.* **2015**, *25*, R526–R532.

(6) Lönnberg, H. *Org. Biomol. Chem.* **2011**, *9*, 1687–1703.

(7) Worthington, F. *Annu. Rev. Biochem.* **1941**, *10*, 221–245.

(8) Duncan, B. K.; Miller, J. H. *Nature* **1980**, *287*, 560–561.

(9) Mortimer, S. A.; Kidwell, M. A.; Doudna, J. A. *Nat. Rev.* **2014**, *15*, 469–479.

(10) Wan, Y.; Kertesz, M.; Spitale, R. C.; Segal, E.; Chang, H. Y. *Nat. Rev.* **2011**, *12*, 641–655.

(11) Watson, J. D.; Crick, F. H. *Nature* **1953**, *171*, 737–738.

(12) Hodes, M. E.; Charlotte, G.; Rakoma, L.; Erwin, C. *J. Biol. Chem.* **1951**, *192*, 223–230.

(13) Dickerson, R. E.; Drew, H. R.; Conner, B. N.; Wing, R. M.; Fratini, A. V; Kopka, M. L. *Science* **1982**, *216*, 475–485.

(14) Schleif, R. *Science* **1988**, *241*, 1182–1187.

(15) Luscombe, N. M.; Austin, S. E.; Berman, H. M.; Thornton, J. M. *Genome Biol.* **2000**, *1*, 1–37.

(16) Nguyen, B.; Neidle, S.; Wilson, W. D. *Acc. Chem. Res.* **2009**, *42*, 11–21.

(17) Woods, K. K.; Lan, T.; Mclaughlin, L. W.; Williams, L. D. *Nucleic Acids Res.* **2003**, *31*, 1536–1540.

(18) Hoogsteen, K. *Acta Cryst.* **1963**, *16*, 907–916.

(19) Zhou, H.; Hintze, B. J.; Kimsey, I. J.; Sathyamoorthy, B.; Yang, S.; Richardson, J. S.; Al-hashimi, H. M. *Nucleic Acids Res.* **2015**, *43*, 3420–3433.

(20) Paul, A.; Bhattacharya, S. *Curr. Sci.* **2012**, *102*, 212–231.

(21) Siggers, T.; Gorda, R. *Nucleic Acids Res*. **2014**, *42*, 2099–2111.

(22) Siggers, T.; Gorda, R. *Nucleic Acids Res.* **2013**, 1–13.

(23) Park, Y.; Breslauer, K. J. *Proc. Natl. Acad. Sci. USA* **1992**, *89*, 6653–6657.

(24) Pizarro, A. M.; Sadler, P. J. *Biochimie* **2010**, *91*, 1198–1211.

(25) Hannon, M. J. *Pure Appl. Chem.* **2007**, *79*, 2243–2261.

(26) Deleavey, G. F.; Damha, M. J. *Chem. Biol.* **2012**, *19*, 937–954.

(27) Eckstein, F. *J. Am. Chem. Soc* **1966**, *18*, 4292–4294.

(28) Eckstein, F. *Tetrahedron Lett.* **1967**, 1157–1160.

(29) Eckstein, F. *Antisense Nucleic Acid Drug Dev.* **2000**, *10*, 117–121.

(30) Appella, D. H. *Curr. Med. Chem.* **2001**, *8*, 545–550.

(31) Gallo, M.; Montserrat, J. M.; Iribarren, A. M. *Brazilian J. Med. Biol. Res.* **2003**, *36* (2), 143–151.

(32) Obika, S.; Nanbu, D.; Hari, Y.; Morio, K.; In, Y.; Ishida, T.; Imanishi, T. *Tetrahedron Lett.* **1997**, *38*, 8735–8738.

(33) Koshkin, A. A.; Singh, S. K.; Nielsen, P.; Rajwanshi, V. K.; Kumar, R.; Meldgaard, M.; Olsen, C. E.; Wengel, J. *Tetrahedron* **1998**, *54*, 3607–3630.

(34) Singh, S. K.; Nielsen, P.; Koshkin, A. A.; Wengel, J. *Chem. Commun.* **1998**, 455–456.

(35) Stulz, E.; Clever, G.; Shionoya, M. *Chem. Soc. Rev.* **2011**, *40*, 5680–5689.

(36) Zhang, Y.; Qu, Z.; Kim, S.; Shi, V.; Liao, B.; Kraft, P.; Bandaru, R.; Wu, Y.; Greenberger, L. M.; Horak, I. D. *Gene Ther.* **2011**, *18*, 326–333.

(37) Veedu, R. N.; Wengel, J. *Chem. Biodivers.* **2010**, *7*, 536–542.

(38) Fujino, T.; Yamazaki, N.; Hasome, A.; Endo, K.; Isobe, H. *Tetrahedron Lett.* **2012**, *53*, 868–870.

(39) Nielsen, P. E.; Egholm, M.; Berg, R. H.; Buchardt, O. *Science* **1991**, *254*, 1497–1500.

(40) Koch, T.; Hansen, H. F.; Andersen, P.; Larsen, T.; Batz, H. G.; Otteson, K.; Orum, H. *J. Pept. Res.* **1997**, *49*, 80–88.

(41) Demidov, V. V; Potaman, V. N.; Frank-Kamenetskii, M. D.; Egholm, M.; Buchard, O.; Sönnichsen, S. H.; Nielsen, P. E. *Biochem. Pharmacol.* **1994**, *48*, 1310–1313.

(42) Ray, A.; Norden, B. *Faseb J* **2000**, *14*, 1041–1060.

(43) Hyrup, B.; Nielsen, P. E. *Bioorg. Med. Chem.* **1996**, *4*, 5–23.

(44) Buchardt, O.; Egholm, M.; Berg, R. H.; Nielsen, P. E. *Trends Biotechnol.* **1993**, *11*, 384–386.

(45) Wittung, P.; Nielsen, P. E.; Buchardt, O.; Egholm, M.; Norden, B. *Nature* **1994**,

368, 561–563.

(46) Brown, S. C.; Thomson, S. A.; Veal, J. M.; Davis, D. G. *Science* **1994**, *265*, 777–780.

(47) Gill, P.; Moghadam, T. T.; Ranjbar, B. *J. Biomol. Tech.* **2010**, *21*, 167–193.

(48) Chakrabarti, M. C.; Schwarz, F. P. *Nucleic Acids Res.* **1999**, *27*, 4801–4806.

(49) Gogoi, K.; Kumar, V. A. *Chem. Commun.* **2008**, 706–708.

(50) Gondeau, C.; Maurizot, J. C.; Durand, M. *Nucleic Acids Res.* **1998**, *26*, 4996–5003.

(51 Siddiquee, S.; Rovina, K.; Azriah, A. *Adv. Tech. Biol. Med.* **2015**, *3*, DOI:10.4172/2379–1764.1000131.

(52) Calabretta, A.; Tedeschi, T.; Corradini, R.; Marchelli, R.; Sforza, S. *Tetrahedron Lett.* **2011**, *52*, 300–304.

(53) Kilsa, K.; Ørum, H.; Nielsen, P. E.; Norde, B. *Biochemistry* **1997**, *36*, 5072–5077.

(54) Egholm, M.; Buchardt, O.; Nielsen, P. E.; Berg, R. H. *J. Am. Chem. Soc.* **1992**, *114*, 1895–1897.

(55) Giesen, U.; Kleider, W.; Berding, C.; Geiger, A.; Ørum, H.; Nielsen, P. E. *Nucleic Acids Res.* **1998**, *26*, 5004–5006.

(56) Tomac, S.; Sarkar, M.; Ratilainen, T.; Wittung, P.; Nielsen, P. E.; Norde, B.; Gra, A.; Nordén, B.; Gräslund, A. *J. Am. Chem. Soc.* **1996**, *118*, 5544–5552.

(57) Wittung, P.; Nielsen, P.; and Nordén, B. *Biochemistry* **1997**, *36*, 7973–7979.

(58) Kuhn, H.; Demidov, V. V; Nielsen, P. E.; Frank-Kamenetskii, M. D. *J. Mol. Biol.* **1999**, *286*, 1337–1345.

(59) Kurakin, A.; Larsen, H. J.; Nielsen, P. E. *Chem. Biol.* **1998**, *5*, 81–89.

(60) Cherny, D. Y.; Belotserkovskii, B. P.; Frank-Kamenetskii, M. D.; Egholm, M.; Buchardt, O.; Berg, R. H.; Nielsen, P. E. *Proc. Natl. Acad. Sci. USA* **1993**, *90*, 1667–1670.

(61) Demidov, V. V; Yavnilovich, M. V; Belotserkovskii, B. P.; Frank-Kamenetskii, M. D.; Nielsen, P. E. *Proc. Natl. Acad. Sci. USA* **1995**, *92*, 2637–2641.

(62) Kuhn, H.; Demidov, V. V; Nielsen, P. E.; Frank-Kamenetskii, M. D. *J. Mol. Biol.* **1999**, *286*, 1337–1345.

(63) Egholm, M.; Christensen, L.; Dueholm, K. L.; Buchardt, O.; Coull, J.; Nielsen, P. E. *Nucleic Acids Res.* **1995**, *23*, 217–222.

(64) Nielsen, P. E.; Christensen, L. *J. Am. Chem. Soc.* **1996**, *118*, 2287–2288.

(65) Lohse, J.; Dahl, O.; Nielsen, P. E. *Proc. Natl. Acad. Sci. USA* **1999**, *96*, 11804–11808.

(66) Paulasova, P.; Pellestor, F. *Ann. Genet.* **2004**, *47*, 349–358.

(67) Karkare, S.; Bhatnagar, D. *Appl. Microbiol. Biotechnol.* **2006**, *71*, 575–586.

(68) Haaima, G.; Hansen, H. F.; Christensen, L.; Dahl, O.; Nielsen, P. E. *Nucleic Acids Res.* **1997**, *25*, 4639–4643.

(69) Hanvey, J. C.; Peffer, N. J.; Bisi, J. E.; Thomson, S. A.; Cadilla, R.; Josey, J. A.; Ricca, D. J.; Hassman, C. F.; Bonham, M. A.; Au, K. G.; Carter, S. G.; Bruckenstein, D. A.; Boyd, A. L.; Noble, S. A.; Babiss, L. E. *Science* **1992**, *258*, 1481–1485.

(70) Chendrimada, T. P.; Finn, K. J.; Ji, X.; Baillat, D.; Gregory, R. I.; Liebhaber, S. a; Pasquinelli, A. E.; Shiekhattar, R. *Nature* **2007**, *447*, 823–828.

(71) Chiarantini, L.; Cerasi, A.; Fraternale, A.; Millo, E.; Benatti, U.; Sparnacci, K.; Laus, M.; Ballestri, M.; Tondelli, L. *J. Control. Release* **2005**, *109*, 24–36.

(72) Knudsen, H.; Nielsen, P. E. *Nucleic Acids Res.* **1996**, *24*, 494–500.

(73) Koppelhus, U.; Zachar, V.; Nielsen, P. E.; Liu, X.; Eugen-olsen, J.; Ebbesen, P. *Nucleic Acids Res.* **1997**, *25*, 2167–2173.

(74) Larsen, J. H.; Nielsen, P. E. *Nucleic Acids Res.* **1996**, *24*, 458–463.

(75) Diviacco, S.; Rapozzi, V.; Xodo, L.; Helene, C.; Quadrifoglio, F.; Giovannangeli, C. *FASEB J.* **2001**, *15*, 2660–2668.

(76) Merrifield, R. B. *J. Am. Chem. Soc* **1963**, *85*, 2149–2154.

(77) Egholm, M.; Nielsen, P. E.; Buchardt, O. *J. Am. Chem. Soc.* **1992**, *114*, 9677–9678.

(78) Valeur, E.; Bradley, M. *Chem. Soc. Rev.* **2009**, *38*, 606–631.

(79) El-faham, A.; Funosas, S.; Prohens, R. *Chem. Eur. J.* **2009**, *15*, 9404–9416.

(80) Montalbetti, C. A.; Falque, V. *Tetrahedron* **2005**, *61*, 10827–10852.

(81) Han, S.; Kim, Y. *Tetrahedron* **2004**, *60*, 2447–2467.

(82) Dueholm, K. L.; Egholm, M.; Buchardt, O. *Org. Prep. Proced. Int.* **1993**, *25*,

457–461.

(83) Finn, P. J.; Gibson, N. J.; Fallon, R.; Hamilton, A.; Brown, T. *Nucleic Acids Res.* **1996**, *24*, 3357–3363.

(84) Will, D. W.; Breipohl, G.; Langner, D.; Knolle, J.; Uhlmann, E. *Tetrahedron* **1995**, *51*, 12069–12082.

(85) Stetsenko, D. A.; Lubyako, E. N.; Potapov, V. K.; Azhikina, T. L.; Sverdlov, E. D. *Tetrahedron Lett.* **1996**, *37*, 3571–3574.

(86) Thomson, S. A.; Josey, J. A.; Cadilla, R.; Gaul, M. D.; Fred Hassman, C.; Luzzio, M. J.; Pipe, A. J.; Reed, K. L.; Ricca, D. J.; Wiethe, R. W.; Noble, S. A. *Tetrahedron* **1995**, *51*, 6179–6194.

(87) Feagin, T. A.; Shah, N. I.; Heemstra, J. M. *J. Nucleic Acids* **2012**, *2012*, ID354549.

(88) Kofoed, T.; Hansen, H. F.; Ørum, H.; Koch, T. *J. Pept. Sci.* **2001**, *7*, 402–412.

(89) Uhlmann, E.; Peyman, A.; Breipohl, G.; Will, D. W. *Angew. Chemie - Int. Ed.* **1998**, *37*, 2796–2823.

(90) Porcheddu, A; Giacomelli, G.; Piredda, I.; Carta, M.; Nieddu, G. *European J. Org. Chem.* **2008**, 5786–5797.

(91) Francois, D.; Winssinger, N. *Org. Lett.* **2003**, *5*, 4445–4447.

(92) Sugiyama, T.; Kittaka, A. *Molecules* **2013**, *18*, 287–310.

(93) Hyrup, B.; Egholm, M.; Rolland, M.; Nielsen, P. E.; Berg, R. H.; Buchardt, O. *J. Chem. Soc. Chem. Commun.* **1993**, 518–519.

(94) Hyrup, B.; Egholm, M.; Nielsen, P. E.; Wittung, P.; Nordc, B.; Buchardt, O. *J. Am. Chem. Soc.* **1994**, *116*, 7964–7970.

(95) Govindaraju, T.; Kumar, V. A.; Ganesh, K. N. *Chem. Commun.* **2004**, *1*, 860–861.

(96) Pokorski, J. K.; Witschi, M. A.; Purnell, B. L.; Appella, D. H. *J. Am. Chem. Soc.* **2004**, *126*, 15067–15073.

(97) Govindaraju, T.; Kumar, V. A.; Ganesh, K. N. *J. Am. Chem. Soc.* **2005**, *127*, 4144–4145.

(98) Lagriffoule, P.; Wittung, P.; Eriksson, M.; Jensen, K. K.; Nordkn, B.; Buchardt, O.; Nielsen, P. E. *Chem. Eur. J.* **1997**, *3*, 912–919.

(99) Bregant, S.; Burlina, F.; Vaissermann, J.; Chassaing, G. *European J. Org. Chem.* **2001**, 3285–3294.

(100) Bregant, S.; Burlina, F.; Chassaing, G. *Bioorganic Med. Chem. Lett.* **2002**, *12*, 1047–1050.

(101) Dueholm, K. L.; Petersen, K. H.; Jensen, D. K.; Egholm, M.; Nielsen, P. E.; Buchardt, O. *Bioorganic Med. Chem. Lett.* **1994**, *4*, 1077–1080.

(102) Haaima, G.; Lohse, A.; Buchardt, O.; Nielsen, P. E. *Angew. Chemie Int. Ed. Engl.* **1996**, *35*, 1939–1942.

(103) Sugiyama, T.; Imamura, Y.; Demizu, Y.; Kurihara, M.; Takano, M.; Kittaka, A. *Bioorganic Med. Chem. Lett.* **2011**, *21*, 7317–7320.

(104) Manicardi, A.; Fabbri, E.; Tedeschi, T.; Sforza, S.; Bianchi, N.; Brognara, E.; Gambari, R.; Marchelli, R.; Corradini, R. *ChemBioChem* **2012**, *13*, 1327–1337.

(105) Sahu, B.; Sacui, I.; Rapireddy, S.; Zanotti, K. J.; Bahal, R.; Armitage, A. A.; Ly, D. H. *J. Org. Chem.* **2011**, *76*, 5614–5627.

(106) Yeh, J. I.; Shivachev, B.; Rapireddy, S.; Crawford, M. J.; Roberto, R.; Du, S.; Madrid, M.; Ly, D. H. *J. Am. Chem. Soc* **2011**, *132*, 10717–10727.

(107) Sahu, B.; Chenna, V.; Lathrop, K. L.; Thomas, S. M.; Zon, G.; Livak, K. J.; Ly, D. H. *J. Org. Chem.* **2009**, *74*, 1509–1516.

(108) Dean, D. *Adv. Drug Deliv. Rev.* **2000**, *44*, 81–95.

(109) David, Q. L.; Segal, J.; Ghiara, J. B.; Barbas, C. F. *Proc. Natl. Acad. Sci. USA* **1997**, *94*, 5525–5530.

(110) Molenaar, C.; Wiesmeijer, K.; Verwoerd, N. P.; Khazen, S.; Eils, R.; Tanke, H. J.; Dirks, R. W. *EMBO J.* **2003**, *22*, 6631–6641.

(111) Norton, J. C.; Piatyszek, M. A.; Wright, W. E.; Shay, J. W.; Corey, D. R. *Nat. Biotechnol.* **1996**, *14*, 615–619.

(112) Mayfield, L. D.; Corey, D. R. *Anal. Biochem.* **1999**, *268*, 401–404.

(113) Dose, C.; Seitz, O. *Org. Lett.* **2005**, *7*, 4365–4368.

(114) Singhal, A.; Nielsen, P. E. *Org. Biomol. Chem.* **2014**, *12*, 6901–6907.

(115) Ficht, S.; Mattes, A.; Seitz, O. *J. Am. Chem. Soc.* **2004**, *126*, 9970–9981.

(116) Stetsenko, D. A.; Gait, M. J. *J. Org. Chem.* **2000**, *65*, 4900–4908.

(117) Koppitz, M.; Nielsen, P. E.; Orgel, L. E. *J. Am. Chem. Soc* **1998**, *120*, 4563–

4569.

(118) Kolb, H. C.; Finn, M. G.; Sharpless, K. B. *Angew. Chemie - Int. Ed.* **2001**, *40*, 2004–2021.

(119) Rostovtsev, V. V.; Green, L. G.; Fokin, V. V.; Sharpless, K. B. *Angew. Chemie - Int. Ed.* **2002**, *41*, 2596–2599.

(120) Tornøe, C. W.; Christensen, C.; Meldal, M. *J. Org. Chem.* **2002**, *67*, 3057–3064.

(121) El-Sagheer, A. H.; Brown, T. *Chem. Soc. Rev.* **2010**, *39*, 1388–1405.

(122) Ji, P.; Atherton, J. H.; Page, M. I. *Org. Biomol. Chem.* **2012**, *10*, 7965–7969.

(123) Huisgen, R. *Proc. Chem. Soc.* **1961**, 357–396.

(124) Labbe, G. *Bull. Soc. Chim. Belg.* **1984**, *93*, 579–592.

(125) Ötvös, S. B.; Georgiádes, Á.; Ádok-Sipiczki, M.; Mészáros, R.; Pálinkó, I.; Sipos, P.; Fülöp, F. *Appl. Catal. A, Gen.* **2015**, *501*, 63–73.

(126) Meldal, M.; Tornøe, C. W. *Chem. Rev.* **2008**, *108*, 2952–3015.

(127) Timothy, R. C.; Hilgraf, R.; Sharpless, K. B.; Fokin, V. V. *Org. Lett.* **2004**, *6*, 2853–2855.

(128) Tron, G. C.; Pirali, T.; Billington, R. A.; Canonico, P. L.; Sorba, G.; Genazzani, A. A. *Med. Res. Rev.* **2008**, *28*, 278–308.

(129) Brik, A.; Alexandratos, J.; Lin, Y. C.; Elder, J. H.; Olson, A. J.; Wlodawer, A.; Goodsell, D. S.; Wong, C. H. *ChemBioChem* **2005**, *6*, 1167–1169.

(130) Peng, X.; Li, H.; Seidman, M. *European J. Org. Chem.* **2010**, *22*, 4194–4197.

(131) Chouikhi, D.; Barluenga, S.; Winssinger, N. *Chem. Commun. (Camb).* **2010**, *46*, 5476–5478.

(132) Castro, V.; Rodríguez, H.; Albericio, F. *ACS Comb. Sci.* **2016**, *18*, 1–14.

(133) Zaragoza, F.; Petersen, S. V. *Tetrahedron* **1996**, *52*, 10823–10826.

(134) Devi, G.; Ganesh, K. N. *Artif. DNA PNA XNA* **2010**, *1*, 68–75.

(135) Oyelere, A. K.; Chen, P. C.; Yao, L. P.; Boguslavsky, N. *J. Org. Chem.* **2006**, *71*, 9791–9796.

(136) Wang, J. *Biosens. Bioelectron.* **1998**, *13*, 757–762.

(137) Mateo-Mart, E.; Briones, C.; Pradier, C. M.; Martn-Gago, J. A. *Biosens. Bioelectron.* **2007**, *22*, 1926–1932.

(138) Hüsken, N.; Gasser, G.; Köster, S. D.; Metzler-Nolte, N. *Bioconjug. Chem.* **2009**, *20*, 1578–1586.

(139) Amant, A. H.; Engbers, C.; Hudson, R. H. E. *Artif. DNA. PNA XNA* **2013**, *4*, 4–10.

(140) Rugheimer, L.; Olerud, J.; Johnsson, C.; Takahashi, T.; Shimizu, K.; Hansell, P. *Matrix Biol.* **2009**, *28*, 390–395.

(141) Chao, H.; Spicer, A. P. *J. Biol. Chem.* **2005**, *280*, 27513–27522.

(142) Girish, K. S.; Kemparaju, K. *Life Sci.* **2007**, *80*, 1921–1943.

(143) DeAngelis, P. L.; Jing, W.; Graves, M. V; Burbank, D. E.; Van Etten, J. L. *Science* **1997**, *278*, 1800–1803.

(144) Suagahara, K.; Schwartz, N. B.; Dorfman, A. *J. Biol. Chem.* **1979**, *254*, 6252–6261.

(145) Yoshida, M.; Itano, N.; Yamada, Y.; Kimata, K. *J. Biol. Chem.* **2000**, *275*, 497–506.

(146) Weigel, P. H.; Hascall, V. C.; Tammi, M. *J. Biol. Chem.* **1997**, *272*, 13997–14000.

(147) Vigetti, D.; Karousou, E.; Viola, M.; Deleonibus, S.; Luca, G. De; Passi, A. *Biochim. Biophys. Acta* **2014**, *1840*, 2452–2459.

(148) Lukens, C. M.; Farrell, L. N. *J. Biol. Chem.* **1995**, *270*, 3400–3408.

(149) Spicer, A. P.; McDonald, J. A. *J. Biol. Chem.* **1998**, *273*, 1923–1932.

(150) Michael, D. R.; Phillips, A. O.; Krupa, A.; Martin, J.; Redman, J. E.; Altaher, A.; Neville, R. D.; Webber, J.; Kim, M.; Bowen, T. *J. Biol. Chem.* **2011**, *286*, 19523–19532.

(151) Vigetti, D.; Deleonibus, S.; Moretto, P.; Bowen, T.; Fischer, J. W.; Grandoch, M.; Oberhuber, A.; Love, D. C.; Hanover, J. A.; Cinquetti, R.; Karousou, E.; Viola, M.; Angelo, M. L. D.; Hascall, V. C.; Luca, G. De; Passi, A. *J. Biol. Chem.* **2014**, *289*, 28816–28826.

(152) Vigetti, D.; Karousou, E.; Viola, M.; Deleonibus, S.; De Luca, G.; Passi, A. *Biochimica et Biophysica Acta.* **2014**, *1840*, 2452–2459.

(153) Moccia, M.; Adamo, M. F. A.; Saviano, M.; Moccia, M.; Adamo, M. F. A.; Saviano, M. *Artif. DNA. PNA XNA* **2016**, *5*, e1107176–1 – e1107176–15.

(154) Li, J.; Sha, Y. *Molecules* **2008**, *13*, 1111–1119.

(155) Borthwick, A. D. *Chem. Rev.* **2012**, *12*, 3641–3716.

(156) Kosynkina, L.; Wang, W.; Liang, T. C. *Tetrahedron Lett.* **1994**, *35*, 5173–5176.

(157) Schwergold, C.; Depecker, G.; Di Giorgio, C.; Patino, N.; Jossinet, F.; Ehresmann, B.; Terreux, R.; Cabrol-Bass, D.; Condom, R. *Tetrahedron* **2002**, *58*, 5675–5687.

(158) Bialy, L.; Díaz-Mochón, J. J.; Specker, E.; Keinicke, L.; Bradley, M. *Tetrahedron* **2005**, *61*, 8295–8305.

(159) Verdolino, V.; Cammi, R.; Munk, B. H.; Schlegel, H. B.; Verdolino, V.; Cammi, R.; Munk, B. H.; Schlegel, H. B. *J. Phys. Chem.* **2008**, *112*, 16860–16873.

(160) Geen, G. R.; Gritnet, T. J.; Kincey, P. M.; Jarvest, R. L. *Tetrahedron* **1990**, *46*, 6903–6914.

(161) Chen, S. M.; Mohan, V.; Kiely, J. S.; Griffith, M. C.; Griffey, R. H. *Tetrahedron Lett.* **1994**, *35*, 5105–5108.

(162) Howarth, N. M.; Ricci, J. *Tetrahedron* **2011**, *67*, 9588–9594.

(163) Bräse, S.; Gil, C.; Knepper, K.; Zimmermann, V. *Angew. Chemie - Int. Ed.* **2005**, *44*, 5188–5240.

(164) Deans, T. L.; Singh, A.; Gibson, M.; Elisseeff, J. H. *Proc. Natl. Acad. Sci. USA* **2012**, *109*, 15217–15222.

(165) Mouna, A. M.; Nguyen, C.; Rage, I.; Xie, J.; Nee, G.; Mazaleyrat, J. P.; Wakselman, M. *Synth. Commun.* **1994**, *24*, 2429–2435.

(166) Dahiya, R. *J. Chil. Chem. Soc.* **2007**, *52*, 1224–1229.

(167) Amant, A. H.; Hudson, R. H. E. *Org. Biomol. Chem.* **2012**, *10*, 876–881.

(168) Palomo, J. M. *RSC Adv.* **2014**, *4*, 32658–32672.

(169) Dose, C.; Seitz, O. *Org. Lett.* **2005**, *7*, 4365–4368.

(170) Dawson, P. E.; Muir, T. W.; Clark-Lewis, I.; Kent, S. B. H. *Science* **1994**, *266*, 776–779.

(171) Mattes, A.; Seitz, O. *Chem. Commun.* **2001**, 2050–2051.

(172) Ficht, S.; Dose, C.; Seitz, O. *ChemBioChem* **2005**, *6*, 2098–2103.

(173) Jang, M.; Kim, J.; Park, H. *J. Microbiol. Biotechnol.* **2010**, *20*, 287–293.

(174) Giesen, U.; Kleider, W.; Berding, C.; Geiger, A.; Ørum, H.; Nielsen, P. E. *Nucleic*

Acids Res. **1998**, *26*, 5004–5006.

(175) Igloi G. L. *Proc. Natl. Acad. Sci. USA* **1998**, *95*, 8562–8567.

(176) Ratilainen, T.; Holmen, A.; Tuite, E.; Nielsen, P. E.; Norde, B. *Biochemistry* **2000**, *39*, 7781–7791.

(177) Kypr, J.; Kejnovská, I.; Renčiuk, D.; Vorlíčková, M. *Nucleic Acids Res.* **2009**, *37*, 1713–1725.

(178) Chakrabarti, M. C.; Schwarz, F. P. *Nucleic Acids Res.* **1999**, *27*, 4801–4806.

(179) Freifelder, D.; Davison, P. F. *Biophys. J.* **1962**, *2*, 249–256.

(180) Nielsen, P. E. ; Haairna, G. *Chem. Soc. Rev.* **1997**, *26*, 73–78.

(181) Katritzky, A. R.; Narindoshvili, T. *Org. Biomol. Chem.* **2008**, *6*, 3171–3176.

(182) Christensen, L.; Hansen, H. F.; Koch, T.; Nielsen, P. E. *Nucleic Acids Res.* **1998**, *26*, 2735–2739.

(183) Norgren, A. S.; Budke, C.; Majer, Z.; Heggemann, C.; Koop, T.; Sewald, N. *Synthesis,* **2009***, 488-494.*

Appendixes

Appendix 1: HPLC Chromatogram and mass spectrum of PNA oligomer 131

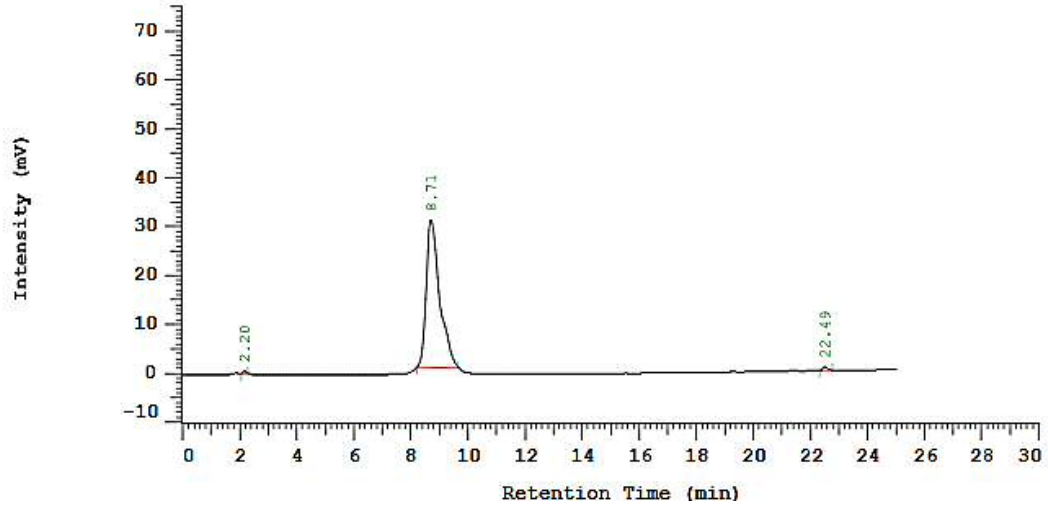

Finger 1: HPLC chromatogram of PNA oligomer **131**.

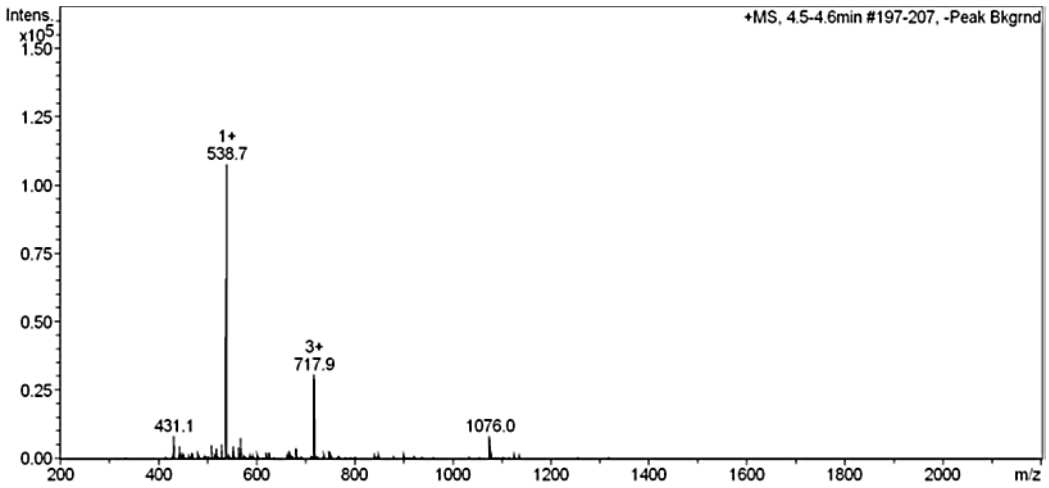

Figure 2: Mass spectrum of PNA oligomer **131**.

Appendix 2: HPLC Chromatogram and mass spectrum of PNA oligomer 132

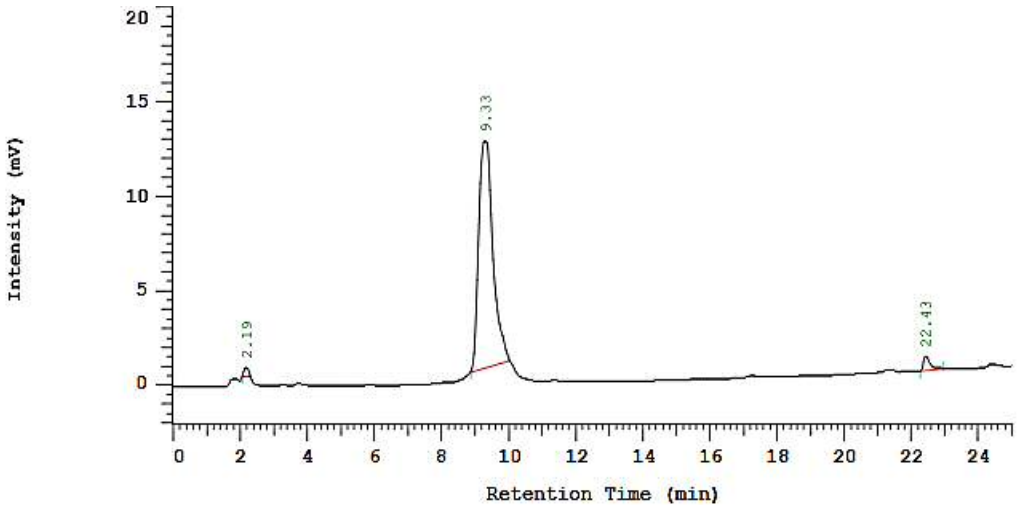

Figure 3: HPLC chromatogram of PNA oligomer **132**.

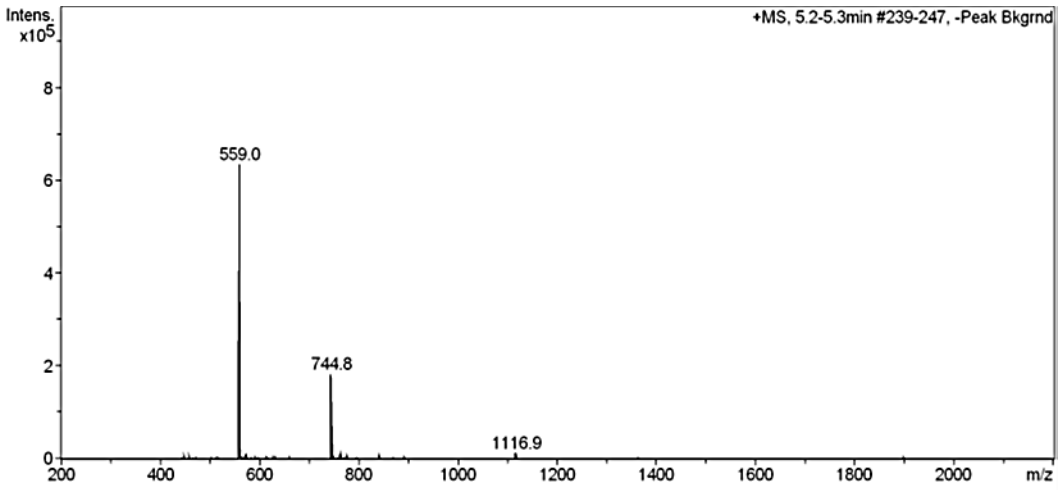

Figure 4: Mass spectrum of PNA oligomer **132**.

Appendix 3: HPLC Chromatogram and mass spectrum of PNA oligomer 133

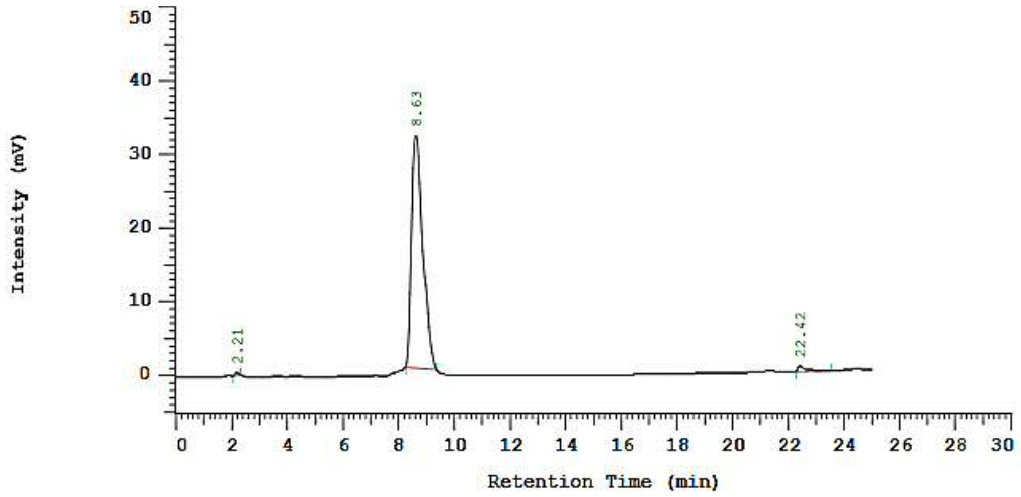

Figure 5: HPLC chromatogram of PNA oligomer **133**.

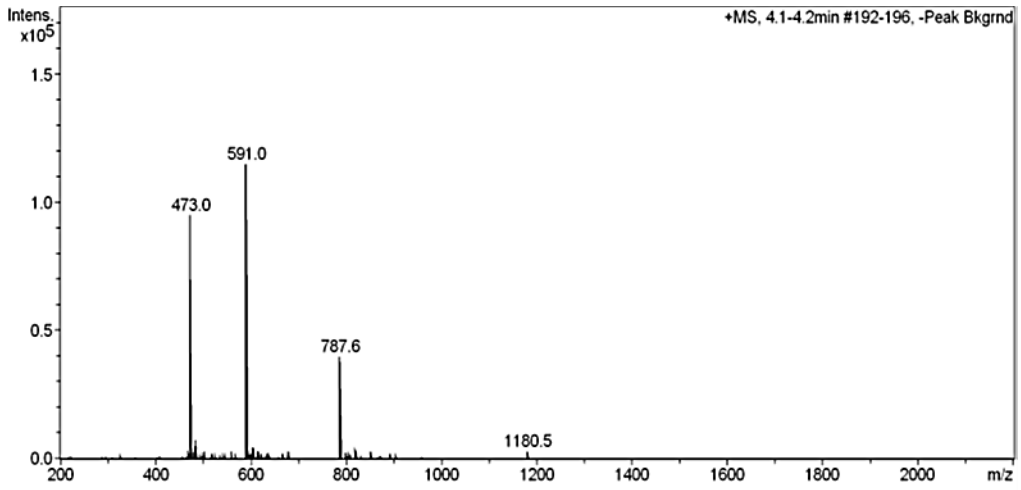

Figure 6: Mass spectrum of PNA oligomer **133**.

Appendix 4: HPLC Chromatogram and mass spectrum of PNA oligomer 134

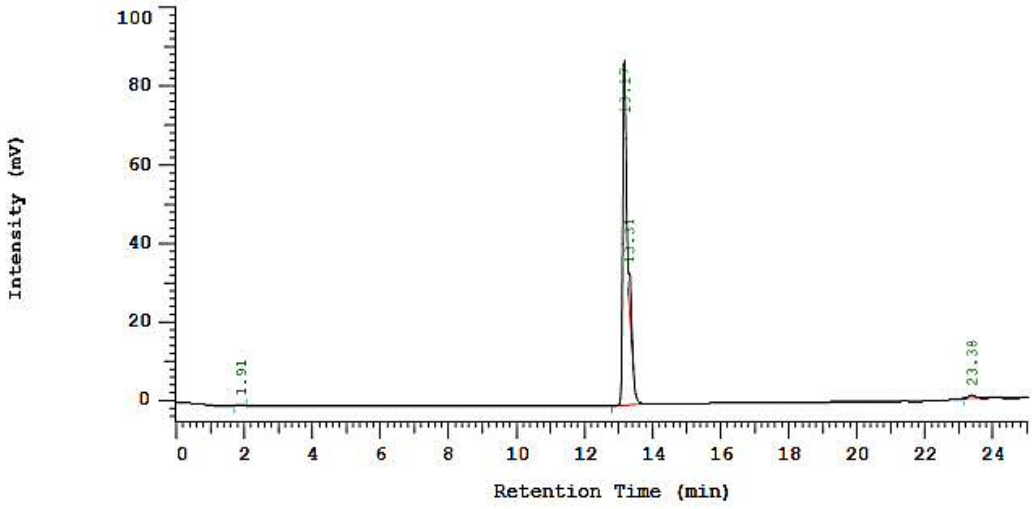

Figure 7: HPLC chromatogram of PNA oligomer **134**.

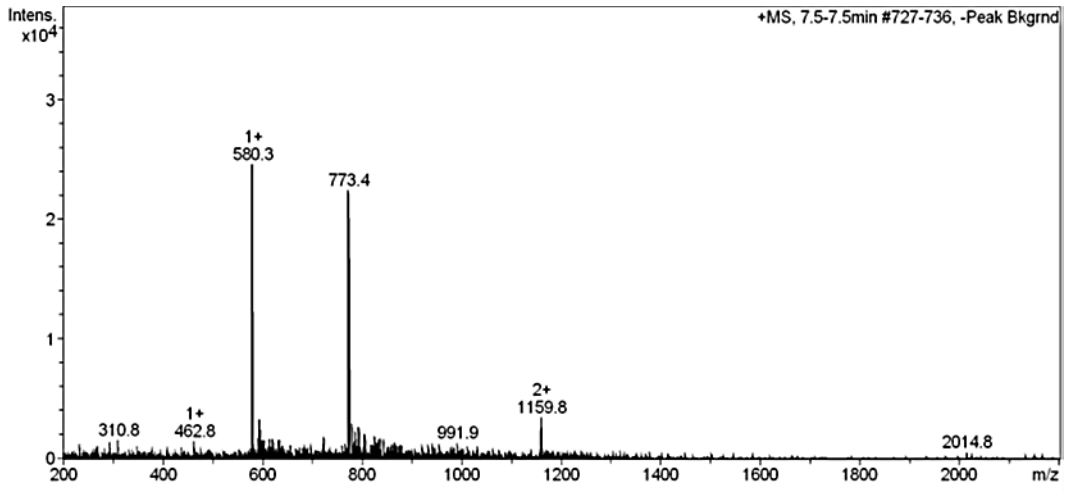

Figure 8: Mass spectrum of PNA oligomer **134**.

Appendix 5: HPLC Chromatogram and mass spectrum of PNA oligomer 135

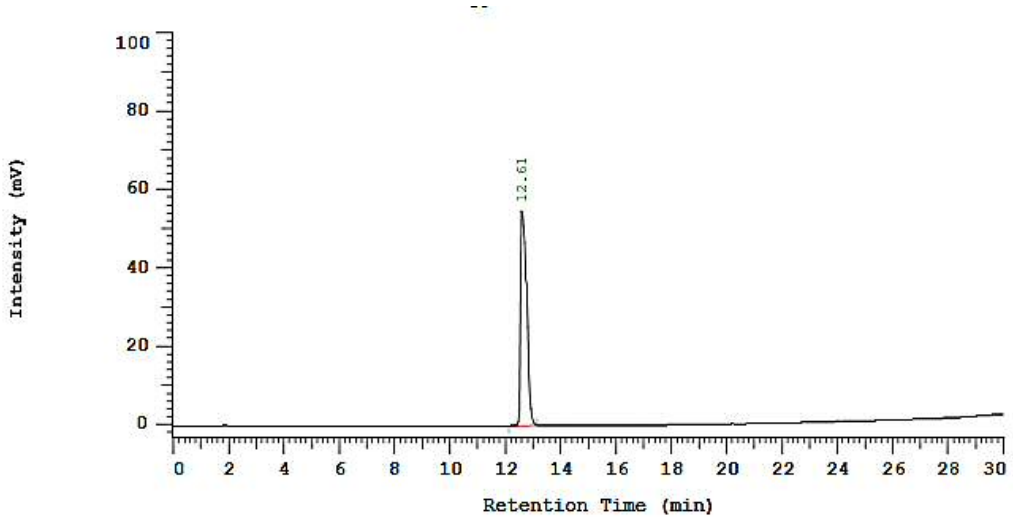

Figure 9: HPLC chromatogram of PNA oligomer **135**.

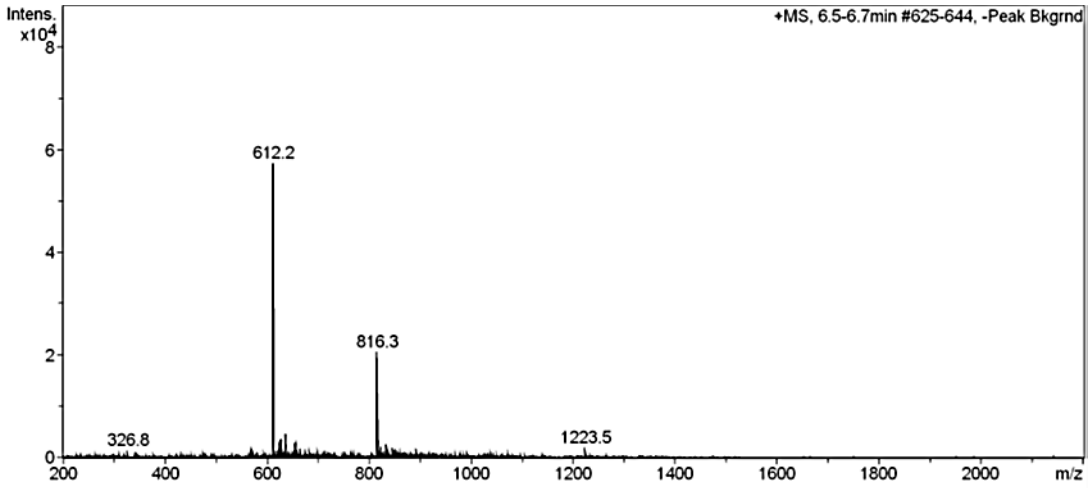

Figure 10: Mass spectrum of PNA oligomer **135**.

Appendix 6: HPLC Chromatogram and mass spectrum of PNA oligomer 136

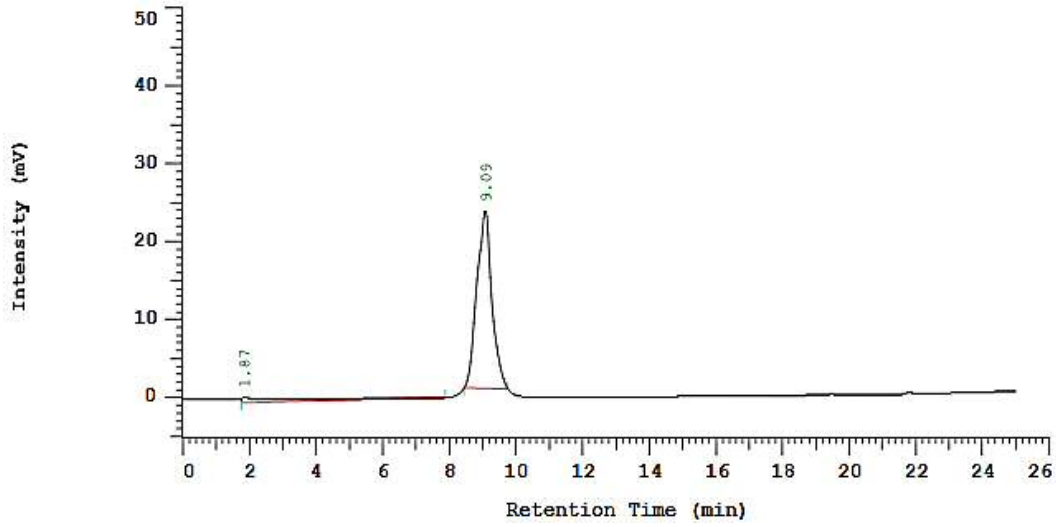

Figure 11: HPLC chromatogram of PNA oligomer **136**.

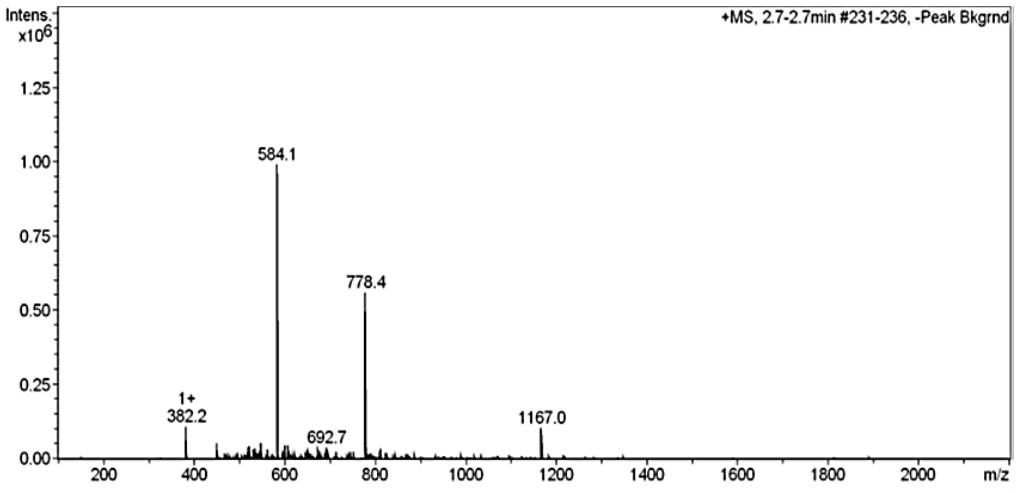

Figure 12: Mass spectrum of PNA oligomer **136**.

Appendix 7: HPLC Chromatogram and mass spectrum of PNA oligomer 137

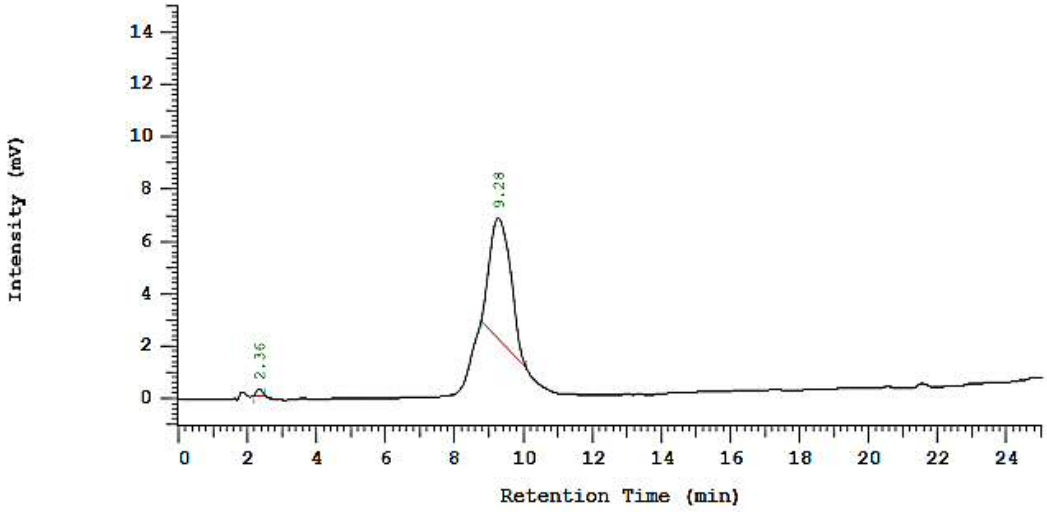

Figure 13: HPLC chromatogram of PNA oligomer **137**.

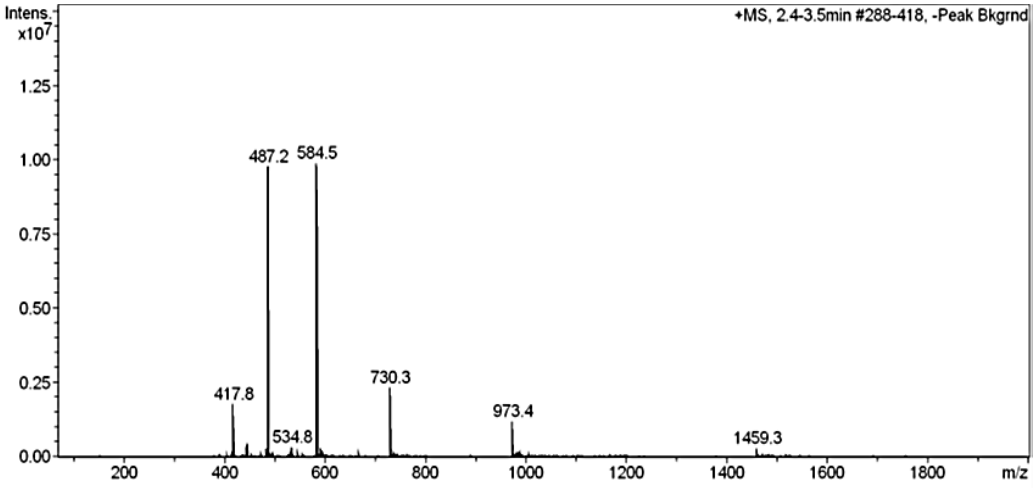

Figure 14: Mass spectrum of PNA oligomer **137**.

Appendix 8: HPLC Chromatogram and mass spectrum of PNA oligomer 138

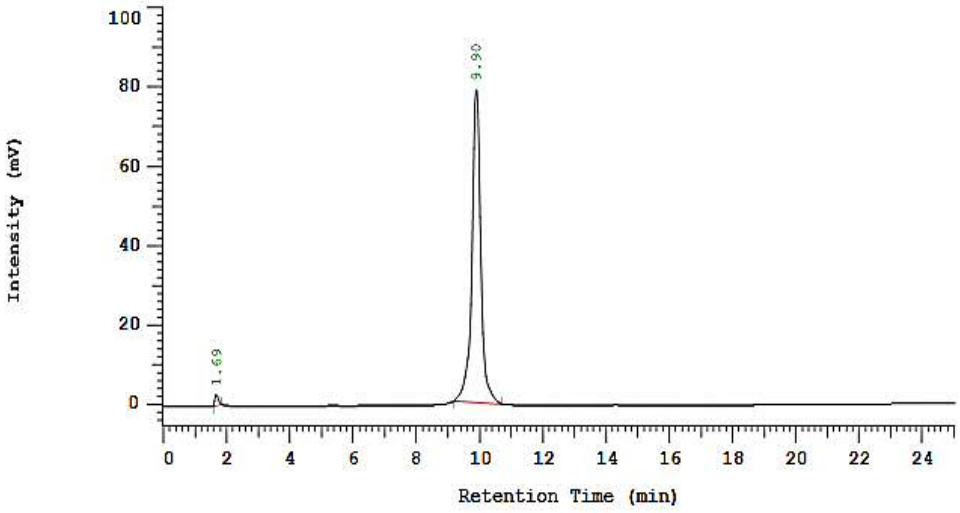

Figure 15: HPLC chromatogram of PNA oligomer **138**.

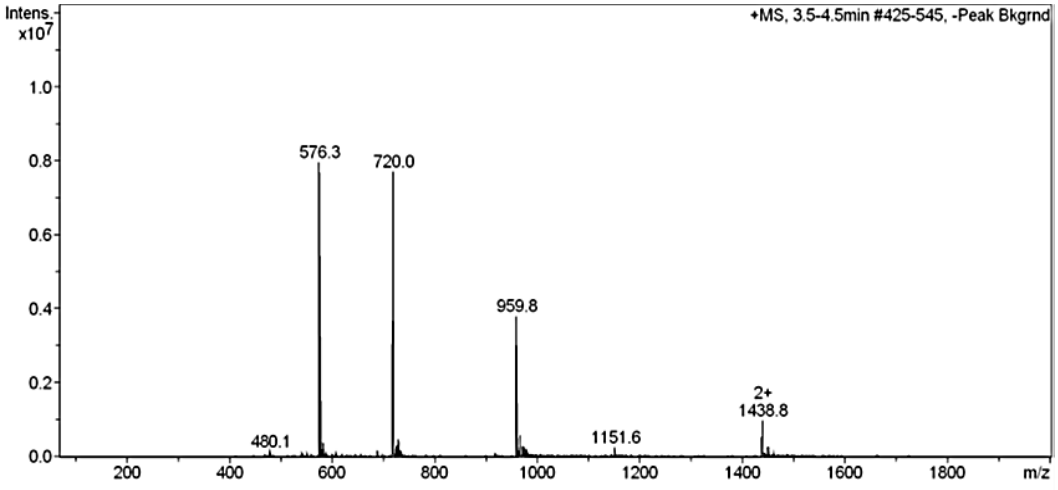

Figure 16: Mass spectrum of PNA oligomer **138**.

Appendix 9: HPLC Chromatogram and mass spectrum of PNA oligomer 139

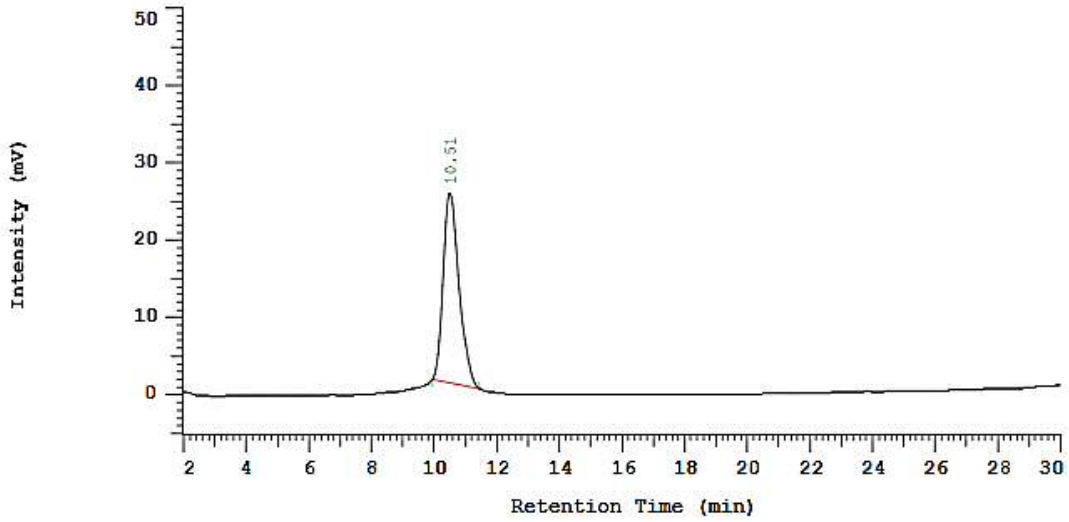

Figure 17: HPLC chromatogram of PNA oligomer **139**.

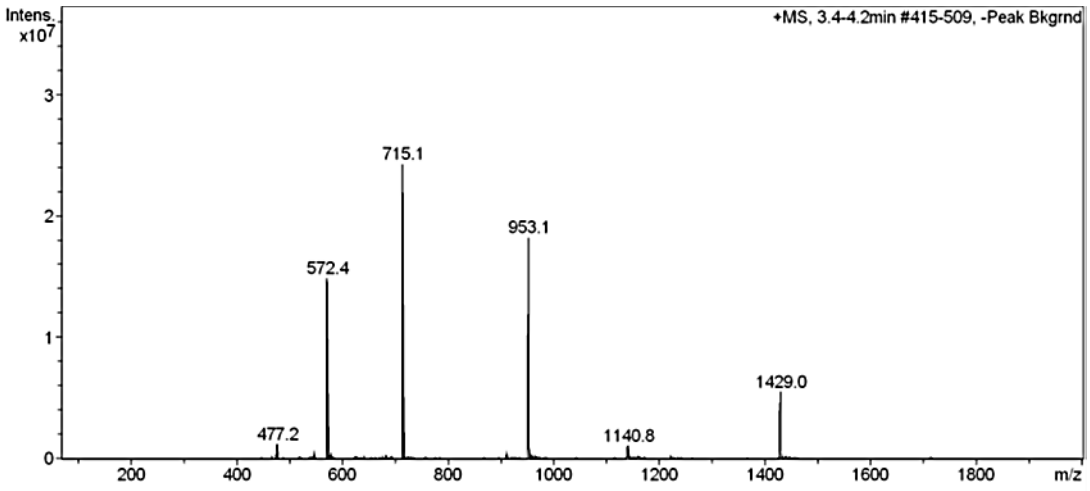

Figure 18: Mass spectrum of PNA oligomer **139**.